Neural Plasticity

Neural Plasticity during Aging

Lead Guest Editor: Mauricio Arcos-Burgos
Guest Editors: Francisco Lopera, Diego Sepulveda-Falla,
and Claudio A. Mastronardi

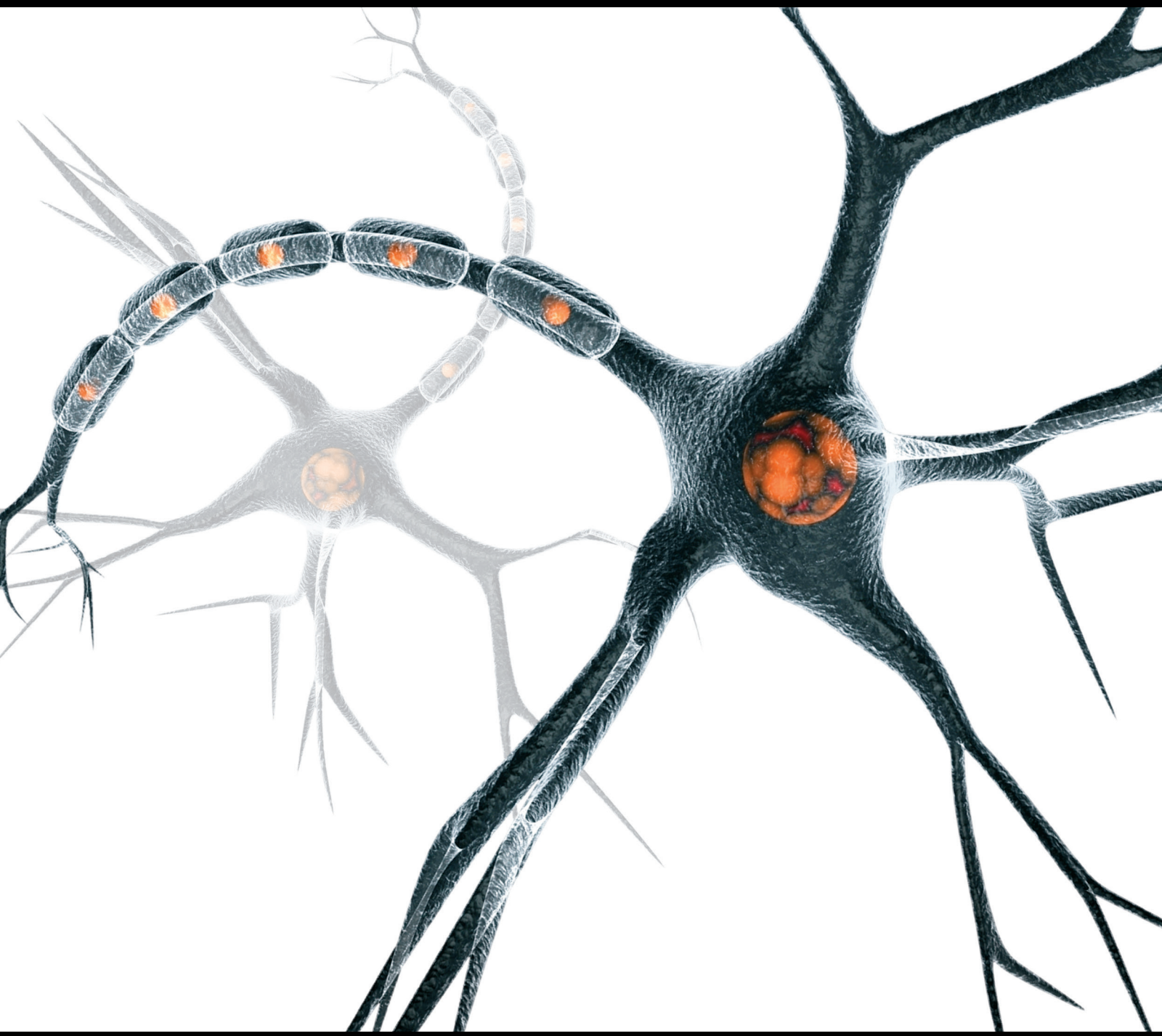

Neural Plasticity during Aging

Neural Plasticity during Aging

Lead Guest Editor: Mauricio Arcos-Burgos
Guest Editors: Francisco Lopera, Diego Sepulveda-Falla, and Claudio A. Mastronardi

Editorial Board

Contents

Hindawi
Neural Plasticity
Volume 2019, Article ID 6042132, 3 pages
https://doi.org/10.1155/2019/6042132

Editorial
Neural Plasticity during Aging

Mauricio Arcos-Burgos,[1,2,3] **Francisco Lopera**,[3] **Diego Sepulveda-Falla**,[3,4] **and Claudio Mastronardi**[1,2]

[1]*Institute of Translational Medicine, Universidad del Rosario, Bogotá, Colombia*
[2]*INPAC Research Group, Fundación Universitaria Sanitas, Bogotá, Colombia*
[3]*Neuroscience Research Group, University of Antioquia, Medellín, Colombia*
[4]*Institute of Neuropathology, University Medical Center Hamburg-Eppendorf, Hamburg, Germany*

Correspondence should be addressed to Mauricio Arcos-Burgos; oscarma.arcos@urosario.edu.co

Received 25 November 2018; Accepted 25 November 2018; Published 26 March 2019

The percentage of older people is increasing steadily in the proportion of the total population of the world. In a recent report published by the National Institute on Aging, in March of 2016, it was estimated that 8.5 percent of people, globally accounting for nearly 617 million, are aged 65 and over [1]. Additionally, it is also predicted that this ratio is going to double, reaching 17 percent of the global population (1.6 billion elders) in 2050 [1]. Consequently, the incidence of neurodegenerative diseases will continue to rise as a result of the increase in life expectancy.

Emerging evidence suggests that mental health decline due to neurodegenerative conditions constitutes the largest cause of global disability, which is accountable for over 20% of lifespan [2]. Data arising from family studies that compared the age of death of monozygotic and dizygotic twins suggested that approximately 25% of the variation in human longevity could be due to genetic factors [3]. It is noteworthy to remark that this genetic component appears to have a larger impact at older ages. However, only a few genes have been so far associated with lifespan, and the interaction among these genes, epigenetic factors, and environmental regulators are far from being well understood.

The neural plasticity processes occurring during aging are astonishing. For instance, there is mounting evidence supporting the concept that development, ageing, and brain degeneration are not mutually exclusive. It is now quite clear that once the brain is fully developed, it gradually shrinks at different levels during the ageing process [4]. All aged brains exhibit small distinctive alterations linked to neurodegeneration, namely, progressive loss of structure, function, or number of neurons [5, 6]. Neurodegeneration is, to some extent, a natural process occurring towards the end of life [7]. However, it is noteworthy to remark that developmentally related processes, i.e., neurogenesis, can also occur within the adult and ageing brain. In fact, approximately two decades ago, it became evident that a new type of neuroplasticity, one that is related to the addition of new neurons, occurs in the human brain [8, 9]. One of the key brain areas where adult neurogenesis occurs during the human's lifetime is the dentate gyrus, a region of the hippocampus that is essential for memory encoding [8, 10, 11]. There are a number of factors that can alter all of the neural plasticity changes that occur during aging. The understanding of the impact they exert particularly on the brain, and generally on the body, may aid in the development of novel therapeutic strategies to overcome the deleterious effects occurring during the aging process.

Therefore, there is an increased need to expand the knowledge on the different genetic, epigenetic, and molecular pathways and environmental factors that affect brain plasticity and healthy aging. Some of the topics covered in this special issue include the following:

(i) Environmental factors affecting healthy aging: possible impact of exercise and proton pump inhibitors (PPI)

(ii) Genetic structural variants associated with healthy aging

(iii) The updating of imaging studies to assess neural plasticity during aging

(iv) Possible novel brain areas undergoing neural plasticity

(v) Preclinical models of healthy aging: protective role of environmental enrichment preventing declarative learning and memory decline

Fourteen papers were submitted for this special issue. Our distinguished reviewers from respective research fields narrowed the field to seven papers, which were finally accepted. The following is a short summary of the findings of each of these papers.

Debate continues in regard to the possible impact of the use of proton pump inhibitors (PPI) and its consequences and links to dementia including Alzheimer's disease. G. Ortiz-Guerrero et al. reviewed preclinical and clinical studies regarding the action of PPI on the central nervous system and their possible implication in the pathophysiology of dementia including Alzheimer's disease. The authors summarized a comprehensive amount of data from a neurobiological and clinical perspective. They discussed both possible neurotoxic and antineurotoxic actions of PPI. They concluded that there is no real consensus on the role of PPIs and the associated risk of dementia. Nevertheless, they gave a word of caution stating that "nutritional and electrolyte monitoring is required in patients who chronically use PPIs, mainly older adults and patients with chronic malnutrition or debilitating chronic conditions".

With more than 350 million sufferers, depression continues to be the most prevalent mental health problem that largely affects the elderly population worldwide. X. Liu et al. designed a neuroimaging study that could be useful to predict the impact of major depressive disorders on dementia. They used resting-state functional magnetic resonance imaging to study 16 patients who had mild cognitive impairment (MCI) with depressive symptoms and 18 patients with nondepressed MCI. The authors studied their brains to measure the amplitude and synchronization of low-frequency brain fluctuations (ALFF), functional connectivity density (FCD), and coupling, which were quantified as the correlations between ALFF values and their associated FCDs. The authors described specific differences between the two experimental groups in some of these parameters in brain areas such as the medial prefrontal cortex, right precentral gyrus, and medial temporal gyrus that could be relevant to define the impact of depression on the neuropathophysiology of MCI.

Declarative learning involves memorizing concepts and events of our life, which can be expressed explicitly. The decline in memory performance is a distinctive feature of the normal aging process. In their original mouse study, S. Cintoli et al. described for the first time the protective role of environmental enrichment in preventing declarative learning and memory decline in aged mice. Thus, their exciting results in mice suggest that exposure to stimulating environmental conditions could be used as a powerful paradigm to promote better memory performance during aging in the elderly population.

Genetics plays an essential role in the aging process. Interestingly, the genome of neuronal cells displays genomic mosaicism, which includes DNA copy number variations (CNVs). D. Villela et al. investigated for the first time the features of somatic CNV mosaicism in nondiseased elderly brains. In their original study, the authors demonstrated a highly significant increase in the number of CNVs in two brain areas (frontal cortex and cerebellum) when compared with paired blood samples (same individuals). It is noteworthy to remark that almost all evidence of genome structural variation in human brains is derived from studies describing changes in single cells, which were interpreted as originating from independent, isolated mutational events. In their studies, D. Vilella et al. indicated the occurrence of extensive clonal mosaicism of CNVs within the human brain, which reveals a novel type of variation that had not been previously characterized.

Even though a decline in motor function is a common phenomenon that takes place during aging, the functional changes occurring in neural networks responsible for generating movement are far from being understood. Recordings from the primary motor cortex during periods of steady muscle contraction show oscillatory neural activity that is coherent with the activity of contralateral muscles. M. E. Spedden et al. investigated the functional oscillatory coupling between activities in the sensorimotor cortex and ankle muscles during static contraction in fifteen young and fifteen older subjects. Their results show that there is an age-related decrease in the strength of oscillatory corticospinal activity during steady-state motor output. They also conclude that their novel findings might be instrumental in developing new preventive and therapeutic interventions that may strengthen sensorimotor control in elderly subjects.

Mounting evidence suggests that exercise causes beneficial effects on neural plasticity and cognition. Exercise triggers the release of neurotrophins, which can increase neurogenesis, synaptogenesis, and angiogenesis. Additionally, exercise can induce neuroendocrinological changes, which impact positively on cognitive, affective, and behavioral functioning. Even though motor performance declines during aging, learning capabilities remain intact. In their original paper, L. Hübner et al. (in press) reveal for the first time that acute exercise facilitates fine motor control performance and learning, as well as electrophysiological processing in healthy older adults. The authors suggest that their findings could be translated into practice by implementing acute exercise as a method to create successful experiences in fine motor control performance, which ultimately could contribute in motivating older patients' rehabilitation process (Lena Hübner et al. in press).

There are an estimated 47 million people worldwide that suffer from dementia, a number that is projected to increase to approximately 131 million by 2050. Alzheimer's disease

is the most common type of dementia accounting for 60-70% of all of the dementia cases. Novel biomarkers for prediction, diagnosis, and follow-up of this neurodegenerative condition are very much needed. Interestingly, functional and pathological mechanisms of the visual system share some similarities with the CNS. In their comprehensive review "Visual Features in Alzheimer's Disease: From Basic Mechanisms to Clinical Overview," the authors summarize the current evidence describing the pathophysiological alterations occurring in the vision system of patients suffering Alzheimer's disease. The authors foresee that novel objective measurement of vascular and inflammatory changes in the eye may play an essential role in the evaluation of early stages of dementia and AD.

We believe that this special issue would provide new insights into important aspects of neural plasticity-associated aging. The different research perspectives described in this special issue might encourage the undertaking of novel projects aimed at developing novel therapeutic strategies and scientific approaches to tackle some of the health issues that are aggravated by the aging process.

Finally, we would like to give thanks to all of the authors, the reviewers, the editorial board members, and the general staff of Neural Plasticity for their concerted effort in constructing this special issue.

Conflicts of Interest

The editors declare that they have no conflicts of interest regarding the publication of this special issue.

Mauricio Arcos-Burgos
Francisco Lopera
Diego Sepulveda-Falla
Claudio Mastronardi

References

[1] W. He, D. Goodkind, and P. Kowal, *An Aging World: 2015. International Populations Reports*, U.S. Census Bureau, 2015.

[2] K. Jin, J. W. Simpkins, X. Ji, M. Leis, and I. Stambler, "The critical need to promote research of aging and aging-related diseases to improve health and longevity of the elderly population," *Aging and Disease*, vol. 6, no. 1, pp. 1–5, 2015.

[3] G. Passarino, F. De Rango, and A. Montesanto, "Human longevity: genetics or lifestyle? It takes two to tango," *Immunity & Ageing*, vol. 13, no. 1, pp. 12–12, 2016.

[4] R. Peters, "Ageing and the brain," *Postgraduate Medical Journal*, vol. 82, no. 964, pp. 84–88, 2006.

[5] M. F. Beal, "Aging, energy, and oxidative stress in neurodegenerative diseases," *Annals of Neurology*, vol. 38, no. 3, pp. 357–366, 1995.

[6] A. Elobeid, S. Libard, M. Leino, S. N. Popova, and I. Alafuzoff, "Altered proteins in the aging brain," *Journal of Neuropathology and Experimental Neurology*, vol. 75, no. 4, pp. 316–325, 2016.

[7] T. Wyss-Coray, "Ageing, neurodegeneration and brain rejuvenation," *Nature*, vol. 539, no. 7628, pp. 180–186, 2016.

[8] P. S. Eriksson, E. Perfilieva, T. Bjork-Eriksson et al., "Neurogenesis in the adult human hippocampus," *Nature Medicine*, vol. 4, no. 11, pp. 1313–1317, 1998.

[9] E. Gould, P. Tanapat, T. Rydel, and N. Hastings, "Regulation of hippocampal neurogenesis in adulthood," *Biological Psychiatry*, vol. 48, no. 8, pp. 715–720, 2000.

[10] R. Knoth, I. Singec, M. Ditter et al., "Murine features of neurogenesis in the human hippocampus across the lifespan from 0 to 100 years," *PLoS One*, vol. 5, no. 1, article e8809, 2010.

[11] V. G. Kukekov, E. D. Laywell, O. Suslov et al., "Multipotent stem/progenitor cells with similar properties arise from two neurogenic regions of adult human brain," *Experimental Neurology*, vol. 156, no. 2, pp. 333–344, 1999.

Hindawi
Neural Plasticity
Volume 2018, Article ID 4756785, 20 pages
https://doi.org/10.1155/2018/4756785

Research Article

Acute Exercise as an Intervention to Trigger Motor Performance and EEG Beta Activity in Older Adults

Lena Hübner,[1] Ben Godde,[2] and Claudia Voelcker-Rehage[1]

[1]*Professorship of Sports Psychology, Institute of Human Movement Science and Health, Chemnitz University of Technology, Thüringer Weg 11, 09126 Chemnitz, Germany*
[2]*Psychology & Methods, Focus Area Diversity, Jacobs University Bremen gGmbH, Campus Ring 1, 28759 Bremen, Germany*

Correspondence should be addressed to Claudia Voelcker-Rehage; claudia.voelcker-rehage@hsw.tu-chemnitz.de

Received 6 July 2018; Accepted 29 August 2018; Published 23 December 2018

Academic Editor: Claudio A. Mastronardi

Acute bouts of exercise have been shown to improve fine motor control performance and to facilitate motor memory consolidation processes in young adults. Exercise effects might be reflected in EEG task-related power (TRPow) decreases in the beta band (13–30 Hz) as an indicator of active motor processing. This study aimed to investigate those effects in healthy older adults. Thirty-eight participants (65–74 years of age) were assigned to an experimental (EG, acute exercise) or a control group (CG, rest). Fine motor control was assessed using a precision grip force modulation (FM) task. FM performance and EEG were measured at (1) baseline (immediately before acute exercise/rest), (2) during practice sessions immediately after, (3) 30 minutes, and (4) 24 hours (FM only) after exercise/rest. A marginal significant effect indicated that EG revealed more improvement in fine motor performance immediately after exercise than CG after resting. EG showed enhanced consolidation of short-term and long-term motor memory, whereas CG revealed only a tendency for short-term motor memory consolidation. Stronger TRPow decreases were revealed immediately after exercise in the contralateral frontal brain area as compared to the control condition. This finding indicates that acute exercise might enhance cortical activation and thus, improves fine motor control by enabling healthy older adults to better utilize existing frontal brain capacities during fine motor control tasks after exercise. Furthermore, acute exercise can act as a possible intervention to enhance motor memory consolidation in older adults.

1. Introduction

Fine motor control performance declines with increasing age [1], affecting activities of daily and professional life [2]. Although older adults are able to learn new and relearn motor skills [3], the consolidation of motor memory is diminished in older adulthood [4–7]. Acute bouts of cardiovascular exercise facilitate neuroplasticity in the primary motor cortex (M1) and enhance corticospinal excitability [8]. These effects are not specific to lower extremity motor areas and muscles engaged during exercise but also apparent in motor areas responsible for upper limbs, indicating that exercise has a generalized effect on M1 [9, 10]. Accordingly, several studies have investigated the effect of acute exercise on upper extremity visuomotor performance as well as acute exercise as a possible intervention to trigger motor consolidation processes in healthy young adults [11–18]. However, previous studies were inconsistent with respect to the time points of measurement, definition of motor performance/learning, and respective results, and were conducted only with young adults.

1.1. Effects of Acute Exercise on Motor Behavior. In the present study, we distinguished between (fine) *motor performance,* indicating a temporary status of motor behavior; *initial motor learning,* representing the very early phase of motor skill acquisition, and *motor memory,* characterized as a stable improvement of motor performance relative to baseline after a certain delay after practice [12, 19].

The influence of a bout of acute exercise on *motor performance* is usually assessed by performing a motor task immediately after an exercise session. Findings in studies with young adults are inconsistent: some indicate better fine motor control performance immediately after moderate intensity exercise than after rest [11], whereas others do not

report such effects after moderate [15, 16] or high-intensity exercise [14].

The effect of acute exercise on *initial motor learning* can be measured by practicing the motor task immediately after exercise. Two studies report enhanced learning after moderate intensity exercise in young adults [11, 16], but others did not find altered motor learning behavior after moderate [15, 20] or high-intensity exercise [14, 18] in upper limb tasks.

Consolidation of *motor memory* refers to the transformation from a fragile to a stable memory trace evolving during online and offline processes after motor practice [21–23]. Memory consolidation processes can be distinguished with respect to different time scales, such as *short-term*, i.e., seconds to hours, and *long-term memory*, i.e., hours to months [24]. Accordingly, motor learning and acute exercise literature have assessed short-term motor memory up to one hour after practice/exercise and long-term motor memory 24 hours or seven days after practice/exercise [12, 25]. In healthy young adults, short-term motor memory in upper limb motor tasks seemed unaffected by acute exercise (one hour after exercise: [12, 14]). In contrast, participants revealed improved upper limb performance compared to resting control groups 24 hours and seven days [12, 14, 17, 18] after a bout of high-intensity exercise as well as 24 hours and seven days after low-intensity exercise [18]. This indicates that exercise triggers long-term motor consolidation processes, probably mediated by enhanced levels of norepinephrine, nerve growth factors, or metabolic signaling [14].

However, the influence of a bout of acute exercise on *motor performance*, *initial motor learning,* or *motor memory* in upper extremity fine motor tasks has not yet been studied in healthy older adults [26]. Several studies have revealed that acute exercise benefits cognitive performance in older adults immediately after moderate cardiovascular exercise [27–29], which was explained by higher arousal, improved information processing, and attention [28, 30]. As older adults require enhanced cognitive resources during motor performance and initial motor learning [31–33], and as motor consolidation processes are diminished in older adults [4–7], acute exercise might be an appropriate intervention to facilitate motor performance, initial motor learning, and motor memory consolidation in this age group.

1.2. Effects of Acute Exercise on Electrophysiological Data. Bilateral pre- and postcentral sensorimotor brain areas are involved in fine motor control performance [34–37], initial learning processes [38, 39], and consolidation of motor memory [23]. Task-related power (TRPow) decreases in the beta frequency band (13–30 Hz) over sensorimotor areas as obtained with electroencephalography (EEG) are discussed to be indicative of enhanced cortical activation and active processing of motor tasks [40–42]. In young adults, such desynchronization of beta oscillations has been shown during visuomotor force-matching tasks [41, 43, 44] and seems to reflect the efficiency of online and feedback processing of the motor system [45]. Furthermore, practicing a motor task led to weaker beta TRPow decreases not only in sensorimotor but also in frontal cortical areas in young adults [46–48], probably indicating increased automaticity and therefore, reflecting initial motor learning processes. With regard to age-related differences, in older as compared to young adults, stronger beta TRPow decreases during the performance of a force modulation task were found [49]. Following these results and as frontal brain activity is of particular interest in aging research [50], we focused our analysis on frontal and sensorimotor cortical areas by analyzing the beta frequency band.

Cardiovascular exercises have a modulating effect on activity in sensorimotor areas. For example, activity in the M1 or the primary somatosensory cortex (S1) was increased immediately after cardiovascular exercises [51–53]. In most studies, the cortical EEG was measured after acute exercise in young [54–57] and older adults [58] at rest. A recent study by Dal Maso et al. [59] investigated event-related desynchronization (ERD) during a power grip force modulation task after a bout of high-intensity exercise in young healthy adults. They revealed weaker ERD (analogous to less TRPow decrease) over bilateral sensorimotor cortical areas during early motor memory consolidation 30 to 90 minutes after exercise as compared to rest [59].

The aim of this study was, first, to investigate whether a moderate intensity cardiovascular exercise session facilitates (1) *motor performance*, (2) *initial motor learning* immediately after exercise, (3) *short-term motor memory* (30 minutes after exercise), and *long-term motor memory* (24 hours after exercise) in older adults. This was examined using a force modulation (FM) task performed with a precision grip. While existing studies with similar motor tasks conducted with young adults revealed controversial findings, effects might be more explicit in older adults due to age-related changes in motor processing. Greater improvement in fine motor control was expected during the motor performance and initial motor learning following acute exercise (experimental group) compared to after rest (control group). Furthermore, we hypothesized that the experimental group would show enhanced short-term and long-term motor memory consolidation, whereas the control group would not.

Secondly, this study aimed at investigating whether an acute exercise session influences TRPow in the beta band over the frontal and sensorimotor cortex during the performance of an FM task at the measurement points after exercise termination. We refer to TRPow decreases as indicators of enhanced motor processing [41, 42] and hypothesized that TRPow decreases were stronger directly after exercise as compared to after the control condition. Throughout practice, we expected that the experimental group would learn more than the control group, which might be reflected in stronger declines of the TRPow decreases. Analyses of EEG beta power at a reference spectrum at rest (before/after FM performance) were performed to confirm that beta power values did not differ between groups over time. Finally, we examined whether changes in beta TRPow were associated with changes in motor performance.

2. Methods

2.1. Participants. Forty-one older adults between the ages of 65 and 74 (69.51 ± 2.97 years of age, 22 female) participated

Table 1: Participant characteristics for EG and CG.

	EG (n = 17, 9 female)		CG (n = 21, 11 female)		F-statistics		
	M	SD	M	SD	$F(1, 36)$	p	η_p^2
Age	68.17	3.18	70.48	2.75	3.39	.074	.09
Education	16.38	2.17	15.76	1.99	0.84	.365	.02
Subj. health	4.12	0.60	4.10	0.63	0.01	.912	<.01
MMSE	28.88	0.86	28.52	0.98	1.40	.244	.04
Subj. hand usage	19.18	4.93	18.57	4.73	0.15	.698	<.01
Pegboard	12.35	1.13	12.19	1.72	0.11	.740	<.01
MVC	55.53	16.14	58.28	16.12	0.77	.387	.02
Physical activity	39.44	18.40	39.03	15.41	0.01	.940	<.01
Maximum Watt	142.82	42.68	143.00	35.73	< 0.01	.989	<.01
VO_2-peak	1.95	0.59	1.85	0.53	0.25	.619	.01

Notes. EG = experimental group; CG = control group; age = age in years; education = years of education; subj. health = self-rated health status in a Likert scale from 1 (poor) to 5 (excellent); MMSE = sum score of the Mini-Mental State Examination; subj. hand usage = self-reported hand use (sum score of 9 items, 5-point scale); Pegboard = mean score of three trials with the right hand; MVC = maximum voluntary contraction of index finger and thumb, maximal value out of three trials; physical activity = kcal/kg*wk; maximum Watt = maximum Watt performed during cardiovascular fitness test; VO_2-peak = VO_2-peak performed during cardiovascular fitness test in l/min.

in this study. Participants were recruited by local newspapers and were screened for the following prerequisites using telephone interviews: (1) age between 65 and 74, (2) absence of neurological and cardiovascular diseases, (3) physically active lifestyle, i.e., moderate intensity exercise for at least 150 minutes per week (in accordance to the recommendations of the American College of Sports Medicine [60]), and (4) right-handedness. The Ethics Committee of the Faculty of Humanities of the Saarland University (4.3.13) approved the study protocol. All participants took part voluntarily and provided informed consent regarding the general study information, receiving EEG and cardiovascular fitness tests, and also provided consent from their personal physician to complete the cardiovascular fitness test. Participants received 35 € as monetary compensation.

To validate the oral information and complete the screening process, participants answered a questionnaire assessing demographic information, education level (years of education), subjective health status ("in general, how would you say your health is?"—5-point Likert scale from *poor* to *excellent*), and physical activity level (adapted version of [61]). Participants were screened for dementia using the Mini-Mental State Examination (MMSE) [62], inclusion criteria ≥ 27 [63]. Further, they conducted the Edinburgh handedness inventory [64] to confirm their right-handedness (score: 84.95 ± 24.57) as well as a questionnaire to assess subjective hand use [65] to control for the exertion of fine motor activities during daily life. To control for restrictions in fine motor control, clinical manual dexterity was measured using the Purdue Pegboard test (Purdue Pegboard test, model 32020, Lafayette Instruments, Lafayette, IN, USA) [66]. The mean number of pins was calculated out of three trials placed with the dominant right hand. In the Purdue Pegboard test, all participants scored within the normative values for the right hand [67].

After screening and exercise testing, participants were assigned to an experimental (EG) or a control group (CG). Participants were matched with respect to their gender, age, MMSE score, and cardiovascular fitness level (VO_2-peak, cf. below). Three participants had to be excluded from data analysis: one participant was not able to perform the fine motor control task adequately (EG), one was regarded as left-handed (CG) [64], and one due to noise in the EEG signal (EG). Therefore, 38 participants between 65 and 74 (69.68 ± 3.04 years of age, 20 female) were included in further analysis (descriptive statistics see Table 1). In the final sample, groups did not differ with respect to gender, age, education, subjective health, subjective hand usage, MMSE score, Pegboard performance, maximum voluntary contraction (MVC, see MVC task), physical activity, or cardiovascular fitness level (see Table 1).

2.2. Measures

2.2.1. Cardiovascular Fitness Test. Cardiovascular fitness was measured by spiroergometry (ZAN600, nSpire Health, Oberthulba, Germany) on a stationary bicycle (Lode Corival cpet, Groningen, the Netherlands) using a ramp protocol to determine peak oxygen consumption (VO_2-peak). The protocol was adjusted according to the participant's gender and self-reported physical activity level to ensure an adequate physical load. For this purpose, the participants were asked how often they perform cardiovascular exercise per week immediately before testing. If participants performed cardiovascular exercise less than three hours per week, a ramp protocol with a progressively increasing load of 10 W/min, starting with 10 W, was chosen for female participants, and a load of 15 W/min, starting with 10 W, was used for male participants. If participants exercised three hours or more per week, a progressive protocol starting at 10 W and increasing load of 15 W/min were used for females, and male participants started at 20 W and increased the load by 20 W/min. All tests were supervised by an experienced sports scientist. Electrocardiography (ECG, recorded with a ten-lead ECG fully

digital stress system; Kiss, GE Healthcare, Munich, Germany), breath-by-breath respiration, heart rate, and blood pressure were continuously monitored. All spiroergometry protocols started with a three-minute rest period, then had participants cycled until a respiratory exchange ratio of 1.05 was maintained for about 30 seconds, and were finished with a five-minute cool-down period. Tests were terminated by volitional exhaustion or the occurrence of risk factors (i.e., systolic blood pressure > 230/115 mmHg, heart rate approximately > [220 – age]). The values of the highest complete performance level (about ≥ 4-5 seconds) achieved by the participants were averaged and regarded as VO_2-peak, expressed as VO_2 l/min.

2.2.2. Fine Motor Control Performance and Learning: Apparatus and Setup. Fine motor control was measured with a force transducer (FT, FX1901 OEM sensor, Variohm EuroSensor, Heidelberg, Germany). The sensor plate (diameter 25 mm) was encased with a plastic sheath (diameter 2.6 mm), which was located 45 to 71 mm above the tabletop on a 45 × 50 mm plastic pedestal (see Figure 1(a)). The FT was placed on a table in front of the participants in a comfortable position. Participants were seated about 60 cm in front of a 23.8-inch monitor (hardware resolution: 1920 × 1080 pixels). The monitor presented online visual feedback about the target (green) and applied force (yellow) on a black background. Target and applied force appeared on the right side of the screen and moved to the left. Target force appeared 200 ms before the applied force. Five seconds of force were presented continuously on the *x*-axis. For the maximum voluntary contraction (MVC) task, the *y*-axis was a fixed window from 0 to 100 N; for the force modulation (FM) task, the *y*-axis was set to 0 to 16 N. Force data were recorded at a sampling rate of 120 Hz and a resolution of 0.06 N with a customized LabVIEW program (LabVIEW 2015, National Instruments Austin, TX, USA). Participants had to pinch the FT with a precision grip, placing their thumb on the force sensor and the index finger on the plastic backside of the sensor (see Figure 1(b)). No participant had experience with this fine motor task. Participants received no feedback in terms of a quantified performance score.

2.2.3. MVC Task. Participants' *maximum voluntary contraction* (*MVC*) was assessed by asking them to exert as much power as possible with their thumb and index finger on the FT (three trials of five seconds, ≥ 30 seconds rest between trials). The highest value out of the three trials was regarded as *MVC*.

2.2.4. Force-Matching Task (FM Task). For an overview of the FM task procedure see Figure 2. First, *familiarization* for the FM task was performed. Participants were instructed to try out how the FT reacts during pinching with low forces without a target curve (one trial, length: 10 seconds). Then, participants had to apply force to match a target force as accurately as possible (part 1: constant target line at 4 N, three trials, 5 seconds each; part 2: regular sine-wave patterns between 1 N and 5 N, frequency of 0.4 Hz, three trials, 6.67 seconds each). For all FM task sessions, participants were again instructed to apply their own force to match the target curve as accurately as possible.

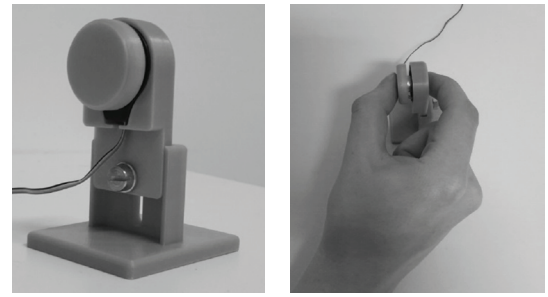

(a) (b)

Figure 1: (a) Force transducer (FT). (b) Participant performs a precision grip.

The target curve of the actual FM task sessions consisted of an irregular sine-wave pattern of eight sine waves with the same minima (2 N) and varying maxima (5.1 N–11.3 N; see Figure 3). Sine-wave frequency (0.35 Hz–0.78 Hz) was adapted to the varying maxima so that tracking velocity was identical within each sine wave. The same sine-wave pattern was performed repetitively throughout the whole experiment. One trial had a length of 15 seconds. Trials were intermitted by a four-second intertrial break, during which a white fixation cross appeared on a black screen. During *baseline*, participants performed eight trials with the irregular sine wave. During the FM practice sessions, participants performed four blocks of eight trials immediately, 30 minutes, and 24 hours after intervention. The blocks were intermitted by breaks of approximately 30 seconds, during which participants were asked to relax their hands.

2.2.5. Acute Exercise Session. The EG performed a moderate intensity exercise session by cycling on a stationary ergometer (Lode Corival cpet, Groningen, the Netherlands) for 25 minutes. The exercise started with a two-minute warm-up without Watt resistance, followed by 20 minutes at 60% of participants' maximum Watt performed during the cardiovascular fitness test (range: 54 W to 130 W, mean: 86.53 ± 25.17 W). The exercise session concluded with a three-minute cool-down without Watt resistance. Heart rate was monitored using a Polar A300 (Polar Electro Oy, Kempele, Finland) with an H7 heart rate sensor (Polar Electro Oy, Kempele, Finland).

2.2.6. EEG Recording. Continuous EEG data were recorded with an active electrode system (actiCHamp, BrainProducts, Gilching, Germany) at a sampling rate of 500 Hz. Thirty-two electrodes were placed according to a modified 10–20 system [68] at the positions Fp1, Fp2, F7, F3, Fz, F4, F8, FC5, FC3, FC1, FC2, FC4, FC6, T7, C3, Cz, C4, T8, CP5, CP3, CP1, CP2, CP4, CP6, P7, P3, Pz, P4, P8, O1, Oz, and O2. The ground electrode was placed at position Fpz, and Fz was used as the reference electrode. Participants were instructed to sit comfortably on the chair and relax their facial muscles before EEG measurement started. EEG was recorded during the FM task as well as for 30 seconds immediately before and after all FM sessions on day 2 (i.e., baseline,

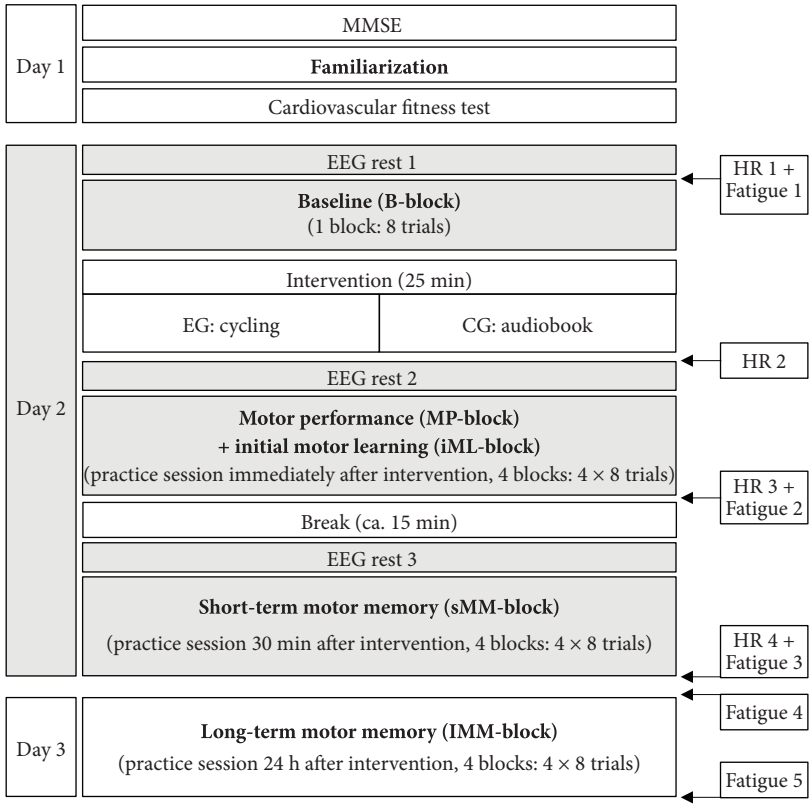

Figure 2: Schematic illustration of the study design. Italic text represents practice time points of the FM task. The grey boxes denote time points of EEG measurement. The white boxes on the right side represent measurement times of heart rate (HR) and subjective fatigue of the participants.

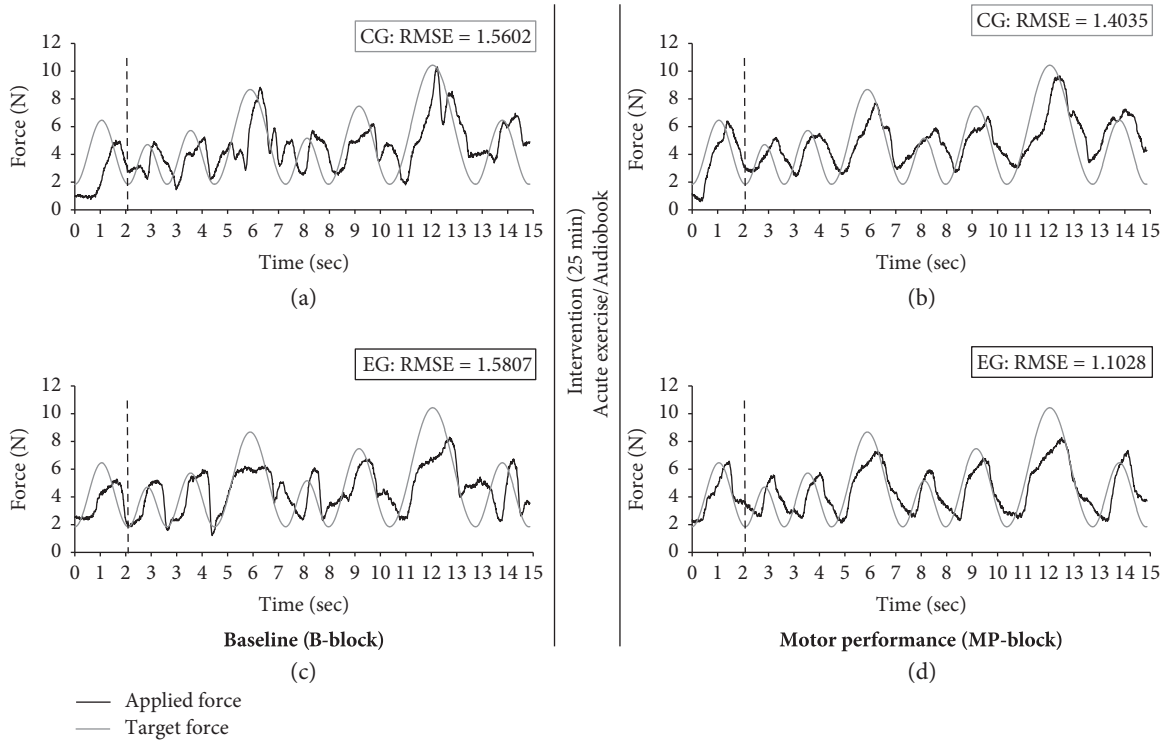

Figure 3: Example FM trials for one participant of each group (CG: a-b; EG: c-d) during *baseline* (*B-block*; a, c) and *motor performance* (*MP-block*; b, d). The grey target curves represent the irregular sine wave pattern. The black lines characterize the force applied by the participants. The black vertical dotted line symbolizes the start of data analyses.

Table 2: Descriptive results and *F*-statistics of heart rate and fatigue values at day 2 for EG and CG.

	EG (n = 17, 9 female)		CG (n = 21, 11 female)		*F*-statistics		
	M	*SD*	*M*	*SD*	$F(1, 36)$	p	η_p^2
HR 1	69.71	10.72	71.14	9.41	0.17	.680	.01
HR 2	99.92	11.20	n.a.	n.a.	—	—	—
HR 3	74.94	11.84	69.63	9.44	1.97	.171	.06
HR 4	69.46	11.65	68.07	7.62	0.17	.677	.01
Fatigue 1	0.66	0.83	0.81	1.03	0.24	.630	.01
Fatigue 2	2.35	1.46	2.18	1.93	0.10	.757	<.01
Fatigue 3	2.47	1.87	2.57	1.57	0.03	.858	<.01
Fatigue 4	0.71	1.21	0.86	0.91	0.19	.663	.01
Fatigue 5	1.25	1.44	1.60	1.57	0.48	.495	.01

Notes. EG = experimental group; CG = control group; HR = heart rate; Fatigue = subjective fatigue of the performing hand (scale from 0 to 10). HR 1 + fatigue 1: before baseline; HR 2: three minutes after acute exercise; HR 3 + fatigue 2: after practice session immediately after intervention; HR 4 + fatigue 3: after practice session 30 minutes after intervention; fatigue 4 + 5: before and after practice session 24 h after intervention.

practice immediately after, and 30 minutes after intervention) to calculate a reference spectrum (EEG rest). During these periods, participants were further instructed to sit calmly on their chair with both hands laying on the table and look at a white fixation cross on a black screen.

2.3. Procedure. Day 1: participants provided a written statement of consent from their physician for the cardiovascular fitness test and signed a declaration of consent for study participation. Then, they performed the MMSE, the FM *MVC*, and *familiarization*, followed by the cardiovascular fitness test. Day 2: the delay between days 1 and 2 was at least 48 hours (to ensure full recovery from the cardiovascular fitness test) and up to 14 days (mean: 5:27 ± 3:19 days). After EEG, caps were mounted and heart rate monitor was placed, participants started with the FM *baseline* measurement. Subsequently, EG performed the 25-minute acute exercise session in an adjoining room. CG stayed on the chair and listened to an audiobook (narrative short story) for 25 minutes. Participants performed the first practice session of the FM task immediately after the intervention (2 to 5 minutes). During the subsequent break (12 to 15 minutes), participants stayed on the chair and talked to one of the investigators. About thirty minutes (27 to 36 minutes) after the end of the intervention, participants performed another practice session. Participant's heart rate was recorded continuously during day 2 (see Figure 2; Table 2). EEG was measured only during day 2. Day 3: 24 hours after the intervention (range: 23.5 to 24.5 hours after the beginning of the first FM practice session on day 2) participants performed the last FM practice session. The order of testing days did not vary between participants. Fatigue of the performing right hand was controlled on a scale from zero (not at all fatigued) to ten (totally fatigued, see Table 2) at different time points on day 2 and day 3 (see Figure 2).

2.4. Data Analysis

2.4.1. FM Task Performance. Data analysis of the FM task was processed in Matlab R2015b software (the MathWorks, Inc., Natick, Massachusetts, US). The first 211 data points (approximately 1.75 seconds, representing the first sine wave of every trial) were excluded from analysis to avoid variation due to differences in ramp time (cf. dotted vertical lines in Figure 3). Fine motor control performance was quantified using the root mean square error (RMSE) as a difference of the target and applied force. A mean of eight trials was calculated for *baseline* (= *B-block*), *motor performance* (= *MP-block*, i.e., first block of the practice session immediately after intervention), *initial motor learning* (= *iML-block*, i.e., block four of the practice session immediately after intervention), *short-term motor memory* (= *sMM-block*, i.e., first block of the practice session 30 minutes after intervention) and *long-term motor memory* (= *lMM-block*, i.e., first block of the practice session 24 hours after intervention). Outliers were presumed per trial across all participants as standardized z-scores greater than 3.29 or below −3.29 per trial (n = 11, in 7 different participants) and were replaced according to the last observation carried forward method [69].

2.4.2. EEG Data. When not stated differently, the following preprocessing steps were performed identically for data from EEG rest and EEG during FM task. Offline EEG data processing was accomplished with the Brain Vision Analyzer software (Version 2.1, Brain Products GmbH, Gilching, Germany). A phase shift-free Butterworth infinite impulse response (IIR) filter was applied with a low cutoff at 1 Hz and a high cutoff at 70 Hz, with a slope of 48 db/Oct as well as a notch filter at 50 Hz to reduce line noise. Subsequently, a raw data inspection (criteria: gradient with a maximally allowed voltage step of 25 μV, lowest allowed activity of 0.5 μV) was performed. The electrode C4 revealed continuous artefacts for one participant. Accordingly, this channel was recalculated with a topographic interpolation for all measurement time points. To remove ocular artifacts, a semiautomatic ocular correction was conducted using an extended infomax independent component analysis (ICA), with the Fp1 electrode above the left eye detecting both vertical and horizontal ocular movements. Visual inspection confirmed that horizontal eye movements were detected and could be

removed. Continuous EEG data during FM task were cut into segments from the beginning of the first trial of the force-tracking task to the end of the last trial of each session on day 2. Intertrial breaks and the first 1.75 seconds (corresponding to the curve of each trial, see Data Analysis FM task) were removed from the continuous EEG data during the task. All data during EEG rest were cut into 20-second segments (second 5 to 25 used for analysis). Continuous data were further separated into epochs of two seconds (overlapping segments of 150 ms), resulting in 7 epochs per FM trial and 10 epochs per EEG rest. Bad segments with obvious remaining artefacts were excluded based on visual inspection. In two participants, electrode CP3 and CP4 had to be excluded from further analyses for *EEG rest* 3, in one participant electrode CP4 had to be excluded for *EEG rest 1*.

After preprocessing, a fast Fourier transform (FFT) algorithm was applied (output was set to power measured in μV^2) using full spectrum and a Hanning window of 10% for each trial or each EEG rest, separately. Power spectra for the beta band (13–30 Hz) were calculated for six electrodes of interest, which are presumed to overlie the left (C3) and right (C4) M1, left (CP3) and right (CP4) S1, and the left (F3) and right (F4) frontal cortex. As operating the precision grip during the FM task required considerable activations of motor areas in both hemispheres [34, 36], power was calculated bilaterally. Power spectra were also calculated for each trial during FM task/EEG rest and each electrode separately. Subsequently, a mean power value for eight segments (corresponding to eight trials of the FM task, i.e., baseline/one block of practice) per electrode was calculated. Then, mean power values were log-transformed [42]. Finally, log-transformed task-related power ($TR(logPow_x)$) was calculated by subtracting log-transformed beta power during EEG rest (*EEG rest 1*, *2*, and *3*, see Figure 2) from log-transformed beta power during FM task for each electrode separately: $TR(logPow_x) = log\ power\ task_x – log\ power\ rest_x$ [42, 70], abbreviated TRPow in the following. For *B-block*, *EEG rest 1* was subtracted from the mean power value of *B-block*. For *MP-block*, *EEG rest 2* was subtracted from the mean power value of the first block directly after intervention. For *iML-block*, *EEG rest 2* from the mean power value of the fourth block directly after intervention. For *sMM*-block, *EEG rest 3* was subtracted from the mean power value of the first block 30 minutes after intervention (see Figure 2).

2.5. Statistical Analysis. All statistical analyses were conducted using SPSS for Windows, version 25 (IBM Corp., Armonk, NY, USA). If not stated differently, p values $< .05$ were regarded as significant, and p values $< .10$ as marginally significant (trend). The nominal alpha level was adjusted for particular analyses using Bonferroni adjustment $(\alpha = 1 - (1 - \alpha)^{1/m})$; m = number of analyses/comparisons to control for multiple testing. Greenhouse-Geisser adjustment was reported in case the sphericity assumption was violated. Effect sizes were reported as partial eta squares (η_p^2). Demographic information (age, education, subjective health, and subjective hand usage), cognitive status (MMSE), MVC, cardiovascular fitness level (VO_2-peak), and heart rate during day 2 were compared using analysis of variance (ANOVA) to assess any differences between EG and CG which may have affected motor performance (cf. Table 1).

2.5.1. FM Task Performance. First, we performed a repeated measures analysis of variance (RM-ANOVA) with TIME (*B-block*, *MP-block*, *iML-block*, *sMM-block*, *lMM-block*) as within-subject factor and 2 GROUP (EG, CG) as between-subject factor to calculate the influence of the intervention (acute exercise or control condition) on FM performance and learning (Analysis 1). This was followed by three analyses to answer our a priori determined research questions, regardless whether the main effects of Analysis 1 were significant. A 2 TIME (*B-block*, *MP-block*) × 2 GROUP (EG, CG) RM-ANOVA (Analysis 1.1) was performed to investigate the influence of the acute exercise session on *MP-block* in the FM task. To examine the influence of acute exercise on *iML-block*, a 2 TIME (*B-block*, *iML-block*) × 2 GROUP (EG, CG) RM-ANOVA (Analysis 1.2) was conducted. Additionally, a 3 TIME (*iML-block*, *sMM-block*, *lMM-block*) × 2 GROUP (EG, CG) RM-ANOVA was performed to assess whether acute bouts of exercise facilitate *sMM-* and *lMM-block* (Analysis 1.3). The nominal alpha level was adjusted for Analyses 1.1–1.3 as well as for the post hoc *t*-tests of Analysis 1.3 using Bonferroni adjustment.

2.5.2. EEG Data. A 4 TIME (*B-block*, *MP-block*, *iML-block*, *sMM-block*) × 2 HEMISPHERE (contralateral, ipsilateral) × 3 REGION (frontal, central, centro-parietal) × 2 GROUP (EG, CG) RM-ANOVA was calculated for TRPow (Analysis 2). Again, to answer a priori determined research questions and in correspondence to the behavioral FM task data, three further analyses were performed per electrode of interest. 2 TIME (*B-block*, *MP-block*) (Analysis 2.1) as well as 2 TIME (*B-block*, *iML-block*) × 2 GROUP (EG, CG) (Analysis 2.2) RM-ANOVAs for TRPow were calculated. Due to technical problems during *EEG rest 1* and *B-block* with the EEG, Analysis 2, 2.1, and 2.2 were conducted with $n = 18$ participants (instead of $n = 21$) for CG. As EEG was not assessed 24 hours after intervention, the last EEG analyses consisted of 2 TIME (*iML-block*, *sMM-block*) × 2 GROUP (EG, CG) RM-ANOVAs (Analysis 2.3).

Identical analyses were performed for *EEG rest 1*, *2*, and *3* to test whether acute exercise influenced beta power at rest: we conducted a 3 TIME (*EEG rest 1*, *EEG rest 2*, *EEG rest 3*) × 2 HEMISPHERE (contralateral, ipsilateral) × 3 REGION (frontal, central, centro-parietal) × 2 GROUP (EG, CG) RM-ANOVA (Analysis 3), followed by a 2 TIME (*EEG rest 1*, *EEG rest 2*) × 2 GROUP (EG, CG) (Analysis 3.1) as well as a 2 TIME (*EEG rest 2, EEG rest 3*) × 2 GROUP (EG, CG) (Analysis 3.3 RM-ANOVA. Note: *EEG rest 2* was used to calculate TRPow of *MP-block* as well as *iML-block*. For EEG at rest only a priori defined follow-up analyses per electrode were calculated. Again, the nominal alpha level was adjusted for Analyses 2.1-2.3, 3.1, and 3.3 as well as post hoc *t*-tests for Analysis 2 and 3 using Bonferroni adjustment to control for multiple testing.

FM and EEG analyses were controlled for a possible influence of participant age (see Table 1, marginal significant

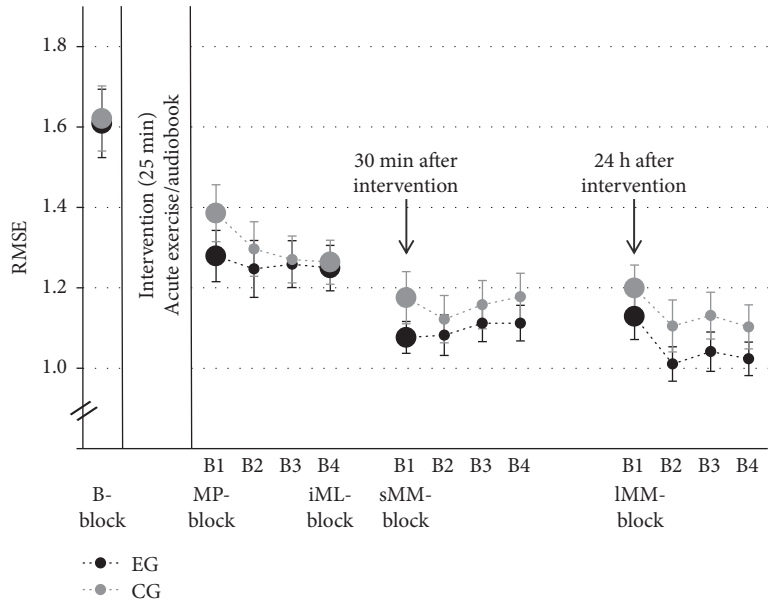

Figure 4: Means and SE of the FM task per group. Large circles indicate measurement time point included in statistical analysis: *B-block = baseline*, *MP-block = motor performance*, *iML-block = initial motor learning*, *sMM-block = short-term motor memory*, and *lMM-block = long-term motor memory*. Small circles indicate time points of practice blocks (B2-B4 = Block 2–4).

effect of age: $p = .074$). Age had no significant influence on FM or EEG statistics. Therefore, results were reported without the covariate age.

2.5.3. Association between Behavioral Performance, EEG Data, and Load during Exercise. Subsequently, Pearson's correlation between FM performance (RMSE) and TRPow in analyses with significant TIME × GROUP interactions was performed to examine the association between behavioral performance and electrophysiological data. Moreover, Pearson's correlation between the Watt values performed during acute exercise and FM performance (RMSE) and TRPow were conducted to explore a possible association of exercise intensity and behavioral or electrophysiological data. Correlation analyses were controlled for multiple testing (Bonferroni adjustment).

3. Results

3.1. FM Task Performance. Figure 4 displays group means and standard errors (SE) of the FM task. Performance of EG and CG was similar at preintervention, differed immediately after intervention, and converged after the initial learning phase and motor memory consolidation. Analysis 1 confirmed a significant improvement for both groups from *B-block* to *lMM-block* (main effect of TIME: $F(4, 36) = 73.99$, $p < .001$, $\eta_p^2 = .67$), but no TIME × GROUP interaction ($F(4, 36) = 1.00$, $p = .388$, $\eta_p^2 = .03$) and no main effect of GROUP ($F(1, 36) = 0.52$, $p = .475$, $\eta_p^2 = .01$). Based on our a priori hypotheses, we further detail the results from three different analyses.

3.1.1. Analysis 1.1. Effect of acute exercise on FM *motor performance (MP-block;* adjusted $\alpha = .017$; see Table 3(a)).

Table 3: *F*-statistics for (a) Analysis 1.1, (b) Analysis 1.2, and (c) Analysis 1.3 for FM task performance (adjusted $\alpha = .017$).

Analysis	*F*-statistics			
	F	*df*	*p*	η_p^2
(a) 1.1				
TIME	175.94	1	**<.001**	.83
GROUP	0.31	1	.579	.01
TIME × GROUP	4.91	1	.033	.12
(b) 1.2				
TIME	101.43	1	**<.001**	.74
GROUP	0.20	1	.888	<.01
TIME × GROUP	<0.01	1	.975	<.01
(c) 1.3				
TIME	12.62	2	**<.001**	.26
GROUP	0.67	1	.420	.02
TIME × GROUP	1.28	2	.284	.03

Performance of EG and CG was similar at *B-block* (preintervention) and improved in the first block of practice immediately after intervention (acute exercise or control condition: listening to an audiobook), with a more pronounced improvement in EG than CG. Figure 3 displays representative grip force profiles of one participant from CG and one from EG, and illustrates the different development from pre- to postintervention. More specifically, Figure 5 indicates that both groups improved similarly at *B-block*, but that EG learned more than CG at *MP-block*. We confirmed the development of CG and EG by a RM-ANOVA revealing a main effect of TIME on RMSE. TIME × GROUP interaction remained marginally significant after adjusting α level. A post

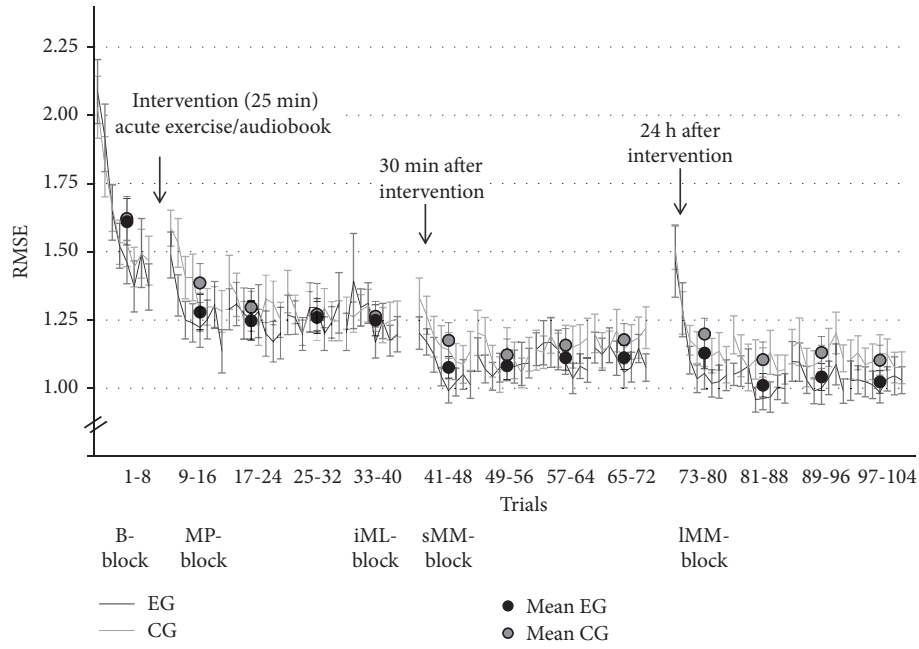

Figure 5: Mean and SE for all FM trials for EG and CG. The black (EG) and gray (CG) circles represent the means per block.

hoc *t*-test further affirmed that EG and CG did not differ pre-intervention (*B-block:* $F(1, 36) = 0.01$, $p = .918$, $\eta_p^2 = .01$).

3.1.2. Analysis 1.2. Effect of acute exercise on FM *initial motor learning* (*iML-block*; adjusted $\alpha = .017$; see Table 3(b)). Exercise did not seem to foster motor learning during the first practice session after intervention, as FM performance in EG and CG improved similarly (see Figure 4). Analysis 1.2, comparing performance in *B-block* and performance in the last block of the first practice session (*iML-block*), resulted in a significant main effect of TIME, but no GROUP or TIME × GROUP interaction effect.

3.1.3. Analysis 1.3. Effect of acute exercise on FM *motor memory* (*sMM-* & *lMM-block*; adjusted $\alpha = .017$; see Table 3(c)). Motor memory was assessed 30 minutes (*sMM-block*) and 24 hours (*lMM-block*) after this initial phase of motor learning. Both groups revealed better *sMM-block* and *lMM-block* performance when compared to *iML-block* performance (main effect of TIME). Although TIME × GROUP interaction was not significant, we performed priori defined post hoc tests to specifically investigate the influence of exercise on short- and long-term motor memory consolidation. Post hoc *t*-tests between *iML-block*, *sMM-block*, and *lMM-block* per group (EG, CG) indicated that acute exercise significantly enhanced performance in *sMM-block* ($p < .001$) and in tendency in *lMM-block* ($p = .027$) compared to *iML-block*, whereas CG only revealed a tendency toward improvement in the *sMM-block* ($p = .057$), and no change in performance in the *lMM-block* ($p = .321$).

3.2. EEG Data. Figure 6 shows TRPow group means and SE for different measurement time points (see Table 4 for all descriptive values for EEG beta power at rest and TRPow for EG and CG).

For the contralateral electrodes (F3, C3, CP3), TRPow of EG and CG was similar at *B-block*, different immediately after exercise, and coincided again after the initial learning phase. EG and CG did not differ for the ipsilateral electrodes (F4, C4, CP4).

3.2.1. Analysis 2. Effect of acute exercise on TRPow. RM-ANOVA confirmed a significant effect of TIME (see Table 5(a) for all statistical results). As compared to *B-block*, the TRPow decrease was stronger in *MP-Block* directly after the intervention, weaker in *iML-block*, and even stronger during *sMM-block* (both compared to *MP-block*). A significant main effect of REGION revealed that TRPow decreases were stronger at centro-parietal and central than at frontal electrodes (centro-parietal/central vs. frontal: both $p < .001$, centro-parietal vs. central: $p = .156$). Furthermore, a significant TIME × HEMISPHERE interaction indicated that contralateral electrodes developed differently over time than ipsilateral electrodes. More specifically, TRPow decreases at contralateral compared to ipsilateral electrodes were weaker at *B-block* ($F(1, 33) = 5.97$, $p = .020$, $\eta_p^2 = .15$), and stronger at *MP-block* ($F(1, 33) = 9.16$, $p = .005$, $\eta_p^2 = .22$). A significant TIME × HEMISPHERE × GROUP interaction further indicated that the TIME × HEMISPHERE interaction stemmed mainly from regional differences in the EG group: TRPow decreases of contralateral compared to ipsilateral electrodes were weaker at *B-block* ($F(1, 33) = 16.70$, $p < .001$, $\eta_p^2 = .34$) and stronger at *MP-block* and *iML-block* ($F(1, 33) = 12.08$, $p = .001$, $\eta_p^2 = .27$; $F(1, 33) = 16.21$, $p < .001$, $\eta_p^2 = .33$, respectively). In contrast, post hoc *t*-tests did not reveal any significant difference in CG between contra- and ipsilateral

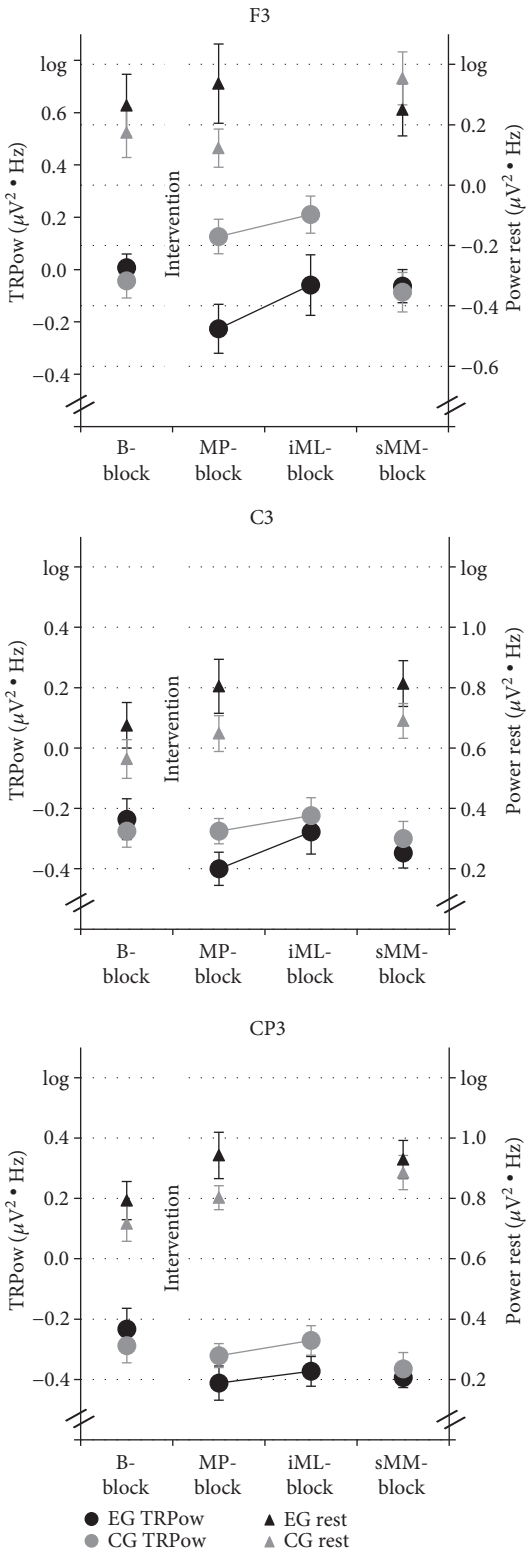

Figure 6: Means and SE of EEG TRPow (left *y*-axis) and EEG at rest (right *y*-axis) values in beta frequency band of the contralateral electrodes F3, C3, and CP3. Four measurement time points were included in the statistical analysis for TRPow (circles): *B-block* = *baseline, motor performance (MP-block) iML-block* = *initial motor learning*, *sMM-block* = *short-term motor memory*, and three for EEG at rest (triangles): *EEG rest 1*, *2*, and *3*.

electrodes at any time point (all $p > .440$). Finally, the TIME × GROUP interaction was marginally significant, indicating that the TRPow values of EG and CG tended to develop differently over the experiment.

3.2.2. Analysis 3. Effect of acute exercise on EEG at rest (see Table 5(b)). The overarching analysis for EEG at rest revealed a significant TIME × HEMISPHERE × REGION × GROUP interaction. Generally, beta power increased from *EEG rest 1* to *EEG rest 3* and from frontal over central to centroparietal electrodes but differed with regard to electrode and hemisphere. Important to note, the follow-up TIME × GROUP interaction was not significant.

In line with our a priori hypotheses, EEG results were further analyzed using three distinct analyses.

3.2.3. Analysis 2.1. Effect of acute exercise on TRPow during FM *MP-block* (adjusted $\alpha = .017$, see Table 6(a)). Figure 7 illustrates group means of the power frequency spectra for EEG rest and during FM task separately for EG and CG for electrode F3 and F4. For electrode F3, EG and CG started at a similar beta power level during FM task (*B-block*), whereas EG revealed a tendency for more beta power at *EEG rest* (see also Figure 6, F3). After exercise during *MP-block*, beta power for EG was higher at EEG rest and lower during FM task compared to the *B-block*, reflecting a stronger TRPow decrease during *MP-block* than during *B-block* (see Figure 7 upper row). In contrast, participants in CG revealed a TRPow increase during *MP-block* (see Figure 7 upper row). This pattern was affirmed when comparing group means (Table 6(a): significant TIME × GROUP interaction) and calculating corresponding post hoc *t*-tests (EG: stronger TRPow decreases immediately after exercise ($F(1, 33) = 12.53$, $p = .001$, $\eta_p^2 = .28$); CG: marginally significant change from a small TRPow decrease to a TRPow increase immediately after intervention ($F(1, 33) = 4.08$, $p = .051$, $\eta_p^2 = .11$). In contrast, such a group difference was not visible for electrode F4 (see Figure 7). Accordingly, statistical analyses confirmed no significant TIME × GROUP interaction for TRPow.

Furthermore, the main effects of TIME were significant for electrode CP3 and C4. For CP3, TRPow decreases became stronger from *B-block* to *MP-block*; TRPow decreases for C4 became weaker from *B-block* to *MP-block*.

3.2.4. Analysis 2.2. Effect of acute exercise on TRPow during FM *iML-block* (adjusted $\alpha = .017$; see Table 6(b)). TRPow decreases of contralateral electrodes at the end of the first practice session were mainly affected by the intervention (see Figure 6; significant TIME × GROUP interactions for contralateral F3 and marginally significant for CP3). Post hoc comparison for electrode F3 showed that TRPow decreases were significantly weaker during *iML-block* than during *B-block* in CG ($F(1, 33) = 9.67$, $p = .004$, $\eta_p^2 = .23$), whereas EG did not change significantly ($F(1, 33) = 0.67$, $p = .418$, $\eta_p^2 = .02$). In contrast, for electrode CP3, TRPow decreases became significantly stronger in EG ($F(1, 33) = 7.98$, $p = .008$, $\eta_p^2 = .20$), whereas CG did not change ($F(1, 33) = 0.04$, $p = .841$, $\eta_p^2 < .01$). As for *MP-block*, C4

Table 4: Descriptive results for EEG beta power at rest and TRPow for EG and CG.

	EEG rest			EEG TRPow			
	1	*2*	*3*	*B-block*	*MP-block*	*iML-block*	*sMM-block*
				F3			
EG	.26 ± .10	.34 ± .13	.25 ± .09	.01 ± .05	−.23 ± .09	−.06 ± .12	−.06 ± .06
CG	.17 ± .08	.12 ± .06	.35 ± .09	−.04 ± .07	.13 ± .07	.21 ± .07	−.09 ± .08
				C3			
EG	.67 ± .08	.08 ± .09	.81 ± .08	−.24 ± .07	−.40 ± .06	−.28 ± .07	−.35 ± .05
CG	.56 ± .06	.65 ± .06	.69 ± .06	−.28 ± .05	−.28 ± .04	−.22 ± .06	−.30 ± .06
				CP3			
EG	.79 ± .06	.94 ± .08	.93 ± .06	−.23 ± .07	−.41 ± .06	−.37 ± .05	−.39 ± .03
CG	.72 ± .06	.80 ± .04	.89 ± .06	−.29 ± .06	−.32 ± .04	−.27 ± .05	−.36 ± .05
				F4			
EG	.13 ± .09	.13 ± .10	.26 ± .09	.10 ± .06	−.01 ± .08	.19 ± .11	−.13 ± .07
CG	.28 ± .09	.31 ± 07	.40 ± .07	.01 ± .06	.02 ± .06	.11 ± .06	−.11 ± .06
				C4			
EG	.71 ± 09	.75 ± .09	.82 ± .08	−.57 ± .08	−.35 ± .06	−.26 ± .06	−.39 ± .06
CG	.53 ± .06	.66 ± .06	.70 ± 05	−.50 ± .04	−.24 ± .07	−.21 ± .06	−.30 ± .06
				CP4			
EG	.83 ± .08	.86 ± 07	.90 ± .07	−.19 ± .08	−.23 ± .06	−.21 ± .06	−.23 ± .06
CG	.67 ± .06	.81 ± .05	.85 ± .05	−.11 ± .04	−.21 ± .05	−.15 ± .05	−.24 ± .05

Note. Mean ± SEM; EG = experimental group; CG = control group; B-block = baseline; MP-block = motor performance; iML-block = initial motor learning; sMM-block = short-term motor memory.

revealed a TIME effect only, showing more TRPow decreases in EG and CG during *iML-block* after exercise compared to *B-block* in ipsilateral sensorimotor cortex.

3.2.5. Analysis 2.3. Effect of acute exercise on TRPow during FM *sMM-block* (adjusted $\alpha = .017$; see Table 6(c)). Thirty minutes after the intervention, TRPow values in EG and CG converged again, similar to *B-block* (see Figure 6). RM-ANOVAs comparing TRPow at *iML-block* and *sMM-block* confirmed a significant effect of TIME and TIME × GROUP interaction for electrode F3 (remained significant after adjusting alpha to $\alpha = .017$). TRPow during *sMM-block* in CG was accompanied by stronger TRPow decreases in the contralateral frontal cortex compared to *iML-block* ($F(1, 36) = 15.98$, $p < .001$, $\eta_p^2 = .31$), whereas TRPow for EG remained stable ($F(1, 36) < 0.01$, $p = .960$, $\eta_p^2 < .01$). Again, for C4, we found a main effect of TIME, showing that TRPow decreases became stronger for both groups from *iML-block* to *sMM-block*.

3.2.6. Analysis 3.1. Effect of acute exercise on *EEG rest 2* (adjusted $\alpha = .025$; see Table 7(a)). Although EG revealed a trend for more beta power at electrode F3 for *EEG rest 1* (as noted above) and *rest 2* (see Figures 6 and 7), the main effect of GROUP and TIME × GROUP interaction were not significant. The main effect of TIME was significant for electrode CP3 and marginally significant for C3, indicating a general increase of beta power from *EEG rest 1* to *EEG rest 2*.

3.2.7. Analysis 3.3. Effect of acute exercise on *EEG rest 3* (adjusted $\alpha = .025$; see Table 7(b)). Beta power increased from *EEG rest 2* to *rest 3* at electrode F4 (TIME effect). For F3, the TIME × GROUP interaction was significant. Beta power increased for CG from *EEG rest 2* to *rest 3* ($F(1, 33) = 7.33$, $p = .010$, $\eta_p^2 = .17$) but remained stable for the EG ($F(1, 33) = 0.84$, $p = .366$, $\eta_p^2 = .02$).

3.3. Association between Motor Behavior, EEG Data, and Load during Exercise. A marginally significant correlation between FM task performance (RMSE) and EEG data (TRPow) was revealed for EG during *sMM-block* at electrode C4 ($r = -.443$, $p = .075$), pointing to a better FM performance with reduced TRPow decrease. However, after controlling for multiple testing, none of the correlation analyses reached statistical significance.

Correlation analyses between the Watt values performed during acute exercise and FM task performance (RMSE) indicated a marginally significant correlation ($r = -.426$, $p = .088$) for *lMM-block*: better FM performance 24 hours after exercise was associated with increasing Watt values (see Table 8 and Figure 8). After controlling for multiple testing, no correlation between Watt values performed during acute exercise and EEG TRPow revealed a significant association (see Table 9).

4. Discussion

This study examined the effect of an acute exercise session on (1) behavioral performance and learning in a precision grip force modulation (FM) task as well as on (2) the electrophysiological correlates of FM task performance and learning in healthy older adults. First, results revealed a marginally significant trend indicating that, as compared

Table 5: *F*-statistics of (a) Analysis 2 (TRPow) and (b) Analysis 3 (EEG rest).

	F-statistics			
	F	*df*	*p*	η_p^2
(a) Analysis 2: TRPow				
TIME	5.03	3	**.009**	.13
HEMISPHERE	2.63	1	.114	.07
REGION	37.85	2	**<.001**	.53
GROUP	3.36	1	.076	.09
TIME × HEMISPHERE	4.65	3	**.017**	.12
TIME × REGION	2.03	6	.102	.06
TIME × GROUP	2.65	3	0.76	.07
HEMISPHERE × REGION	1.42	2	.250	.04
HEMISPHERE × GROUP	0.01	1	.920	<.01
REGION × GROUP	2.15	2	.131	.06
TIME × HEMISPHERE × GROUP	5.81	3	**.007**	.15
TIME × REGION × GROUP	0.76	6	.539	.02
TIME × HEMISPHERE × REGION	1.14	6	.343	.03
HEMISPHERE × REGION × GROUP	1.82	2	.169	.05
TIME × HEMISPHERE × REGION × GROUP	0.58	6	.669	.02
(b) Analysis 3: EEG rest				
TIME	7.07	2	**.002**	.18
HEMISPHERE	0.19	1	.665	.01
REGION	136.45	2	**<.001**	.81
GROUP	0.83	1	.370	.02
TIME × HEMISPHERE	0.48	2	.623	.01
TIME × REGION	1.13	4	.344	.03
TIME × GROUP	0.76	2	.460	.02
HEMISPHERE × REGION	0.52	2	.594	.02
HEMISPHERE × GROUP	6.18	1	**.018**	.16
REGION × GROUP	2.65	2	.098	.07
TIME × HEMISPHERE × GROUP	3.42	2	**.041**	.09
TIME × REGION × GROUP	0.70	4	.504	.02
TIME × HEMISPHERE × REGION	0.68	4	.535	.02
HEMISPHERE × REGION × GROUP	6.21	2	**.009**	.16
TIME × HEMISPHERE × REGION × GROUP	2.95	4	**.049**	.08

to *baseline*, participants of the experimental group (EG) improved their *motor performance* in the FM task immediately after exercise more than the control group (CG) after rest. Secondly, EG had steeper beta TRPow decreases (i.e., higher activity) than CG directly after exercise (measurement time point *motor performance*) at the contralateral frontal electrode, probably indicating that acute exercise facilitated motor compensation processes in the aged brain.

4.1. Effect of Acute Exercise on Motor Behavior. Although over the whole experiment both groups improved their performance with practice, our analyses revealed that acute exercise significantly influenced FM performance at particular time points.

4.1.1. Motor Performance. In a sample of older adults, acute exercise facilitated *motor performance* in the FM task immediately after exercise in tendency more than a control condition. Similarly, Mierau et al. [71] reported more performance improvement in a motor adaptation paradigm immediately after exercise than after rest in young adults. The underlying mechanisms of superior motor performance immediately after exercise remain unknown. Findings from cognitive research revealed improved information processing indicated by electrophysiological markers (shorter latencies and larger amplitudes of the P3) immediately after exercise in older adults [29]. Skriver et al. [14] revealed that enhanced motor performance correlated with enhanced norepinephrine release and higher lactate level immediately after exercise in young adults. Furthermore, enhanced cerebral blood flow

Table 6: *F*-statistics of (a) Analysis 2.1, (b) Analysis 2.2, and (c) Analysis 2.3 for EEG TRPow (adjusted $\alpha = .017$).

	TIME				GROUP				TIME × GROUP			
	F	*df*	*p*	η_p^2	*F*	*df*	*p*	η_p^2	*F*	*df*	*p*	η_p^2
(a) Analysis 2.1												
F3	1.28	1	.266	.04	2.24	1	.144	.06	15.58	1	**<.001**	.32
C3	4.12	1	.051	.11	0.32	1	.577	.01	3.23	1	.081	.09
CP3	8.18	1	**.007**	.20	0.50	1	.825	<.01	3.59	1	.067	.10
F4	2.86	1	.100	.08	0.28	1	.603	.01	1.17	1	.287	.03
C4	28.75	1	**<.001**	.47	1.43	1	.240	.10	0.42	1	.524	.01
CP4	1.94	1	.173	.06	0.91	1	.348	.03	0.19	1	.670	.01
(b) Analysis 2.2												
F3	2.49	1	.124	.07	1.12	1	.297	.03	7.59	1	**.009**	.19
C3	<0.01	1	.995	<.01	<0.01	1	.971	<.01	1.01	1	.322	.03
CP3	3.55	1	.068	.10	0.07	1	.795	<.01	4.69	1	.038	.12
F4	1.73	1	.197	.05	1.24	1	.273	.04	0.07	1	.799	<.01
C4	71.83	1	**<.001**	.69	0.52	1	.476	.02	0.07	1	.799	<.01
CP4	0.04	1	.844	<.01	1.50	1	.229	.04	<0.01	1	.951	<.01
(c) Analysis 2.3												
F3	7.35	1	**.010**	.04	1.43	1	.240	.04	6.95	1	**.012**	.16
C3	2.83	1	.101	.07	0.49	1	.487	.01	0.01	1	.943	<.01
CP3	3.09	1	.087	.08	0.10	1	.753	<.01	1.27	1	.267	.03
F4	29.25	1	**<.001**	.45	0.15	1	.700	<.01	1.00	1	.336	.03
C4	9.36	1	**.004**	.21	0.68	1	.414	.02	0.36	1	.555	.01
CP4	2.42	1	.129	.06	0.08	1	.783	<.01	1.05	1	.312	.03

in the M1 during a finger tapping task [72] as well as an increase in the resting-state connectivity of the sensorimotor areas [73] in young adults immediately after exercise indicated better preconditions for motor task execution (see also Section 4.2).

4.1.2. Initial Motor Learning. As especially, the initial phase of learning requires a high amount of cognitive resources [33], and acute exercise was found to improve cognitive performance in older adults [27–29], we examined whether acute exercise impacts this very early stage of learning. However, there was no superior effect of acute exercise on *initial motor learning* compared to a resting control condition in older adults. Thus, the positive influence of acute exercise on *motor performance* disappeared until the end of the practice session, revealing that the superiority of EG immediately after exercise was compensated by a higher performance gain of CG within the first FM practice session. We can only speculate about the underlying mechanism. One explanation might be that exercise itself already brought EG closer to their limits, whereas participants in CG made use of their capacity to improve during the practice session.

4.1.3. Motor Memory Consolidation. There is a consensus that older adults, in general, reveal diminished long-term motor consolidation processes [4–7]. It was hypothesized that acute exercise could be a proper intervention to facilitate consolidation processes in older adults, because effects of acute exercise on *long-term motor memory* consolidation, but not *short-term motor memory* consolidation, have been shown in young adults [12, 14, 17]. However, such a positive effect of acute exercise could neither be confirmed on *short-term* nor *long-term motor memory* consolidation in our group of older adults. This seems to be in line with studies examining the effect of acute exercise on (not motor related) short- and long-term memory, exposing higher effects for young than for older adults [74]. Interestingly, the a priori post hoc tests revealed enhanced consolidation of *short-term* and *long-term motor memory* for EG after exercise, but only a tendency toward improvement of *short-term motor memory* for CG after rest. Thus, based on our results we cannot exclude that an acute exercise session might be a possible intervention to enhance motor consolidation in a FM task in older adults.

4.2. Effect of Acute Exercise on Electrophysiological Data. In addition to the FM data, the electrophysiological correlates of FM task performance were investigated. To this aim, beta TRPow decreases in electrodes supposed to lie over the frontal cortex, M1, and S1 were calculated as indicators of task-related cortical activation of the corresponding brain areas [41, 42].

In general, beta power at rest was highest over centro-parietal and lowest over frontal electrodes. Consistent with other studies [49, 75], also TRPow decreases were stronger at centro-parietal and central than at frontal electrodes. Although the exact origin of beta oscillations is unknown, the latter finding indicates a strong sensorimotor cortical activation during the motor task [76]. A trend for a TIME × GROUP interaction revealed that TRPow of EG

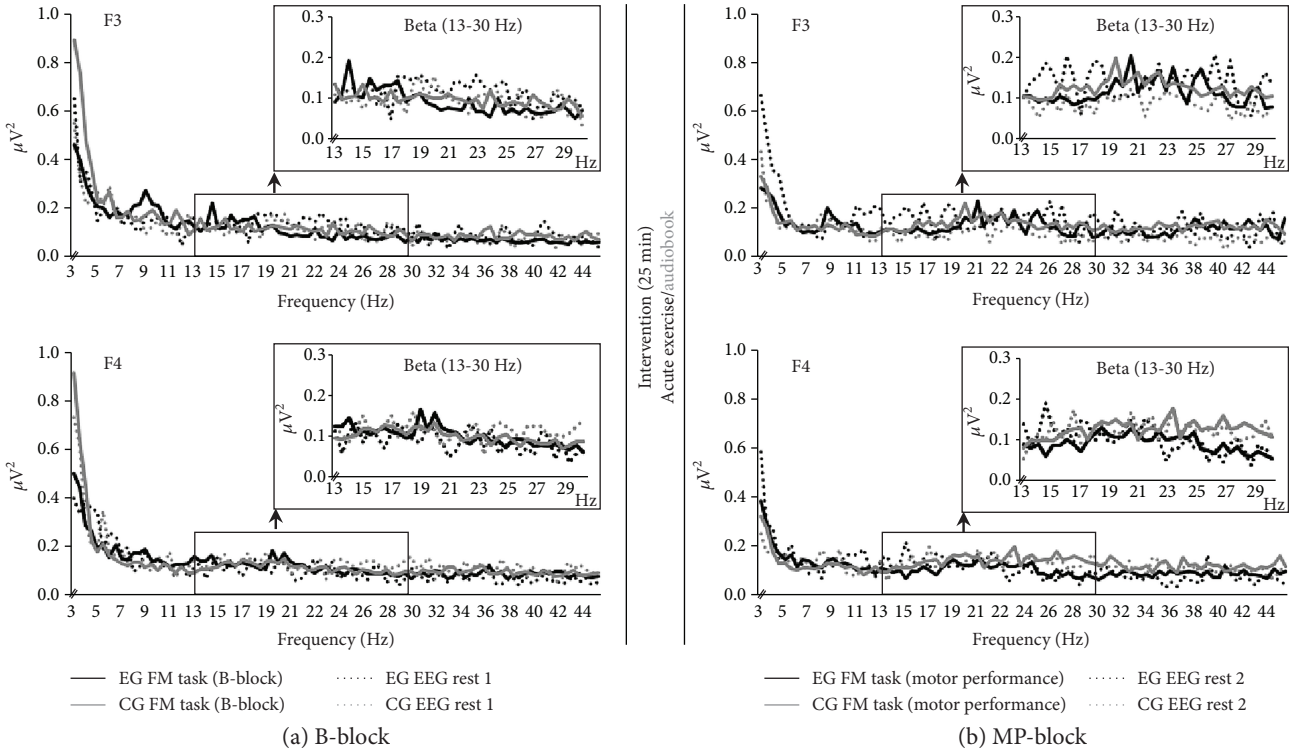

Figure 7: Means of the frequency (3–45 Hz) for EG (black line) and CG (grey line) for electrodes F3 (upper row) and F4 (lower row). The solid lines indicate data during FM task; dotted lines represent data at EEG rest. Data from FM trials during *baseline* (*B-block*) (a), *motor performance* (*MP-block*) (b), and *EEG rest 1* before intervention (a) and *EEG rest 2* after intervention (b) are illustrated. Inlets reveal the enlarged view of analyzed frequency band (beta: 13–30 Hz).

and CG tended to develop differently throughout the experiment. For specific electrodes and time points, this was confirmed by our a priori defined analyses as discussed in the following.

4.2.1. Motor Performance. The acute exercise session caused stronger TRPow decreases at electrode F3 (but not C3 or CP3), and therefore, higher activation of the contralateral frontal cortex during the FM practice session immediately after acute exercise. It has been shown that older as compared to young adults need to activate more frontal brain resources to successfully perform a motor task [50]. One prominent theory claims that this additional activation reflects compensation processes associated with maintained or enhanced motor performance [77]. Therefore, the increased contralateral frontal activity might indicate that acute exercise enables healthy older adults to better utilize existing frontal brain capacities during the FM task immediately after exercise. Our findings are also supported by functional near-infrared spectroscopy (fNIRS) studies, in which acute exercise as compared to rest led to compensatory frontal brain activity during the performance of a subsequent cognitive task in older adults [78, 79].

4.2.2. Initial Motor Learning. It has been shown that practicing visuomotor force-matching tasks in general leads to an attenuation of beta TRPow decreases in frontal and sensorimotor cortical areas in young adults, interpreted as that task execution became less demanding due to increased automaticity [46, 48]. In line with these results, the CG in our study also revealed less contralateral frontal activation (less TRPow decrease) at the end of the first FM practice session compared to baseline. Interestingly, the contralateral frontal activity of the EG also decreased again in the course of the initial learning bock (after an initial increase of activity immediately after exercise, cf. 4.2.1), resulting in a nonsignificant effect from *baseline* to *initial motor learning*. As the cognitive load during the performance of a motor task decreases with practice [33], it might be that the initial strong compensatory contralateral frontal activity of the EG was not needed anymore to perform the FM task with ongoing practice. Furthermore, results indicate that acute exercise facilitated contralateral frontal beta activity directly after exercise but had no further effect on frontal beta activity during the learning course (similar to the behavioral FM data). In line with this finding, acute exercise led to a positive effect on cognitive performance only immediately after exercise in older adults, but not after a certain time delay [27].

4.2.3. Motor Memory Consolidation. From the last block of the first FM practice session after intervention (i.e., *initial motor learning*) to the first block of the second FM practice session after a very short consolidation period (i.e., *short-term motor memory*), CG but not EG revealed a strong reduction of contralateral frontal cortical activity (i.e., weaker beta TRPow decreases). EG, in turn, did not change from *initial motor learning* to *short-term motor memory*, resulting in frontal TRPow decreases that did not differ significantly

Table 7: *F*-statistics of (a) Analysis 3.1 and (b) Analysis 3.3 for EEG rest (adjusted $\alpha = .025$).

	TIME				GROUP				TIME × GROUP			
	F	*df*	*p*	η_p^2	*F*	*df*	*p*	η_p^2	*F*	*df*	*p*	η_p^2
(a) Analysis 3.1												
F3	0.08	1	.780	<.01	2.14	1	.153	.06	2.29	1	.139	.07
C3	5.34	1	.027	.14	2.43	1	.128	.07	0.76	1	.388	.02
CP3	11.43	1	**.002**	.26	1.83	1	.185	.05	0.82	1	.372	.02
F4	0.03	1	.869	<.01	1.71	1	.200	.05	<0.01	1	.969	<.01
C4	3.94	1	.056	.11	2.07	1	.160	.06	0.65	1	.426	.02
CP4	2.34	1	.136	.07	2.34	1	.136	.07	0.65	1	.426	.02
(b) Analysis 3.3												
F3	1.28	1	.266	.03	21.55	1	.636	.01	6.21	1	**.017**	.15
C3	0.47	1	.449	.01	2.34	1	.135	.06	0.19	1	.665	.01
CP3	1.12	1	.298	.03	1.43	1	.239	.04	2.15	1	.151	.06
F4	6.37	1	**.016**	.15	0.16	1	.696	<.01	0.16	1	.696	<.01
C4	2.41	1	.130	.06	1.20	1	.281	.03	0.22	1	.644	.01
CP4	1.35	1	.253	.04	0.39	1	.535	.01	0.01	1	.910	<.01

from the baseline level. Thus, the effect of the intervention (exercise or control condition) as well as the effect of practicing the FM task (first practice session) disappeared during the 15-minute break between FM practice sessions. Therefore, different to young adults [59], in older adults, efficient short-term motor memory consolidation was not reflected by weaker beta TRPow decreases. The different results might be related to the intensity of exercise, i.e., a moderate intensity exercise might not be strong enough to trigger motor memory consolidation in older adults or to a general age-related decline in memory consolidation after acute exercise [74].

Interestingly, the significant effects of acute exercise on EEG beta activity were restricted to the contralateral side; no influence was found for the ipsilateral brain areas. Although the FM task requires bilateral brain activity [34, 36], especially in older adults [49], acute exercise seemed to trigger the dominant contralateral brain side only.

A general increase of beta power at rest was revealed from *EEG rest 1* to *3*. Beta power at rest was interpreted as a correlate of processing of content-specific information [80, 81]. Therefore, one might assume that both groups increased processing throughout the FM practice on day 2 (regardless of the intervention). The lack of TIME × GROUP interactions for beta power at rest indicated that sweating did not systematically affect EEG data at rest.

4.3. Association between Motor Behavior, EEG Data, and Load during Exercise. After, correcting for multiple comparisons, no significant associations between FM task performance and TRPow during FM task were found. Thus, we might conclude that our results confirm earlier studies reporting no direct correlation between visuomotor performance, task-related beta power, and electrophysiological data [44, 82]. However, as the (marginally significant) correlation during short-term motor memory consolidation at electrode C4 for the experimental group was medium high, we might carefully interpret that as that good short-term motor memory consolidation came along with weaker TRPow decrease. This fits to our finding that TRPow decreases got weaker with practice. In contrast, a motor sequence learning study (without acute exercise) revealed that a high learning gain (i.e., a high decrease of reaction times) correlated with a high beta suppression after a short-term consolidation phase of ten minutes in young adults [83]. Diverging results might indicate different control strategies between the (key pressing) motor sequence task and our FM task and/or between age groups.

It was further investigated whether the individual exercise load was associated with FM task performance after exercise, as exercise loads varied highly within the EG (range: 54 W to 130 W). Although only marginally significant, there was a moderate association between exercise load and long-term motor memory consolidation, indicating better performance in the FM task 24 hours after acute exercise with higher exercise loads. The level of significance might be due to the small sample size of $n = 17$ and the high variation in the data. It has to be examined whether there is an objective criterion (i.e., exercise load in Watt) or relative criterion (exercise load as a percentage of maximum performance) that triggers these processes. Based on the correlational results, one could speculate that acute exercise needs to be performed at a certain exercise load to increase motor consolidation processes.

4.4. Limitations and Future Directions. To our knowledge, this study revealed for the first time that acute exercise facilitates fine motor control performance and learning as well as electrophysiological processing in healthy older adults. However, several factors might have influenced (or weakened) the effect of an acute exercise session on motor processes.

The aim of the *baseline* measurement was to assess a status quo of the initial fine motor performance of the participants. Participants in both groups revealed high improvements within these first eight trials of the FM task (see Figure 5). As the rate of improvement was nearly identical between the experimental and control groups, it

Table 8: Correlations between the Watt load performed during exercise and FM performance (RMSE) after different time points of exercise (adjusted $\alpha = .013$).

RMSE	Watt load during exercise	
	r	*p*
MP-block	−.291	.257
iML-block	−.300	.242
sMM-block	−.157	.547
lMM-block	−.426	.088

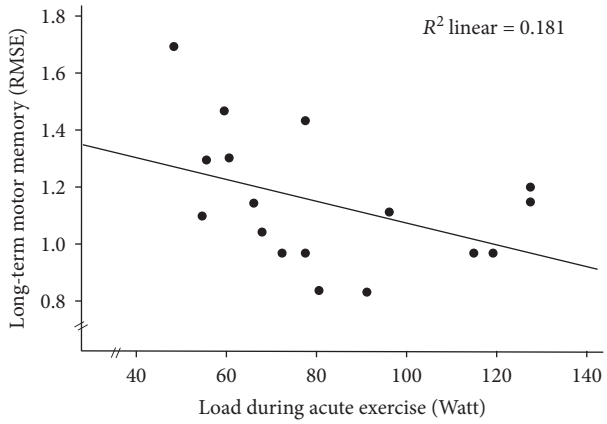

Figure 8: Scatterplot of the FM performance during long-term motor memory block (*lMM-block*) and the Watt load during acute exercise.

Table 9: Correlations between the Watt load performed during exercise and TRPow after different time points of exercise (adjusted $\alpha = .017$).

TRPow	Watt load during exercise	
	r	*p*
MP-block	.217	.403
C3	.227	.381
CP3	.142	.585
C4	.334	.190
CP4	.378	.134
F3	−.069	.793
iML-block	.006	.981
C3	.336	.188
CP3	.195	.453
C4	.373	.140
CP4	.345	.175
F3	.112	.669
sMM-block	−.081	.758
C3	.171	.513
CP3	.559	.020
C4	.474	.054
CP4	.328	.198
F3	.377	.135

rather represents a baseline familiarization than a baseline fine motor performance level. Based on the mean values, one could assume that the intervention time led to a short-term motor memory consolidation. However, considering the particular trials within the analyzed blocks during *baseline* and *motor performance*, we see that both groups started at a slightly lower performance level than the last trial of the baseline block. This contradicts the assumption of a general short-term consolidation due to the intervention break.

Although the intensity of exercise is discussed as an important factor in acute exercise research [84], no systematic association can be derived from studies using motor paradigms with young adults. That is, exercise intensity did not influence the consolidation of long-term motor memory systematically: better motor memory was found 24 hours after a high intensity [12, 14, 17, 18] and after a low-intensity exercise session [18], but, surprisingly, not after a moderate intensity exercise session [15, 16]. These heterogeneous results might have been influenced by the method of defining exercise intensity (% of VO_2-peak vs. % of estimated age-related maximum heart rate vs. % of maximum Watt) or by the exercise type (cycling vs. running). In the current study, a moderate intensity exercise session was used, as this load could be transferred from laboratory-based acute exercise studies to the setting of rehabilitation, i.e., patients or persons not experienced with exercise [8]. High-intensity exercise did not seem appropriate, as it is performed by or recommended only for older persons with exercise experience [85, 86]. Nevertheless, exercise intensity might be a determining factor and should be systematically analyzed in future studies.

The order of acute exercise and practicing the motor task might also be an important factor. Roig et al. [12] found that practicing a motor task before acute exercise led to better long-term motor memory than practice after exercise. However, this finding was not supported by another study (using a motor adaptation paradigm), revealing that the order of practice and exercise did not influence the effect of exercise [87]. Thus, we decided to perform the practice sessions after exercise, as this design has been repeatedly shown to facilitate cognitive performance in older adults [27–29].

Furthermore, the physical activity/cardiovascular fitness level of the participants might mediate results. We generated a controlled sample in terms of the physical activity level, which could prevent generalizability to the general population of older adults. However, homogenizing the sample was necessary, as the physical activity level seems to mediate plasticity of the brain [88, 89] and the response to acute exercise sessions [90]. Further influencing factors might be the specific kind of upper extremity motor tasks (motor sequence learning: [91–94]; motor adaptation paradigms: [71, 87]), the kind of (cardiovascular) exercise [95], timing, or the duration of exercise. In sum, further studies with older adults are needed that systematically vary the potential influencing factors [26].

With respect to associated neural mechanisms, we restricted our analysis to the beta band (cf. introduction for argumentation). In addition, alpha oscillations (8–13 Hz) of the sensorimotor cortex were described as possible markers

of sensorimotor processing [96, 97]. We did not find any acute exercise-related effects on EEG alpha power at rest or TRPow in our data (results not reported) and abstained from including it in the current report.

5. Conclusions

A moderate intensity acute exercise session tended to improve fine motor control performance immediately after exercise in a precision grip FM task in healthy older adults more than a resting control condition. Therefore, acute exercise might be a potential candidate to enhance motor performance in older adults. This could have important practical implications for the setting of rehabilitation: acute exercise could be implemented as a method to create successful experiences in fine motor control performance and therefore, to contribute in motivating older patients in the rehabilitation process. Further, the stronger contralateral frontal beta TRPow decreases immediately after the exercise session compared to after the control condition was interpreted as higher frontal brain activity [41, 42]. This higher beta activity might indicate enhanced compensation processes, implicating that acute exercise facilitates the ability to better use existing frontal brain capacities during fine motor control tasks.

Data Availability

The data used to support the findings of this study are available from the corresponding author upon request.

Conflicts of Interest

The authors declare that there is no conflict of interest regarding the publication of this paper.

Acknowledgments

The authors would like to thank Tim Albrecht, Marie Fernau, Anna Lena Flagmeier, and Kai Hoffmann for their help during data collection as well as our research group for carefully reading the manuscript. This work was supported by a grant of the German Research Foundation (VO-15/1 Re-LOAD, GO-8 Re-LOAD).

References

[1] G. Diermayr, T. L. McIsaac, and A. M. Gordon, "Finger force coordination underlying object manipulation in the elderly - a mini-review," *Gerontology*, vol. 57, no. 3, pp. 217–227, 2011.

[2] M. Zimerman, M. Nitsch, P. Giraux, C. Gerloff, L. G. Cohen, and F. C. Hummel, "Neuroenhancement of the aging brain: restoring skill acquisition in old subjects," *Annals of Neurology*, vol. 73, no. 1, pp. 10–15, 2013.

[3] C. Voelcker-Rehage, "Motor-skill learning in older adults—a review of studies on age-related differences," *European Review of Aging and Physical Activity*, vol. 5, no. 1, pp. 5–16, 2008.

[4] K. M. Berghuis, M. P. Veldman, S. Solnik, G. Koch, I. Zijdewind, and T. Hortobágyi, "Neuronal mechanisms of motor learning and motor memory consolidation in healthy old adults," *Age*, vol. 37, no. 3, p. 9779, 2015.

[5] R. M. Brown, E. M. Robertson, and D. Z. Press, "Sequence skill acquisition and off-line learning in normal aging," *PLoS One*, vol. 4, no. 8, article e6683, 2009.

[6] D. Nemeth and K. Janacsek, "The dynamics of implicit skill consolidation in young and elderly adults," *The Journals of Gerontology: Series B*, vol. 66B, no. 1, pp. 15–22, 2011.

[7] M. Roig, A. Ritterband-Rosenbaum, J. Lundbye-Jensen, and J. B. Nielsen, "Aging increases the susceptibility to motor memory interference and reduces off-line gains in motor skill learning," *Neurobiology of Aging*, vol. 35, no. 8, pp. 1892–1900, 2014.

[8] A. M. Singh and W. R. Staines, "The effects of acute aerobic exercise on the primary motor cortex," *Journal of Motor Behavior*, vol. 47, no. 4, pp. 328–339, 2015.

[9] A. M. Singh, R. E. Duncan, J. L. Neva, and W. Richard Staines, "Aerobic exercise modulates intracortical inhibition and facilitation in a nonexercised upper limb muscle," *BMC Sports Science, Medicine and Rehabilitation*, vol. 6, no. 1, p. 23, 2014.

[10] A. E. Smith, M. R. Goldsworthy, T. Garside, F. M. Wood, and M. C. Ridding, "The influence of a single bout of aerobic exercise on short-interval intracortical excitability," *Experimental Brain Research*, vol. 232, no. 6, pp. 1875–1882, 2014.

[11] R. Perini, M. Bortoletto, M. Capogrosso, A. Fertonani, and C. Miniussi, "Acute effects of aerobic exercise promote learning," *Scientific Reports*, vol. 6, no. 1, p. 25440, 2016.

[12] M. Roig, K. Skriver, J. Lundbye-Jensen, B. Kiens, and J. B. Nielsen, "A single bout of exercise improves motor memory," *PLoS One*, vol. 7, no. 9, article e44594, 2012.

[13] A. M. Singh, J. L. Neva, and W. R. Staines, "Aerobic exercise enhances neural correlates of motor skill learning," *Behavioural Brain Research*, vol. 301, pp. 19–26, 2016.

[14] K. Skriver, M. Roig, J. Lundbye-Jensen et al., "Acute exercise improves motor memory: exploring potential biomarkers," *Neurobiology of Learning and Memory*, vol. 116, pp. 46–58, 2014.

[15] N. J. Snow, C. S. Mang, M. Roig, M. N. McDonnell, K. L. Campbell, and L. A. Boyd, "The effect of an acute bout of moderate-intensity aerobic exercise on motor learning of a continuous tracking task," *PLoS One*, vol. 11, no. 2, article e0150039, 2016.

[16] M. A. Statton, M. Encarnacion, P. Celnik, and A. J. Bastian, "A single bout of moderate aerobic exercise improves motor skill acquisition," *PLoS One*, vol. 10, no. 10, article e0141393, 2015.

[17] R. Thomas, M. M. Beck, R. R. Lind et al., "Acute exercise and motor memory consolidation: the role of exercise timing," *Neural Plasticity*, vol. 2016, Article ID 6205452, 11 pages, 2016.

[18] R. Thomas, L. K. Johnsen, S. S. Geertsen et al., "Acute exercise and motor memory consolidation: the role of exercise intensity," *PLoS One*, vol. 11, no. 7, article e0159589, 2016.

[19] A. Shumway-Cook and M. H. Woollacott, *Motor Control: Translating Research into Clinical Practice*, Lippincott Williams & Wilkins, 2007.

[20] A. M. Singh, J. L. Neva, and W. R. Staines, "Acute exercise enhances the response to paired associative stimulation-induced plasticity in the primary motor cortex," *Experimental Brain Research*, vol. 232, no. 11, pp. 3675–3685, 2014.

[21] J. Doyon and H. Benali, "Reorganization and plasticity in the adult brain during learning of motor skills," *Current Opinion in Neurobiology*, vol. 15, no. 2, pp. 161–167, 2005.

[22] Y. Dudai, "The neurobiology of consolidations, or, how stable is the engram?," *Annual Review of Psychology*, vol. 55, no. 1, pp. 51–86, 2004.

[23] W. Muellbacher, U. Ziemann, J. Wissel et al., "Early consolidation in human primary motor cortex," *Nature*, vol. 415, no. 6872, pp. 640–644, 2002.

[24] J. L. McGaugh, "Memory–a century of consolidation," *Science*, vol. 287, no. 5451, pp. 248–251, 2000.

[25] S. S. Kantak and C. J. Winstein, "Learning-performance distinction and memory processes for motor skills: a focused review and perspective," *Behavioural Brain Research*, vol. 228, no. 1, pp. 219–231, 2012.

[26] L. Hübner and C. Voelcker-Rehage, "Does physical activity benefit motor performance and learning of upper extremity tasks in older adults?–a systematic review," *European Review of Aging and Physical Activity*, vol. 14, no. 1, p. 15, 2017.

[27] L. A. Barella, J. L. Etnier, and Y. K. Chang, "The immediate and delayed effects of an acute bout of exercise on cognitive performance of healthy older adults," *Journal of Aging and Physical Activity*, vol. 18, no. 1, pp. 87–98, 2010.

[28] Y. K. Chang, C. H. Chu, C. C. Wang, T. F. Song, and G. X. Wei, "Effect of acute exercise and cardiovascular fitness on cognitive function: an event-related cortical desynchronization study," *Psychophysiology*, vol. 52, no. 3, pp. 342–351, 2015.

[29] K. Kamijo, Y. Hayashi, T. Sakai, T. Yahiro, K. Tanaka, and Y. Nishihira, "Acute effects of aerobic exercise on cognitive function in older adults," *The Journals of Gerontology. Series B, Psychological Sciences and Social Sciences*, vol. 64B, no. 3, pp. 356–363, 2009.

[30] K. Lambourne and P. Tomporowski, "The effect of exercise-induced arousal on cognitive task performance: a meta-regression analysis," *Brain Research*, vol. 1341, pp. 12–24, 2010.

[31] E. Dayan and L. G. Cohen, "Neuroplasticity subserving motor skill learning," *Neuron*, vol. 72, no. 3, pp. 443–454, 2011.

[32] B. Godde and C. Voelcker-Rehage, "More automation and less cognitive control of imagined walking movements in high- versus low-fit older adults," *Frontiers in Aging Neuroscience*, vol. 2, p. 139, 2010.

[33] U. Halsband and R. K. Lange, "Motor learning in man: a review of functional and clinical studies," *Journal of Physiology, Paris*, vol. 99, no. 4–6, pp. 414–424, 2006.

[34] H. H. Ehrsson, A. Fagergren, T. Jonsson, G. Westling, R. S. Johansson, and H. Forssberg, "Cortical activity in precision- versus power-grip tasks: an fMRI study," *Journal of Neurophysiology*, vol. 83, no. 1, pp. 528–536, 2000.

[35] M. F. Ghilardi, C. Ghez, V. Dhawan et al., "Patterns of regional brain activation associated with different forms of motor learning," *Brain Research*, vol. 871, no. 1, pp. 127–145, 2000.

[36] J. P. Kuhtz-Buschbeck, H. H. Ehrsson, and H. Forssberg, "Human brain activity in the control of fine static precision grip forces: an fMRI study," *European Journal of Neuroscience*, vol. 14, no. 2, pp. 382–390, 2001.

[37] P. E. Roland, B. Larsen, N. A. Lassen, and E. Skinhoj, "Supplementary motor area and other cortical areas in organization of voluntary movements in man," *Journal of Neurophysiology*, vol. 43, no. 1, pp. 118–136, 1980.

[38] A. Floyer-Lea and P. M. Matthews, "Changing brain networks for visuomotor control with increased movement automaticity," *Journal of Neurophysiology*, vol. 92, no. 4, pp. 2405–2412, 2004.

[39] W. Muellbacher, U. Ziemann, B. Boroojerdi, L. Cohen, and M. Hallett, "Role of the human motor cortex in rapid motor learning," *Experimental Brain Research*, vol. 136, no. 4, pp. 431–438, 2001.

[40] A. K. Engel and P. Fries, "Beta-band oscillations – signalling the status quo?," *Current Opinion in Neurobiology*, vol. 20, no. 2, pp. 156–165, 2010.

[41] S. Erla, L. Faes, G. Nollo, C. Arfeller, C. Braun, and C. Papadelis, "Multivariate EEG spectral analysis evidences the functional link between motor and visual cortex during integrative sensorimotor tasks," *Biomedical Signal Processing and Control*, vol. 7, no. 3, pp. 221–227, 2012.

[42] C. Gerloff, J. Richard, J. Hadley, A. E. Schulman, M. Honda, and M. Hallett, "Functional coupling and regional activation of human cortical motor areas during simple, internally paced and externally paced finger movements," *Brain*, vol. 121, no. 8, pp. 1513–1531, 1998.

[43] J. Classen, C. Gerloff, M. Honda, and M. Hallett, "Integrative visuomotor behavior is associated with interregionally coherent oscillations in the human brain," *Journal of Neurophysiology*, vol. 79, no. 3, pp. 1567–1573, 1998.

[44] A. J. Rilk, S. R. Soekadar, P. Sauseng, and C. Plewnia, "Alpha coherence predicts accuracy during a visuomotor tracking task," *Neuropsychologia*, vol. 49, no. 13, pp. 3704–3709, 2011.

[45] S. N. Baker, "Oscillatory interactions between sensorimotor cortex and the periphery," *Current Opinion in Neurobiology*, vol. 17, no. 6, pp. 649–655, 2007.

[46] C. Kranczioch, S. Athanassiou, S. Shen, G. Gao, and A. Sterr, "Short-term learning of a visually guided power-grip task is associated with dynamic changes in EEG oscillatory activity," *Clinical Neurophysiology*, vol. 119, no. 6, pp. 1419–1430, 2008.

[47] H. Nakano, M. Osumi, K. Ueta, T. Kodama, and S. Morioka, "Changes in electroencephalographic activity during observation, preparation, and execution of a motor learning task," *The International Journal of Neuroscience*, vol. 123, no. 12, pp. 866–875, 2013.

[48] B. Studer, S. Koeneke, J. Blum, and L. Jancke, "The effects of practice distribution upon the regional oscillatory activity in visuomotor learning," *Behavioral and Brain Functions*, vol. 6, no. 1, p. 8, 2010.

[49] L. Hübner, B. Godde, and C. Voelcker-Rehage, "Older adults reveal enhanced task-related beta power decreases during a force modulation task," *Behavioural Brain Research*, vol. 345, pp. 104–113, 2018.

[50] R. D. Seidler, J. A. Bernard, T. B. Burutolu et al., "Motor control and aging: links to age-related brain structural, functional, and biochemical effects," *Neuroscience and Biobehavioral Reviews*, vol. 34, no. 5, pp. 721–733, 2010.

[51] L. O. D. Christensen, P. Johannsen, T. Sinkjær, N. Petersen, H. S. Pyndt, and J. B. Nielsen, "Cerebral activation during bicycle movements in man," *Experimental Brain Research*, vol. 135, no. 1, pp. 66–72, 2000.

[52] E. B. Fontes, A. H. Okano, F. de Guio et al., "Brain activity and perceived exertion during cycling exercise: an fMRI study," *British Journal of Sports Medicine*, vol. 49, no. 8, pp. 556–560, 2015.

[53] M. Hiura, T. Nariai, K. Ishii et al., "Changes in cerebral blood flow during steady-state cycling exercise: a study using oxygen-15-labeled water with PET," *Journal of Cerebral Blood Flow and Metabolism*, vol. 34, no. 3, pp. 389–396, 2014.

[54] J. B. Crabbe and R. K. Dishman, "Brain electrocortical activity during and after exercise: a quantitative synthesis," *Psychophysiology*, vol. 41, no. 4, pp. 563–574, 2004.

[55] M. Fumoto, T. Oshima, K. Kamiya et al., "Ventral prefrontal cortex and serotonergic system activation during pedaling exercise induces negative mood improvement and increased alpha band in EEG," *Behavioural Brain Research*, vol. 213, no. 1, pp. 1–9, 2010.

[56] S. Schneider, C. D. Askew, J. Diehl et al., "EEG activity and mood in health orientated runners after different exercise intensities," *Physiology & Behavior*, vol. 96, no. 4-5, pp. 709–716, 2009.

[57] P. Wollseiffen, A. Ghadiri, A. Scholz et al., "Short bouts of intensive exercise during the workday have a positive effect on neuro-cognitive performance," *Stress and Health*, vol. 32, no. 5, pp. 514–523, 2015.

[58] H. Moraes, A. Deslandes, H. Silveira et al., "The effect of acute effort on EEG in healthy young and elderly subjects," *European Journal of Applied Physiology*, vol. 111, no. 1, pp. 67–75, 2011.

[59] F. Dal Maso, B. Desormeau, M. H. Boudrias, and M. Roig, "Acute cardiovascular exercise promotes functional changes in cortico-motor networks during the early stages of motor memory consolidation," *NeuroImage*, vol. 174, pp. 380–392, 2018.

[60] M. E. Nelson, W. J. Rejeski, S. N. Blair et al., "Physical activity and public health in older adults: recommendation from the American College of Sports Medicine and the American Heart Association," *Circulation*, vol. 116, no. 9, pp. 1094–1105, 2007.

[61] J. A. Baecke, J. Burema, and J. E. Frijters, "A short questionnaire for the measurement of habitual physical activity in epidemiological studies," *The American Journal of Clinical Nutrition*, vol. 36, no. 5, pp. 936–942, 1982.

[62] M. F. Folstein, S. E. Folstein, and P. R. McHugh, "Mini-mental state. A practical method for grading the cognitive state of patients for the clinician," *Psychiatry Research*, vol. 12, no. 3, pp. 189–198, 1975.

[63] R. M. Crum, J. C. Anthony, S. S. Bassett, and M. F. Folstein, "Population-based norms for the mini-mental state examination by age and educational level," *JAMA*, vol. 269, no. 18, pp. 2386–2391, 1993.

[64] R. C. Oldfield, "The assessment and analysis of handedness: the Edinburgh inventory," *Neuropsychologia*, vol. 9, no. 1, pp. 97–113, 1971.

[65] S. Vieluf, J. Mahmoodi, B. Godde, E. M. Reuter, and C. Voelcker-Rehage, "The influence of age and work-related expertise on fine motor control," *GeroPsych*, vol. 25, no. 4, pp. 199–206, 2012.

[66] J. Tiffin and E. J. Asher, "The Purdue Pegboard: norms and studies of reliability and validity," *Journal of Applied Psychology*, vol. 32, no. 3, pp. 234–247, 1948.

[67] J. Desrosiers, R. Hébert, G. Bravo, and E. Dutil, "The Purdue Pegboard Test: normative data for people aged 60 and over," *Disability and Rehabilitation*, vol. 17, no. 5, pp. 217–224, 1995.

[68] H. H. Jasper, "The ten twenty electrode system of the international federation," *Electroencephalography and Clinical Neurophysiology*, vol. 10, pp. 371–375, 1958.

[69] B. G. Tabachnick and L. S. Fidell, "Computer-assisted research design and analysis," Allyn & Bacon, Boston, MA, USA, 2001.

[70] D. J. Serrien, A. H. Pogosyan, and P. Brown, "Cortico-cortical coupling patterns during dual task performance," *Experimental Brain Research*, vol. 157, no. 1, pp. 79–84, 2004.

[71] A. Mierau, S. Schneider, T. Abel, C. Askew, S. Werner, and H. K. Strüder, "Improved sensorimotor adaptation after exhaustive exercise is accompanied by altered brain activity," *Physiology & Behavior*, vol. 96, no. 1, pp. 115–121, 2009.

[72] J. C. Smith, E. S. Paulson, D. B. Cook, M. D. Verber, and Q. Tian, "Detecting changes in human cerebral blood flow after acute exercise using arterial spin labeling: implications for fMRI," *Journal of Neuroscience Methods*, vol. 191, no. 2, pp. 258–262, 2010.

[73] A. S. Rajab, D. E. Crane, L. E. Middleton, A. D. Robertson, M. Hampson, and B. J. MacIntosh, "A single session of exercise increases connectivity in sensorimotor-related brain networks: a resting-state fMRI study in young healthy adults," *Frontiers in Human Neuroscience*, vol. 8, p. 625, 2014.

[74] M. Roig, S. Nordbrandt, S. S. Geertsen, and J. B. Nielsen, "The effects of cardiovascular exercise on human memory: a review with meta-analysis," *Neuroscience and Biobehavioral Reviews*, vol. 37, no. 8, pp. 1645–1666, 2013.

[75] M. P. Rearick, J. A. Johnston, and S. M. Slobounov, "Feedback-dependent modulation of isometric force control: an EEG study in visuomotor integration," *Cognitive Brain Research*, vol. 12, no. 1, pp. 117–130, 2001.

[76] R. Salmelin and R. Hari, "Spatiotemporal characteristics of sensorimotor neuromagnetic rhythms related to thumb movement," *Neuroscience*, vol. 60, no. 2, pp. 537–550, 1994.

[77] S. Heuninckx, N. Wenderoth, and S. P. Swinnen, "Systems neuroplasticity in the aging brain: recruiting additional neural resources for successful motor performance in elderly persons," *The Journal of Neuroscience*, vol. 28, no. 1, pp. 91–99, 2008.

[78] K. Hyodo, I. Dan, K. Suwabe et al., "Acute moderate exercise enhances compensatory brain activation in older adults," *Neurobiology of Aging*, vol. 33, no. 11, pp. 2621–2632, 2012.

[79] T. Tsujii, K. Komatsu, and K. Sakatani, "Acute effects of physical exercise on prefrontal cortex activity in older adults: a functional near-infrared spectroscopy study," *Advances in Experimental Medicine and Biology*, vol. 765, pp. 293–298, 2013.

[80] C. Moisello, D. Blanco, J. Lin et al., "Practice changes beta power at rest and its modulation during movement in healthy subjects but not in patients with Parkinson's disease," *Brain and Behavior*, vol. 5, no. 10, article e00374, 2015.

[81] B. Spitzer and S. Haegens, "Beyond the status quo: a role for beta oscillations in endogenous content (re)activation," *eNeuro*, vol. 4, no. 4, pp. ENEURO.0170–ENEU17.2017, 2017.

[82] H. E. Rossiter, E. M. Davis, E. V. Clark, M. H. Boudrias, and N. S. Ward, "Beta oscillations reflect changes in motor cortex inhibition in healthy ageing," *NeuroImage*, vol. 91, pp. 360–365, 2014.

[83] B. Pollok, D. Latz, V. Krause, M. Butz, and A. Schnitzler, "Changes of motor-cortical oscillations associated with motor learning," *Neuroscience*, vol. 275, pp. 47–53, 2014.

[84] C. Voelcker-Rehage, C. Niemann, L. Hübner, B. Godde, and A. H. Winneke, "Benefits of physical activity and fitness for lifelong cognitive and motor development—brain and behavior," in *Sport and Exercise Psychology Research*, M. Raab, P. Wylleman, R. Seiler, A.-M. Elbe, and A. Hatzigeorgiadis, Eds., pp. 43–73, Elsevier, Amsterdam, 2016.

[85] M. E. Cress, D. M. Buchner, T. Prohaska et al., "Physical activity programs and behavior counseling in older adult populations," *Medicine & Science in Sports & Exercise*, vol. 36, no. 11, pp. 1997–2003, 2004.

[86] P. B. Sparling, B. J. Howard, D. W. Dunstan, and N. Owen, "Recommendations for physical activity in older adults," *BMJ*, vol. 350, p. h100, 2015.

[87] B. Ferrer-Uris, A. Busquets, V. Lopez-Alonso, M. Fernandez-del-Olmo, and R. Angulo-Barroso, "Enhancing consolidation of a rotational visuomotor adaptation task through acute exercise," *PLoS One*, vol. 12, no. 4, article e0175296, 2017.

[88] J. Cirillo, A. P. Lavender, M. C. Ridding, and J. G. Semmler, "Motor cortex plasticity induced by paired associative stimulation is enhanced in physically active individuals," *The Journal of Physiology*, vol. 587, no. 24, pp. 5831–5842, 2009.

[89] T. Lulic, J. el-Sayes, H. J. Fassett, and A. J. Nelson, "Physical activity levels determine exercise-induced changes in brain excitability," *PLoS One*, vol. 12, no. 3, article e0173672, 2017.

[90] M. E. Hopkins, F. C. Davis, M. R. VanTieghem, P. J. Whalen, and D. J. Bucci, "Differential effects of acute and regular physical exercise on cognition and affect," *Neuroscience*, vol. 215, pp. 59–68, 2012.

[91] M. Coco, V. Perciavalle, P. Cavallari, and V. Perciavalle, "Effects of an exhaustive exercise on motor skill learning and on the excitability of primary motor cortex and supplementary motor area," *Medicine*, vol. 95, no. 11, article e2978, 2016.

[92] C. S. Mang, N. J. Snow, K. L. Campbell, C. J. D. Ross, and L. A. Boyd, "A single bout of high-intensity aerobic exercise facilitates response to paired associative stimulation and promotes sequence-specific implicit motor learning," *Journal of Applied Physiology*, vol. 117, no. 11, pp. 1325–1336, 2014.

[93] B. Lauber, S. Franke, W. Taube, and A. Gollhofer, "The effects of a single bout of exercise on motor memory interference in the trained and untrained hemisphere," *Neuroscience*, vol. 347, pp. 57–64, 2017.

[94] J. Rhee, J. Chen, S. M. Riechman, A. Handa, S. Bhatia, and D. L. Wright, "An acute bout of aerobic exercise can protect immediate offline motor sequence gains," *Psychological Research*, vol. 80, no. 4, pp. 518–531, 2015.

[95] R. Thomas, M. Flindtgaard, K. Skriver et al., "Acute exercise and motor memory consolidation: does exercise type play a role?," *Scandinavian Journal of Medicine & Science in Sports*, vol. 27, no. 11, pp. 1523–1532, 2017.

[96] E. Başar, C. Başar-Eroğlu, S. Karakaş, and M. Schürmann, "Brain oscillations in perception and memory," *International Journal of Psychophysiology*, vol. 35, no. 2-3, pp. 95–124, 2000.

[97] G. Pfurtscheller and F. L. Da Silva, "Event-related EEG/MEG synchronization and desynchronization: basic principles," *Clinical Neurophysiology*, vol. 110, no. 11, pp. 1842–1857, 1999.

Hindawi
Neural Plasticity
Volume 2018, Article ID 2941783, 21 pages
https://doi.org/10.1155/2018/2941783

Review Article

Visual Features in Alzheimer's Disease: From Basic Mechanisms to Clinical Overview

María Alejandra Cerquera-Jaramillo,[1] Mauricio O. Nava-Mesa,[2] Rodrigo E. González-Reyes,[2] Carlos Tellez-Conti,[1] and Alejandra de-la-Torre[2]

[1]*Escuela Superior de Oftalmología-Instituto Barraquer de América, Bogotá, Colombia*
[2]*Grupo de Investigación en Neurociencias (NeURos), Escuela de Medicina y Ciencias de la Salud, Universidad del Rosario, Bogotá, Colombia*

Correspondence should be addressed to Alejandra de-la-Torre; alejadelatorre@yahoo.com

Received 21 February 2018; Accepted 7 August 2018; Published 14 October 2018

Academic Editor: Diego Sepulveda-Falla

Alzheimer's disease (AD) is the leading cause of dementia worldwide. It compromises patients' daily activities owing to progressive cognitive deterioration, which has elevated direct and indirect costs. Although AD has several risk factors, aging is considered the most important. Unfortunately, clinical diagnosis is usually performed at an advanced disease stage when dementia is established, making implementation of successful therapeutic interventions difficult. Current biomarkers tend to be expensive, insufficient, or invasive, raising the need for novel, improved tools aimed at early disease detection. AD is characterized by brain atrophy due to neuronal and synaptic loss, extracellular amyloid plaques composed of amyloid-beta peptide (Aβ), and neurofibrillary tangles of hyperphosphorylated tau protein. The visual system and central nervous system share many functional components. Thus, it is plausible that damage induced by Aβ, tau, and neuroinflammation may be observed in visual components such as the retina, even at an early disease stage. This underscores the importance of implementing ophthalmological examinations, less invasive and expensive than other biomarkers, as useful measures to assess disease progression and severity in individuals with or at risk of AD. Here, we review functional and morphological changes of the retina and visual pathway in AD from pathophysiological and clinical perspectives.

1. Introduction

Alzheimer's disease (AD) is the most prevalent progressive neurodegenerative disease in humans and the main cause of dementia worldwide [1]. Together with vascular dementia, AD corresponds to 60%–80% of all dementia cases [2]. According to the World Alzheimer Report [3], an estimated 47 million people worldwide currently have dementia, a number that is projected to rise to approximately 131 million by 2050. Several modifiable and nonmodifiable risk factors have been described for AD, although aging remains the most significant [4]. Consequently, after 65 years of age, AD prevalence is expected to double every 5 years [5]. According to the US National Institute on Aging-Alzheimer's Association workgroup, there are three different stages of AD: preclinical AD (presymptomatic with early AD-related brain changes observed by neuroimaging or other biomarker studies such as amyloid and tau studies in cerebrospinal fluid (CSF)), mild cognitive impairment (MCI) caused by AD (mild cognitive decline but still able to perform daily activities), and dementia caused by AD (major cognitive decline that interferes with daily activities) [6]. Globally, AD has significant direct and indirect costs, which increased from US$ 604 billion in 2010 to US$ 818 billion in 2015, totaling around 1% of the worldwide gross domestic product (GDP) [3].

Two types of AD have been characterized based on age of onset: early-onset AD (EOAD), referred to as familial, and late-onset AD (LOAD), which is regarded as sporadic. EOAD presents before the age of 65 and corresponds to around 5% of AD cases [7], while LOAD appears after 65 years of age and represents the most common type of

AD, accounting for >90% of AD cases [8]. No direct cause has been described for LOAD, but its disease development is influenced by various environmental and genetic risk factors [9]. The main risk factors include aging, genetics (presenilin 1 (PSEN1), PSEN2, and APP1 genes) [7, 10], hypertension, diabetes, hypercholesterolemia, stroke, obesity, sedentary lifestyle, depression, low socioeconomic status, and alcohol and tobacco use [1, 4, 9].

AD is characterized by formation and aggregation of extracellular plaques of abnormal amyloid-beta (Aβ) peptides, as well as presence of intracellular aggregates of hyperphosphorylated tau protein, known as neurofibrillary tangles (NFT) [11, 12]. In AD, Aβ peptides are produced from abnormal cleavage of the amyloid precursor protein (APP) by the beta-site amyloid precursor protein cleaving enzyme 1 (BACE-1 or β-secretase) and γ-secretase complex [13]. Aβ peptides promote intracellular tau phosphorylation, with hyperphosphorylated tau protein posteriorly aggregating into NFT [11, 14]. Aβ and NFT activate astrocytes and microglia, inducing production of proinflammatory factors such as interleukins and nitric oxide (NO), and ultimately resulting in excessive neuroinflammation, oxidative stress (OS), neuronal damage, and cell death [15–17].

Currently, the diagnosis and classification of AD are based on clinical and neuropsychological examinations complemented by neuroimaging studies. Nonetheless, a conclusive diagnosis still relies on pathological examination of postmortem brain tissue [18]. While many exploratory biomarkers have been proposed for AD, cerebrospinal fluid levels of tau and Aβ levels, together with imaging studies (such as positron emission tomography carbon 11-labeled Pittsburgh compound B), are the most widely accepted [19]. Unfortunately, these techniques are not easily accessible to patients with dementia worldwide owing to elevated costs and a lack of adequate medical facilities. Therefore, it is important to find easy-to-acquire, cost-effective methods that can provide information on the main disease manifestations, even at early stages, to favor timely interventions and improve the quality of life for patients. In this regard, a recent strategic roadmap aimed at improving early diagnosis of AD based on biomarkers was proposed and is centered on several phases that evaluate analytical validity, clinical validity, and clinical utility [20].

The visual system may be a helpful marker for the early stages of AD. Brain alterations in AD can be accompanied by ocular symptoms [21–24] which may be related to progression, cognitive deterioration, and disease severity [25]. This may be explained because the visual system shares the same embryological origin, namely, the neural tube of the brain, and indeed is considered an extension of the diencephalon [26]. In addition, both components have several functional and structural similarities, including microvasculature and neuronal projections [27]. Furthermore, examination of the visual system may provide markers for identifying dementia subtypes, thereby helping to differentiate AD from vascular dementia [28].

Hence, the aim of this review is to describe functional and morphological changes of the eye and visual pathway that are observed in AD from a clinical and pathophysiological perspective. Considering that the visual system shares vascular and cellular components with the central nervous system (CNS), ocular alterations observed in patients with AD may represent an initial manifestation of the disease and serve as possible candidates for complementary diagnostic biomarkers of MCI and the early stage of AD.

2. Pathological Mechanisms of Aβ and Tau Toxicity in the Eye

2.1. General Mechanisms of Aβ and Tau Production. Senile plaques (SP) are formed from extracellular aggregation of Aβ deposits, which are derived from excessive or inadequate cleavage of APP by BACE-1 and the γ-secretase complex [13]. PSEN1 and PSEN2 are part of the γ-secretase complex, which also includes nicastrin, anterior pharynx-defective 1, and presenilin enhancer 2 [29]. Although its function is not fully understood, APP has been involved in regulation of synaptic plasticity and acts as a cell adhesion molecule that participates in several neurodevelopmental aspects such as migration, neurite outgrowth, growth cone pathfinding, and synaptogenesis [30, 31]. Inadequate cleavage of APP may lead to formation of abnormally long peptides, such as Aβ1–42 fragments, which are more likely to oligomerize and form plaques, compared with shorter fragments such as Aβ1–40 [32]. Although the precise neurotoxic mechanisms of Aβ are not yet fully elucidated, the presence and aggregation of these peptides compromise the function of various cells including astrocytes, microglia, and neurons, leading to systemic failure of brain activity, mainly related, but not limited, to cognitive aspects [33, 34].

In vitro evidence indicates that Aβ induces the release of proinflammatory factors from astrocytes and microglia, including interleukin-1β (IL-1β), IL-6, NO, and tumor necrosis factor alpha (TNFα) [15, 16]. In addition, Aβ oligomers may generate free radicals and induce mitochondrial dysfunction via abnormal activation of glial cells [35, 36]. Other pathological mechanisms include glutamate-induced neuronal excitotoxicity [37], GABAergic dysfunction [38], and reduced cerebral glucose intake [39, 40]. Ultimately, accumulation of Aβ peptides may trigger intracellular signaling for tau hyperphosphorylation, with formation of tau oligomers and NFT [11, 14] leading to neuronal degeneration [41]. Tau appears to be involved in disease progression, as tau aggregates propagate in a prion-like fashion, initiating a self-amplifying cascade and spreading to other brain regions [42]. In AD, these aberrant proteins are deposited in several brain areas including the frontal, parietal, temporal, and occipital lobes and cause neuroinflammation, OS, metabolic dysfunction, excitotoxicity, and perturbation of synaptic plasticity [43–48].

2.2. Aβ Mechanisms in the Retina. Retinal cells share a common embryonic origin with the brain and indeed are a projection of the CNS [49]. Further, they have similarities in vasculature, glial cells, neurotransmitter systems, and connectivity with the visual cortex [50]. Moreover, insoluble aggregation of Aβ peptides in the eye of double transgenic AD mice has been observed in different retinal layers, mainly

the ganglion cell layer (GCL), nerve fiber layer (NFL), photoreceptor layer, and inner plexiform layer (IPL), leading to neuronal damage and visual symptoms [51]. Although this has not been confirmed in humans, it is hypothesized that similar changes may occur.

Glial cells play a crucial role in the biochemical and molecular mechanisms that induce neurodegeneration and are highly expressed in the mammalian retina, optic nerve, and retinal blood vessels. Astrocytes predominate in the NFL, interacting with retinal ganglion cells and in close relationship with blood vessels of the inner nuclear layer (INL) [52]. Thus, Aβ-induced toxic effects on astrocytes and microglia may generate alterations in the eye and visual system like those found in other nervous tissues, such as the hippocampus or cortex.

Moreover, Aβ has been shown to produce changes in Müller cells, the main glial cells resident in the retina. An *in vitro* model using the immortalized human Müller cell line MIO-M1 reported that treatment with Aβ_{1-42} induced caspase-independent apoptosis through activation of the purinergic receptor P2X7 in these cells [53]. A subretinal injection of Aβ_{1-42} in C57BL/6 mice stimulated the development of gliosis and a proinflammatory phenotype in Müller cells, together with an increase in protein expression of cyclooxygenase 2 (COX-2), glutamine synthetase (GS), the inwardly rectifying potassium channel Kir4.1, and the aquaporin-4 (AQP-4) water channel [54]. However, studies in AD animal models have found contradictory results. A study using the triple transgenic mouse model, 3x-TG-AD [55], observed strong gliotic responses and increased processes in Müller cells close to amyloid deposits, while a more recent study using the APPSWE/PS1ΔE9 mouse model failed to see any significant gliotic response or changes in GS expression [56].

Aggregation of Aβ plaques can lead to inflammatory reactions, reactive gliosis, and cellular and neuronal apoptosis in both the brain and retina [43, 57]. At the very early disease stage, an increase in macular layer size is observed in amnestic MCI patients, which may correspond to inflammatory processes and/or gliosis [58]. Also, astrocytes induce the release of vascular factors such as prostaglandins, NO, and arachidonic acid, which may lead to neurovascular dysfunction in AD as indicated by pathological and experimental studies [59–61]. Similarly, it has been shown that levels of complement (C1q) are elevated in close vicinity to amyloid plaques and astrocyte processes in transgenic mice [62]. In addition, C1q activation generates endothelial cell adhesion in human dermal microvascular endothelial cells [63]. Together, these mechanisms may affect retinal vessels and metabolic supply and increase metabolic injury in the GCL of the retina in the early stage of AD as well as during MCI (Figure 1).

Several studies in humans and animal models have identified Aβ plaques in the photoreceptor layer, GCL, NFL, IPL, and outer plexiform layer (OPL), which manifest at the early stage of disease, even before the appearance of neurological symptoms [64–66]. The retinal and visual effects of these plaques are not entirely clear, but activation of astrocytes and microglia, together with neuroinflammatory changes induced by Aβ, lead to an initial increase in the retinal epithelium (RPE) and GCL degeneration in a transgenic rodent model of AD [64, 67]. In addition, an increase in the number of astrocytes and astrocyte/neuron ratio (which is associated with increased neuronal loss), especially in the superior and inferior quadrants of the retina, has been reported in humans [68]. Similar changes where neuronal numbers are reduced and nonneuronal cells are increased have been observed in human brain regions such as the hippocampus and cerebral cortex [69], as well as in the visual cortex [70]. Nonetheless, despite the previous observations of Aβ effects on the eye, there are limitations to mimic the clinical findings in animal models, which may point to other endogenous mechanisms present in these models and diverse adaptive changes in early phases of AD [71, 72]. Additionally, it is noteworthy to remark that Aβ aggregation was also shown within the eye of individuals undergoing normal cognitive aging; however, this pathophysiological process is quite distinct from the one described in patients suffering AD as it is discussed below in Section 2.4.

2.3. Tau Mechanisms in the Retina. One of the hallmarks of AD is the presence of intraneuronal hyperphosphorylated tau protein. These tau oligomers assemble in large insoluble fibrillar structures, known as NFT, and spread between cells in both the brain and retina. Tau oligomers seem to be one of the main structures that promote inflammation in the retina at the early disease stage. Tau oligomers induce neuroinflammation in a perpetuating feed-forward cycle, propagating neural damage, augmenting tau oligomer production, and consequently triggering the appearance of more inflammation [73]. Other studies detected tau accumulation in the retina at an early phase of AD: before the onset of cognitive impairment and even before tau aggregation in the brain in the mouse model of AD. In the retina, tau accumulates principally in GCL dendrites and intraretinal axons, but is depleted in optic nerve axons [74]. Some studies have demonstrated predominant accumulation of tau in GCL, but it has also been observed in the INL, IPL, OPL, and NFL [65, 75]. Conversely, hyperphosphorylated tau has not been found in other structures such as optic nerve, cornea, and lens in AD transgenic mice [76, 77]. Tau accumulation causes dysfunction in anterograde axonal transport, which is a feature of neuronal impairment that occurs before the appearance of retinal cell death [74]. Tau aggregation inhibits mitochondrial transport towards the GCL periphery, leading to loss of energy production and formation of reactive oxygen species (ROS). Altogether, retinal neurons in AD tend to be more susceptible to OS, produce hyperphosphorylated tau aggregates, and prolong the delay in vesicular transport that is necessary for synapse function and cellular growth [75]. Future studies comparing tau aggregation between AD patients, MCI, and individuals undergoing healthy aging could be useful to clarify if tau plays any role in retinal changes in AD pathology.

2.4. Aβ, Aging, and Age-Related Macular Degeneration. During aging, the brain and retina develop extracellular deposits recognized as plaques and drusen, respectively.

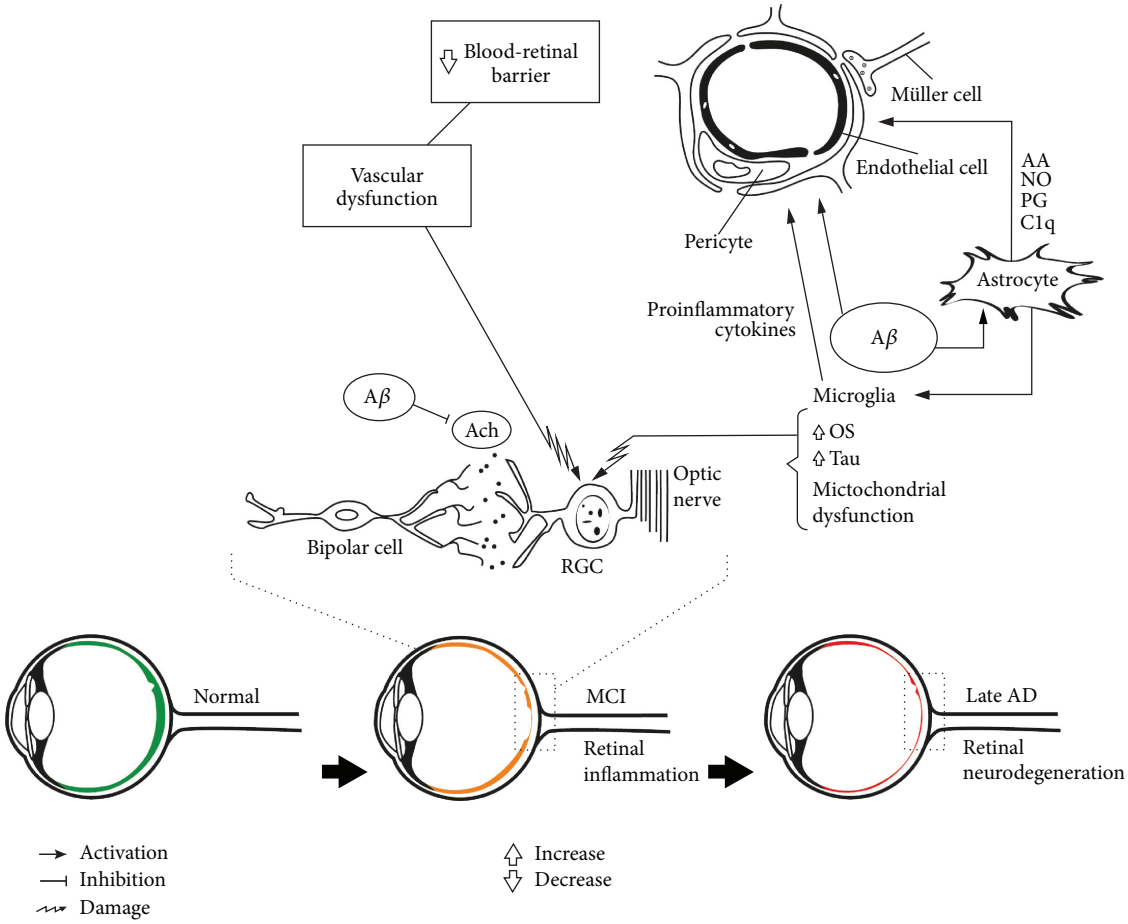

Figure 1: Pathophysiological events in the retina during Alzheimer's disease progression. Amyloid-beta (Aβ) induces microglia and astrocyte activation, synaptic dysfunction, and neurodegeneration. These interactions can be observed by noninvasive ophthalmological examinations in the retina at different stages of Alzheimer's disease (AD). Reduction in the peripapillary region and macular volume has been described in MCI and AD. AA: arachidonic acid; Aβ: amyloid-beta; ACh: acetylcholine; AD: Alzheimer's disease; MCI: mild cognitive impairment; NO: nitric oxide; OS: oxidative stress; PG: prostaglandins; RGC: retinal ganglion cells.

"Drusen" in the retina are deposits of insoluble cellular debris and lipids localized beneath the RPE and inner collagenous layer of Bruch's membrane (BM) [71]. Two types of "drusen" have been identified (hard and soft which differ in their location, and in their clinical and morphological appearance). Both soft and hard "drusen" have similar compositions; however, some authors suggest that each type of "drusen" may be composed by a certain variety of proteins or may be constituted by different amounts of the same components. Differences in "drusen's" morphology, composition, physical properties, and location (peripheral or central) could most likely be based on different formative mechanisms that may contribute to macular susceptibility for age-related macular degeneration (AMD) progression. Although "hard drusen" can appear everywhere in the retina, they are usually located in the peripheral retina and are characterized by hemispherical structures with well-defined borders. "Hard drusen" are considered part of the normal aging process. "Soft drusen" are located exclusively in the macula, characterized by poorly defined borders and larger size [78]. They are linked to the early stage of AMD [72, 79]. AMD is a slow, progressive disease that compromises the macula and the primary cause of irreversible blindness during aging [43].

Two types of AMD have been described: dry AMD type, characterized by significant atrophy of RPE and the photoreceptor layer, and wet, or exudative, AMD type, with invasive blood vessels through the blood–retinal barrier [43]. These invasive vessels come from the choroid and proliferate in the retinal layers between BM and RPE or sometimes proliferate between RPE and the neurosensory retina. In turn, this leads to vascular leakage and fluid accumulation, with formation of fibrovascular disciform scars in the retina that can be observed by ophthalmoscopy [79].

The extracellular deposits in the brain and retina share the presence of Aβ, ApoE, proteoglycans, immunoglobulins, metal ions, acute-phase reactants, fibrinogen, prothrombin, membrane debris, and protease elements [43, 72]. Aβ formation is found in both AD and AMD, suggesting a common mechanism related to proteinopathic Aβ1–42 peptide deposition [80, 81] and imbalance between increased Aβ synthesis and reduced Aβ removal [12]. Specifically, in the aging eye, Aβ accumulation occurs primarily in the outer segments of photoreceptors and at the interface between RPE and BM

[82]. This process appears to initiate at the apical region of the outer segments and progresses through the retinal layers with age, also accumulating in choroidal blood vessels. In drusen, Aβ is localized in vesicular components known as "amyloid vesicles" or "amyloid assemblies" [43, 78] and exhibits several shapes, diameters, and fusion processes. In addition, some drusen are described as a single large vesicle occupying a sizable portion of the drusen, or densely packed with several amyloid vesicles [43]. Amyloid vesicles are formed by amyloid oligomer cores composed of toxic oligomeric Aβ1–42 peptides that are centrally organized in a ring structure [82], in close proximity to the inner collagenous layer of BM [71]. Aβ1–42 interacts with different drusen components, including complement proteins (HF1, C3b/iC3b, and C5), interleukins (IL-1β, IL-8, and IL-33), and lipids (cholesterol and phosphatidylcholine) to form mature Aβ fibrils, which compose the shell of amyloid vesicles [43, 82].

Overall, these interactions increase ROS production, which contributes to formation of glycation and lipoxidation end products [79]. Additionally, it is hypothesized that Aβ promotes retinal microglia translocation from the inner retina (normal position) to the subretinal space, inducing changes in RPE cells and leading to secretion of proinflammatory, chemotactic, and proangiogenic molecules [82]. Furthermore, complement proteins appear to play a key role in the pathophysiological mechanisms of AD owing to activation by membrane proteins, lipids, cholesterol, and Aβ deposits. Complement molecules promote inflammatory stimuli [72], disrupt the RPE junctional complex [82], impair trans-epithelial permeability, and induce mitochondrial damage. Moreover, they also promote an increase in angiogenic factors, such as vascular endothelial growth factor (VEGF), and decrease in anti-angiogenic factors, such as pigment epithelium-derived factor [43, 83].

The role of tau in AMD is debated and likely underestimated, as tau has not been found in drusen, but has been reported in OPL, INL, IPL, and NFL of patients with AD. Some studies suggest that tau aggregation in aged retina causes defective transportation of molecules, cells, and proteins, which may promote drusen formation and subsequently AMD [75].

2.5. Apolipoprotein E Mechanisms. ApoE is involved in the transport of cholesterol and triglycerides and is considered one of the most important risk factors for development of AD [84]. ApoE protein is mainly expressed in the brain on astrocytes, but also in microglia, neurons, pericytes, smooth muscle cells, and brain endothelial cells [85]. Of the different ApoE alleles (ε2, ε3, and ε4), ApoE4 shows a strong relationship with increased risk of developing AD, while ApoE2 provides protection against AD [86]. ApoE4 interacts with Aβ to increase Aβ aggregation [87]. Furthermore, the risk of amyloidosis in AD is suggested to be related to the interaction between ApoE, aging, and amyloid burden [88].

ApoE4 is associated with vascular pathology in AD and promotes cerebral amyloid angiopathy. Further, ApoE4 is related to other vascular diseases such as atherosclerosis, stroke, cerebrovascular disease, and coronary heart disease. Consequently, it has been proposed that the pathological effects of ApoE4 are initiated by cerebrovascular insult, which subsequently leads to neurodegeneration. In the retina of transgenic mice, ApoE4 is implicated in reduced vascular density and increased vascular buds and branching in early postnatal days, which ends during the neonatal period. These findings are associated with decreased synaptic expression after the neonatal period, due to low VEGF levels in ApoE4 models. VEGF is implicated in angiogenesis and vascular plasticity and as a neuronal growth factor in retina development. This determined that ApoE4 has transitory synaptic and vascular effects during retinal development, before and after the neonatal period, respectively. Moreover, VEGF in aged retina has proangiogenic effects that promote macular edema, diabetic retinopathy, and macular holes [89, 90].

ApoE can be expressed in RPE, GCL, and BM and is synthesized in Müller cells [89]. ApoE is involved in uptake, processing, transport, and clearance of lipids for retinal metabolism; therefore, disturbance of this process may lead to cholesterol and lipid accumulation in BM [43]. Distinct to AD, ApoE4 confers protection against AMD because it improves BM permeability, facilitates lipid transportation, and consequently leads to reduced debris accumulation in drusen formation. In contrast, ApoE2 increases the risk of AMD apparition because it induces VEGF as a proangiogenic agent [43, 89, 91, 92]. Contradictorily, some studies have shown increased AMD in AD patients [93], while others show no association [94].

3. Functional and Pathological Findings in the Visual System

Neuronal and synaptic dysfunction in AD may compromise visual system pathways in associated cortical and subcortical brain structures, as well as peripheral nerves. Complex visual disruptions are described in AD, which are related to neural dysfunction and modifications in varied eye structures. Depending on the area affected, these lead to diverse clinical manifestations, making the visual system a potential diagnostic aid [95].

3.1. Cortical, Subcortical, and Brainstem Regions. Aβ and NFT aggregation as well as neurodegeneration and axonal damage are found in different brain structures related to visual system functioning [50]. For instance, in the primary cortex (Brodmann areas 17 and 18) of AD patients, has been described a decrease in neuronal density, and increase in glial density only in area 17. These cellular changes are related with the presence of Aβ-plaques and NFT [70]. In the case of the secondary visual cortex, involvement of the cuneal and lingual areas of the occipital lobe of AD cases may correspond with impairment in selective visual attention, emotion, and visual processing [96–98]. Meanwhile, reduced glucose metabolism in the visual association cortex and inferior parietal cortex might be related to abnormalities in figure copying, color vision tested by isochromatic plates, and stereopsis [99].

Regarding subcortical structures, Aβ aggregation and neuritic plaques have been found in the pulvinar nucleus of

the thalamus of AD postmortem samples. This nucleus participates in visual attention and in the control of eye movements [100]. Similarly, amyloid pathology in the lateral geniculate nucleus of the thalamus, the initial processor of visual information, has been reported. In this regard, a reduction in the number of parvocellular neurons and magnocellular gliosis was found [101]. Indeed, the magnocellular system is involved in recognition of movement, spatial perception, and luminosity, meanwhile parvocellular on identification of color and form. Correspondingly, color and motion perception is affected in AD patients [21]. Another structure involved would be the suprachiasmatic nucleus, responsible of the circadian cycle, sleep, melatonin secretion, pupil regulation, and learning. In fact, clinical and animal models of AD indicate severe disturbance in the circadian rhythms, as well as neurodegeneration in brain structures which control those cycles [102–105]. Altogether, cortical and subcortical dysfunction of the visual system may partially explain the difficulties AD patients have with writing, reading, color and structure differentiation, facial recognition, and visual acuity.

Amyloid aggregation, NFT, and neuritic plaques in the superior colliculus, responsible for the onset of ocular movements, have been reported in postmortem samples from the brainstem of AD patients [106, 107]. Accumulation of Aβ has also been observed in the Edinger-Westphal nucleus of the parasympathetic oculomotor system (which is responsible for pupillary constriction), resulting in degeneration, neuronal loss, and decreased acetylcholine (ACh) in this nucleus, with consequent pupillary reflex alterations [22, 46]. The sympathetic system, involved in the dilatation of the pupil, is also affected in more advanced AD stages [46].

ACh is well known as an excitatory neurotransmitter in the learning and memory process [108] and is compromised in AD. Indeed, changes in neurotransmitter function may explain retinal and visual dysfunction in early AD and MCI before neurodegeneration is established. Different studies have shown neurotransmitter synthesis in amacrine cells, and nicotinic receptors in bipolar cells, horizontal cells, photoreceptors, and the GCL [108, 109]. In the retina of a transgenic mouse model of AD (Tg-SwDI), specific cholinergic cell loss together with reactive gliosis was found [108]. Cholinergic dysfunction induced by Aβ is established at distinct levels: neurodegeneration of cholinergic cells [110], ACh depletion [111], impaired ACh release [112], and finally Aβ-induced impairment of muscarinic [113] and nicotinic acetylcholine receptors (e.g., α7-nAChR) [114], as well as associated effectors (e.g., potassium voltage-gated channels, KCNQ) [115–117]. In older animal models, downregulation of α4, α7, α9, and α10 nAChR, and m4 and m5 muscarinic acetylcholine receptor (mAChR) subunits, was found. These changes are observed in photoreceptors and INL cells, accompanied by cholinergic cell loss in the retina [108]. Contrast sensitivity and visual attention has been found to be deteriorated in AD patients [118]. In this regard, the use of cholinergic drugs such as donepezil leads to improvement in visual selective attention [119]. Similarly, donepezil also increases contrast sensitivity and accuracy in non-AD subjects [120]. Therefore, the stimulation of the cholinergic system in AD patients not only may generate improvement in learning and memory processes but also might improve visual alteration at retinal, subcortical, and cortical levels.

3.2. Retina. In the retina, GCL, NFL, IPL, and the photoreceptor layer can generate Aβ, as each layer expresses APP [30]. As described earlier, aberrant APP cleavage leads to neurotoxic Aβ aggregation, enabling inflammatory processing, degeneration, and thinning in all quadrants of the retina in these layers, but mainly in the superior and inferior quadrants. These layers are present in a third of the macula; therefore, any alterations can contribute to reduced macula and fovea volume, which may partially explain the ocular manifestations that these patients exhibit [25, 48, 121–124]. Study in retinas from postmortem patients with AD found a reduction in the number of GCL neurons related to progressive aging [125]. In contrast, GCL thinning was aggravated in patients with AD and not related to aging in other studies [126]. AD ocular findings in human studies are summarized in Table 1, and findings in animal studies are summarized in Table 2.

3.3. Optic Nerve. Analysis of the optic disc has been performed in AD patients, with increased cup-to-disc ratio [50], higher pallor area-to-disc area ratio, and decreased disc rim area of the optic nerve observed as indirect signs of axonal damage [21, 127, 128]. These optic nerve alterations are due to degeneration of axons and larger cells of the GCL and NFL [127] in the central and peripheral portions of the retina, which are involved in the magnocellular pathway and ensure greater optic nerve caliber [129]. In addition, reduced hemoglobin percentage in the neuroretinal rim and increased cup-to disc ratio (by 39%–43%) have been demonstrated [128, 130, 131]. Nonetheless, despite significant reduction of the density of axons from the optic nerve in AD when compared with the age-matched control subjects, no correlation between optic nerve volume and cerebral volume in AD patients was observed [132].

3.4. Retinal Vasculature. Regarding the vasculature, Aβ protein can be found in the walls of retinal blood vessels. Its integrity is important in maintaining the blood–brain barrier [44]. However, with aging, Aβ protein aggregates and accumulates in blood vessels of the cerebral and retinal vasculature [126]. As already described, retinal microvasculature has the same embryological origin as brain microvasculature, sharing disease-specific pathological mechanisms [44]. Different clinical studies have shown venular narrowing [133] with a decrease in flow, vessel diameter [134, 135], arteriolar–venular fractal dimension [133], and branching pattern [136] in AD. Similarly, increased arterial tortuosity has been observed in clinical studies [133], with standard deviation of vessel width [136] and amplitude of arterial pulsation [126, 133, 136, 137]. Moreover, these findings relate to cognitive impairment, disease progression, and reduction in NFL diameter in the superior quadrant [21, 26, 27, 138–140]. Although other studies differ in these conclusions, no significant variations were shown for

Table 1: AD ocular findings in human studies.

Ocular histopathological hallmarks in human studies				
Ref.	Population (mean age, range years)	Tissue analyzed	AD stage (early vs. late-onset)	Findings
Williams et al. 2017 [198]	AD $n = 17$ (77) Controls $n = 2$ (77)	Retina, lens, and optic nerve	Late	No presence of tau, Aβ, ubiquitin, TDP-43, or a-synuclein.
Tsai et al. 2014 [67]	AD $n = 10$ (63–95) Control $n = 10$ (63–95)	Nasal and temporal regions of the retina	NS	Aβ plaques in retina and reduced choroidal thickness.
Ho et al. 2014 [204]	AD $n = 11$ (82/61–92) Controls $n = 6$ (74/66–86)	Peripheral nasal retina, posterior retina including the macular region and optic nerve head, and peripheral temporal retina	Late Definite AD ($n = 9$) Probable AD ($n = 2$)	Cytoplasmic α-synuclein positivity, but not Aβ deposits and abnormal tau accumulation.
Schön et al. 2012 [77]	AD $n = 6$ (37–79) Controls $n = 4$ (53–60)	Retina	Early and late	Hyperphosphorylated tau but no Aβ plaques or fibrillar tau aggregates.
Koronyo-Hamaoui et al. 2011 [66]	AD $n = 8$ (80/48–94) $n = 5$ (79/65–92) Controls $n = 5$ (76/66–85)	Retina	Late ($n = 9$) Early ($n = 1$)	Aβ40 plaques.
Syed et al. 2005 [205]	AD $n = 12$ (81.9 ± 6.54/69–84) Controls $n = 13$ (78.5 ± 8.57/66–82)	Optic nerve	Late	The density of axons was reduced in both the center and peripheral portions of the optic nerve with preferential loss of the smaller-sized axons.
Blanks et al. 1996 [68]	(GFAP-ir) AD $n = 12$ (64–88) Controls $n = 19$ (63–89) Neuronal and cell numbers (GCL) AD $n = 11$ (16 retinas 45–92 years) Control $n = 9$ (11 retinas 60–89 years)	Retina	Late	Extensive neuronal loss in the entire retina (36.4%), most pronounced in the superior and inferior quadrants, throughout the midperipheral regions (40–49%), and in the far peripheral inferior retina (50–59%). Increase in the astrocyte : neuron ratio. Also, more extensive labeling of glial fibrillary acidic protein immunoreactivity (GFAP-ir) in astrocytes in the GCL, in the Müller cells, and in radial processes.
Curcio and Drucker [206]	AD $n = 4$ (67–86) Controls $n = 4$ (66–86)	Retina	Late	No evidence of GCL loss between AD and controls.
Blanks et al. 1991 [207]	AD $n = 11$ (13 retinas 83/69–93 years) Controls $n = 11$ (14 retinas 78/60–98 years)	Retina	Late	The fovea shows a loss of neurons within the GCL, mainly in large and small ganglion cells.
Sadun and Bassi 1990 [129]	AD (10 optic nerves, 3 retinas 76–89 years) Controls (8 optic nerves, 2 retinas 70–79 years)	Optic nerve and retina	Late	Predominant loss of the largest class of retinal ganglion cells (M cells). Retina of 1/3 AD patients also showed degeneration of GCL and their axons in the NFL.

Table 1: Continued.

Ocular histopathological hallmarks in human studies				
Ref.	Population (mean age, range years)	Tissue analyzed	AD stage (early vs. late-onset)	Findings
Blanks et al. 1989 [208]	AD $n = 16$ (76–93) Controls $n = 19$ (60–91)	Optic nerve and retina	Late	Degeneration in the GCL is characterized by a vacuolated appearance of the cytoplasm. Absence of neurofibrillary tangles, neuritic plaques, or amyloid angiopathy.
Hinton et al. 1986 [128]	AD $n = 10$ (10 optic nerves, 4 retinas 73–89 years) Controls $n = 10$ (73–89)	Optic nerve and retina	Late	Widespread axonal degeneration in optic nerves, decreased in the number of cells in GCL, and reduction in the thickness of NFL. There was no retinal neurofibrillary degeneration or amyloid angiopathy.

Table 2: AD ocular findings in animal studies.

Ocular hallmarks in experimental animal models		
Ref.	Model	Findings
Oliveira-Souza et al. 2017 [108]	Tg-SwDI mice 6.5 to 15 months	Upregulation of AChR gene expression and significant cell loss in the photoreceptor layer and inner retina on young groups. Specific cholinergic cell loss and increased astrocytic gliosis in the middle-aged and AChR downregulation in older adult groups.
Joly et al. 2017 [209]	Tg APPswe/PS1DE9 mice 3 to 13 months	No Aβ or amyloid plaques were detected in the Tg retinas. However, the CTFb/CTFa ratio was significantly lower. Response mediated by cones was preserved. Retinal-specific processing of amyloid may confer protection against AD and selectively preserve cone-dependent vision during aging.
Nilson et al. 2017 [73]	P301L mouse Htau mouse	Tau oligomers colocalize with astrocytes, microglia, HMGB1, and inflammatory cells in the retina.
Chiasseu et al. 2017 [74]	3xTg mice 3 to 6 months	Age-related increase in endogenous retinal tau accumulation, previous to the reported onset of behavioral deficits, and tau aggregation in the brain. Tau build-up occurred in GCL soma and dendrites, but not in axons.
Chidlow et al. 2017 [56]	Tg APPSWE/PS1ΔE9 mouse 3 to 12 months	No presence of amyloid plaques, dystrophic neurites, neuronal loss, macro- or microgliosis, OS, tau hyperphosphorylation, or upregulations of proinflammatory cytokines in the retina.
Gupta et al. 2016 [47]	Tg APP/PS1 mice 13 to 16 months	Increased Aβ deposition in the retinas with thinning in inner retinal layers and decline in scotopic threshold response. Reduction of axonal density in the optic nerve.
Du et al. 2015 [65]	*Octodon degus* 6.7–70 months	Aβ deposition in the inner and outer segment of the photoreceptors, NFL, and GCL. Aβ expression was higher in the central retinal region than in the retinal periphery. Phosphorylated tau was seen more consistently in NFL-GCL regardless of age.
Pogue et al. 2015 [80]	Tg 5xFAD Tg-AD mice 0–5 months	Presence of Aβ42 peptides in the brain and retina, accompanied by inflammatory markers such as cyclooxygenase-2 and C-protein reactive.
Maharshak et al. 2016 [90]	ApoE3 and ApoE4 targeted replacement mice 4–7–12–120 days old	Transient changes in vascular branching and decrease in retinal synaptic density in the apoE4 mice. Additionally, lower levels of retinal VEGF were observed in apoE4 mice compared to the ApoE3 mouse retinas.
Tsai et al. 2014 [67]	TgF344-AD rat 14–19 months	Reduction in choroidal thickness, hypertrophic retinal pigment epithelial cells, inflammatory cells, Aβ plaques, and upregulation of complement factor C3 in the retina.
Williams et al. 2013 [210]	Tg 2576 mice 14 months	No significant changes in GCL synaptic densities but a highly significant change in mitochondrial morphology. GCL dendritic atrophy preceded cell loss, and this may be due to the accumulations of Aβ.
Zhao et al. 2013 [76]	Tg APP/PS1 mice	Hyperexpression of phosphorylated tau was detected in retina, accompanied with an increase in senile plaques and NFTs. The increased tau phosphorylation was associated with a significant augment in the production of p35 and p25, and upregulation of calpain.
Schon et al. 2012 [77]	Tg P301S mice	*In vivo* detection of fibrillar tau in the retina and the progression of tau pathology over several months was demonstrated.
Koronyo-Hamaoui et al. 2011 [66]	Tg APPSWE/PS1ΔE9 mouse 7–17 months	Retinal Aβ plaques were detected following systemic administration of curcumin in Tg, previous to the appearance of Aβ plaques in the brain.
Perez et al. 2009 [64]	Tg APPSWE/PS1DeltaE9 mouse 12–19 months	Aβ plaques appeared in the OPL and IPL of the retina, displaying syntaxin 1 and ChAT, but no neuronal degeneration was observed. ERG revealed reduction in the amplitudes of a and b waves.

arteriolar–venular caliber, branching angle, or venular tortuosity in AD patients [133].

4. Visual Impairments in AD: Clinical Features

AD affects different structures of the visual system in a similar pathological manner as the brain, with manifestation of distinct signs and symptoms that can be determined by adequate clinical history and ophthalmological examination. To our knowledge, there are no studies showing the chronological clinical manifestations specifically correlated with changes in the retina in patients with AD. Therefore, it is important to conduct clinical prospective studies in order to clarify this aspect. Regarding structural changes in the retina, thinning of the superior or inferior quadrants has been described in AD patients associated with visual field impairment. Other visual findings have been correlated with alterations in the brain [141]. Regarding early visual manifestations, it has been observed that contrast sensitivity is the first visual dysfunction found in animal models and AD patients [142, 143]. The rest of visual symptoms are evident depending on the compromised brain structure [22, 95, 144].

Complex visual disturbances are described in patients with AD, including constructional and visuoperceptual disorientation, specifically difficulties in searching for objects (figure–ground discrimination), finding their way in familiar surroundings (environmental agnosia) [99, 145], and spatial recognition or spatial order memory (spatial agnosia) [146]. Additionally, distinct alterations in daily life activities due to deterioration in visual attention [147] and impairments in tasks requiring semantic access from visual information (e.g., disproportionate reading [148] and facial recognition [149]) are observed. With facial recognition, transient misidentification, abnormal self-identification, Capgras syndrome (denial of a familiar person and identifying them as a replacement, imposter, or double), and in some cases prosopagnosia (disordered recognition of familiar faces) have been described [150]. These disturbances are due to disordered visual processing because of disrupted cortico-cortical projections as a result of alterations in cortical and visual pathways (i.e., occipito–parietal and occipito–temporal) [151, 152]. Disordered visual processing can lead to complications in perceiving and comparing visual stimuli, alterations in processing visual stimuli, and impairments in long-term memory and generating verbal or action responses [148].

Another visual disturbance identified in AD is Balint's syndrome. This is an uncommon and incompletely understood visuospatial defect reported in patients with bilateral parieto-occipital damage associated with Brodmann's area 7b in the posterior parietal lobe (which is involved in control of pursuit ocular movements and target gaze on a stimulus) and superior occipital cortex areas 17, 18, and 19 (which are involved in visual field construction) [153]. Balint's syndrome is characterized by simultanagnosia (difficulties in locating, reaching, or attending to multiple items in a visual space), ocular motor apraxia (inability to maintain fixation on a specific point located in the peripheral visual field), and optic ataxia (inappropriate coordination of voluntary movements in response to a visual stimulus) [149].

Recently, alterations in ophthalmologic examination of AD patients have been described. These alterations include decreased visual acuity, with difficulties in writing and reading [154] increasing along with disease progression [139, 155, 156]. Similarly, compromised contrast sensitivity (ability to distinguish an object on a background of different frequencies) [142–144, 157] has been observed as a principal manifestation during the initial disease stage, with progressive impairment throughout the disease course [143]. Contrast sensitivity is associated with damage to the magnocellular pathway in the geniculate nucleus of the CNS, which is involved in the ability to identify luminosity and motion perception [158]. Another manifestation in AD patients is fluctuations in color perception, mainly errors in color recognition, due to involvement of the parvocellular pathway, which is characterized by smaller axons of the optic nerve [159]. Additionally, pupillary reflex deficits are reported as a deficiency of the sympathetic and parasympathetic systems, with the principal findings being decreased amplitude, speed, and latency of reflexes. Further, smaller resting pupil diameter and maximum dilatation velocity in the dark [160] as well as reduced amplitude and 75% recovery time of the light reflex response [22, 160] are also reported. Other abnormalities in ocular movement, decreased movement perception, and stereopsis dysfunction have been observed in patients with AD [46]. These abnormalities include inability to focus on an object (less relative fixation time) [161], irregular convergence angle, difficulty performing saccadic ocular movements [162, 163], poorer heading and speed perception at lower temporal periodicity [24], and inability to identify three-dimensional objects [164]. Finally, loss of the visual field mainly occurs in the inferior quadrant and is related to GCL damage in the superior quadrant of the corresponding retina [96]. Visual field loss is characterized by accumulation of larger SP and greater amounts of NFT in the cuneal gyrus than lingual gyrus of the visual cortex, which is where nerve fiber projections of the GCL in the superior and inferior quadrants terminate, respectively [135].

5. Paraclinical Visual Studies in AD

Different noninvasive imaging methods have been developed to study structures of the visual system and visual pathways in AD patients. In this section, we describe findings obtained by optical coherence tomography (OCT) and bioelectrical changes through electrophysiological examinations, specifically electroretinograms (ERG) and visual evoked potentials (VEP).

5.1. Optical Coherence Tomography in the Retina. In the retina, different OCT methods based on cross-sectional images of the retinal layers have been performed in AD patients, including spectral domain-optical coherence tomography (SD-OCT). Using SD-OCT, thinning and thickening of NFL in the superior and inferior quadrants, respectively, of the nasal and temporal regions were related [165] to cognitive impairment [131, 166, 167]. Degeneration of NFL,

GCL, and IPL has been related to AD duration, with longer disease duration associated with greater damage to the retinal layers. The most affected quadrants were the temporal, temporal–inferior, and temporal–superior sectors, with increased nasal/temporal ratio reflecting higher temporal sector commitment. In addition, reduction of the GCL was associated with axonal degeneration, which may predict greater disease severity [168].

Among other OCT studies, progressive compromise of the NFL was shown between an intermediate group with MCI and different disease stages. Thinning of NFL in the superior quadrant was gradually affected among patients with MCI and mild AD. The inferior quadrant was involved in severe disease stages, demonstrating engagement of the NFL throughout disease progression [169]. In addition, another study detected a decrease in NFL in AD and MCI groups in the inferior quadrant, with the superior quadrant significantly compromised in AD patients only [170]. Contrarily, NFL thinning was evident in all MCI and AD groups, indicating that NFL involvement is observed in the early disease stage [171]. Furthermore, significant NFL thinning was identified in patients at the early stage of AD [165]. A meta-analysis of 51 articles in the last 5 years recognized that loss of NFL mainly occurred in the superior quadrant, yet corresponded to visual field impairments in the inferior quadrant. This deterioration in NFL was related to disease duration in AD [140].

When comparing AD patients and healthy controls, a significant NFL reduction has been observed in AD patients, more prominent in the inferior [172, 173] and superior quadrants [140, 174]. A meta-analysis including 887 AD patients and 864 controls evidenced peripapillary NFL thinning in the superior and inferior quadrants of the retina in AD patients that was not present in controls [175]. Additionally, AD patients had reduced thickness in GCL, NFL, IPL, and outer nuclear layer (ONL) compared with controls [176].

In contrast, a relationship between NFL involvement (through OCT) and cognitive impairment by Mini-Mental State Examination (MMSE) was reported in AD patients, suggesting that measurement of NFL may be used as a disease progression marker [177]. However, other studies have observed NFL thinning in all quadrants, especially the nasal region, with no relationship to the MMSE and AD severity [178].

5.2. Optical Coherence Tomography in the Macula. The macula is the principal structure affected at the early stage in AD patients. By OCT, decreased macula volume was observed in the four internal quadrants and one temporal external quadrant, with no significant difference in decrease in peripapillary region volume in AD patients [179]. However, a recent meta-analysis has shown that AD and MCI patients had lower peripapillary retinal NFL compared with controls [180]. Using SD-OCT, increased macular size and IPL was shown in patients with MCI and those at risk of developing AD, suggesting an inflammatory process and reactive gliosis in the early disease stage before establishment of AD [172, 174]. Conversely, macular thinning was identified in MCI [178] and in all sectors except the fovea, mainly in NFL of the superior quadrant in AD [156]. Decreased IPL in the inferonasal, inferotemporal, and superotemporal sectors was observed, as well as reduced NFL in the temporal sector in patients with MCI who developed AD two years later. Corroboratively, these results were related to cognitive impairment [176]. Macular atrophy has been described as the first manifestation in patients with AD and is related to degree of cognitive impairment in the MMSE [140]. By frequency domain optical coherence tomography in AD, NFL, GCL, and IPL are shown to be reduced in size in the macula, except in the inferior external quadrant. Again, this thinning is related to MMSE results [181].

5.3. Optical Coherence Tomography in the Choroid. Choroid reduction and thinning are observed in AD. Using SD-OCT, thinning of the choroid was measured in the macula at 13 locations (separated by 500 mm) in elderly compared with healthy subjects. A significant decrease in the choroid was shown in all 13 locations, but principally in two locations temporal to the fovea. This indicates that compromise in the choroid is not related to age [182]. By OCT examination over a period of 12 months, greater choroid reduction was characterized in AD patients compared with controls of the same age [183]. Another study measured thickness of GCL in the macula, the choroid, and external retina, and compared them with MMSE results. GCL thinning in the superior and inferior quadrants of the macula was observed, with significant thinning of the choroid in all regions. Further, a relationship was observed between GCL thinning in the macula and MMSE results, but not with choroid thinning, which was unrelated to severity of cognitive damage [173].

5.4. Electrophysiological Examination. Electrophysiological examinations (i.e., bioelectrical changes in the visual system) such as VEP and ERG have been performed in patients with AD [140]. VEP extracts signals directly from the visual cortex, which are dependent on adequate integrity of the visual system (eye, retina, optic nerve, and visual cortex). In patients with AD, decreased amplitude of P2 or P100 components are observed at 100 ms [45, 46, 48, 96, 138–140, 175, 184–186]. Yet, other studies have shown no changes in pattern-VEP nor association with NFL thinning [187] in the peripapillary or macular regions [188].

The pattern ERG (PERG) test presents three peaks: negative–positive–negative, which are observed at 35–50–95 ms, respectively [46]. Most studies show decreased amplitudes and time delays, mainly in N35, P50, and N95 components, in PERG of patients with AD [140, 189]. In contrast, only reduced P50–N95 amplitudes with increased implicit P50 time [190] were shown in other studies, while a compromised magnocellular pathway was also reported [158]. All these findings relate to damage at the GCL level (N95) [190]. Conversely, further studies detected no PERG changes [191]. In another type of exam, the multifocal ERG, which evaluates macula functionality, even in early or intermediate states of the disease in patients with AD, a statistically significant reduction in the electric activity of the macula has been registered, especially in the foveal and parafoveal regions, due to the decrease in the amplitude of the P1 component

[145]. In PERG, reduced mean amplitudes in these components were observed in patients with AD. This anomaly may be due to axonal depletion within the optic nerve as well as GCL degeneration [192]. Additionally, PERG at different frequencies showed amplitude reductions at high frequencies in patients with AD [193]. In other types of examination, namely, pattern-reversal VEP and ERG, no alterations were detected, but delays were occasionally demonstrated in the second positive component of flash VEP [192]. Scotopic and photopic flash ERG and oscillatory potentials show no alterations between both methods in patients with AD, suggesting no visual pathway involvement [194]. With VEP, decreased latency in the magnocellular pathway was observed in AD patients [158].

6. Future Clinical Directions

The clinical study of the visual system offers several benefits owing to the relatively scarce invasiveness of the examination, as well as the associated low cost of procedures. Structural eye components such as the cornea, lens, retina, and optic nerve can be observed with an ophthalmoscope. Additionally, functional aspects related to autonomic features, such as pupillary reflex, can be directly studied. Further, a wide array of visual paraclinical tests have been developed including VEP, ERG, tonometry, and OCT. These procedures are not limited to evaluating aspects of the visual system and can also be used to examine neurological or systemic components of many conditions. This has led to the proposition that studying the visual system is a helpful and complementary approach with biomarker potential in neurodegenerative conditions, including AD [45]. Many visual changes manifest in AD patients (as already discussed), including alterations in visual acuity, color perception, contrast sensitivity, the visual field, pupillary reflexes, ocular movements, and stereopsis. All can be examined by simple, noninvasive, and easily accessible methods such as adequate ophthalmologic examination, OCT, and electrophysiological examinations. These are supporting diagnostic tools that could potentially even be used in the early disease stage. Current biomarkers for AD tend to be either expensive or invasive, and in particular for countries with poor and inadequate healthcare systems. Moreover, no current biomarkers predict with absolute confidence, conversion of MCI to AD, or development of sporadic AD. For a recent review on the advantages and disadvantages of current AD biomarkers, refer to [20]. Several findings in the visual system point to the useful role of eye examinations for determination of AD. One of the challenges of this approach is to differentiate changes related to normal aging from those of pathological origin. To date, three structural components of the eye, the retina, eye vasculature, and lens, have emerged as interesting research areas in AD [45].

Study of the retina and associated structures has shown AD-related changes in preclinical (phase 1) animal exploratory models, thereby providing hints for their utility as biomarkers in humans. Many of these studies have been performed in transgenic humanized rodent models expressing AD characteristics. Accumulation of Aβ in plaques was observed at 12 months in the retina of transgenic APPswe/PS1ΔE9 mice. These plaques localized mainly in the OPL and IPL and increased in number and size with age [64]. Similar results were also observed in transgenic APPswe/PS1ΔE9 rats, with Aβ plaque-like structures present in the retina, together with choroidal thinning [67]. Aβ peptides were observed in the inner and outer segments of photoreceptors, NFL, and GCL, with higher expression in the central retinal region, in the Chilean rodent, *Octodon degus* [65], which has been suggested as a possible natural model of AD [195]. Some studies in transgenic mice have even reported earlier appearance of plaques in the retina than brain [42]. Furthermore, changes in retinal plaques can be individually monitored in real time following glatiramer acetate immunization in mice [66]. Regrettably, these results using similar animal models have not always been consistent, with contradictory findings reported. In a recently published study on APPswe/PS1ΔE9 mice, researchers were unable to demonstrate the presence of amyloid plaques, dystrophic neurites, neuronal loss, macro- or microgliosis, aberrant cell cycle re-entry, OS, tau hyperphosphorylation, or upregulation of proinflammatory cytokines or stress signaling molecules in the retina [56]. Despite promising results obtained in preclinical models, more investigations are needed to address the reasons why AD-related changes are not constant in all animal models and explore the mechanisms inducing cellular and molecular alterations in the retina. Comprehension of these questions is vital if visual components are to be translated from basic science to clinical practice as reliable biomarkers.

Changes in the human retina have also been reported in relation to AD. A recent meta-analysis, which included 25 studies comprising 887 AD patients, 216 MCI patients, and 864 healthy controls, concluded that AD and MCI patients show decreased retinal thickness measured by OCT [180]. Another meta-analysis, which included a lower number of studies and patients, reached a similar conclusion, corroborating the role of OCT and retinal measurement in assessment of AD [123, 196]. Accordingly, retinal measurements in humans may help distinguish between different neurodegenerative conditions. Patients with frontotemporal degeneration have a thinner outer retina, including a thinner ONL. In contrast, AD patients tend to exhibit inner retinal thinning [197]. Despite these encouraging results, in a similar fashion to the animal models, some reports challenge this evidence. In a recent paper, Tau, Aβ, transactive response DNA-binding protein 43, ubiquitin, and α-synuclein were examined by immunohistochemistry in postmortem AD patient brains, showing no evidence of inclusions, deposits, or accumulation of other proteins in any part of the ocular globe [198]. As in preclinical experiments, human studies need to be expanded to clarify these controversial aspects of AD-induced changes in the retina and visual system.

Other aspects of the eye and visual system are also reported to show alterations related to AD, although the retina is the component that has been most thoroughly studied. In the lens, some but not all clinical studies show Aβ deposition [199], while others have concluded that cataract grade or lens opacity is unlikely to provide a noninvasive

measure of the risk of developing AD dementia [200]. These controversial results do not support the use of lens examination as a biomarker of AD, underscoring the importance of conducting more detailed, controlled clinical studies with a larger number of patients. Ocular vascular changes have also been reported in AD patients [26, 201], which suggest similar microvascular damage in the eye as the well-described cerebral amyloid angiopathy owing to vascular Aβ deposition [202]. Direct and minimally invasive observation of eye vasculature, mainly retinal, provides an advantage to using vascular changes as a marker of AD. Unfortunately, the current evidence is not strong enough to offer a definitive answer on using this approach as a biomarker for AD. A recent systematic review, which included all published studies applying fundus camera imaging to examine association between retinal vasculature/retinopathy and any form of dementia, found many inconsistent results regarding changes in vessel caliber, tortuosity, and fractal dimension, although the authors concluded that retinopathy was more prevalent in dementia [203]. One possible explanation for the variation in results was suggested to be the absence of histopathological confirmation of AD diagnosis as well as lack of dementia severity reports. However, some studies using immunohistochemistry have reported absence of markers for AD in the visual system (Tables 1 and 2). A recent investigation done on postmortem eye tissue obtained from AD patients failed to report any indication of tau, Aβ, TDP-43, ubiquitin, or α-synuclein and showed no evidence of inclusions, deposits, or other protein accumulation in any region of the globe [198]. A similar result was obtained in another postmortem study, where no Aβ deposits or abnormal tau accumulations were detected in the lens, retina, or other structures in the eyes of AD patients [204]. Another study found hyperphosphorylated tau but not Aβ aggregates in postmortem retinas from AD patients [77]. These results contrast previously mentioned studies where AD pathological changes in the eyes were found. Differences in experimental procedures or in AD disease stage may partly explain some of these discrepancies. Nonetheless, the reported absence of AD markers in the eye may suggest that the disease compromises or develops in a dissimilar manner in the brain and in the eye. As well, other biochemical, structural, or imaging markers (i.e., OCT) in the visual system may be more adequate than Aβ or tau in the eye. This points to the need for developing future studies with more precise inclusion/exclusion criteria, larger patient populations with clear AD severity classifications and staging (for example, MCI, EOAD, and LOAD), and standardized measurements for vasculature analysis.

Currently, several clinical trials are being conducted to help clarify the use of visual components as possible biomarkers for AD. The National Institutes of Health- (NIH-) supported webpage that is responsible for the registry of clinical trials (https://clinicaltrials.gov/) has 38 studies related to AD and the eye. These studies have a wide range of objectives including measurement of saccades and eye-tracking, visuospatial attention, retinal thickness, and amyloid deposition. Although studying optic changes in AD is not without controversy, it represents a promising target that needs to be carefully studied in the future, both in preclinical and clinical studies, as the potential benefit of eye examinations as biomarkers for AD, in particular for detection of early changes, could have a significant impact in clinical practice.

7. Conclusions

The visual system might rise to be an important biomarker of AD because the functional and pathological mechanisms with the CNS are similar. AD patients manifest a reduction in thickness of the retina, explained by a selective neurodegenerative process induced by Aβ. Although the precise reason why certain retinal layers or quadrants are affected is not clear, neuronal loss is the result of the presence of several mechanisms such as inflammation, oxidative stress, and vascular dysfunction. There are divergent points of view about the relationship between ocular manifestations that need to be clarified. However, a better knowledge of pathophysiological mechanisms could lead to the development of new biomarkers during early stages of the disease. Ocular and visual examinations in AD would be a less invasive and more cost-effective method, than the techniques that are currently used. Noninvasive ophthalmological assessment could complement the AD diagnosis and would be a helpful tool to evaluate the disease progression. Novel functional studies of the visual system, as well as objective measurements of vascular and inflammatory changes in the eye, may play an important role in the evaluation of early stages of AD, including MCI and people at risk of dementia.

Abbreviations

ACh: Acetylcholine
AD: Alzheimer's disease
Aβ: Amyloid-beta
AMD: Age-related macular degeneration
ApoE: Apolipoprotein E
APP: Amyloid precursor protein
BACE-1: Beta-site amyloid precursor protein cleaving enzyme 1
BM: Bruch's membrane
CNS: Central nervous system
EOAD: Early-onset Alzheimer's disease
ERG: Electroretinogram
GCL: Ganglion cell layer
IL-1β: Interleukin-1β
IL-6: Interleukin-6
IL-8: Interleukin-8
IL-33: Interleukin-33
INL: Inner nuclear layer
IPL: Inner plexiform layer
LOAD: Late-onset AD
mAChR: Muscarinic acetylcholine receptor
MCI: Mild cognitive impairment
MMSE: Mini-Mental State Examination
nAChR: Nicotinic acetylcholine receptor
NIH: National Institutes of Health
NFL: Nerve fiber layer
NFT: Neurofibrillary tangles
NO: Nitric oxide

OCT: Optical coherence tomography
ONL: Outer nuclear layer
OPL: Outer plexiform layer
OS: Oxidative stress
ROS: Reactive oxygen species
RPE: Retinal pigment epithelium
SD-OCT: Spectral domain-optical coherence tomography
SP: Senile plaques
VEP: Visual evoked potential.

Conflicts of Interest

The authors declare no conflicts of interest.

Authors' Contributions

María Alejandra Cerquera-Jaramillo and Mauricio O. Nava-Mesa have contributed equally to this paper.

Acknowledgments

We thank Rachel James, Ph.D., from Edanz Group (http://www.edanzediting.com/ac) for editing a draft of this manuscript.

References

[1] P. Scheltens, K. Blennow, M. M. B. Breteler et al., "Alzheimer's disease," *The Lancet*, vol. 388, no. 10043, pp. 505–517, 2016.

[2] G. M. Ashraf, S. Chibber, Mohammad et al., "Recent updates on the association between Alzheimer's disease and vascular dementia," *Medicinal Chemistry*, vol. 12, no. 3, pp. 226–237, 2016.

[3] M. Prince, A. Wimo, M. Guerchet, G.-C. Ali, Y.-T. Wu, and M. Prina, *World Alzheimer Report 2015: The Global Impact of Dementia: an Analysis of Prevalence, Incidence, Cost and Trends*, Alzheimer's Disease International, London, 2015.

[4] R. A. Hickman, A. Faustin, and T. Wisniewski, "Alzheimer disease and its growing epidemic: risk factors, biomarkers, and the urgent need for therapeutics," *Neurologic Clinics*, vol. 34, no. 4, pp. 941–953, 2016.

[5] C. A. Lane, J. Hardy, and J. M. Schott, "Alzheimer's disease," *European Journal of Neurology*, vol. 25, no. 1, pp. 59–70, 2018.

[6] C. R. Jack Jr, M. S. Albert, D. S. Knopman et al., "Introduction to the recommendations from the National Institute on Aging-Alzheimer's Association workgroups on diagnostic guidelines for Alzheimer's disease," *Alzheimer's & Dementia: The Journal of the Alzheimer's Association*, vol. 7, no. 3, pp. 257–262, 2011.

[7] M. F. Mendez, "Early-onset Alzheimer disease," *Neurologic Clinics*, vol. 35, no. 2, pp. 263–281, 2017.

[8] A. L. Pierce, S. S. Bullain, and C. H. Kawas, "Late-onset Alzheimer disease," *Neurologic Clinics*, vol. 35, no. 2, pp. 283–293, 2017.

[9] I. Bos, S. J. Vos, L. Frölich et al., "The frequency and influence of dementia risk factors in prodromal Alzheimer's disease," *Neurobiology of Aging*, vol. 56, pp. 33–40, 2017.

[10] S. L. Rosenthal and M. I. Kamboh, "Late-onset Alzheimer's disease genes and the potentially implicated pathways," *Current Genetic Medicine Reports*, vol. 2, no. 2, pp. 85–101, 2014.

[11] R. B. Maccioni, J. P. Muñoz, and L. Barbeito, "The molecular bases of Alzheimer's disease and other neurodegenerative disorders," *Archives of Medical Research*, vol. 32, no. 5, pp. 367–381, 2001.

[12] H. W. Querfurth and F. M. LaFerla, "Alzheimer's disease," *The New England Journal of Medicine*, vol. 362, no. 4, pp. 329–344, 2010.

[13] P. Agostinho, A. Pliássova, C. R. Oliveira, and R. A. Cunha, "Localization and trafficking of amyloid-β protein precursor and secretases: impact on Alzheimer's disease," *Journal of Alzheimer's Disease*, vol. 45, no. 2, pp. 329–347, 2015.

[14] A. Chiarini, U. Armato, E. Gardenal, L. Gui, and I. Dal Prà, "Amyloid β-exposed human astrocytes overproduce phospho-tau and overrelease it within exosomes, effects suppressed by calcilytic NPS 2143-further implications for Alzheimer's therapy," *Frontiers in Neuroscience*, vol. 11, 2017.

[15] C. Lindberg, M.-L. B. Selenica, A. Westlind-Danielsson, and M. Schultzberg, "β-Amyloid protein structure determines the nature of cytokine release from rat microglia," *Journal of Molecular Neuroscience*, vol. 27, no. 1, pp. 1–12, 2005.

[16] L. Hou, Y. Liu, X. Wang et al., "The effects of amyloid-β42 oligomer on the proliferation and activation of astrocytes in vitro," *In Vitro Cellular & Developmental Biology-Animal*, vol. 47, no. 8, pp. 573–580, 2011.

[17] R. E. González-Reyes, M. O. Nava-Mesa, K. Vargas-Sánchez, D. Ariza-Salamanca, and L. Mora-Muñoz, "Involvement of astrocytes in Alzheimer's disease from a neuroinflammatory and oxidative stress perspective," *Frontiers in Molecular Neuroscience*, vol. 10, p. 427, 2017.

[18] F. M. Elahi and B. L. Miller, "A clinicopathological approach to the diagnosis of dementia," *Nature Reviews Neurology*, vol. 13, no. 8, pp. 457–476, 2017.

[19] N. El Kadmiri, N. Said, I. Slassi, B. El Moutawakil, and S. Nadifi, "Biomarkers for Alzheimer disease: classical and novel candidates' review," *Neuroscience*, vol. 370, pp. 181–190, 2018.

[20] G. B. Frisoni, M. Boccardi, F. Barkhof et al., "Strategic roadmap for an early diagnosis of Alzheimer's disease based on biomarkers," *The Lancet Neurology*, vol. 16, no. 8, pp. 661–676, 2017.

[21] L. Y. L. Chang, J. Lowe, A. Ardiles et al., "Alzheimer's disease in the human eye. Clinical tests that identify ocular and visual information processing deficit as biomarkers," *Alzheimer's & Dementia*, vol. 10, no. 2, pp. 251–261, 2014.

[22] F. Z. Javaid, J. Brenton, L. Guo, and M. F. Cordeiro, "Visual and ocular manifestations of Alzheimer's disease and their use as biomarkers for diagnosis and progression," *Frontiers in Neurology*, vol. 7, 2016.

[23] D.-H. Lee, A. B. Laemmer, A. Waschbisch et al., "Neuromyelitis optica presenting with relapses under treatment with natalizumab: a case report," *Journal of Medical Case Reports*, vol. 8, no. 1, p. 155, 2014.

[24] V. Kavcic, W. Vaughn, and C. J. Duffy, "Distinct visual motion processing impairments in aging and Alzheimer's disease," *Vision Research*, vol. 51, no. 3, pp. 386–395, 2011.

[25] M. P. Bambo, E. Garcia-Martin, S. Otin et al., "Visual function and retinal nerve fibre layer degeneration in patients with Alzheimer disease: correlations with severity

of dementia," *Acta Ophthalmologica*, vol. 93, no. 6, pp. e507–e508, 2015.

[26] C. Y.-L. Cheung, Y.-T. Ong, M. K. Ikram, C. Chen, and T. Y. Wong, "Retinal microvasculature in Alzheimer's disease," *Journal of Alzheimer's Disease*, vol. 42, Supplement 4, pp. S339–S352, 2014.

[27] M. K. Ikram, C. Y. Cheung, T. Y. Wong, and C. P. L. H. Chen, "Retinal pathology as biomarker for cognitive impairment and Alzheimer's disease," *Journal of Neurology, Neurosurgery, and Psychiatry*, vol. 83, no. 9, pp. 917–922, 2012.

[28] N. A. Arnaoutoglou, M. Arnaoutoglou, P. Nemtsas, V. Costa, S. J. Baloyannis, and K. P. Ebmeier, "Color perception differentiates Alzheimer's disease (AD) from vascular dementia (VaD) patients," *International Psychogeriatrics*, vol. 29, no. 8, pp. 1355–1361, 2017.

[29] C. M. Carroll and Y.-M. Li, "Physiological and pathological roles of the γ-secretase complex," *Brain Research Bulletin*, vol. 126, Part 2, pp. 199–206, 2016.

[30] L. J. Sosa, A. Cáceres, S. Dupraz, M. Oksdath, S. Quiroga, and A. Lorenzo, "The physiological role of the amyloid precursor protein as an adhesion molecule in the developing nervous system," *Journal of Neurochemistry*, vol. 143, no. 1, pp. 11–29, 2017.

[31] E. Montagna, M. M. Dorostkar, and J. Herms, "The role of APP in structural spine plasticity," *Frontiers in Molecular Neuroscience*, vol. 10, 2017.

[32] A. T. Rao, A. J. Degnan, and L. M. Levy, "Genetics of Alzheimer disease," *American Journal of Neuroradiology*, vol. 35, no. 3, pp. 457-458, 2014.

[33] R. Aleksis, F. Oleskovs, K. Jaudzems, J. Pahnke, and H. Biverstål, "Structural studies of amyloid-β peptides: unlocking the mechanism of aggregation and the associated toxicity," *Biochimie*, vol. 140, pp. 176–192, 2017.

[34] B. De Strooper and E. Karran, "The cellular phase of Alzheimer's disease," *Cell*, vol. 164, no. 4, pp. 603–615, 2016.

[35] D. Zhu, Y. Lai, P. B. Shelat, C. Hu, G. Y. Sun, and J. C.-M. Lee, "Phospholipases A2 mediate amyloid-beta peptide-induced mitochondrial dysfunction," *The Journal of Neuroscience*, vol. 26, no. 43, pp. 11111–11119, 2006.

[36] S. Askarova, X. Yang, W. Sheng, G. Y. Sun, and J. C.-M. Lee, "Role of Aβ-receptor for advanced glycation endproducts interaction in oxidative stress and cytosolic phospholipase A_2 activation in astrocytes and cerebral endothelial cells," *Neuroscience*, vol. 199, pp. 375–385, 2011.

[37] Z. Esposito, L. Belli, S. Toniolo, G. Sancesario, C. Bianconi, and A. Martorana, "Amyloid β, glutamate, excitotoxicity in Alzheimer's disease: are we on the right track?," *CNS Neuroscience & Therapeutics*, vol. 19, no. 8, pp. 549–555, 2013.

[38] M. O. Nava-Mesa, L. Jiménez-Díaz, J. Yajeya, and J. D. Navarro-Lopez, "GABAergic neurotransmission and new strategies of neuromodulation to compensate synaptic dysfunction in early stages of Alzheimer's disease," *Frontiers in Cellular Neuroscience*, vol. 8, p. 167, 2014.

[39] L. Mosconi, S. Sorbi, M. J. de Leon et al., "Hypometabolism exceeds atrophy in presymptomatic early-onset familial Alzheimer's disease," *Journal of Nuclear Medicine*, vol. 47, no. 11, pp. 1778–1786, 2006.

[40] L. Mosconi, A. Pupi, and M. J. De Leon, "Brain glucose hypometabolism and oxidative stress in preclinical Alzheimer's disease," *Annals of the New York Academy of Sciences*, vol. 1147, no. 1, pp. 180–195, 2008.

[41] M. S. Forman, D. Lal, B. Zhang et al., "Transgenic mouse model of tau pathology in astrocytes leading to nervous system degeneration," *The Journal of Neuroscience*, vol. 25, no. 14, pp. 3539–3550, 2005.

[42] M. Goedert, D. S. Eisenberg, and R. A. Crowther, "Propagation of tau aggregates and neurodegeneration," *Annual Review of Neuroscience*, vol. 40, no. 1, pp. 189–210, 2017.

[43] J. A. Ratnayaka, L. C. Serpell, and A. J. Lotery, "Dementia of the eye: the role of amyloid beta in retinal degeneration," *Eye*, vol. 29, no. 8, pp. 1013–1026, 2015.

[44] T. M. Shah, S. M. Gupta, P. Chatterjee, M. Campbell, and R. N. Martins, "Beta-amyloid sequelae in the eye: a critical review on its diagnostic significance and clinical relevance in Alzheimer's disease," *Molecular Psychiatry*, vol. 22, no. 3, pp. 353–363, 2017.

[45] P. van Wijngaarden, X. Hadoux, M. Alwan, S. Keel, and M. Dirani, "Emerging ocular biomarkers of Alzheimer disease," *Clinical & Experimental Ophthalmology*, vol. 45, no. 1, pp. 54–61, 2017.

[46] J. K. H. Lim, Q.-X. Li, Z. He et al., "The eye as a biomarker for Alzheimer's disease," *Frontiers in Neuroscience*, vol. 10, 2016.

[47] V. K. Gupta, N. Chitranshi, V. B. Gupta et al., "Amyloid β accumulation and inner retinal degenerative changes in Alzheimer's disease transgenic mouse," *Neuroscience Letters*, vol. 623, pp. 52–56, 2016.

[48] N. J. Hart, Y. Koronyo, K. L. Black, and M. Koronyo-Hamaoui, "Ocular indicators of Alzheimer's: exploring disease in the retina," *Acta Neuropathologica*, vol. 132, no. 6, pp. 767–787, 2016.

[49] A. London, I. Benhar, and M. Schwartz, "The retina as a window to the brain-from eye research to CNS disorders," *Nature Reviews Neurology*, vol. 9, no. 1, pp. 44–53, 2013.

[50] Y. Kusne, A. B. Wolf, K. Townley, M. Conway, and G. A. Peyman, "Visual system manifestations of Alzheimer's disease," *Acta Ophthalmologica*, vol. 95, no. 8, pp. e668–e676, 2017.

[51] K. Chiu, T.-F. Chan, A. Wu, I. Y.-P. Leung, K.-F. So, and R. C.-C. Chang, "Neurodegeneration of the retina in mouse models of Alzheimer's disease: what can we learn from the retina?," *Age*, vol. 34, no. 3, pp. 633–649, 2012.

[52] E. Vecino, F. D. Rodriguez, N. Ruzafa, X. Pereiro, and S. C. Sharma, "Glia-neuron interactions in the mammalian retina," *Progress in Retinal and Eye Research*, vol. 51, pp. 1–40, 2016.

[53] A. Wakx, M. Dutot, F. Massicot, F. Mascarelli, G. A. Limb, and P. Rat, "Amyloid β peptide induces apoptosis through P2X7 cell death receptor in retinal cells: modulation by marine omega-3 fatty acid DHA and EPA," *Applied Biochemistry and Biotechnology*, vol. 178, no. 2, pp. 368–381, 2016.

[54] V. Dinet, J. Bruban, N. Chalour et al., "Distinct effects of inflammation on gliosis, osmohomeostasis, and vascular integrity during amyloid beta-induced retinal degeneration," *Aging Cell*, vol. 11, no. 4, pp. 683–693, 2012.

[55] M. M. Edwards, J. J. Rodríguez, R. Gutierrez-Lanza, J. Yates, A. Verkhratsky, and G. A. Lutty, "Retinal macroglia changes in a triple transgenic mouse model of Alzheimer's disease," *Experimental Eye Research*, vol. 127, pp. 252–260, 2014.

[56] G. Chidlow, J. P. M. Wood, J. Manavis, J. Finnie, and R. J. Casson, "Investigations into retinal pathology in the early stages of a mouse model of Alzheimer's disease," *Journal of Alzheimer's Disease*, vol. 56, no. 2, pp. 655–675, 2017.

[57] R. T. Liu, A. Wang, E. To et al., "Vinpocetine inhibits amyloid-beta induced activation of NF-κB, NLRP3 inflammasome and cytokine production in retinal pigment epithelial cells," *Experimental Eye Research*, vol. 127, pp. 49–58, 2014.

[58] J. P. Cunha and A. Castanheira-Dinis, "Alzheimer disease: OCT retinal and choroidal thickness," in *Proceedings of the 5th International Conference on Photonics, Optics and Laser Technology*, Porto, Portugal, 2017.

[59] A. M. Birch, "The contribution of astrocytes to Alzheimer's disease," *Biochemical Society Transactions*, vol. 42, no. 5, pp. 1316–1320, 2014.

[60] C. Iadecola and M. Nedergaard, "Glial regulation of the cerebral microvasculature," *Nature Neuroscience*, vol. 10, no. 11, pp. 1369–1376, 2007.

[61] K. Kisler, A. R. Nelson, A. Montagne, and B. V. Zlokovic, "Cerebral blood flow regulation and neurovascular dysfunction in Alzheimer disease," *Nature Reviews Neuroscience*, vol. 18, no. 7, pp. 419–434, 2017.

[62] T. Iram, D. Trudler, D. Kain et al., "Astrocytes from old Alzheimer's disease mice are impaired in Aβ uptake and in neuroprotection," *Neurobiology of Disease*, vol. 96, pp. 84–94, 2016.

[63] B. Ghebrehiwet, X. Feng, R. Kumar, and E. I. B. Peerschke, "Complement component C1q induces endothelial cell adhesion and spreading through a docking/signaling partnership of C1q receptors and integrins," *International Immunopharmacology*, vol. 3, no. 3, pp. 299–310, 2003.

[64] S. E. Perez, S. Lumayag, B. Kovacs, E. J. Mufson, and S. Xu, "β-Amyloid deposition and functional impairment in the retina of the APPswe/PS1ΔE9 transgenic mouse model of Alzheimer's disease," *Investigative Ophthalmology & Visual Science*, vol. 50, no. 2, pp. 793–800, 2009.

[65] L. Y. Du, L. Y.-L. Chang, A. O. Ardiles et al., "Alzheimer's disease-related protein expression in the retina of *Octodon degus*," *PloS One*, vol. 10, no. 8, article e0135499, 2015.

[66] M. Koronyo-Hamaoui, Y. Koronyo, A. V. Ljubimov et al., "Identification of amyloid plaques in retinas from Alzheimer's patients and noninvasive in vivo optical imaging of retinal plaques in a mouse model," *NeuroImage*, vol. 54, Supplement 1, pp. S204–S217, 2011.

[67] Y. Tsai, B. Lu, A. V. Ljubimov et al., "Ocular changes in TgF344-AD rat model of Alzheimer's disease," *Investigative Ophthalmology & Visual Science*, vol. 55, no. 1, pp. 523–534, 2014.

[68] J. C. Blanks, S. Y. Schmidt, Y. Torigoe, K. V. Porrello, D. R. Hinton, and R. H. I. Blanks, "Retinal pathology in Alzheimer's disease. II. Regional neuron loss and glial changes in GCL," *Neurobiology of Aging*, vol. 17, no. 3, pp. 385–395, 1996.

[69] C. H. Andrade-Moraes, A. V. Oliveira-Pinto, E. Castro-Fonseca et al., "Cell number changes in Alzheimer's disease relate to dementia, not to plaques and tangles," *Brain*, vol. 136, no. 12, pp. 3738–3752, 2013.

[70] G. Leuba and R. Kraftsik, "Visual cortex in Alzheimer's disease: occurrence of neuronal death and glial proliferation, and correlation with pathological hallmarks," *Neurobiology of Aging*, vol. 15, no. 1, pp. 29–43, 1994.

[71] V. Luibl, J. M. Isas, R. Kayed, C. G. Glabe, R. Langen, and J. Chen, "Drusen deposits associated with aging and age-related macular degeneration contain nonfibrillar amyloid oligomers," *The Journal of Clinical Investigation*, vol. 116, no. 2, pp. 378–385, 2006.

[72] D. H. Anderson, R. F. Mullins, G. S. Hageman, and L. V. Johnson, "A role for local inflammation in the formation of drusen in the aging eye," *American Journal of Ophthalmology*, vol. 134, no. 3, pp. 411–431, 2002.

[73] A. N. Nilson, K. C. English, J. E. Gerson et al., "Tau oligomers associate with inflammation in the brain and retina of tauopathy mice and in neurodegenerative diseases," *Journal of Alzheimer's Disease*, vol. 55, no. 3, pp. 1083–1099, 2017.

[74] M. Chiasseu, L. Alarcon-Martinez, N. Belforte et al., "Tau accumulation in the retina promotes early neuronal dysfunction and precedes brain pathology in a mouse model of Alzheimer's disease," *Molecular Neurodegeneration*, vol. 12, no. 1, p. 58, 2017.

[75] W. Ho, Y. Leung, A. W. Tsang, K. F. So, K. Chiu, and R. C. Chang, "Review: Tauopathy in the retina and optic nerve: does it shadow pathological changes in the brain?," *Molecular Vision*, vol. 18, pp. 2700–2710, 2012.

[76] H. Zhao, R. Chang, H. Che et al., "Hyperphosphorylation of tau protein by calpain regulation in retina of Alzheimer's disease transgenic mouse," *Neuroscience Letters*, vol. 551, pp. 12–16, 2013.

[77] C. Schön, N. A. Hoffmann, S. M. Ochs et al., "Long-term in vivo imaging of fibrillar tau in the retina of P301S transgenic mice," *PloS One*, vol. 7, no. 12, article e53547, 2012.

[78] M. Rudolf, M. E. Clark, M. F. Chimento, C.-M. Li, N. E. Medeiros, and C. A. Curcio, "Prevalence and morphology of druse types in the macula and periphery of eyes with age-related maculopathy," *Investigative Ophthalmology & Visual Science*, vol. 49, no. 3, pp. 1200–1209, 2008.

[79] S. McHarg, S. J. Clark, A. J. Day, and P. N. Bishop, "Age-related macular degeneration and the role of the complement system," *Molecular Immunology*, vol. 67, no. 1, pp. 43–50, 2015.

[80] A. I. Pogue, P. Dua, J. M. Hill, and W. J. Lukiw, "Progressive inflammatory pathology in the retina of aluminum-fed 5xFAD transgenic mice," *Journal of Inorganic Biochemistry*, vol. 152, pp. 206–209, 2015.

[81] V. V. Ermilov and A. A. Nesterova, "β-Amyloidopathy in the pathogenesis of age-related macular degeneration in correlation with neurodegenerative diseases," *Advances in Experimental Medicine and Biology*, vol. 854, pp. 119–125, 2016.

[82] K. Ohno-Matsui, "Parallel findings in age-related macular degeneration and Alzheimer's disease," *Progress in Retinal and Eye Research*, vol. 30, no. 4, pp. 217–238, 2011.

[83] T. Yoshida, K. Ohno-Matsui, S. Ichinose et al., "The potential role of amyloid β in the pathogenesis of age-related macular degeneration," *The Journal of Clinical Investigation*, vol. 115, no. 10, pp. 2793–2800, 2005.

[84] L. M. Tai, R. Thomas, F. M. Marottoli et al., "The role of APOE in cerebrovascular dysfunction," *Acta Neuropathologica*, vol. 131, no. 5, pp. 709–723, 2016.

[85] J.-T. Yu, L. Tan, and J. Hardy, "Apolipoprotein E in Alzheimer's disease: an update," *Annual Review of Neuroscience*, vol. 37, no. 1, pp. 79–100, 2014.

[86] J. Hardy and D. J. Selkoe, "The amyloid hypothesis of Alzheimer's disease: progress and problems on the road to therapeutics," *Science*, vol. 297, no. 5580, pp. 353–356, 2002.

[87] H. K. Dong, J.-A. Gim, S. H. Yeo, and H.-S. Kim, "Integrated late onset Alzheimer's disease (LOAD) susceptibility genes:

cholesterol metabolism and trafficking perspectives," *Gene*, vol. 597, pp. 10–16, 2017.

[88] A. T. Baker-Nigh, K. G. Mawuenyega, J. G. Bollinger et al., "Human central nervous system (CNS) ApoE isoforms are increased by age, differentially altered by amyloidosis, and relative amounts reversed in the CNS compared with plasma," *The Journal of Biological Chemistry*, vol. 291, no. 53, pp. 27204–27218, 2016.

[89] T. Masuda, M. Shimazawa, Y. Hashimoto et al., "Apolipoprotein E2 and E3, but not E4, promote retinal pathologic neovascularization," *Investigative Ophthalmology & Visual Science*, vol. 58, no. 2, pp. 1208–1217, 2017.

[90] I. Maharshak, S. Salomon-Zimri, R. Antes et al., "The effects of the apoE4 genotype on the developing mouse retina," *Experimental Eye Research*, vol. 145, pp. 17–25, 2016.

[91] O. Levy, S. Lavalette, S. J. Hu et al., "APOE isoforms control pathogenic subretinal inflammation in age-related macular degeneration," *The Journal of Neuroscience*, vol. 35, no. 40, pp. 13568–13576, 2015.

[92] J. M. Ong, N. C. Zorapapel, K. A. Rich et al., "Effects of cholesterol and apolipoprotein E on retinal abnormalities in ApoE-deficient mice," *Investigative Ophthalmology & Visual Science*, vol. 42, no. 8, pp. 1891–1900, 2001.

[93] S. Frost, R. Guymer, K. Zaw Aung et al., "Alzheimer's disease and the early signs of age-related macular degeneration," *Current Alzheimer Research*, vol. 13, no. 11, pp. 1259–1266, 2016.

[94] M. A. Williams, V. Silvestri, D. Craig, A. P. Passmore, and G. Silvestri, "The prevalence of age-related macular degeneration in Alzheimer's disease," *Journal of Alzheimer's Disease*, vol. 42, no. 3, pp. 909–914, 2014.

[95] V. S. Pelak and W. Hills, "Vision in Alzheimer's disease: a focus on the anterior afferent pathway," *Neurodegenerative Disease Management*, vol. 8, no. 1, pp. 49–67, 2018.

[96] R. A. Armstrong, "Visual field defects in Alzheimer's disease patients may reflect differential pathology in the primary visual cortex," *Optometry and Vision Science*, vol. 73, no. 11, pp. 677–682, 1996.

[97] X. Liu, W. Chen, H. Hou et al., "Decreased functional connectivity between the dorsal anterior cingulate cortex and lingual gyrus in Alzheimer's disease patients with depression," *Behavioural Brain Research*, vol. 326, pp. 132–138, 2017.

[98] A. A. Brewer and B. Barton, "Visual cortex in aging and Alzheimer's disease: changes in visual field maps and population receptive fields," *Frontiers in Psychology*, vol. 5, p. 74, 2014.

[99] M. Kiyosawa, T. M. Bosley, J. Chawluk et al., "Alzheimer's disease with prominent visual symptoms: clinical and metabolic evaluation," *Ophthalmology*, vol. 96, no. 7, pp. 1077–1086, 1989.

[100] R. O. Kuljis, "Lesions in the pulvinar in patients with Alzheimer's disease," *Journal of Neuropathology & Experimental Neurology*, vol. 53, no. 2, pp. 202–211, 1994.

[101] D. Erskine, J. P. Taylor, M. J. Firbank et al., "Changes to the lateral geniculate nucleus in Alzheimer's disease but not dementia with Lewy bodies," *Neuropathology and Applied Neurobiology*, vol. 42, no. 4, pp. 366–376, 2016.

[102] R. Feng, L. Li, H. Yu, M. Liu, and W. Zhao, "Melanopsin retinal ganglion cell loss and circadian dysfunction in Alzheimer's disease (review)," *Molecular Medicine Reports*, vol. 13, no. 4, pp. 3397–3400, 2016.

[103] A. N. Coogan, B. Schutová, S. Husung et al., "The circadian system in Alzheimer's disease: disturbances, mechanisms, and opportunities," *Biological Psychiatry*, vol. 74, no. 5, pp. 333–339, 2013.

[104] L. Zhou, Q. Gao, M. Nie et al., "Degeneration and energy shortage in the suprachiasmatic nucleus underlies the circadian rhythm disturbance in ApoE−/− mice: implications for Alzheimer's disease," *Scientific Reports*, vol. 6, no. 1, article 36335, 2016.

[105] J. Van Erum, D. Van Dam, and P. P. De Deyn, "Sleep and Alzheimer's disease: a pivotal role for the suprachiasmatic nucleus," *Sleep Medicine Reviews*, vol. 40, pp. 17–27, 2018.

[106] G. Leuba and K. Saini, "Pathology of subcortical visual centres in relation to cortical degeneration in Alzheimer's disease," *Neuropathology and Applied Neurobiology*, vol. 21, no. 5, pp. 410–422, 1995.

[107] J. Parvizi, G. W. Van Hoesen, and A. Damasio, "The selective vulnerability of brainstem nuclei to Alzheimer's disease," *Annals of Neurology*, vol. 49, no. 1, pp. 53–66, 2001.

[108] F. G. Oliveira-Souza, M. L. DeRamus, T. van Groen, A. E. Lambert, M. S. Bolding, and C. E. Strang, "Retinal changes in the Tg-SwDI mouse model of Alzheimer's disease," *Neuroscience*, vol. 354, pp. 43–53, 2017.

[109] L. Nobili and W. G. Sannita, "Cholinergic modulation, visual function and Alzheimer's dementia," *Vision Research*, vol. 37, no. 24, pp. 3559–3571, 1997.

[110] A. Patricio-Martínez, L. Mendieta, I. Martínez, J. Aguilera, and I. D. Limón, "The recombinant C-terminal fragment of tetanus toxin protects against cholinotoxicity by intraseptal injection of β-amyloid peptide (25-35) in rats," *Neuroscience*, vol. 315, pp. 18–30, 2016.

[111] S. H. Deibel, N. Weishaupt, A. M. Regis et al., "Subtle learning and memory impairment in an idiopathic rat model of Alzheimer's disease utilizing cholinergic depletions and β-amyloid," *Brain Research*, vol. 1646, pp. 12–24, 2016.

[112] R. Schliebs and T. Arendt, "The significance of the cholinergic system in the brain during aging and in Alzheimer's disease," *Journal of Neural Transmission*, vol. 113, no. 11, pp. 1625–1644, 2006.

[113] H. Janíčková, V. Rudajev, P. Zimčík et al., "Uncoupling of M1 muscarinic receptor/G-protein interaction by amyloid β1-42," *Neuropharmacology*, vol. 67, pp. 272–283, 2013.

[114] J. J. Dougherty, J. Wu, and R. A. Nichols, "β-Amyloid regulation of presynaptic nicotinic receptors in rat hippocampus and neocortex," *The Journal of Neuroscience*, vol. 23, no. 17, pp. 6740–6747, 2003.

[115] S. Kar, D. Seto, P. Gaudreau, and R. Quirion, "Beta-amyloid-related peptides inhibit potassium-evoked acetylcholine release from rat hippocampal slices," *The Journal of Neuroscience*, vol. 16, no. 3, pp. 1034–1040, 1996.

[116] J. Mayordomo-Cava, J. Yajeya, J. D. Navarro-López, and L. Jiménez-Díaz, "Amyloid-β modulates the expression of GirK and KCNQ channel genes in the hippocampus," *PLoS One*, vol. 10, no. 7, article e0134385, 2015.

[117] R. N. Leão, L. V. Colom, L. Borgius, O. Kiehn, and A. Fisahn, "Medial septal dysfunction by Aβ-induced KCNQ channel-block in glutamatergic neurons," *Neurobiology of Aging*, vol. 33, no. 9, pp. 2046–2061, 2012.

[118] L. Guo, J. Duggan, and M. Cordeiro, "Alzheimer's disease and retinal neurodegeneration," *Current Alzheimer Research*, vol. 7, no. 1, pp. 3–14, 2010.

[119] N. S. Foldi, R. E. C. White, and L. A. Schaefer, "Detecting effects of donepezil on visual selective attention using signal detection parameters in Alzheimer's disease," *International Journal of Geriatric Psychiatry*, vol. 20, no. 5, pp. 485–488, 2005.

[120] M. Boucart, G. Bubbico, S. szaffarczyk et al., "Donepezil increases contrast sensitivity for the detection of objects in scenes," *Behavioural Brain Research*, vol. 292, pp. 443–447, 2015.

[121] J. P. Cunha, N. Moura-Coelho, R. P. Proença et al., "Alzheimer's disease: a review of its visual system neuropathology. Optical coherence tomography-a potential role as a study tool in vivo," *Graefe's Archive for Clinical and Experimental Ophthalmology*, vol. 254, no. 11, pp. 2079–2092, 2016.

[122] M. H. Madeira, A. F. Ambrósio, and A. R. Santiago, "Glia-mediated retinal neuroinflammation as a biomarker in Alzheimer's disease," *Ophthalmic Research*, vol. 54, no. 4, pp. 204–211, 2015.

[123] G. Coppola, A. di Renzo, L. Ziccardi et al., "Optical coherence tomography in Alzheimer's disease: a meta-analysis," *PLoS One*, vol. 10, no. 8, article e0134750, 2015.

[124] S. Krantic and A. Torriglia, "Retina: source of the earliest biomarkers for Alzheimer's disease?," *Journal of Alzheimer's Disease*, vol. 40, no. 2, pp. 237–243, 2014.

[125] C. La Morgia, F. N. Ross-Cisneros, J. Hannibal, P. Montagna, A. A. Sadun, and V. Carelli, "Melanopsin-expressing retinal ganglion cells: implications for human diseases," *Vision Research*, vol. 51, no. 2, pp. 296–302, 2011.

[126] C. Laske, H. R. Sohrabi, S. M. Frost et al., "Innovative diagnostic tools for early detection of Alzheimer's disease," *Alzheimer's & Dementia*, vol. 11, no. 5, pp. 561–578, 2015.

[127] C. S. Tsai, R. Ritch, B. Schwartz et al., "Optic nerve head and nerve fiber layer in Alzheimer's disease," *Archives of Ophthalmology*, vol. 109, no. 2, pp. 199–204, 1991.

[128] D. R. Hinton, A. A. Sadun, J. C. Blanks, and C. A. Miller, "Optic-nerve degeneration in Alzheimer's disease," *New England Journal of Medicine*, vol. 315, no. 8, pp. 485–487, 1986.

[129] A. A. Sadun and C. J. Bassi, "Optic nerve damage in Alzheimer's disease," *Ophthalmology*, vol. 97, no. 1, pp. 9–17, 1990.

[130] M. P. Bambo, E. Garcia-Martin, F. Gutierrez-Ruiz et al., "Analysis of optic disk color changes in Alzheimer's disease: a potential new biomarker," *Clinical Neurology and Neurosurgery*, vol. 132, pp. 68–73, 2015.

[131] Y. Lu, Z. Li, X. Zhang et al., "Retinal nerve fiber layer structure abnormalities in early Alzheimer's disease: evidence in optical coherence tomography," *Neuroscience Letters*, vol. 480, no. 1, pp. 69–72, 2010.

[132] T. Kusbeci, O. Y. Kusbeci, N. G. Mas, H. S. Karabekir, G. Yavas, and A. Yucel, "Stereological evaluation of the optic nerve volume in Alzheimer disease," *The Journal of Craniofacial Surgery*, vol. 26, no. 5, pp. 1683–1686, 2015.

[133] M. A. Williams, A. J. McGowan, C. R. Cardwell et al., "Retinal microvascular network attenuation in Alzheimer's disease," *Alzheimer's & Dementia: Diagnosis, Assessment & Disease Monitoring*, vol. 1, no. 2, pp. 229–235, 2015.

[134] G. T. Feke, B. T. Hyman, R. A. Stern, and L. R. Pasquale, "Retinal blood flow in mild cognitive impairment and Alzheimer's disease," *Alzheimer's & Dementia: Diagnosis, Assessment & Disease Monitoring*, vol. 1, no. 2, pp. 144–151, 2015.

[135] F. Berisha, G. T. Feke, C. L. Trempe, J. W. McMeel, and C. L. Schepens, "Retinal abnormalities in early Alzheimer's disease," *Investigative Ophthalmology & Visual Science*, vol. 48, no. 5, pp. 2285–2289, 2007.

[136] S. Frost, Y. Kanagasingam, H. Sohrabi et al., "Retinal vascular biomarkers for early detection and monitoring of Alzheimer's disease," *Translational Psychiatry*, vol. 3, no. 2, article e233, 2013.

[137] S. M. Golzan, K. Goozee, D. Georgevsky et al., "Retinal vascular and structural changes are associated with amyloid burden in the elderly: ophthalmic biomarkers of preclinical Alzheimer's disease," *Alzheimer's Research & Therapy*, vol. 9, no. 1, p. 13, 2017.

[138] M. H. Dehabadi, B. M. Davis, T. K. Wong, and M. F. Cordeiro, "Retinal manifestations of Alzheimer's disease," *Neurodegenerative Disease Management*, vol. 4, no. 3, pp. 241–252, 2014.

[139] R. Tzekov and M. Mullan, "Vision function abnormalities in Alzheimer disease," *Survey of Ophthalmology*, vol. 59, no. 4, pp. 414–433, 2014.

[140] D. Mahajan and M. Votruba, "Can the retina be used to diagnose and plot the progression of Alzheimer's disease?," *Acta Ophthalmologica*, vol. 95, no. 8, pp. 768–777, 2017.

[141] Y. Shao, H. Jiang, Y. Wei et al., "Visualization of focal thinning of the ganglion cell–inner plexiform layer in patients with mild cognitive impairment and Alzheimer's disease," *Journal of Alzheimer's Disease*, vol. 64, no. 4, pp. 1261–1273, 2018.

[142] V. Jindal, "Interconnection between brain and retinal neurodegenerations," *Molecular Neurobiology*, vol. 51, no. 3, pp. 885–892, 2015.

[143] S. L. Risacher, D. WuDunn, S. M. Pepin et al., "Visual contrast sensitivity in Alzheimer's disease, mild cognitive impairment, and older adults with cognitive complaints," *Neurobiology of Aging*, vol. 34, no. 4, pp. 1133–1144, 2013.

[144] T. J. Crawford, A. Devereaux, S. Higham, and C. Kelly, "The disengagement of visual attention in Alzheimer's disease: a longitudinal eye-tracking study," *Frontiers in Aging Neuroscience*, vol. 7, p. 118, 2015.

[145] G. Binetti, S. F. Cappa, E. Magni, A. Padovani, A. Bianchetti, and M. Trabucchi, "Disorders of visual and spatial perception in the early stage of Alzheimer's disease," *Annals of the New York Academy of Sciences*, vol. 777, no. 1, pp. 221–225, 1996.

[146] T. B. Adelstein, R. P. Kesner, and D. S. Strassberg, "Spatial recognition and spatial order memory in patients with dementia of the Alzheimer's type," *Neuropsychologia*, vol. 30, no. 1, pp. 59–67, 1992.

[147] M. Rizzo, S. W. Anderson, J. Dawson, R. Myers, and K. Ball, "Visual attention impairments in Alzheimer's disease," *Neurology*, vol. 54, no. 10, pp. 1954–1959, 2000.

[148] C. Flicker, S. H. Ferris, T. Crook, and R. T. Bartus, "Impaired facial recognition memory in aging and dementia," *Alzheimer Disease and Associated Disorders*, vol. 4, no. 1, pp. 43–54, 1990.

[149] M. F. Mendez, M. A. Mendez, R. Martin, K. A. Smyth, and P. J. Whitehouse, "Complex visual disturbances in Alzheimer's disease," *Neurology*, vol. 40, no. 3, Part 1, pp. 439–443, 1990.

[150] M. F. Mendez, R. J. Martin, K. A. Smyth, and P. J. Whitehouse, "Disturbances of person identification in Alzheimer's disease. A retrospective study," *The Journal*

of Nervous and Mental Disease, vol. 180, no. 2, pp. 94–96, 1992.

[151] A. Cronin-Golomb, S. Corkin, J. F. Rizzo, J. Cohen, J. H. Growdon, and K. S. Banks, "Visual dysfunction in Alzheimer's disease: relation to normal aging," *Annals of Neurology*, vol. 29, no. 1, pp. 41–52, 1991.

[152] P. R. Hof and C. Bouras, "Object recognition deficit in Alzheimer's disease: possible disconnection of the occipito-temporal component of the visual system," *Neuroscience Letters*, vol. 122, no. 1, pp. 53–56, 1991.

[153] P. R. Hof, C. Bouras, J. Constantinidis, and J. H. Morrison, "Selective disconnection of specific visual association pathways in cases of Alzheimer's disease presenting with Balint's syndrome," *Journal of Neuropathology and Experimental Neurology*, vol. 49, no. 2, pp. 168–184, 1990.

[154] P.-F. Kaeser, J. Ghika, and F.-X. Borruat, "Visual signs and symptoms in patients with the visual variant of Alzheimer disease," *BMC Ophthalmology*, vol. 15, no. 1, p. 65, 2015.

[155] R. Armstrong and A. Syed, "Alzheimer's disease and the eye," *Ophthalmic and Physiological Optics*, vol. 16, pp. S2–S8, 1996.

[156] V. Polo, M. J. Rodrigo, E. Garcia-Martin et al., "Visual dysfunction and its correlation with retinal changes in patients with Alzheimer's disease," *Eye*, vol. 31, no. 7, pp. 1034–1041, 2017.

[157] S. A. Neargarder, E. R. Stone, A. Cronin-Golomb, and S. Oross, "The impact of acuity on performance of four clinical measures of contrast sensitivity in Alzheimer's disease," *The Journals of Gerontology Series B: Psychological Sciences and Social Sciences*, vol. 58, no. 1, pp. P54–P62, 2003.

[158] F. Sartucci, D. Borghetti, T. Bocci et al., "Dysfunction of the magnocellular stream in Alzheimer's disease evaluated by pattern electroretinograms and visual evoked potentials," *Brain Research Bulletin*, vol. 82, no. 3-4, pp. 169–176, 2010.

[159] G. Salamone, C. di Lorenzo, S. Mosti et al., "Color discrimination performance in patients with Alzheimer's disease," *Dementia and Geriatric Cognitive Disorders*, vol. 27, no. 6, pp. 501–507, 2009.

[160] R. Prettyman, P. Bitsios, and E. Szabadi, "Altered pupillary size and darkness and light reflexes in Alzheimer's disease," *Journal of Neurology, Neurosurgery, and Psychiatry*, vol. 62, no. 6, pp. 665–668, 1997.

[161] R. J. Molitor, P. C. Ko, and B. A. Ally, "Eye movements in Alzheimer's disease," *Journal of Alzheimer's Disease*, vol. 44, no. 1, pp. 1–12, 2015.

[162] W. A. Fletcher and J. A. Sharpe, "Saccadic eye movement dysfunction in Alzheimer's disease," *Annals of Neurology*, vol. 20, no. 4, pp. 464–471, 1986.

[163] O. A. Coubard, "What do we know about eye movements in Alzheimer's disease? The past 37 years and future directions," *Biomarkers in Medicine*, vol. 10, no. 7, pp. 677–680, 2016.

[164] C.-N. Lee and K.-W. Park, "Cognitive functions and stereopsis in patients with parkinson's disease and Alzheimer's disease," *Alzheimer's & Dementia*, vol. 10, no. 4, article P767, 2014.

[165] H. Kergoat, M. J. Kergoat, L. Justino, H. Chertkow, A. Robillard, and H. Bergman, "An evaluation of the retinal nerve fiber layer thickness by scanning laser polarimetry in individuals with dementia of the Alzheimer type," *Acta Ophthalmologica Scandinavica*, vol. 79, no. 2, pp. 187–191, 2001.

[166] S. Kirbas, K. Turkyilmaz, O. Anlar, A. Tufekci, and M. Durmus, "Retinal nerve fiber layer thickness in patients with Alzheimer disease," *Journal of Neuro-Ophthalmology*, vol. 33, no. 1, pp. 58–61, 2013.

[167] A. Trebbastoni, F. D'Antonio, A. Bruscolini et al., "Retinal nerve fibre layer thickness changes in Alzheimer's disease: results from a 12-month prospective case series," *Neuroscience Letters*, vol. 629, pp. 165–170, 2016.

[168] E. Garcia-Martin, M. P. Bambo, M. L. Marques et al., "Ganglion cell layer measurements correlate with disease severity in patients with Alzheimer's disease," *Acta Ophthalmologica*, vol. 94, no. 6, pp. e454–e459, 2016.

[169] D. Liu, L. Zhang, Z. Li et al., "Thinner changes of the retinal nerve fiber layer in patients with mild cognitive impairment and Alzheimer's disease," *BMC Neurology*, vol. 15, no. 1, p. 14, 2015.

[170] A. Kesler, V. Vakhapova, A. D. Korczyn, E. Naftaliev, and M. Neudorfer, "Retinal thickness in patients with mild cognitive impairment and Alzheimer's disease," *Clinical Neurology and Neurosurgery*, vol. 113, no. 7, pp. 523–526, 2011.

[171] C. Paquet, M. Boissonnot, F. Roger, P. Dighiero, R. Gil, and J. Hugon, "Abnormal retinal thickness in patients with mild cognitive impairment and Alzheimer's disease," *Neuroscience Letters*, vol. 420, no. 2, pp. 97–99, 2007.

[172] P. J. Snyder, L. N. Johnson, Y. Y. Lim et al., "Nonvascular retinal imaging markers of preclinical Alzheimer's disease," *Alzheimer's & Dementia: Diagnosis, Assessment & Disease Monitoring*, vol. 4, pp. 169–178, 2016.

[173] H. A. Bayhan, S. Aslan Bayhan, A. Celikbilek, N. Tanık, and C. Gürdal, "Evaluation of the chorioretinal thickness changes in Alzheimer's disease using spectral-domain optical coherence tomography," *Clinical & Experimental Ophthalmology*, vol. 43, no. 2, pp. 145–151, 2015.

[174] F. J. Ascaso, N. Cruz, P. J. Modrego et al., "Retinal alterations in mild cognitive impairment and Alzheimer's disease: an optical coherence tomography study," *Journal of Neurology*, vol. 261, no. 8, pp. 1522–1530, 2014.

[175] D. Rodriguez-Mena, C. Almarcegui, I. Dolz, L. E. Pablo, and E. Garcia-Martin, "Application of electrophysiological tests in the study of neurological diseases with visual involvement," *Archivos De La Sociedad Espanola De Oftalmologia*, vol. 87, no. 10, pp. 311–314, 2012.

[176] S. H. Choi, S. J. Park, and N. R. Kim, "Macular ganglion cell -inner plexiform layer thickness is associated with clinical progression in mild cognitive impairment and Alzheimers disease," *PLoS One*, vol. 11, no. 9, article e0162202, 2016.

[177] E. O. Oktem, E. Derle, S. Kibaroglu, C. Oktem, I. Akkoyun, and U. Can, "The relationship between the degree of cognitive impairment and retinal nerve fiber layer thickness," *Neurological Sciences*, vol. 36, no. 7, pp. 1141–1146, 2015.

[178] L. Gao, Y. Liu, X. Li, Q. Bai, and P. Liu, "Abnormal retinal nerve fiber layer thickness and macula lutea in patients with mild cognitive impairment and Alzheimer's disease," *Archives of Gerontology and Geriatrics*, vol. 60, no. 1, pp. 162–167, 2015.

[179] E. Salobrar-Garcia, I. Hoyas, M. Leal et al., "Analysis of retinal peripapillary segmentation in early Alzheimer's disease patients," *BioMed Research International*, vol. 2015, Article ID 636548, 8 pages, 2015.

[180] J. den Haan, F. D. Verbraak, P. J. Visser, and F. H. Bouwman, "Retinal thickness in Alzheimer's disease: a systematic review and meta-analysis," *Alzheimer's & Dementia: Diagnosis, Assessment & Disease Monitoring*, vol. 6, pp. 162–170, 2017.

[181] L. P. Cunha, L. C. Lopes, L. V. F. Costa-Cunha et al., "Macular thickness measurements with frequency domain-OCT for quantification of retinal neural loss and its correlation with cognitive impairment in Alzheimer's disease," *PLoS One*, vol. 11, no. 4, article e0153830, 2016.

[182] J. P. Cunha, R. Proença, A. Dias-Santos et al., "Choroidal thinning: Alzheimer's disease and aging," *Alzheimer's & Dementia : Diagnosis, Assessment & Disease Monitoring*, vol. 8, pp. 11–17, 2017.

[183] A. Trebbastoni, M. Marcelli, F. Mallone et al., "Attenuation of choroidal thickness in patients with Alzheimer disease: evidence from an Italian prospective study," *Alzheimer Disease and Associated Disorders*, vol. 31, no. 2, pp. 128–134, 2017.

[184] V. E. Pollock, L. S. Schneider, H. C. Chui, V. Henderson, M. Zemansky, and R. B. Sloane, "Visual evoked potentials in dementia: a meta-analysis and empirical study of Alzheimer's disease patients," *Biological Psychiatry*, vol. 25, no. 8, pp. 1003–1013, 1989.

[185] S. Holroyd and M. L. Shepherd, "Alzheimer's disease: a review for the ophthalmologist," *Survey of Ophthalmology*, vol. 45, no. 6, pp. 516–524, 2001.

[186] B. Katz and S. Rimmer, "Ophthalmologic manifestations of Alzheimer's disease," *Survey of Ophthalmology*, vol. 34, no. 1, pp. 31–43, 1989.

[187] R. Kromer, N. Serbecic, L. Hausner, L. Froelich, and S. C. Beutelspacher, "Comparison of visual evoked potentials and retinal nerve fiber layer thickness in Alzheimer's disease," *Frontiers in Neurology*, vol. 4, 2013.

[188] P. K. Iseri, Ö. Altinaş, T. Tokay, and N. Yüksel, "Relationship between cognitive impairment and retinal morphological and visual functional abnormalities in Alzheimer disease," *Journal of Neuro-Ophthalmology*, vol. 26, no. 1, pp. 18–24, 2006.

[189] V. Parisi, R. Restuccia, F. Fattapposta, C. Mina, M. G. Bucci, and F. Pierelli, "Morphological and functional retinal impairment in Alzheimer's disease patients," *Clinical Neurophysiology*, vol. 112, no. 10, pp. 1860–1867, 2001.

[190] K. Krasodomska, W. Lubiński, A. Potemkowski, and K. Honczarenko, "Pattern electroretinogram (PERG) and pattern visual evoked potential (PVEP) in the early stages of Alzheimer's disease," *Documenta Ophthalmologica*, vol. 121, no. 2, pp. 111–121, 2010.

[191] H. Kergoat, M.-J. Kergoat, L. Justino, H. Chertkow, A. Robillard, and H. Bergman, "Visual retinocortical function in dementia of the Alzheimer type," *Gerontology*, vol. 48, no. 4, pp. 197–203, 2002.

[192] B. Katz, S. Rimmer, V. Iragui, and R. Katzman, "Abnormal pattern electroretinogram in Alzheimer's disease: evidence for retinal ganglion cell degeneration?," *Annals of Neurology*, vol. 26, no. 2, pp. 221–225, 1989.

[193] G. L. Trick, M. C. Barris, and M. Bickler-Bluth, "Abnormal pattern electroretinograms in patients with senile dementia of the Alzheimer type," *Annals of Neurology*, vol. 26, no. 2, pp. 226–231, 1989.

[194] L. Justino, M. J. Kergoat, H. Bergman, H. Chertkow, A. Robillard, and H. Kergoat, "Neuroretinal function is normal in early dementia of the Alzheimer type," *Neurobiology of Aging*, vol. 22, no. 4, pp. 691–695, 2001.

[195] F. Altimiras, B. Uszczynska-Ratajczak, F. Camara et al., "Brain transcriptome sequencing of a natural model of Alzheimer's disease," *Frontiers in Aging Neuroscience*, vol. 9, 2017.

[196] X.-F. He, Y.-T. Liu, C. Peng, F. Zhang, S. Zhuang, and J.-S. Zhang, "Optical coherence tomography assessed retinal nerve fiber layer thickness in patients with Alzheimer's disease: a meta-analysis," *International Journal of Ophthalmology*, vol. 5, no. 3, pp. 401–405, 2012.

[197] B. J. Kim, D. J. Irwin, D. Song et al., "Optical coherence tomography identifies outer retina thinning in frontotemporal degeneration," *Neurology*, vol. 89, no. 15, pp. 1604–1611, 2017.

[198] E. A. Williams, D. McGuone, M. P. Frosch, B. T. Hyman, N. Laver, and A. Stemmer-Rachamimov, "Absence of Alzheimer disease neuropathologic changes in eyes of subjects with Alzheimer disease," *Journal of Neuropathology and Experimental Neurology*, vol. 76, no. 5, pp. 376–383, 2017.

[199] T. Tian, B. Zhang, Y. Jia, and Z. Li, "Promise and challenge: the lens model as a biomarker for early diagnosis of Alzheimer's disease," *Disease Markers*, vol. 2014, Article ID 826503, 5 pages, 2014.

[200] L. Bei, Y.-B. Shui, F. Bai, S. K. Nelson, G. P. Van Stavern, and D. C. Beebe, "A test of lens opacity as an indicator of preclinical Alzheimer disease," *Experimental Eye Research*, vol. 140, pp. 117–123, 2015.

[201] C. Y.-L. Cheung, Y. T. Ong, M. K. Ikram et al., "Microvascular network alterations in the retina of patients with Alzheimer's disease," *Alzheimer's & Dementia: The Journal of the Alzheimer's Association*, vol. 10, no. 2, pp. 135–142, 2014.

[202] G. Banerjee, R. Carare, C. Cordonnier et al., "The increasing impact of cerebral amyloid angiopathy: essential new insights for clinical practice," *Journal of Neurology, Neurosurgery, and Psychiatry*, vol. 88, no. 11, pp. 982–994, 2017.

[203] S. McGrory, J. R. Cameron, E. Pellegrini et al., "The application of retinal fundus camera imaging in dementia: a systematic review," *Alzheimer's & Dementia: Diagnosis, Assessment & Disease Monitoring*, vol. 6, pp. 91–107, 2017.

[204] C.-Y. Ho, J. C. Troncoso, D. Knox, W. Stark, and C. G. Eberhart, "Beta-amyloid, phospho-tau and alpha-synuclein deposits similar to those in the brain are not identified in the eyes of Alzheimer's and Parkinson's disease patients," *Brain Pathology*, vol. 24, no. 1, pp. 25–32, 2014.

[205] A. B. Syed, R. A. Armstrong, and C. U. Smith, "A quantitative analysis of optic nerve axons in elderly control subjects and patients with Alzheimer's disease," *Folia Neuropathologica*, vol. 43, no. 1, pp. 1–6, 2005.

[206] C. A. Curcio and D. N. Drucker, "Retinal ganglion cells in Alzheimer's disease and aging," *Annals of Neurology*, vol. 33, no. 3, pp. 248–257, 1993.

[207] J. C. Blanks, Y. Torigoe, D. R. Hinton, and R. H. I. Blanks, "Retinal degeneration in the macula of patients with Alzheimer's disease," *Annals of the New York Academy of Sciences*, vol. 640, no. 1, pp. 44–46, 1991.

[208] J. C. Blanks, D. R. Hinton, A. A. Sadun, and C. A. Miller, "Retinal ganglion cell degeneration in Alzheimer's disease," *Brain Research*, vol. 501, no. 2, pp. 364–372, 1989.

[209] S. Joly, S. Lamoureux, and V. Pernet, "Nonamyloidogenic processing of amyloid beta precursor protein is associated with retinal function improvement in aging male APP_{swe}/PS1ΔE9 mice," *Neurobiology of Aging*, vol. 53, pp. 181–191, 2017.

[210] P. A. Williams, R. A. Thirgood, H. Oliphant et al., "Retinal ganglion cell dendritic degeneration in a mouse model of Alzheimer's disease," *Neurobiology of Aging*, vol. 34, no. 7, pp. 1799–1806, 2013.

Hindawi
Neural Plasticity
Volume 2018, Article ID 3725087, 12 pages
https://doi.org/10.1155/2018/3725087

Research Article

Environmental Enrichment Induces Changes in Long-Term Memory for Social Transmission of Food Preference in Aged Mice through a Mechanism Associated with Epigenetic Processes

Simona Cintoli,[1,2] **Maria Cristina Cenni**,[1] **Bruno Pinto**,[2,3] **Silvia Morea**,[2] **Alessandro Sale**,[1] **Lamberto Maffei**,[1,3] **and Nicoletta Berardi**[1,2]

[1]*Neuroscience Institute, CNR, Via G. Moruzzi 1, 56124 Pisa, Italy*
[2]*Department of Neuroscience, Psychology, Drug Research and Child Health (NEUROFARBA), University of Florence, Florence, Italy*
[3]*Scuola Normale Superiore, Pisa, Italy*

Correspondence should be addressed to Alessandro Sale; sale@in.cnr.it

Received 7 February 2018; Revised 17 May 2018; Accepted 31 May 2018; Published 16 July 2018

Academic Editor: Claudio A. Mastronardi

Decline in declarative learning and memory performance is a typical feature of normal aging processes. Exposure of aged animals to an enriched environment (EE) counteracts this decline, an effect correlated with reduction of age-related changes in hippocampal dendritic branching, spine density, neurogenesis, gliogenesis, and neural plasticity, including its epigenetic underpinnings. Declarative memories depend on the medial temporal lobe system, including the hippocampus, for their formation, but, over days to weeks, they become increasingly dependent on other brain regions such as the neocortex and in particular the prefrontal cortex (PFC), a process known as system consolidation. Recently, it has been shown that early tagging of cortical networks is a crucial neurobiological process for remote memory formation and that this tagging involves epigenetic mechanisms in the recipient orbitofrontal (OFC) areas. Whether EE can enhance system consolidation in aged animals has not been tested; in particular, whether the early tagging mechanisms in OFC areas are deficient in aged animals and whether EE can ameliorate them is not known. This study aimed at testing whether EE could affect system consolidation in aged mice using the social transmission of food preference paradigm, which involves an ethologically based form of associative olfactory memory. We found that only EE mice successfully performed the remote memory recall task, showed neuronal activation in OFC, assessed with c-fos immunohistochemistry and early tagging of OFC, assessed with histone H3 acetylation, suggesting a defective system consolidation and early OFC tagging in aged mice which are ameliorated by EE.

1. Introduction

Aging of the brain is a complex biological process associated with decline in sensory, motor, and cognitive functions. In particular, a decline in declarative learning and memory performance is a typical feature of the normal aging process. Human and animal model data are in accordance to show that during aging, changes in neuronal morphology and density as well as changes in synaptic density, function, and plasticity are specific to each area of the brain [1–3]; brain areas crucial for declarative memory formation, such as hippocampus and other medial temporal lobe structures, show differential volume decline with age, associated with loss of synaptic density, changes in neuronal electrophysiological properties, deficits in synaptic plasticity [1, 3, 4], and changes in gene transcription [5, 6] and in epigenetic mechanisms, leading to reduction in plasticity factors necessary for the induction and local consolidation of synaptic efficacy changes [7, 8]. Aged rodents have contributed a crucial part of these data [1, 9, 10].

Environmental enrichment (EE) is an experimental protocol classically defined as "a combination of complex

inanimate and social stimulation" [11] which provides animals with the opportunity to attain high levels of voluntary physical activity on running wheels and to enhance exploration, cognitive activity, and social interaction. EE causes brain changes at functional, anatomical, and molecular level, including changes in plasticity factors and mechanisms (see [9]), with clear benefits for learning and memory [12–15], particularly evident in aged animals [9, 12, 16]. Most of the studies have been conducted in aged rodents, but EE has been found to provide cognitive benefits also in other aged mammals (see [9]). Positive effects of EE on cognitive processes have been found in young, adult, and aged rodents both for hippocampal-dependent and hippocampal-independent learning and memory [9, 12–22]. For instance, EE improves spatial memory, (see [9, 23, 24]), object recognition memory [9, 24], social novelty [9, 24], and fear memory [25] in aged mice and in mouse models of neurodegeneration (see [26]). These beneficial effects in aged animals have been related to EE action on neurogenesis, neurotrophic factors (BDNF), IGF-I, synaptic plasticity, and neurotransmitter systems (see [9]). In particular, the improvement in declarative learning and memory performance in EE aged rodents has been correlated with EE attenuating the age-related changes in hippocampal dendritic branching, spine density, neurogenesis, gliogenesis, and neural plasticity, including its epigenetic underpinnings [9, 20–22, 26–31].

Declarative memories (memories for facts and events) are not acquired in their definitive form but undergo a gradual process of stabilization over time to allow long-term maintenance [32–34]. In animals, typical protocols to test declarative memory are those testing spatial memory, recognition memory, and in general associative memory. In the process of associative memory formation, consolidation, and maintenance, the hippocampus is believed to integrate, in the form of an anatomical index, information transmitted from distributed cortical networks that support the various features of a whole experience [34], rapidly merging these different features into a coherent memory trace. Consolidation of this new memory trace at the cortical level would then occur slowly via repeated and coordinated reactivation of hippocampal-cortical networks in order to progressively increase the strength and stability of corticocortical connections that represent the original experience. Therefore, these types of memories depend on the medial temporal lobe system, including the hippocampus, for their formation, but, over days to weeks, they become increasingly dependent on other brain regions such as the neocortex and in particular the prefrontal cortex (PFC) [20–23]. This process of time-dependent gradual reorganization of the brain regions supporting remote memory storage is known as systems-level memory consolidation or system consolidation [24–28]. Recently, it has been shown that early tagging of cortical networks is a necessary neurobiological process for remote associative olfactory memory formation using the social transmission of food preference (STFP) paradigm, an ethologically based form of associative olfactory memory [29–31], and that this tagging involves epigenetic mechanisms in the recipient orbitofrontal (OFC) areas [35, 36].

Whether EE can enhance system consolidation in aged animals has not been tested; in particular, whether the early tagging mechanisms in OFC areas demonstrated by Lesburgueres et al. [36] in young animals are deficient in aged animals and whether EE can ameliorate them is not known.

This study aimed at testing whether EE could affect system consolidation in STFP in aged mice. As already pointed out, aged mice are considered a good model of aging, with translation value [10]. For instance, deficits in the same types of memory appear in aged humans and mice, increases in oxidative stress parameters and neuroinflammation, which are typical alterations of the aged brain, are present in both aged humans and mice [9, 10], and, even if amyloid plaques are not found in aged mouse brain, recent work has shown that aged mice do show an increase in amyloid oligomers, which also characterize human aging [37]. Regarding the estimated correspondence between murine and human age, some comparative studies have estimated [38] that senescence begins in mice around eighteen months of age; the age of mice in the present paper (15-16 months) would then correspond, approximately, with the upper limit of human adulthood (65 years).

We have studied whether EE could affect system consolidation in STFP, a protocol particularly suitable to study recent and remote associative memory [39], in aged mice, using the same protocol used by Lesburgueres et al. [36] to demonstrate for the first time a role for histone acetylation in the early tagging of OFC in young animals. We found that only EE mice successfully performed the remote associative olfactory memory recall task and showed neuronal activation in OFC, assessed with c-fos immunohistochemistry. Early tagging of OFC, assessed with histone H3 acetylation [36], was found in EE but not in SC aged mice.

2. Materials and Methods

2.1. Animal Treatment. Male and female C57BL/6 mice of 14 months of age were used in this study. All the procedures were approved by the Italian Ministry of Health. Animals were housed in the animal house with a 12 h/12 h light/dark cycle and with food and water available ad libitum. At 14 months of age, animals were assigned to one of the following rearing conditions for 40 days: environmental enrichment (EE mice, $n = 32$) or standard condition (SC mice, $n = 40$). SC rearing condition consisted of $26 \times 18 \times 18$ cm cages housing 3 animals per cage. EE rearing condition was achieved using a large cage ($44 \times 62 \times 28$ cm) containing several food hoppers, one running wheel for voluntary physical exercise, and differently shaped objects (tunnels, toys, shelters, and stairs) that were repositioned twice a week and completely substituted with others once a week. The rearing conditions were maintained throughout the behavioral tests.

2.2. Social Transmission of Food Preference (STFP) Test. For the STFP test, mice, male and female, were transferred in same-sex littermate groups (2–5 animals per box) in Plexiglas cages. The test was performed during the light phase of the cycle. The STFP task is based on food neophobia in rodents. Mice show a preference for eating a food that is cued with an

odor previously experienced in the breath of a conspecific, over a flavor cued with a novel scent [40, 41]. In this protocol, "observer" mice interact, during the learning phase, with a "demonstrator" mouse that has recently eaten a novel food. When observer mice are subsequently presented with a choice between the food eaten by the demonstrator and some other novel foods, they prefer the food eaten by the demonstrator, the familiar food. This phenomenon depends on the observer mice detecting olfactory cues in the breath of the demonstrator mouse during their interaction within the learning phase (sniff interaction). The subsequent food preference serves as a measure of memory for those olfactory cues. Before starting the test, one mouse from each cage was designated as the "demonstrator" and the others as the "observers." For the behavioral experiments we have used a total of 17 EE animals and 23 SC animals: in the EE group, 13 EE animals performed the behavioral tasks as observers and 4 EE mice served as demonstrator mice; in the SC group, 16 SC animals performed the task as observers and and 7 SC mice served as demonstrators.

The STFP task consisted of three distinct phases as described in the protocol of Wrenn et al. [41, 42]. To minimize neophobia during the experiments, mice were habituated to eat powdered rodent chow from 4 oz (113.40 g) glass food jar assemblies (Dyets Inc., Bethlehem, PA). Jars were approximately 7 cm in diameter and 5 cm in depth [41]. The jar assemblies have been selected in order to prevent mice from crawling and digging into the food and spilling the food from the jar.

Before the first phase, the experimenter prepared the food jar assemblies using flavored food and recorded the weights of the jars. Cocoa-flavored chow was obtained by mixing ground cocoa with plain powdered chow to give a 2% (*w*/*w*) cocoa mixture. Cumin-flavored chow was obtained by mixing cumin with plain powdered chow to give a 0.5% (*w*/*w*) cumin mixture [36].

In phase I, the demonstrators were exposed to cocoa-flavored food during a 1 h feeding session in a cage without water. At the end of phase I, the jar assemblies were removed and weighed: the demonstrator that did not eat at least 0.2 g of food was not used in the further steps of the experiment. In phase II, the learning phase, the demonstrators, immediately after the 1 h exposure to the flavored food, were placed into the cages containing their respective observers: mice were allowed to interact freely for 30 min. During phase II, the experimenter constantly watched the demonstrator from a distance of ≅50 cm and recorded the number of times that each "observer" sniffed the muzzle of the demonstrator. A sniff is defined as a close (<2 cm) orientation of the observer's nose toward the front or side of the demonstrator's muzzle [41]. The scoring of observer sniffs of the demonstrator's muzzle can provide critical data showing that the impairment in food preference is not due to changes in social behavior and insufficient social interaction. Phase III, the choice phase, started after a selected retention interval (1 h, 24 h, or 30 days). Each observer was placed in an individual cage with two jars in the opposite side of the cage for counterbalancing the position. One jar contained the familiar food (cocoa-flavored), consumed by the demonstrator observer mice had interacted with, the other one the novel food (cumin-flavored). After 1 h of feeding period, the jars were removed from the cages and weighed; the amount of food eaten from each jar was recorded. The preference for the familiar food over the novel food was taken as an index of memory for the familiar food. For all three phases, the experimenter was blind to the rearing conditions of the mice.

To control for the effects of extra handling, novel food sniffing, and consumption and interaction with the demonstrator mouse on c-fos activation and histone H3 acetylation, we used pseudolearning (PL) mice; these animals experienced arena exploration, jar exploration, food consumption, and interaction with the demonstrator, but no learning was involved. Indeed, PL subjects (12 PL-EE and 12 PL-SC) did not detect any olfactory cue in the breath of the demonstrator mouse during the interaction period, since demonstrator mice (3 EE and 5 SC) did not eat any food before interaction. In this way, we can control for differences in c-fos expression or H3 acetylation simply due to extra handling, exposure to the arena, food, and demonstrator mouse, in the learning group and isolate the effect of learning on c-fos activation and H3 acetylation.

For c-fos-positive cell analysis, we used, at 24 h retention interval, EE ($n = 4$), SC ($n = 4$), PL-EE ($n = 4$), and PL-SC ($n = 4$); at 30-day retention interval, EE ($n = 4$), SC ($n = 4$), PL-EE ($n = 4$), and PL-SC ($n = 4$); for histone H3 acetylation analysis in the OFC, we used EE ($n = 4$), SC ($n = 4$), PL-EE ($n = 4$), and PL-SC ($n = 4$).

A possible confounding factor is the presence of an innate flavor preference for one of the flavors used in the experiment. Over the years, several different flavorants have been successfully used in the basic procedure of STFP [43]. The pairs of flavorant used in the present paper and their specific concentrations were based on literature data [36] and on pilot data indicating that by giving naïve mice a choice between the two flavors used in our experiment, mice ate the same amount of each flavored food in the absence of STFP training ($n = 5$, paired t-test cocoa-flavored versus cumin-flavored $p = 0.359$).

2.3. Immunohistochemistry. We used the procedure previously described in [44]. Mice were anaesthetized and perfused via intracardiac infusion with 0.1 M PBS and then 4% paraformaldehyde (PFA, dissolved in 0.1 M phosphate buffer, pH 7.4) 90 min after completion of phase III (choice phase) or 60 minutes after phase II (learning phase) for c-fos and histone H3 acetylation, respectively. Brains were removed, fixed overnight in PFA, and then transferred to 30% sucrose solution and stored at 4°C. Coronal sections were cut at 40 μm thickness on a freezing microtome (Sliding Leica microtome SM2010R, Leica Microsystems) and processed for immunohistochemistry.

For c-fos immunohistochemistry, after a blocking step in 10% NGS and 0.5% Triton X-100 in PBS, free-floating sections were incubated using anti-c-fos rabbit polyclonal antibody (1 : 3000 rabbit anti-c-fos polyclonal antibody, Calbiochem, USA) for 36 h at 4°C. Subsequently, sections were transferred in a solution containing 1% NGS,

0.1% Triton X-100, and 1 : 200 anti-rabbit biotinylated antibody (Vector Labs) in PBS. This was followed by incubation in ABC kit (Vector Labs) and final detection with DAB reaction kit (Vector Labs). Sections were finally mounted on gelatinized slides, dehydrated, and sealed with DPX mounting medium (VWR International, UK).

For acetyl-histone H3 immunohistochemistry, after a blocking step in 10% NGS and 0.05% Triton X-100 in PBS, sections were incubated in a solution containing 10% NGS, 0.05% Triton X-100, and anti-acetyl-histone H3 monoclonal rabbit antibodies (Lys14, 1 : 200 rabbit anti-acetyl-histone H3 monoclonal antibodies, Millipore, USA) overnight at 4°C. Subsequently, sections were transferred in a solution containing 3% NGS, 0.05% Triton X-100, and 1 : 400 Alexa Fluor 568 goat anti-rabbit IgG antibody (Life Technologies) in PBS (Ciccarelli et al., 2013). Sections were then mounted on gelatinized slides with VECTASHIELD (Vector Labs).

2.4. Quantitative Analysis of c-fos-Positive Cells. We used the procedure previously described in [44]. Counting of c-fos-positive cells in different brain areas was performed using a CCD camera (MBF Bioscience, Germany) mounted on a Zeiss Axioskop (Zeiss, Germany) microscope and the Stereo Investigator software (MBF Bioscience). Brain structures were anatomically defined according to a mouse brain atlas (Paxinos and Franklin, 1997), and the regions of interest selected for measurement of c-fos-positive nuclei in the orbitofrontal cortex (OFC) were (numbers indicate the distance in millimeters of the sections from bregma) medial orbital cortex (MO, +2.80 mm), ventral orbital cortex (VO, +2.80 mm), lateral orbital cortex (LO, +2.80 mm), and dorsolateral orbital cortex (DLO, +2.80 mm). The number of c-fos-positive cells was counted at 20x magnification, in 5–10 fields ($50 \times 50\,\mu$m or $100 \times 100\,\mu$m) per section according to the size of brain structure and their density calculated (cells/mm^2), using at least 5 sections for each structure. The experimenter counting c-fos-positive cells was blind to the rearing condition and treatment of the animals.

2.5. Quantitative Analysis of Immunohistochemical Signal of Histone H3 Acetylation in the OFC. The imaging of brain areas was performed using a CCD camera (MBF Bioscience, Germany) mounted on a Zeiss Axioskop (Zeiss, Germany) microscope and QCapture software (QImaging, Canada). Brain structures were anatomically defined according to a mouse brain atlas (Paxinos and Franklin, 1997). Images were acquired at 20x magnification in one field of $200 \times 300\,\mu$m per section, keeping constant both microscope settings and fluorescence-field intensity. The collected images were imported to the image analysis system MetaMorph (molecular devices), and for each animal, the relative signal intensity of AcH3-immunopositive cells was calculated using at least 5 sections for each structure. The relative signal intensity of AcH3-immunopositive cells was calculated as the ratio between the mean intensity of AcH3-immunopositive cells and the intensity of background signal measured in sample areas surrounding AcH3$^+$ cells. All image acquisition and analysis were carried out in blind.

2.6. Statistics. All results were expressed as mean ± SEM, and all statistical analyses were performed using statistical software package SigmaStat (SigmaStat, version 3.5). For STFP performance in phase III, a two-way analysis of variance (ANOVA) for repeated measures (RM) was performed for each retention interval (1 h, 24 h, or 30 days), considering both factor condition (EE or SC or PL-EE or PL-SC) and factor flavor (familiar or novel), with post hoc analysis Holm-Sidak method. The number of c-fos-positive cells in each OFC area was analyzed with a two-way ANOVA, factor condition and retention interval, with post hoc analysis Holm-Sidak method. The level of histone H3 acetylation in each OFC area was analyzed with a two-way ANOVA, factor condition, and area, with post hoc analysis Holm-Sidak method.

3. Results

3.1. Long-Term STFP Memory Deficit in Aged Mice Is Ameliorated by EE. Aged C57BL/6 mice, housed in EE or SC for 40 days, were subjected to the STFP task. During the learning phase (phase II), interactions between demonstrator and observer mice were scored to control for possible differences between EE and SC mice in the amount of interactions (a schematic diagram of the experimental protocol is reported in Figure 1).

Indeed, a difference in interaction with the demonstrator during the learning phase would affect performance in the choice phase: an observer mouse is expected not to show any preference for the cued food if it has not adequately interacted with the demonstrator during the learning phase. We found no difference in the amount of interactions between EE and SC mice (t-test, EE ($n = 13$) versus SC ($n = 16$), $p = 0.111$; data not shown).

Then, we evaluated olfactory memory abilities in the choice phase (phase III) of the STFP task: in this phase, observer mice, after a retention interval, were placed in individual cages allocating two jars: one jar contained a familiar food identical to that consumed by the demonstrator and the other containing a totally novel food. After 1 h spent in the choice phase, the jars were removed from the cage and weighed in order to assess the amount of food eaten from each jar. The choice phase was performed at three different intervals, that is, 1 h, 24 h (day 1), or 30 days (day 30) after the end of phase II.

At 1 h retention interval, we found a clear preference for the familiar food in both groups of animals which underwent associative learning of familiar food in the breath of the demonstrator, SC ($n = 8$) and EE ($n = 5$) (two-way RM ANOVA, post hoc analysis Holm-Sidak method, familiar food versus novel food, $p = 0.007$ for SC, $p < 0.001$ for EE; Figure 1); on the contrary, at retention intervals 24 h (day 1) and 30 days (day 30), we found a significant familiar food preference only for EE mice, while SC mice displayed no preference at either interval (two-way RM ANOVA post hoc analysis Holm-Sidak method, familiar food versus novel food at day 1, $p = 0.153$ for SC mice ($n = 4$), $p = 0.001$ for EE mice ($n = 4$); at day 30, $p = 0.095$ for SC mice ($n = 4$), $p = 0.021$ for EE mice ($n = 4$); Figure 2).

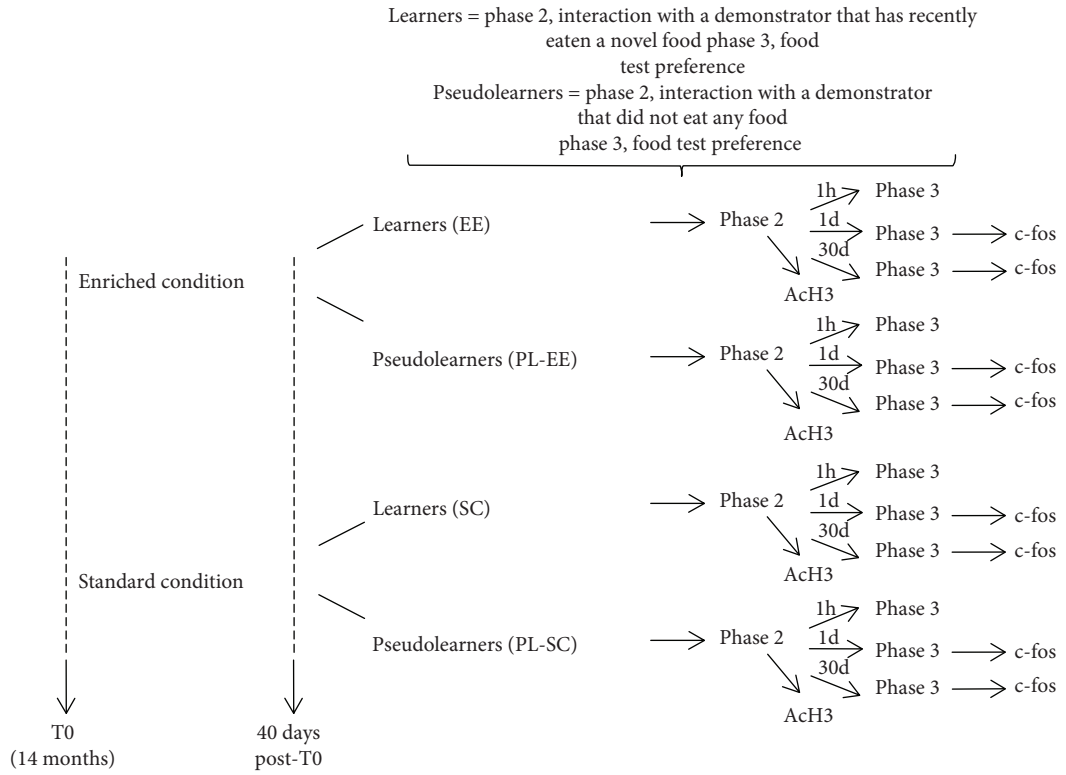

Figure 1: Schematic diagram of the experimental protocol.

As expected, no food preference was displayed by PL-SC and PL-EE mice, which did not undergo associative learning (two-way RM ANOVA, post hoc analysis Holm-Sidak method, novel versus familiar; $p > 0.05$ at both retention intervals; Figure 2).

The good performance of SC mice at 1 h retention interval rules out the possibility of olfactory deficits hampering the preference for the familiar food in aged SC mice. Thus, their failure in eating significantly more the familiar food at day 1 and day 30 indicates a long-term STFP memory deficit in aged SC mice, which is rescued by EE.

3.2. c-fos Expression in the OFC of Aged SC and EE Mice following a Retention Interval of 1 or 30 Days. After the end of the choice test at day 1 and day 30, when SC and EE mice significantly differed in their memory performance, mice were sacrificed and the expression of c-fos protein was assessed as an indicator of neuronal activity in the OFC, the final olfactory memory storage site. c-fos immunohistochemistry is currently used in developing adult and aging animals as a reliable, surrogate marker for neuronal activity, particularly when spatial distribution of neuronal activity and comparison of neural activation between different brain regions is of interest (see, e.g., [10, 44–50]). We separately counted c-fos-positive cells in 4 OFC subregions, medial orbital cortex (MO), ventral orbital cortex (VO), lateral orbital cortex (LO), and dorsolateral orbital cortex (DLO). No difference was present between the two control groups, PL-EE and PL-SC mice, in any OFC region at any retention interval (two-way ANOVA, post hoc analysis Holm-Sidak method, PL-EE versus PL-SC, $p > 0.05$; Figure 3), suggesting that EE and SC condition per se does not affect c-fos expression in the areas of interest during the choice test.

At day 1, we found significant neuronal activation in OFC both for EE and SC mice: indeed, the number of c-fos-positive cells was higher in SC and EE mice with respect to their controls (PL-SC and PL-EE mice) in all OFC areas in EE mice and in LO and DLO in SC mice (two-way ANOVA, post hoc analysis Holm-Sidak method for condition, EE versus PL-EE ($p < 0.01$) for all areas; SC versus PL-SC ($p < 0.01$) for LO and DLO; SC versus PL-SC ($p > 0.05$) for MO and VO; Figure 3). No difference was present between EE and SC mice in any OFC regions (two-way ANOVA, post hoc analysis Holm-Sidak method for condition, EE versus SC ($p > 0.05$) for all areas; Figure 3).

At day 30 retention interval, we found significant neuronal activation only in EE mice: in particular, we found an increased number of c-fos-positive cells in all OFC areas of EE mice (two-way ANOVA, post hoc analysis Holm-Sidak method for condition, EE versus PL-EE ($p < 0.001$) in all areas; Figure 3). No increase in the number of c-fos-positive cells was present in any OFC area at day 30 in SC mice with respect to their controls (two-way ANOVA, post hoc analysis Holm-Sidak method for condition, SC versus PL-SC ($p > 0.05$) in all areas; Figure 2), indicating lack of neuronal activation. A comparison between EE and SC c-fos expression at day 30 showed a greater neuronal activation in EE with respect to SC mice in all OFC areas (two-way ANOVA, post hoc analysis Holm-Sidak method for housing

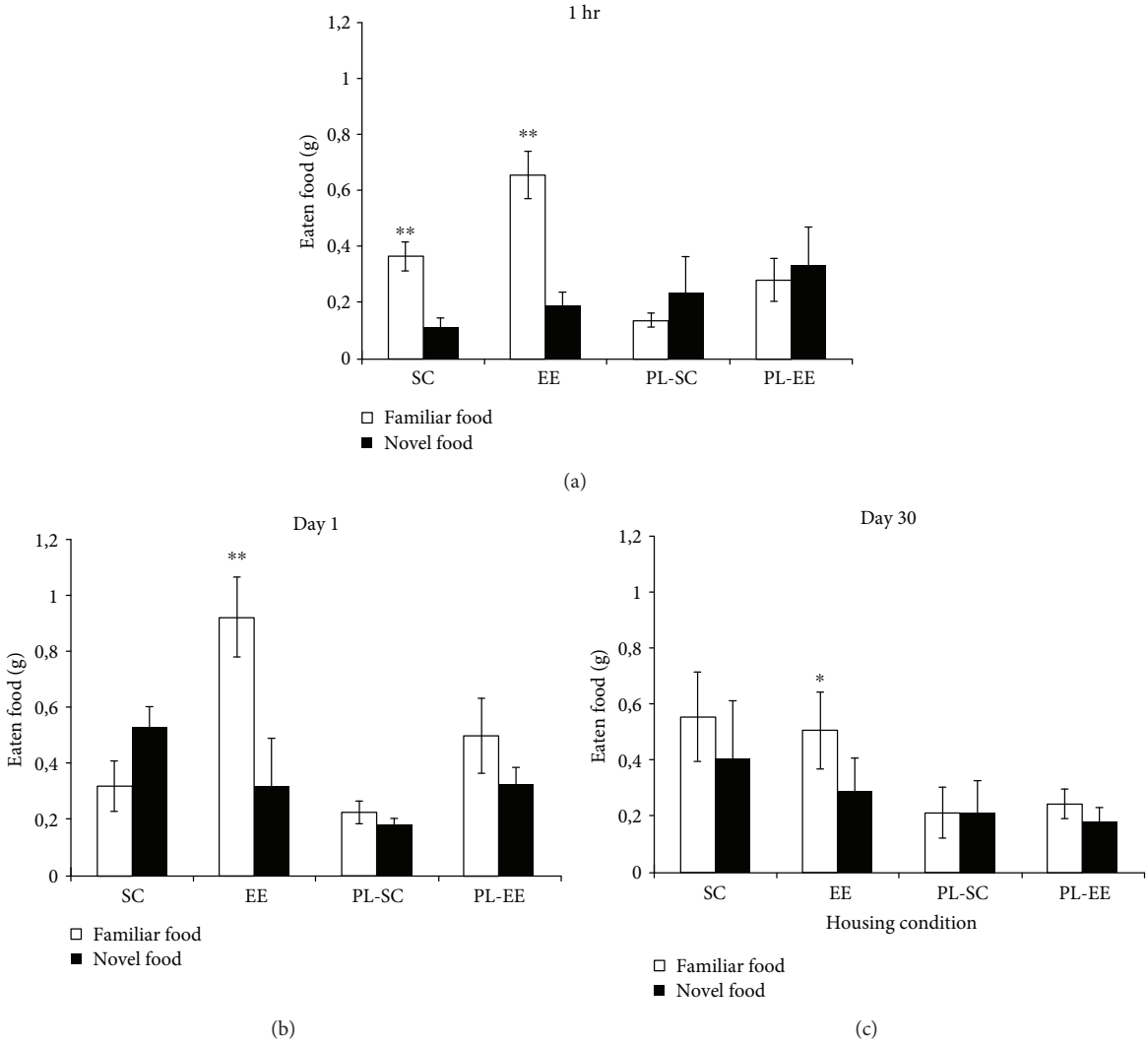

Figure 2: Performance of SC, EE, PL-SC, and PL-EE mice in the STFP. (a) 1-hour retention interval: there is a significant preference for the familiar food (open columns) with respect to the novel food (filled columns) for SC and EE groups, which underwent associative learning of familiar food in the breath of the demonstrator (two-way RM ANOVA post hoc analysis Holm-Sidak method, familiar food versus novel food for SC ($p = 0.007$) and EE ($p < 0.001$)). (b) 24-hour retention interval (day 1). There is a significant preference for the familiar food with respect to the novel food only for EE group (two-way RM ANOVA post hoc analysis Holm-Sidak method, familiar food versus novel food for EE ($p = 0.001$)). (c) 30-day retention interval (day 30): there is a significant preference for the familiar food with respect to the novel food only for EE group (two-way RM ANOVA post hoc analysis Holm-Sidak method, familiar food versus novel food for EE ($p = 0.021$)). There is no preference for the familiar food in pseudolearning mice, PL-SC and PL-EE, for any time interval (two-way RM ANOVA post hoc analysis Holm-Sidak method ($p > 0.05$) for all comparisons). $^{*}p < 0.05$; $^{**}p < 0.01$; error bars = SEM.

condition, EE versus SC, $p = 0.003$ for MO and $p < 0.001$ for VO, LO, and DLO; Figure 3).

In the comparison between c-fos activations at day 1 and day 30, we found a significantly higher number of c-fos-positive cells at day 30 with respect to day 1 in EE mice in all OFC areas but MO (two-way ANOVA, post hoc analysis Holm-Sidak method 30 versus 1 in EE, $p = 0.181$ in MO; $p < 0.001$ in VO; $p = 0.004$ in LO; $p = 0.035$ in DLO; Figure 3); on the contrary, no significantly higher activation of OFC areas was found at day 30 with respect to day 1 in SC mice; rather, we found a decrease in c-fos expression in LO for the SC group (two-way ANOVA, post hoc analysis Holm-Sidak method 30 versus 1 in SC, $p = 0.018$ in LO; $p > 0.05$ in MO, VO, and DLO; Figure 3).

Thus, preserved memory at day 30 in EE mice was associated with a significant activation of OFC and with increased OFC activation with respect to day 1 recall.

3.3. Increased Histone H3 Acetylation in the OFC of EE Aged Mice 1 h after the Learning Phase. Epigenetic changes are crucially involved in memory consolidation [35, 51]. Lesburgueres et al. [36] have shown that the setting of synaptic tags during system consolidation of STFP memory involves epigenetic mechanisms, in particular increased acetylation of histone H3 in the OFC shortly (1 h) after the learning phase; preventing the increase in H3 acetylation impaired remote memory, assessed 30 days later, while pharmacological maintenance of a higher level of acetylation resulted in

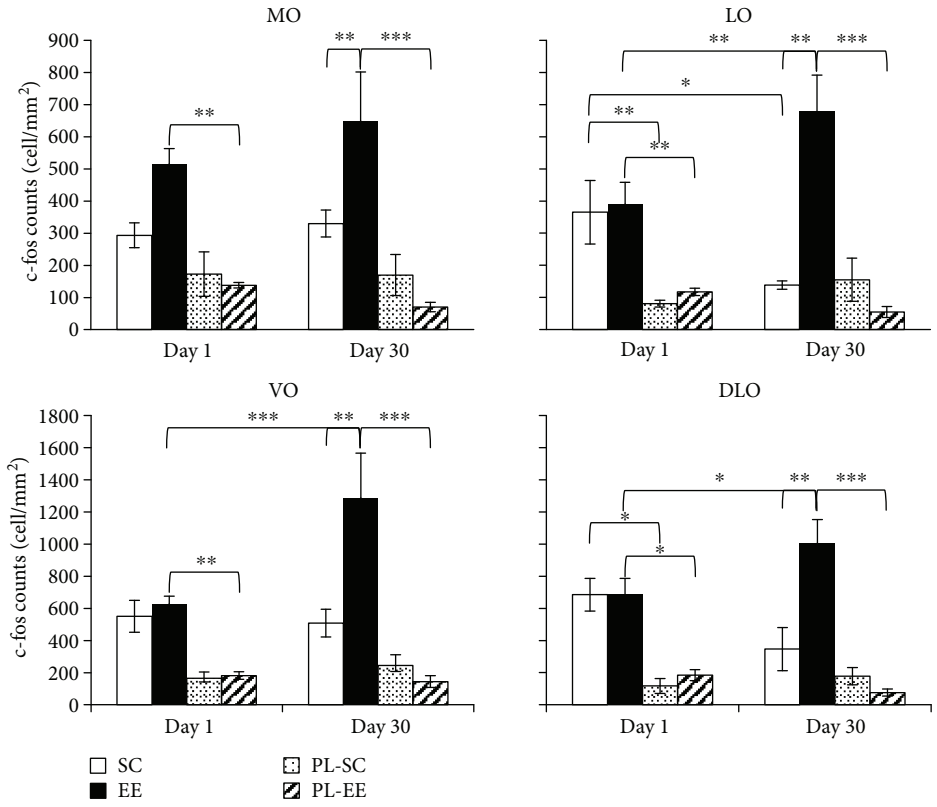

(a)

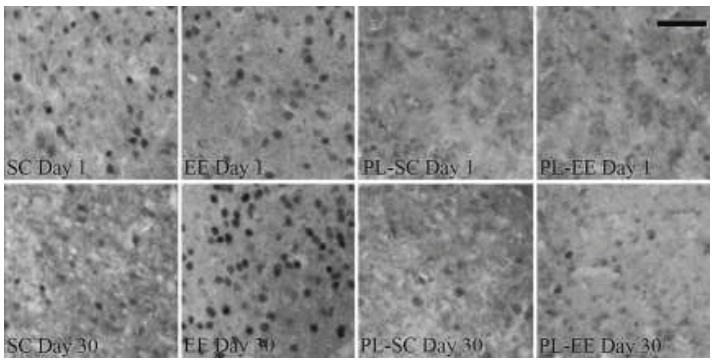

(b)

Figure 3: (a) c-fos expression in subregions of OFC for SC (open columns), EE (filled columns), PL-SC (dotted columns), and PL-EE (hatched columns) mice subjected to choice phase at day 1 and day 30. MO: two-way ANOVA, factor condition ($p < 0.001$), factor time ($p = 0.613$), condition × time ($p = 0.530$), post hoc analysis Holm-Sidak method. SC versus PL-SC and PL-SC versus PL-EE ($p > 0.05$) for all retention intervals. Statistical differences were found between EE versus PL-EE at day 1 ($p = 0.001$) and day 30 ($p < 0.001$); EE versus SC significant at day 30 ($p = 0.003$). LO: two-way ANOVA, factor condition ($p < 0.001$), factor time ($p = 0.688$), condition × time ($p = 0.004$), post hoc analysis Holm-Sidak method. PL-SC versus PL-EE ($p > 0.05$) for all retention intervals. Statistical differences were found between SC versus PL-SC at day 1 ($p = 0.004$); EE versus PL-EE at day 1 ($p = 0.001$) and day 30 ($p < 0.001$); EE versus SC significant at day 30 ($p < 0.001$). Statistical differences within group were found between day 1 and day 30 for SC group ($p = 0.018$) and for EE group ($p = 0.004$). VO: two-way ANOVA, factor condition ($p < 0.001$), factor time ($p = 0.054$), condition × time ($p = 0.015$), post hoc analysis Holm-Sidak method. SC versus PL-SC and PL-SC versus PL-EE ($p > 0.05$) for all retention intervals. Statistical differences were found between EE versus PL-EE at day 1 ($p = 0.001$) and day 30 ($p < 0.001$); EE versus SC significant at day 30 ($p < 0.001$). Statistical differences within EE group were found between day 1 and day 30 ($p < 0.001$). DLO: two-way ANOVA, factor condition ($p < 0.001$), factor time ($p = 0.913$), condition × time ($p = 0.059$), post hoc analysis Holm-Sidak method. PL-SC versus PL-EE ($p > 0.05$) for all retention intervals. Statistical differences were found between SC versus PL-SC at day 1 ($p = 0.003$); EE versus PL-EE at day 1 ($p = 0.002$) and day 30 ($p < 0.001$); EE versus SC significant at day 30 ($p < 0.001$). Statistical differences within EE group were found between day 1 and day 30 ($p = 0.035$). $^{*}p < 0.05$; $^{**}p < 0.01$; $^{***}p < 0.001$; error bars = SEM. (b) Representative panel of c-fos protein expression in DLO for SC, EE, PL-SC, and PL-EE mice, following recall at day 1 and day 30; scale bar: 50 μm.

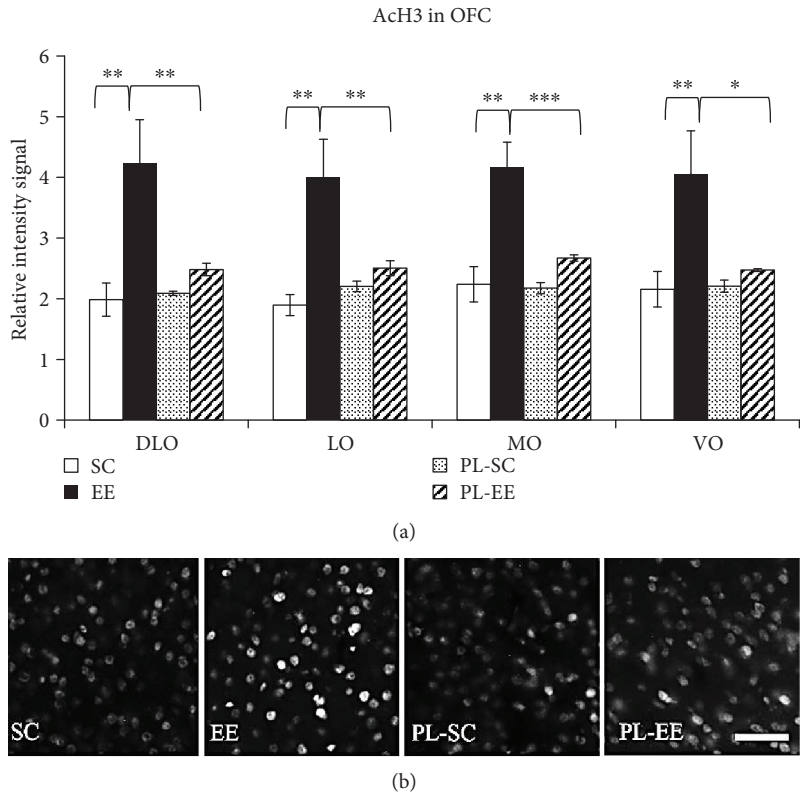

Figure 4: (a) H3 acetylation on L14 in subregions of OFC for SC (open columns), EE (filled columns), PL-SC (dotted columns), and PL-EE (hatched columns) mice 1 hour after the learning phase. PL-SC did not differ from PL-EE mice. Only EE animals showed significant differences with respect to their controls in OFC areas; (one-way ANOVA ($p < 0.01$), post hoc analysis Holm-Sidak method, SC versus PL-SC and PL-SC versus PL-EE ($p > 0.05$) for all subregions). MO: EE versus SC ($p < 0.001$), EE versus PL-EE ($p = 0.001$). LO: EE versus SC ($p < 0.001$), EE versus PL-EE ($p = 0.007$). VO: EE versus SC ($p = 0.004$), EE versus PL-EE ($p = 0.013$). DLO: EE versus SC ($p = 0.001$), EE versus PL-EE ($p = 0.008$). $^{*}p < 0.05$; $^{**}p < 0.01$; $^{***}p < 0.001$; error bars = SEM. (b) Representative panel of histone H3 acetylation in DLO for SC, EE, PL-SC, and PL-EE mice 1 h after learning; scale bar: 50 μm.

improved remote memory retrieval. Using Lesburgueres et al. protocol, we have assessed AcH3 levels in OFC 1 h after the learning phase.

We found that the signal intensity of histone H3 acetylation on lysine 14 was significantly increased with respect to control PL mice only in EE mice, and this was found in all subregions of OFC (one-way ANOVA, $p < 0.01$, post hoc analysis Holm-Sidak method, EE versus PL-EE, $p < 0.01$ for all subregions; Figure 4); no intensity difference was found between SC and PL-SC or between PL-EE and PL-SC mice (one-way ANOVA, $p < 0.01$, post hoc analysis Holm-Sidak method, SC versus PL-SC, $p > 0.05$ for all subregions; Figure 4). Intensity of H3 acetylation in EE mice was significantly higher than in SC mice in all OFC regions (one-way ANOVA, $p < 0.01$, post hoc analysis Holm-Sidak method, EE versus SC, $p < 0.01$ for all subregions; Figure 4).

Thus, the preserved remote memory recall in aged EE mice is associated with enhanced OFC histone acetylation early in the system consolidation process, which suggests a preserved early tagging of OFC.

4. Discussion

Brain aging is a complex physiological process characterized by a progressive deterioration of cognitive functions, especially in the learning and memory domains. Major deficits are particularly evident at the level of declarative memory abilities requiring the precise recall of detailed information, a process initially mediated by the hippocampus and other medial temporal lobe structures [1, 4] and subsequently supported by the process of system consolidation. System consolidation consists in the functional and structural reorganization of cerebral regions prompted by the reactivation of hippocampal-cortical pathways and the strengthening of corticocortical connections, leading to formation of a cortical memory trace which supports remote memory recall [36, 52]. Many papers have investigated the effects of EE on local memory consolidation in the aged hippocampus, responsible for formation and early maintenance of hippocampus-dependent memory; for instance, EE ameliorates CA1 plasticity and cell excitability and reverses age-related epigenetic changes and other age-related negative processes (see, e.g., [20–22, 31, 53]). However, to our knowledge, the effects of EE on system consolidation, that is, on the recruitment of cortical activity to support remote memory, have not been investigated in aged animals. In particular, we found no study on the effects of EE on the early tagging in prefrontal cortex as a correlate of remote memory retrieval.

In this study, we showed that exposure to EE in aged mice modulates system consolidation and enhances performance in

the STFP declarative memory task. STFP is a hippocampus-dependent task which exploits the natural tendency of rodents to prefer food sources based on a previous sampling of their odor in the breath of littermates. In this task, the behavioral performance can be efficiently measured in a single trial session and, given that the underlying memory traces are long-lasting, it allows researchers to perform a characterization of possible changes in the expression levels of potential transcription factors involved in memory acquisition and in the recall phases. Olfactory memories activated by STFP are eventually transferred to the OFC, via a system consolidation process which requires early tagging of cortical networks in this structure [36].

While early tagging of cortical networks has been previously investigated in adult rodents, no evidence for similar mechanisms has been provided, so far, in aged animals. We first report that, while aged SC animals displayed severe deficits in memory recall at both recent (1 day) and remote (30 days) time intervals, EE preserved cognitive performance in the STFP task at both intervals. The performance of aged EE mice thus resembles that of standard-reared young adult rats, performing well both recent and remote STFP memory recall [36].

Focusing on c-fos expression as a marker of neuronal activity, we analyzed the activation of the final recipient of SFTP memory, namely, OFC, during recent and remote recall. A marked environment-dependent effect was found in the OFC, with enriched mice displaying higher c-fos expression levels compared to SC animals at the 30-day interval, in agreement with the differences in recall abilities displayed by enriched versus SC animals in the SFTP declarative memory task at this time point. Importantly, the absence of OFC activation displayed by SC aged mice at the 30 days of retention interval was not dependent on general olfactory discrimination deficits, as demonstrated by the intact performance displayed by the same group at shorter intervals (1 h). Comparable amounts of OFC activation were instead found in SC and EE animals at the 1-day retention interval, when both groups displayed increased c-fos expression compared to their respective controls; however, this activation of OFC areas was paralleled by marked behavioral deficits evident at this time point. These results indicate that OFC activation recorded 24 h past the end of the acquisition phase is not sufficient for, or not correlated with, mouse mnemonic performance. This is in accordance with the late role for OFC in system consolidation and its dispensability for recent memory recall [36, 52, 54, 55].

Looking for possible epigenetic changes acting as an early tagging mechanism for memory formation in olfactory cortical networks, we found an increased H3 acetylation in all analyzed OFC areas of EE subjects compared to SC animals. H3 acetylation levels were found to be enhanced with respect to control animals in EE mice, but not in SC animals. These results suggest a deficit in the initial steps of cortical tagging of memory traces associated with brain aging in SC compared to EE animals and demonstrate that exposure to stimulating environmental conditions preserves remote recall of declarative memory abilities in aged mice by promoting system consolidation through the activation of epigenetic regulatory processes crucial for coding and consolidation of cortical mnemonic traces. System consolidation is the process of time-dependent gradual reorganization of the brain regions supporting remote memory storage. Within this process, early tagging of cortical circuits is a necessary step for the formation of enduring associative memory [35, 36]. In particular, early tagging of OFC cortical networks is a prerequisite for the establishment of remote olfactory memory of the STFP. Synaptic tags may serve as an early and persistent signature of activity in the cortex that is necessary to ensure the progressive rewiring of cortical networks that support remote memory storage. The early increase in histone H3 acetylation following STFP learning phase is involved in the formation of the early synaptic tags in OFC supporting STFP remote memory retrieval: preventing the increase in H3 acetylation impaired remote memory, assessed 30 days later, while pharmacological maintenance of a higher level of acetylation resulted in improved remote memory retrieval probed 30 days later [36]. Our results show that in the absence of H3 acetylation following learning, as is the case of aged SC mice, there is a strong memory deficit. EE ameliorates memory performance in aged mice, allowing a good retrieval of memory 30 days after learning and this is associated with an increased H3 acetylation in OFC of EE mice. This suggests that EE preserves a good early tagging in aged mice and strengthens the hypothesis that early tagging is important for system consolidation.

It has been previously reported that an increased activity of histone acetyltransferase (HAT) enzymes during a hippocampus-dependent task can be accompanied by increased histone acetylation acting as a specific epigenetic tagging for memory consolidation [56]. It is well known that environment-induced beneficial effects on brain plasticity and memory abilities may involve HAT activation [9, 28]. The increased AcH3 found in our EE mice might suggest an involvement of HAT activation; however, further work would be necessary to elucidate the mechanisms underlying this increased acetylation.

At the 24 h retention interval, OFC activation in SC mice was enhanced with respect to their PL controls, reaching levels not significantly different from those displayed by EE mice; however, differently from EE mice, in SC mice, OFC activation at the 24 h of retention interval was not preceded by any early tagging process, suggesting that it is the lack of early tagging and not the lack of general recruitment of OFC areas that is responsible for the main deficits in remote associative memory formation displayed by SC aged mice. Indeed, the crucial and irreplaceable role of early tagging is that of topographically specifying, by means of epigenetic signature [35, 36], which sets of cortical neurons will participate to the hippocampal-cortical dialogue during the course of systems-level consolidation. In the absence of early tagging, that is, of the specification of the recipient circuits in OFC, the general activation of OFC would be unlikely to sustain the fine process of transferring specific information from the hippocampus to OFC to sustain formation of enduring associative memory.

EE is well known to affect synaptic function not only in young or adult but also in aged animals, where EE ameliorates many of the deficits in synaptic physiology, density, and plasticity induced by age (see [1, 9, 20, 22]). We cannot exclude that these effects of EE might have contributed to our results, for instance, via a better encoding/local consolidation process in the hippocampus, especially in the case of the better performance of EE animals at the 24 h interval, where early tagging in PFC is not supposed to play a key role; enhanced synaptic function and plasticity in EE animals might also have contributed to our results enhancing the efficacy of the hippocampal-cortical dialogue during formation of the cortical trace which supports remote memory.

In conclusion, our results show that exposure to stimulating environmental conditions can be used as a powerful paradigm to promote good system consolidation of associative memory in aged mice and suggest that system consolidation may be a crucial target for treatments aimed at ameliorating memory dysfunctions in elderly subjects.

Data Availability

The data used to support the findings of this study are available from the corresponding author upon request.

Conflicts of Interest

The authors declare that they have no conflicts of interest.

Acknowledgments

This work was made possible by the generous funding of "Fondazione Pisa" to project "Train the Brain" and to project "Translational Assessment in Aging" (Bando Ricerca Scientifica in Neuroscienze 2007 and Bando Ricerca Scientifica e Tecnologica 2016, Fondazione Pisa).

References

[1] S. N. Burke and C. A. Barnes, "Neural plasticity in the ageing brain," *Nature Reviews Neuroscience*, vol. 7, no. 1, pp. 30–40, 2006.

[2] T. Hedden and J. D. E. Gabrieli, "Insights into the ageing mind: a view from cognitive neuroscience," *Nature Reviews Neuroscience*, vol. 5, no. 2, pp. 87–96, 2004.

[3] S. A. Small, S. A. Schobel, R. B. Buxton, M. P. Witter, and C. A. Barnes, "A pathophysiological framework of hippocampal dysfunction in ageing and disease," *Nature Reviews Neuroscience*, vol. 12, no. 10, pp. 585–601, 2011.

[4] C. A. Barnes, "Secrets of aging: what does a normally aging brain look like?," *F1000 Biology Reports*, vol. 3, p. 22, 2011.

[5] A. Fleischmann, O. Hvalby, V. Jensen et al., "Impaired long-term memory and NR2A-type NMDA receptor-dependent synaptic plasticity in mice lacking c-Fos in the CNS," *The Journal of Neuroscience*, vol. 23, no. 27, pp. 9116–9122, 2003.

[6] X. Zhou, C. Moon, F. Zheng et al., "N-methyl-D-aspartate-stimulated ERK1/2 signaling and the transcriptional up-regulation of plasticity-related genes are developmentally regulated following in vitro neuronal maturation," *Journal of Neuroscience Research*, vol. 87, no. 12, pp. 2632–2644, 2009.

[7] J. Graff and L. H. Tsai, "Histone acetylation: molecular mnemonics on the chromatin," *Nature Reviews Neuroscience*, vol. 14, no. 2, pp. 97–111, 2013.

[8] S. K. Pirooznia and F. Elefant, "Targeting specific HATs for neurodegenerative disease treatment: translating basic biology to therapeutic possibilities," *Frontiers in Cellular Neuroscience*, vol. 7, p. 30, 2013.

[9] A. Sale, N. Berardi, and L. Maffei, "Environment and brain plasticity: towards an endogenous pharmacotherapy," *Physiological Reviews*, vol. 94, no. 1, pp. 189–234, 2014.

[10] M. Weber, T. Wu, J. E. Hanson et al., "Cognitive deficits, changes in synaptic function, and brain pathology in a mouse model of normal aging (1, 2, 3)," *eNeuro*, vol. 2, no. 5, 2015.

[11] M. R. Rosenzweig, E. L. Bennett, M. Hebert, and H. Morimoto, "Social grouping cannot account for cerebral effects of enriched environments," *Brain Research*, vol. 153, no. 3, pp. 563–576, 1978.

[12] J. Bennett, P. McRae, L. Levy, and K. Frick, "Long-term continuous, but not daily, environmental enrichment reduces spatial memory decline in aged male mice," *Neurobiology of Learning and Memory*, vol. 85, no. 2, pp. 139–152, 2006.

[13] S. N. Duffy, K. J. Craddock, T. Abel, and P. V. Nguyen, "Environmental enrichment modifies the PKA-dependence of hippocampal LTP and improves hippocampus-dependent memory," *Learning & Memory*, vol. 8, no. 1, pp. 26–34, 2001.

[14] H. van Praag, B. R. Christie, T. J. Sejnowski, and F. H. Gage, "Running enhances neurogenesis, learning, and long-term potentiation in mice," *Proceedings of the National Academy of Sciences of the United States of America*, vol. 96, no. 23, pp. 13427–13431, 1999.

[15] H. van Praag, G. Kempermann, and F. H. Gage, "Neural consequences of environmental enrichment," *Nature Reviews Neuroscience*, vol. 1, no. 3, pp. 191–198, 2000.

[16] K. M. Frick and S. M. Fernandez, "Enrichment enhances spatial memory and increases synaptophysin levels in aged female mice," *Neurobiology of Aging*, vol. 24, no. 4, pp. 615–626, 2003.

[17] G. Schoenbaum, M. R. Roesch, T. A. Stalnaker, and Y. K. Takahashi, "Orbitofrontal cortex and outcome expectancies: optimizing behavior and sensory perception," in *Neurobiology of Sensation and Reward*, J. A. Gottfried, Ed., CRC Press/Taylor & Francis, Boca Raton, FL, USA, 2011.

[18] Y. P. Tang, H. Wang, R. Feng, M. Kyin, and J. Z. Tsien, "Differential effects of enrichment on learning and memory function in NR2B transgenic mice," *Neuropharmacology*, vol. 41, no. 6, pp. 779–790, 2001.

[19] A. M. Birch and A. M. Kelly, "Lifelong environmental enrichment in the absence of exercise protects the brain from age-related cognitive decline," *Neuropharmacology*, 2018.

[20] L. E. B. Bettio, L. Rajendran, and J. Gil-Mohapel, "The effects of aging in the hippocampus and cognitive decline," *Neuroscience and Biobehavioral Reviews*, vol. 79, pp. 66–86, 2017.

[21] S. J. Morse, A. A. Butler, R. L. Davis, I. J. Soller, and F. D. Lubin, "Environmental enrichment reverses histone methylation changes in the aged hippocampus and restores age-related memory deficits," *Biology*, vol. 4, no. 2, pp. 298–313, 2015.

[22] A. Kumar, A. Rani, O. Tchigranova, W. H. Lee, and T. C. Foster, "Influence of late-life exposure to environmental enrichment or exercise on hippocampal function and CA1

senescent physiology," *Neurobiology of Aging*, vol. 33, no. 4, pp. 828.e1–828.e17, 2012.

[23] M. Hüttenrauch, G. Salinas, and O. Wirths, "Effects of long-term environmental enrichment on anxiety, memory, hippocampal plasticity and overall brain gene expression in C57BL6 mice," *Frontiers in Molecular Neuroscience*, vol. 9, 2016.

[24] C. Grinan-Ferre, D. Perez-Caceres, S. M. Gutierrez-Zetina et al., "Environmental enrichment improves behavior, cognition, and brain functional markers in young senescence-accelerated prone mice (SAMP8)," *Molecular Neurobiology*, vol. 53, no. 4, pp. 2435–2450, 2016.

[25] P. Obiang, E. Maubert, I. Bardou et al., "Enriched housing reverses age-associated impairment of cognitive functions and tPA-dependent maturation of BDNF," *Neurobiology of Learning and Memory*, vol. 96, no. 2, pp. 121–129, 2011.

[26] J. Nithianantharajah and A. J. Hannan, "Enriched environments, experience-dependent plasticity and disorders of the nervous system," *Nature Reviews Neuroscience*, vol. 7, no. 9, pp. 697–709, 2006.

[27] L. Baroncelli, C. Braschi, M. Spolidoro, T. Begenisic, A. Sale, and L. Maffei, "Nurturing brain plasticity: impact of environmental enrichment," *Cell Death and Differentiation*, vol. 17, no. 7, pp. 1092–1103, 2010.

[28] A. Fischer, F. Sananbenesi, X. Wang, M. Dobbin, and L. H. Tsai, "Recovery of learning and memory is associated with chromatin remodelling," *Nature*, vol. 447, no. 7141, pp. 178–182, 2007.

[29] B. Kolb, G. Gorny, A. H. V. Soderpalm, and T. E. Robinson, "Environmental complexity has different effects on the structure of neurons in the prefrontal cortex versus the parietal cortex or nucleus accumbens," *Synapse*, vol. 48, no. 3, pp. 149–153, 2003.

[30] F. Mora, G. Segovia, and A. del Arco, "Aging, plasticity and environmental enrichment: structural changes and neurotransmitter dynamics in several areas of the brain," *Brain Research Reviews*, vol. 55, no. 1, pp. 78–88, 2007.

[31] K. M. Frick, "Epigenetics, oestradiol and hippocampal memory consolidation," *Journal of Neuroendocrinology*, vol. 25, no. 11, pp. 1151–1162, 2013.

[32] Y. Dudai, "The neurobiology of consolidations, or, how stable is the engram?," *Annual Review of Psychology*, vol. 55, no. 1, pp. 51–86, 2004.

[33] S. H. Wang and R. G. M. Morris, "Hippocampal-neocortical interactions in memory formation, consolidation, and reconsolidation," *Annual Review of Psychology*, vol. 61, no. 1, pp. 49–79, 2010.

[34] L. R. Squire and P. J. Bayley, "The neuroscience of remote memory," *Current Opinion in Neurobiology*, vol. 17, no. 2, pp. 185–196, 2007.

[35] K. M. Lattal and M. A. Wood, "Epigenetics and persistent memory: implications for reconsolidation and silent extinction beyond the zero," *Nature Neuroscience*, vol. 16, no. 2, pp. 124–129, 2013.

[36] E. Lesburgueres, O. L. Gobbo, S. Alaux-Cantin, A. Hambucken, P. Trifilieff, and B. Bontempi, "Early tagging of cortical networks is required for the formation of enduring associative memory," *Science*, vol. 331, no. 6019, pp. 924–928, 2011.

[37] M. Mainardi, A. Di Garbo, M. Caleo, N. Berardi, A. Sale, and L. Maffei, "Environmental enrichment strengthens corticocortical interactions and reduces amyloid-β oligomers in aged mice," *Frontiers in Aging Neuroscience*, vol. 6, 2014.

[38] S. Dutta and P. Sengupta, "Men and mice: relating their ages," *Life Sciences*, vol. 152, pp. 244–248, 2016.

[39] B. Bessieres, O. Nicole, and B. Bontempi, "Assessing recent and remote associative olfactory memory in rats using the social transmission of food preference paradigm," *Nature Protocols*, vol. 12, no. 7, pp. 1415–1436, 2017.

[40] P. Valsecchi, M. Mainardi, A. Sgoifo, and A. Taticchi, "Maternal influences on food preferences in weanling mice Mus domesticus," *Behavioural Processes*, vol. 19, no. 1–3, pp. 155–166, 1989.

[41] C. C. Wrenn, A. P. Harris, M. C. Saavedra, and J. N. Crawley, "Social transmission of food preference in mice: methodology and application to galanin-overexpressing transgenic mice," *Behavioral Neuroscience*, vol. 117, no. 1, pp. 21–31, 2003.

[42] C. C. Wrenn, "Unit 8.5G Social transmission of food preference in mice," *Current Protocols in Neuroscience*, 2004.

[43] B. G. Galef and E. E. Whiskin, "Socially transmitted food preferences can be used to study long-term memory in rats," *Animal Learning & Behavior*, vol. 31, no. 2, pp. 160–164, 2003.

[44] J. Bonaccorsi, S. Cintoli, R. Mastrogiacomo et al., "System consolidation of spatial memories in mice: effects of enriched environment," *Neural Plasticity*, vol. 2013, Article ID 956312, 12 pages, 2013.

[45] J. P. Aggleton and M. W. Brown, "Contrasting hippocampal and perirhinalcortex function using immediate early gene imaging," *Quarterly Journal of Experimental Psychology*, vol. 58, no. 3-4b, pp. 218–233, 2005.

[46] R. Melani, G. Chelini, M. C. Cenni, and N. Berardi, "Enriched environment effects on remote object recognition memory," *Neuroscience*, vol. 352, pp. 296–305, 2017.

[47] A. S. Zannas, J. H. Kim, and A. E. West, "Regulation and function of MeCP2 Ser 421 phosphorylation in U50488-induced conditioned place aversion in mice," *Psychopharmacology*, vol. 234, no. 6, pp. 913–923, 2017.

[48] J. M. Stratford, J. A. Thompson, and T. E. Finger, "Immunocytochemical organization and sour taste activation in the rostral nucleus of the solitary tract of mice," *The Journal of Comparative Neurology*, vol. 525, no. 2, pp. 271–290, 2017.

[49] J. Y. Joo, K. Schaukowitch, L. Farbiak, G. Kilaru, and T. K. Kim, "Stimulus-specific combinatorial functionality of neuronal c-fos enhancers," *Nature Neuroscience*, vol. 19, no. 1, pp. 75–83, 2016.

[50] R. P. Haberman, M. T. Koh, and M. Gallagher, "Heightened cortical excitability in aged rodents with memory impairment," *Neurobiology of Aging*, vol. 54, pp. 144–151, 2017.

[51] M. Korte and D. Schmitz, "Cellular and system biology of memory: timing, molecules, and beyond," *Physiological Reviews*, vol. 96, no. 2, pp. 647–693, 2016.

[52] P. W. Frankland and B. Bontempi, "The organization of recent and remote memories," *Nature Reviews Neuroscience*, vol. 6, no. 2, pp. 119–130, 2005.

[53] S. Peleg, F. Sananbenesi, A. Zovoilis et al., "Altered histone acetylation is associated with age-dependent memory impairment in mice," *Science*, vol. 328, no. 5979, pp. 753–756, 2010.

[54] P. W. Frankland, B. Bontempi, L. E. Talton, L. Kaczmarek, and A. J. Silva, "The involvement of the anterior cingulate cortex in remote contextual fear memory," *Science*, vol. 304, no. 5672, pp. 881–883, 2004.

[55] P. W. Frankland, C. O'Brien, M. Ohno, A. Kirkwood, and A. J. Silva, "Alpha-CaMKII-dependent plasticity in the cortex is required for permanent memory," *Nature*, vol. 411, no. 6835, pp. 309–313, 2001.

[56] O. Bousiges, A. P. Vasconcelos, R. Neidl et al., "Spatial memory consolidation is associated with induction of several lysine-acetyltransferase (histone acetyltransferase) expression levels and H2B/H4 acetylation-dependent transcriptional events in the rat hippocampus," *Neuropsychopharmacology*, vol. 35, no. 13, pp. 2521–2537, 2010.

Hindawi
Neural Plasticity
Volume 2018, Article ID 2406170, 9 pages
https://doi.org/10.1155/2018/2406170

Research Article

Increased DNA Copy Number Variation Mosaicism in Elderly Human Brain

Darine Villela,[1] **Claudia K. Suemoto**,[2,3] **Renata Leite**,[3] **Carlos Augusto Pasqualucci**,[3,4] **Lea T. Grinberg**,[3,5] **Peter Pearson**,[1] **and Carla Rosenberg**[1]

[1]*Human Genome and Stem Cells Research Center, Department of Genetics and Evolutionary Biology, Institute of Biosciences, University of São Paulo, Rua do Matão 277, 05508-090 São Paulo, SP, Brazil*
[2]*Discipline of Geriatrics, Department of Internal Medicine, University of São Paulo Medical School, Avenida Doutor Arnaldo 455, 01246-000 São Paulo, SP, Brazil*
[3]*Brazilian Aging Brain Study Group-LIM22, Department of Pathology, University of São Paulo Medical School, Avenida Doutor Arnaldo 455, 01246-000 São Paulo, SP, Brazil*
[4]*Department of Pathology, University of São Paulo Medical School, Avenida Doutor Arnaldo 455, 01246-000 São Paulo, SP, Brazil*
[5]*Memory and Aging Center, Department of Neurology, University of California, San Francisco 675 Nelson Rising Lane, P.O. Box 1207, San Francisco, CA 94143, USA*

Correspondence should be addressed to Darine Villela; darinevillela@gmail.com

Received 1 March 2018; Accepted 28 May 2018; Published 28 June 2018

Academic Editor: Mauricio Arcos-Burgos

Aging is a complex process strongly determined by genetics. Previous reports have shown that the genome of neuronal cells displays somatic genomic mosaicism including DNA copy number variations (CNVs). CNVs represent a significant source of genetic variation in the human genome and have been implicated in several disorders and complex traits, representing a potential mechanism that contributes to neuronal diversity and the etiology of several neurological diseases and provides new insights into the normal, complex functions of the brain. Nonetheless, the features of somatic CNV mosaicism in nondiseased elderly brains have not been investigated. In the present study, we demonstrate a highly significant increase in the number of CNVs in nondiseased elderly brains compared to the blood. In two neural tissues isolated from paired *postmortem* samples (same individuals), we found a significant increase in the frequency of deletions in both brain areas, namely, the frontal cortex and cerebellum. Also, deletions were found to be significantly larger when present only in the cerebellum. The sizes of the variants described here were in the 150–760 kb range, and importantly, nearly all of them were present in the Database of Genomic Variants (common variants). Nearly all evidence of genome structural variation in human brains comes from studies detecting changes in single cells which were interpreted as derived from independent, isolated mutational events. The observations based on array-CGH analysis indicate the existence of an extensive clonal mosaicism of CNVs within and between the human brains revealing a different type of variation that had not been previously characterized.

1. Introduction

Aging is a complex process that involves altered cellular function, oxidative stress, longevity, and related diseases [1]. An important challenge for future research is to understand how genetics influences cognition and the neurobiological mechanisms underlying normal and pathological aging. It is expected that genetic variants may contribute to the considerable individual differences in cognitive aging by altering brain plasticity [2, 3]. Interestingly, previous reports have shown that individual neurons display somatic genomic mosaicism [4]. Although the effects of this somatic mosaicism are not fully understood, it is expected that alterations in the genome of neuronal cells will influence both the

normal and the diseased brains. The forms of somatic genomic mosaicism identified in the human brain include aneuploidy [5], mobile genetic element insertions (MEIs) [6, 7], single-nucleotide variants (SNVs), indels [8], and, more recently, DNA copy number variations (CNVs) [4, 9].

CNVs represent a prevalent form of genetic variation that contributes to phenotypic diversity, numerous diseases, and complex traits in human populations [10]. The mechanisms by which copy number changes may affect gene expression, and phenotypic traits comprise alteration of gene dosage and disruption of coding sequences or regulatory elements [10]. McConnell and colleagues were the first to demonstrate increased levels of CNVs in cortical neurons derived from *postmortem* specimens and human-induced pluripotent stem cell (hiPSC) fibroblast-derived neurons compared to blood samples using a single-cell sequencing strategy [11]. The authors identified in both samples a subset of aneuploid neurons as well as numerous subchromosomal CNVs. Because of the long lifespan of neurons and their central role in synapses, it is speculated that the accumulation of somatic mutations within neural progenitor cells or in postmitotic neurons could influence neuronal development, complexity, and function. In this regard, genomic mosaicism in single, sporadic Alzheimer's disease neurons characterized by an increase in total DNA content and amyloid precursor protein (*APP*) gene copy number was reported [12]. The authors also showed large differences in the total DNA content between different brain areas, which may indicate distinct functionality for genomic mosaicism in the central nervous system.

The existence of region-specific somatic mosaicism of DNA content was also demonstrated in nondiseased human brains, suggesting that sporadic brain diseases may depend on which pathogenic loci are altered [12, 13]. However, the features of mosaic CNV in nondiseased elderly brains have not been characterized. It is not clear yet when and what promotes CNV formation in human brains or how does it relate to aging. Moreover, it is worth to mention that nearly all evidence of genome structural variation in human brains comes from studies detecting changes in single cells, either by FISH for detection of chromosomal aneuploidy or by total DNA sequencing of single cells for chromosomal structural rearrangements. The genomic changes observed in single cells were interpreted as derived from independent, isolated mutational events. In this study, based on a comparative array-comparative genomic hybridization (array-CGH) analysis of two brain tissues and blood-isolated *postmortem* samples from the same individuals, we report the existence of an extensive clonal mosaicism for CNV in and between the cerebellum and the frontal cortex compared to the blood, which probably reflects a higher mutation rate in neural tissues.

2. Materials and Methods

2.1. Postmortem DNA Samples. All the samples used in this study were provided by the Brain Bank of the Brazilian Aging Brain Study Group (BBBABSG) [14, 15]. The clinical and functional status of all subjects was assessed through the closest family member to the deceased who completed questionnaires on whether or not the subject was demented or suffered from other possible neural conditions, including a previous history of stroke, epilepsy, or Parkinson's disease. All questionnaires were based on a validated clinical protocol that includes a series of semistructured scales covering major functional abilities [16, 17] and cognitive evaluation by the Clinical Dementia Rating Scale [18] and the Informant Questionnaire on Cognitive Decline in the Elderly [19]. As a standard protocol for neuropathological diagnosis, the brain was examined macroscopically, and 15 brain regions were sampled for microscopic evaluation. Neuropathological examinations were carried out using immunohistochemistry following internationally accepted guidelines [20–23]. BBBABSG's procedures are approved by the Ethical Board of the University of São Paulo Medical School, and the next of kin agreed to participate and signed an informed written consent. Initially, investigations on CNV frequencies were derived from array-CGH data taken from 24 blood and 71 cerebellum independent samples (different individuals). Subsequently, 19 paired blood/cerebellum samples from the same individuals were used to confirm the differences in CNV frequencies between the two tissues. In addition to the paired samples from 19 individuals, we obtained matched frontal cortex tissues from 10 of the individuals. Table 1 presents the characterization of all individuals classified from the paired analysis cohort.

2.2. Array-CGH. CNVs were identified using comparative genomic hybridization based on microarrays (array-CGH) containing 180,000 oligonucleotides (Oxford Gene Technologies, UK). Briefly, samples were labeled with Cy3- and Cy5-deoxycytidine triphosphates by random priming. Purification, hybridization, and washing were carried out as previously reported [24]. Scanned images of the arrays were processed using Feature Extraction software, and data were analyzed with the Genomic Workbench software, both software from Agilent Technologies (Santa Clara, CA, USA). CNVs were identified using the aberration detection method 2 statistical algorithm (ADM2) with a sensitivity threshold of 6.7. A genomic segment was considered duplicated or deleted when the $\log_2$ ratio of the test/reference fluorescent intensities of a given region encompassing at least three probes which were above 0.3 or below −0.3, respectively. The equivalency between the $\log_2$ ratios of the test/reference for duplications is 0.58 and for deletions is −1. Detected CNVs were compared to CNV data from oligoarray studies documented in the Database of Genomic Variants (DGV).

2.3. Statistical Analyses. Data are presented as the mean ± SEM. Statistical analyses (GraphPad Prism 6.0 software, San Diego, CA, USA) were performed using the nonparametric Mann–Whitney *U* test for the comparison between two groups. One-way ANOVA followed by Bonferroni's post hoc test was applied to estimate the mean differences between three groups. Two-way ANOVA was used to compare the mean differences between groups with two independent variables.

3. Results

The investigation of CNVs by array-CGH in independent samples of nondemented elderly individuals revealed a highly

Table 1: Clinical data of all individuals classified as nondemented included in the paired analysis cohort.

Case	Sex	Age at death	Schooling (years of formal education)	Neuropathological diagnosis	Cause of death
1	M	83	14	Normal	Ischemic cardiomyopathy
2	F	97	4	Normal	Dilated cardiomyopathy
3	F	73	12	Normal	Acute infarction myocardial
4	F	77	3	Normal	Tromboembolism pulmonar
5	M	64	4	Normal	Acute infarction myocardial
6	F	66	4	Normal	Healed myocardial infarction
7	F	67	4	Normal	Bilateral bronchopneumonia
8	F	62	1	Normal	Hemopericardium
9	F	70	4	Normal	Myocarditis
10	M	63	11	Normal	Acute infarction myocardial
11	F	81	11	Normal	Pulmonary edema
12	F	77	2	Normal	Hemopericardium
13	M	81	13	Normal	Bronchopneumonia
14	F	65	11	Normal	Acute infarction myocardial
15	M	76	4	Normal	Acute lung edema/myocardiopathy
16	F	75	4	Normal	Acute lung edema
17	M	50	13	Normal	Hypertensive cardiopathy
18	F	89	8	Normal	Acute infarction myocardial
19	M	85	2	Normal	Pulmonary edema

significant increase in the frequency of CNVs in *postmortem* samples from the cerebellum ($n = 71$) compared to blood samples ($n = 24$) (Mann–Whitney U test, $p < 0.0001$) (Figure 1(a)). This finding was later confirmed in 19 paired blood/cerebellum samples taken from the same individuals (Mann–Whitney U test, $p < 0.001$) (Figure 1(b)). Figure 1(c) shows an example of many more copies of a segment of chromosome 8 in the cerebellum than in the blood. For some of the paired cerebellum/blood samples, we were also able to obtain matched frontal cortex tissue and determine the distribution of CNVs between these two neural tissues within the same individuals.

The distribution of absolute CNV numbers in the frontal cortex and cerebellum revealed high heterogeneity both between individuals and tissues (two-way ANOVA, $p < 0.001$) (Figure 2(a)). Further inspection using a Venn diagram (Figure 2(b)) shows the proportion of CNVs observed exclusively either in the frontal cortex or in the cerebellum (referred to as unique CNVs). In total, 75% of the CNVs correspond to unique mutations to one of these two neural tissues (43% in the frontal cortex and 32% in the cerebellum). The remaining 25% refers to CNVs in common to both tissues, suggesting that they were acquired earlier during brain development. All the 159 CNVs identified in these two brain areas are presented in Supplementary Table 1. We also evaluated the CNVs regarding the frequency of deletions and duplications, their length, and gene content. For both in common and in unique CNVs from the frontal cortex and cerebellum, the frequency of deletions was higher than that of duplications (two-way ANOVA, $p < 0.05$, Figure 2(c)). Comparing the lengths of the CNVs, the mean sizes of duplications and deletions differed significantly among groups ($^*p < 0.05$, one-way ANOVA), and the unique deletions from the cerebellum were significantly larger than the ones in common (Bonferroni's test, $p < 0.05$). Nonetheless, in the present data, neither the length nor gene content of the unique CNVs from the frontal cortex and cerebellum areas were significantly different from each other (Table 2).

Importantly, nearly all the observed CNVs in this study, either present in both brain tissues or exclusively to one of them, had already been described in the Database of Genomic Variants (DGV) as polymorphic, being most of them segmental duplications (Figure 2(d)). Figure 3 shows two examples of somatic duplications that are present in the frontal cortex but absent in the cerebellum. As in most of the CNVs observed in this study, the amplified segment involves a gene family with variable copy number variation in the population.

Using the ingenuity pathway analysis (IPA) software (QIAGEN Inc., https://www.qiagenbioinformatics.com/products/ingenuitypathway-analysis), we retrieved the predicted target pathways of all the CNVs identified in the frontal cortex and cerebellum and found enrichment for antigen presentation and regulation cytokine production pathways, respectively (Figure 4); the top diseases/function of all networks retrieved from both neural tissues are presented in Supplementary Table 2.

4. Discussion

Several studies have demonstrated that neuronal genomes exhibit somatic genomic mosaicism compared to other tissues including CNVs [4]. Notably, genome structural variation in the human brain has been reported in single cell studies, using either FISH or DNA sequencing involving large-scale changes such as aneuploidy and structural rearrangements of more

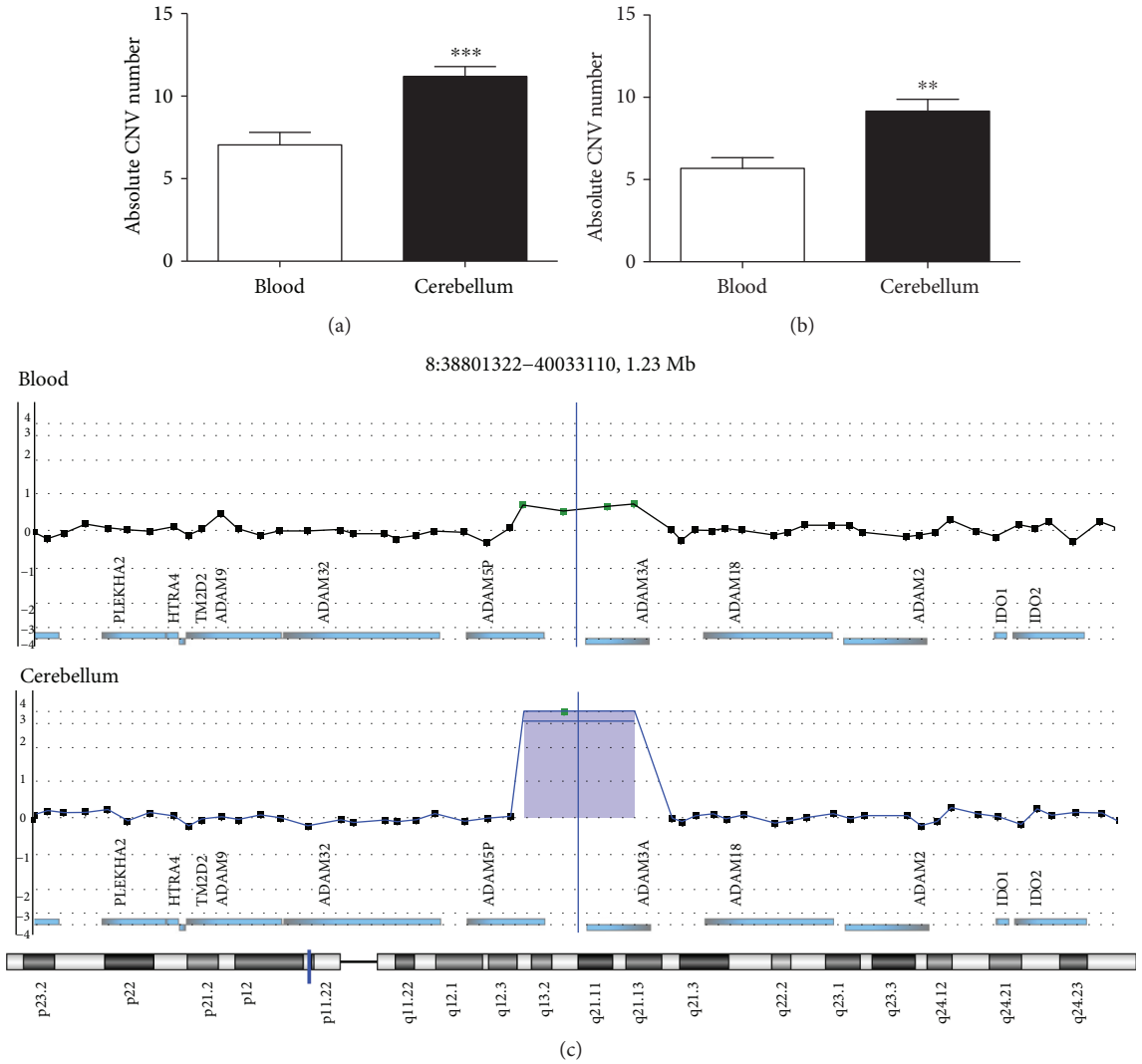

Figure 1: Increase frequency of DNA copy number variation (CNVs) in neural tissue compared to the blood. (a) The mean of the total CNVs detected in independent blood ($n = 24$) and cerebellum tissue ($n = 71$) samples; $^{***}p < 0.0001$, Mann–Whitney U test. (b) The mean of the total CNVs detected in paired blood and cerebellum samples from 19 random individuals; $^{**}p < 0.001$, Mann–Whitney U test. (c) Example of a CNV absent in the blood and observed in the cerebellum. Images extracted from Genomic Workbench software.

than 7 Mb [11, 25]. Our study is the first to investigate the clonal CNV burden within different neural tissues in nondiseased elderly brains using direct microarray analysis.

In contrast to previous studies on single cells using either FISH or DNA sequencing, our results, based on array-CGH analysis, represent genomic changes in DNA pools from a large number of cells from each tissue investigated, which indicates that at least some of these increase in CNV variation in human brains relative to the blood must occur as extensive clones rather than isolated events. The presence of extensive clones involving different CNVs indicates that these CNVs must either have been present in the germline (constitutive) or have originated early in embryonic development and could be distinguished from partial chromosome aneuploidies or large copy number variations as detected by FISH and/or sequencing of single cells [11, 26, 27]. The frequency of unique CNVs in each tissue is probably proportional to the CNV mutation rate for each tissue and should reflect CNV mutation rate differences between tissues. Significantly, nearly all the observed CNVs, both CNVs in common to both neural tissues and presumptively new mutations, had already been described in the Database of Genomic Variants (DGV) as polymorphic, and the amplified segment involves a gene family with variable copy number variation in the population, being most of them segmental duplications. This evidence suggests that many of these variants arose commonly and perhaps involve similar mechanisms in their origin, the nonallelic homologous recombination [10].

The CNV distribution within different human brain areas was highly heterogeneous both between individuals and tissues. A previous study based on flow cytometry demonstrated that the frontal cortex exhibits more variation in DNA content than the cerebellum [13] Although we did not quantify variation in DNA content across our DNA samples from the frontal cortex and cerebellum, we examined whether such differences in DNA content described by

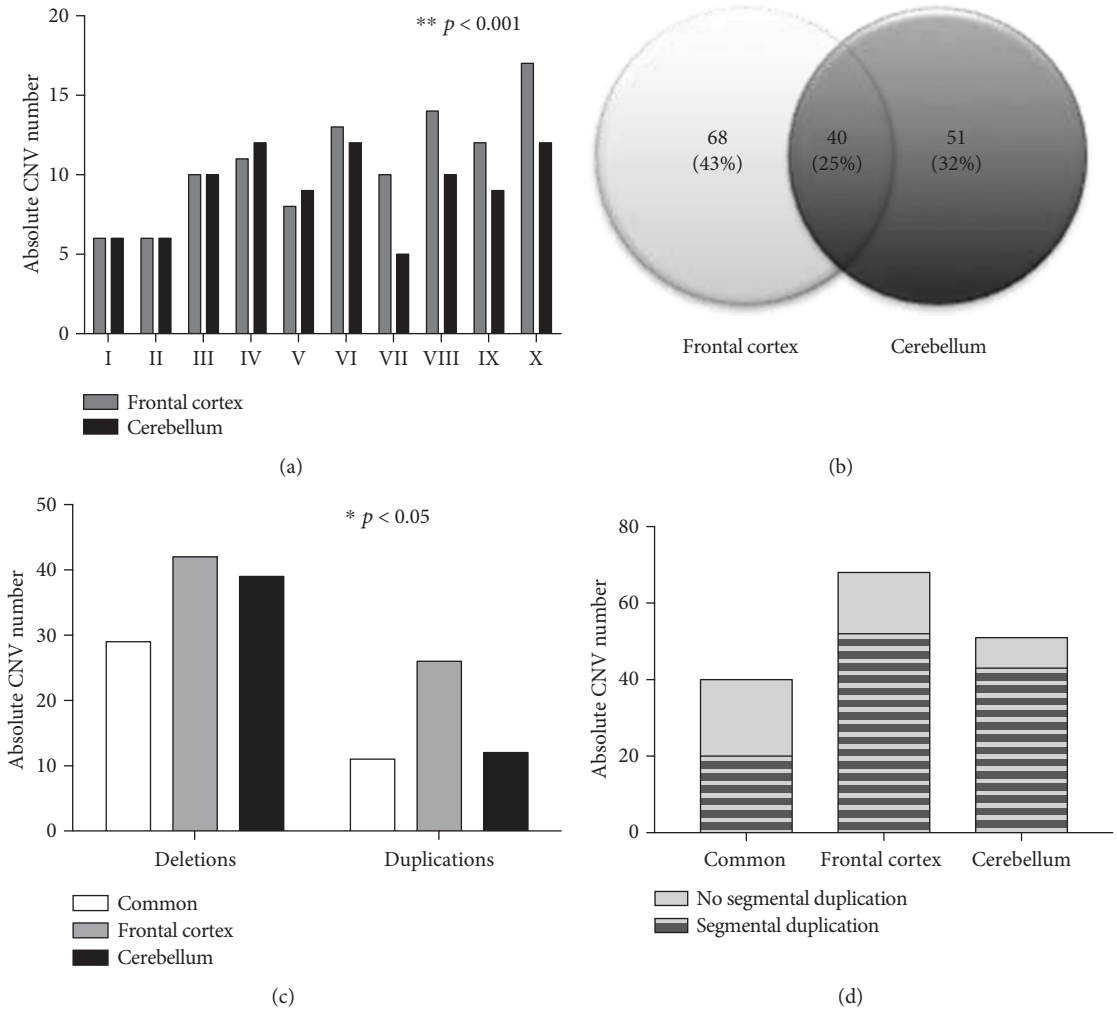

Figure 2: Distribution of DNA copy number variations (CNVs) between two neural tissues from the same individuals. (a) Comparison of the absolute number of CNVs detected in the frontal cortex and cerebellum from 10 paired individuals; $^{**}p < 0.001$ for comparison between individuals, two-way ANOVA. (b) Venn diagram showing the proportion of CNVs observed in the frontal cortex and cerebellum. (c) Total number of deletions and duplications observed in the CNVs in common to both neural tissues and in the unique CNVs from the frontal cortex and cerebellum; $^{*}p < 0.05$ for comparisons between the compared groups as well as deletions and duplications, two-way ANOVA. (d) Proportion of segmental duplications identified in the CNVs in common to both neural tissues and in the unique CNVs from the frontal cortex and cerebellum.

Table 2: Comparison of length and gene content of the in common and unique CNVs from the frontal cortex and cerebellum.

Copy number variation	CNVs in common to both tissues	Unique CNVs (frontal cortex)	Unique CNVs (cerebellum)
Mean size of CNVs (kb)	$319 \pm 85/n = 40$	$295 \pm 60/n = 68$	$436 \pm 84/n = 51$
Deletions (Kb) ($p < 0.05$)$^{*\#}$	$151 \pm 32/n = 29$	$299 \pm 88/n = 42$	$478 \pm 103/n = 39$
Duplications (kb) ($p < 0.05$)*	$760 \pm 261/n = 11$	$290 \pm 72/n = 26$	$301 \pm 125/n = 12$
Gene content (kb)	$1.33 \pm 0.23/n = 40$	$1.57 \pm 0.19/n = 68$	$1.38 \pm 0.27/n = 51$

CNVs: DNA copy number variations. ($^{*}p < 0.05$) One-way ANOVA, significant difference among means. ($^{\#}p < 0.05$) Bonferroni's posttest, in common CNVs versus unique CNVs from the cerebellum.

Westra et al. might be caused by increased rates of deletion and/or duplication in the frontal cortex compared to the cerebellum. Albeit not statistically significant, we observed an increase in the frequency only of duplications in the frontal cortex compared to the cerebellum. However, neither the length nor gene content of the unique CNVs from either these two neural tissues were significantly different from each other. Although Westra et al. reported that the variation in DNA content averaged ~250 Mb more DNA in the frontal cortex compared to the cerebellum by flow cytometry, this

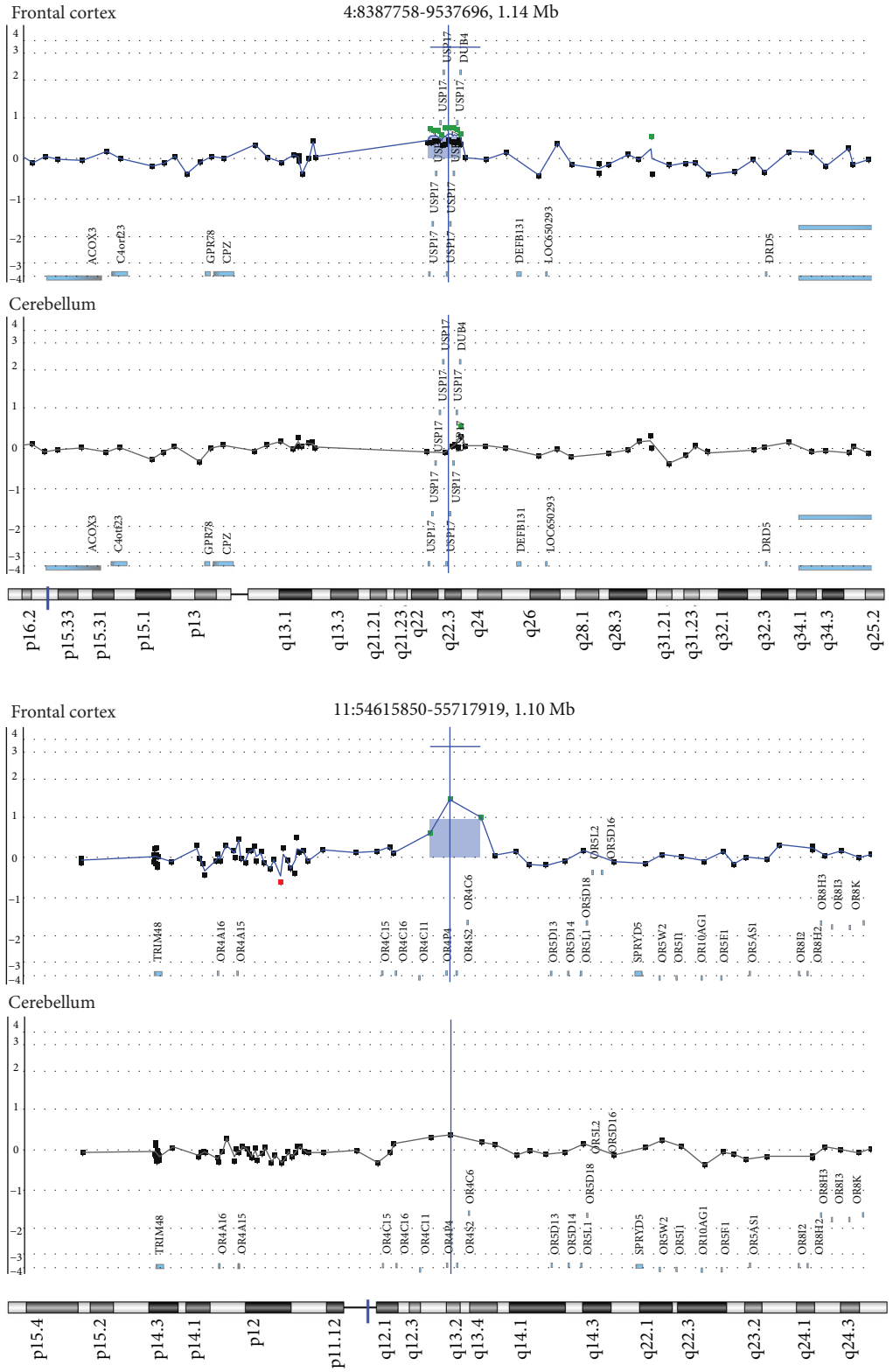

Figure 3: Unique DNA copy number variations (CNVs) from neural tissues. Two examples of somatic duplications that are present in the frontal cortex but absent in the cerebellum. Images extracted from Genomic Workbench software.

difference could not be directly related to DNA copy number variation. Further, their results are possibly explicable by a much higher involvement of retrotransposition in the neural cortex than the cerebellum culminating in a significantly wider variation in DNA content, similar to the differences induced by a higher number of L1 transpositions in the human hippocampus compared to the caudate nucleus [6].

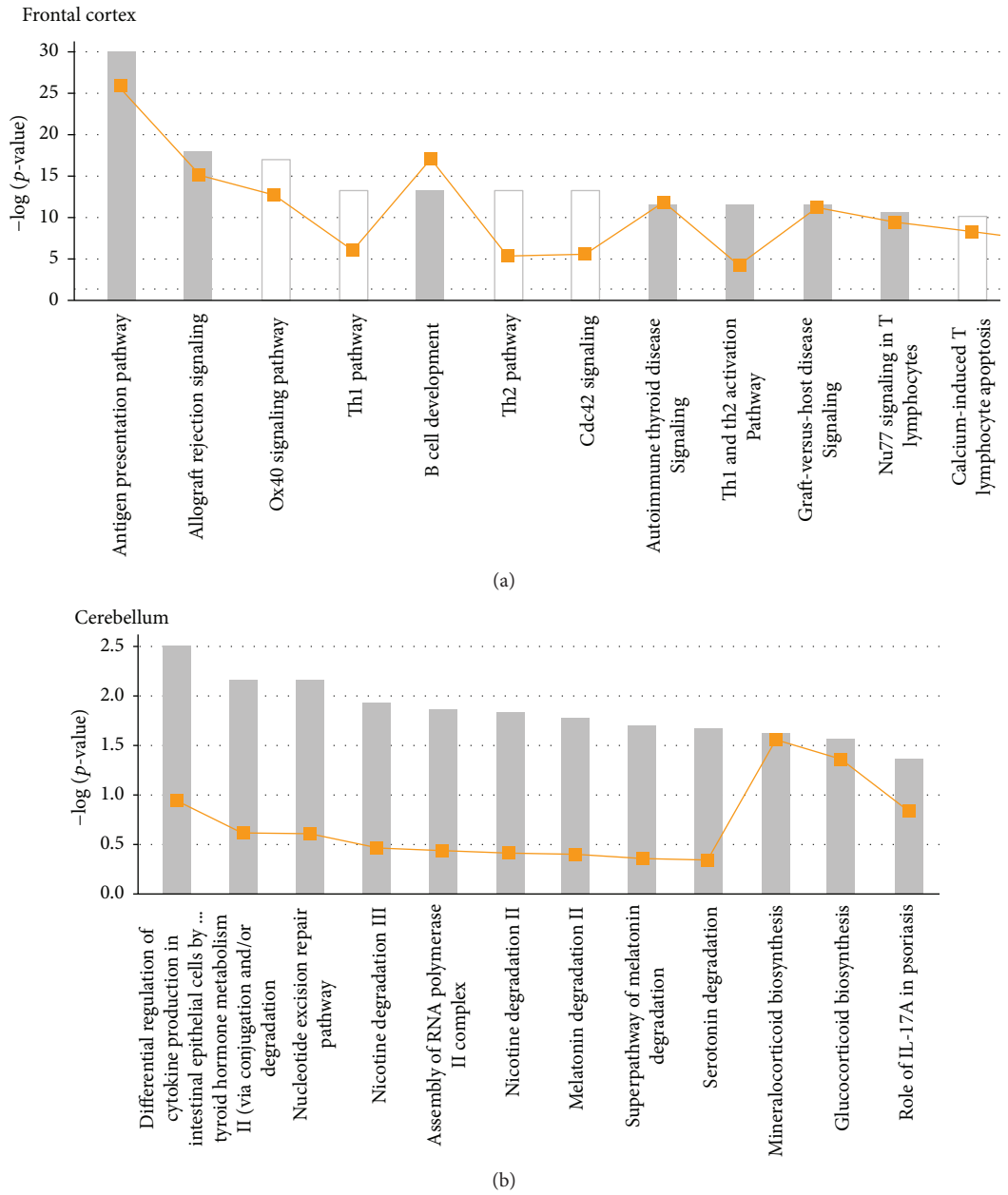

Figure 4: Top canonical pathways identified in ingenuity pathway analysis (IPA). The x-axis represents the top canonical pathways calculated by IPA based on all DNA copy number variations (CNVs) identified in the frontal cortex (a) and cerebellum (b). The yellow line represents the threshold of p value < 0.05 as calculated by Fischer's test.

IPA analysis was performed to investigate whether this increase of CNVs in the brain could be explained by an enrichment of pathways specific for central nervous system function. Based on the fact that the predicted target pathways of all brain CNVs are not specific for the central nervous system functioning, our array-CGH analyses indicate either an increased genomic instability or a less stringent selection against genomic imbalances in brain tissues compared to the blood, resulting in an increased frequency of clonal CNVs in neural tissues. Nonetheless, the exact mechanisms leading to such neuronal genomic instability are still a matter of speculation, but retrotransposon insertion has been demonstrated to mediate the formation of CNVs in various brain tissues [6] and also to involve double-strand DNA breaks [28]. Even so, CNVs represent a significant source of genetic variation in the human genome and have been implicated in several disorders and complex traits, representing a potential mechanism that contributes to neuronal diversity. Besides, the highly significant increase of CNVs that we reported here potentially contributes to physiologic variability and neuronal plasticity and can provide new insights into the complex functioning of the brain.

In summary, this study demonstrates an extensive clonal mosaicism for copy number variation between two different brain tissues. The investigation of genomic changes based on tissue DNA instead of single cells

revealed a different type of variation than previously reported. The variation detected in tissue (clonal) seems to involve smaller segments, which are variable in number in the population, likely having a smaller phenotypic impact than the aneuploidies or chromosome alterations seen in single cells. Even so, they reflect a higher genomic instability or less stringent selection in the brain than in the blood, which deserves attention.

Data Availability

The data used to support the findings of this study are available from the corresponding author upon request.

Conflicts of Interest

None of the authors have any conflict of interest to declare.

Acknowledgments

This work was supported by FAPESP Grants 2013/08028-1 and 2014/17132-0.

Supplementary Materials

Supplementary Table 1: all DNA copy number variations (CNVs) identified in the frontal cortex and cerebellum. The frequency of deletions and duplications of all unique CNVs (observed exclusively either in the frontal cortex or in the cerebellum) as well as the ones in common to both tissues are presented in their respective sheets. Information about CNV gene content, their length, and genomic position are also presented. Supplementary Table 2: top diseases/function of all networks retrieved from both the frontal cortex and the cerebellum. Ingenuity pathway analysis (IPA) software retrieved the predicted target pathways of all DNA copy number variations (CNVs) identified exclusively in the frontal cortex and cerebellum (unique CNVs). *(Supplementary Materials)*

References

[1] A. M. Valdes, D. Glass, and T. D. Spector, "Omics technologies and the study of human ageing," *Nature Reviews Genetics*, vol. 14, no. 9, pp. 601–607, 2013.

[2] H. Y. Zoghbi and S. T. Warren, "Neurogenetics: advancing the "next-generation" of brain research," *Neuron*, vol. 68, no. 2, pp. 165–173, 2010.

[3] I. Reinvang, I. J. Deary, A. M. Fjell, V. M. Steen, T. Espeseth, and R. Parasuraman, "Neurogenetic effects on cognition in aging brains: a window of opportunity for intervention?," *Frontiers in Aging Neuroscience*, vol. 2, p. 143, 2010.

[4] M. J. McConnell, J. V. Moran, A. Abyzov et al., "Intersection of diverse neuronal genomes and neuropsychiatric disease: The Brain Somatic Mosaicism Network," *Science*, vol. 356, no. 6336, p. eaal1641, 2017.

[5] D. M. Bushman and J. Chun, "The genomically mosaic brain: aneuploidy and more in neural diversity and disease," *Seminars in Cell & Developmental Biology*, vol. 24, no. 4, pp. 357–369, 2013.

[6] J. K. Baillie, M. W. Barnett, K. R. Upton et al., "Somatic retrotransposition alters the genetic landscape of the human brain," *Nature*, vol. 479, no. 7374, pp. 534–537, 2011.

[7] G. D. Evrony, X. Cai, E. Lee et al., "Single-neuron sequencing analysis of L1 retrotransposition and somatic mutation in the human brain," *Cell*, vol. 151, no. 3, pp. 483–496, 2012.

[8] M. A. Lodato, M. B. Woodworth, S. Lee et al., "Somatic mutation in single human neurons tracks developmental and transcriptional history," *Science*, vol. 350, no. 6256, pp. 94–98, 2015.

[9] X. Cai, G. D. Evrony, H. S. Lehmann et al., "Single-cell, genome-wide sequencing identifies clonal somatic copy-number variation in the human brain," *Cell Reports*, vol. 10, no. 4, p. 645, 2015.

[10] L. Feuk, A. R. Carson, and S. W. Scherer, "Structural variation in the human genome," *Nature Reviews Genetics*, vol. 7, no. 2, pp. 85–97, 2006.

[11] M. J. McConnell, M. R. Lindberg, K. J. Brennand et al., "Mosaic copy number variation in human neurons," *Science*, vol. 342, no. 6158, pp. 632–637, 2013.

[12] D. M. Bushman, G. E. Kaeser, B. Siddoway et al., "Genomic mosaicism with increased amyloid precursor protein (APP) gene copy number in single neurons from sporadic Alzheimer's disease brains," *eLife*, vol. 4, 2015.

[13] J. W. Westra, R. R. Rivera, D. M. Bushman et al., "Neuronal DNA content variation (DCV) with regional and individual differences in the human brain," *The Journal of Comparative Neurology*, vol. 518, no. 19, pp. 3981–4000, 2010.

[14] L. T. Grinberg, R. E. de Lucena Ferretti, J. M. Farfel et al., "Brain bank of the Brazilian aging brain study group—a milestone reached and more than 1,600 collected brains," *Cell and Tissue Banking*, vol. 8, no. 2, pp. 151–162, 2007.

[15] C. K. Suemoto, R. E. L. Ferretti-Rebustini, R. D. Rodriguez et al., "Neuropathological diagnoses and clinical correlates in older adults in Brazil: a cross-sectional study," *PLoS Medicine*, vol. 14, no. 3, article e1002267, 2017.

[16] S. Katz, A. B. Ford, R. W. Moskowitz, B. A. Jackson, and M. W. Jaffe, "Studies of illness in the aged. The index of Adl: a standardized measure of biological and psychosocial function," *JAMA*, vol. 185, no. 12, pp. 914–919, 1963.

[17] M. P. Lawton and E. M. Brody, "Assessment of older people: self-maintaining and instrumental activities of daily living," *Gerontologist*, vol. 9, 3 Part 1, pp. 179–186, 1969.

[18] J. C. Morris, "The clinical dementia rating (CDR): current version and scoring rules," *Neurology*, vol. 43, no. 11, pp. 2412–2414, 1993.

[19] A. F. Jorm and P. A. Jacomb, "The informant questionnaire on cognitive decline in the elderly (IQCODE): socio-demographic correlates, reliability, validity and some norms," *Psychological Medicine*, vol. 19, no. 04, pp. 1015–1022, 1989.

[20] H. Braak and E. Braak, "Neuropathological stageing of Alzheimer-related changes," *Acta Neuropathologica*, vol. 82, no. 4, pp. 239–259, 1991.

[21] S. S. Mirra, A. Heyman, D. McKeel et al., "The consortium to establish a registry for Alzheimer's disease (CERAD). Part II. Standardization of the neuropathologic assessment of Alzheimer's disease," *Neurology*, vol. 41, no. 4, pp. 479–486, 1991.

[22] H. Braak, K. D. Tredici, U. Rüb, R. A. I. de Vos, E. N. H. Jansen Steur, and E. Braak, "Staging of brain pathology related to

sporadic Parkinson's disease," *Neurobiology of Aging*, vol. 24, no. 2, pp. 197–211, 2003.

[23] I. R. A. Mackenzie, M. Neumann, E. H. Bigio et al., "Nomenclature and nosology for neuropathologic subtypes of frontotemporal lobar degeneration: an update," *Acta Neuropathologica*, vol. 119, no. 1, pp. 1–4, 2010.

[24] A. C. V. Krepischi, J. Knijnenburg, D. R. Bertola et al., "Two distinct regions in 2q24.2-q24.3 associated with idiopathic epilepsy," *Epilepsia*, vol. 51, no. 12, pp. 2457–2460, 2010.

[25] F. Faggioli, J. Vijg, and C. Montagna, "Chromosomal aneuploidy in the aging brain," *Mechanisms of Ageing and Development*, vol. 132, no. 8-9, pp. 429–436, 2011.

[26] S. D. Pack, R. J. Weil, A. O. Vortmeyer et al., "Individual adult human neurons display aneuploidy: detection by fluorescence in situ hybridization and single neuron PCR," *Cell Cycle*, vol. 4, no. 12, pp. 1758–1760, 2005.

[27] Y. B. Yurov, I. Y. Iourov, S. G. Vorsanova et al., "Aneuploidy and confined chromosomal mosaicism in the developing human brain," *PLoS One*, vol. 2, no. 6, article e558, 2007.

[28] E. Suberbielle, P. E. Sanchez, A. V. Kravitz et al., "Physiologic brain activity causes DNA double-strand breaks in neurons, with exacerbation by amyloid-β," *Nature Neuroscience*, vol. 16, no. 5, pp. 613–621, 2013.

Hindawi
Neural Plasticity
Volume 2018, Article ID 1672708, 8 pages
https://doi.org/10.1155/2018/1672708

Research Article

Altered Intrinsic Coupling between Functional Connectivity Density and Amplitude of Low-Frequency Fluctuation in Mild Cognitive Impairment with Depressive Symptoms

Xiaozheng Liu,[1] **Jiuzun Chen**,[1] **Bangli Shen**,[1,2] **Gang Wang**,[3] **Jiapeng Li**,[3] **Hongtao Hou**,[3] **Xingli Chen**,[3] **Zhongwei Guo**,[3] **and Chuanwan Mao**[1]

[1]*Department of Radiology, China-USA Neuroimaging Research Institute, The Second Affiliated Hospital and Yuying Children's Hospital, Wenzhou Medical University, Wenzhou, Zhejiang 325027, China*
[2]*Department of Pain, The Second Affiliated Hospital and Yuying Children's Hospital, Wenzhou Medical University, Wenzhou, Zhejiang 325027, China*
[3]*Tongde Hospital of Zhejiang Province, Hangzhou, Zhejiang 310012, China*

Correspondence should be addressed to Zhongwei Guo; guozw1977@aliyun.com and Chuanwan Mao; maocwwz@163.com

Received 4 December 2017; Revised 6 March 2018; Accepted 7 May 2018; Published 29 May 2018

Academic Editor: Claudio A. Mastronardi

Neuroimaging studies have demonstrated that major depressive disorder increases the risk of dementia in older individuals with mild cognitive impairment. We used resting-state functional magnetic resonance imaging to explore the intrinsic coupling patterns between the amplitude and synchronisation of low-frequency brain fluctuations using the amplitude of low-frequency fluctuations (ALFF) and the functional connectivity density (FCD) in 16 patients who had mild cognitive impairment with depressive symptoms (D-MCI) (mean age: 69.6 ± 6.2 years) and 18 patients with nondepressed mild cognitive impairment (nD-MCI) (mean age: 72.1 ± 9.7 years). Coupling was quantified as the correlations between the ALFF values and their associated FCDs. The results showed that the ALFF values in the D-MCI group were higher in the left medial prefrontal cortex (mPFC) and lower in the right precentral gyrus (preCG), and the FCD values were higher in the left medial temporal gyrus (MTG) than those in the nD-MCI group. Further, correlation analyses demonstrated that, in the D-MCI group, the mPFC was negatively correlated with the MTG. These findings may relate to the characteristics of mood disorders in patients with MCI, and they offer further insight into the neuropathophysiology of MCI with depressive symptoms.

1. Introduction

Mild cognitive impairment (MCI) is a neurological disorder that is associated with minimal cognitive impairments that are beyond those expected based on a person's age and education, but the changes are not severe enough to interfere with daily living, and they do not meet the criteria for dementia [1]. The conversion rate from MCI to dementia is approximately 12–16% per year [2]. Depression is a common symptom among individuals with MCI, with a prevalence of 32% [3].

Gao et al. [4] reported that depression was a major risk factor for the incidences of dementia and MCI. Further, recent meta-analyses showed that depressive symptoms increase the risk of MCI progressing to dementia and that depressive symptoms predict conversion from any type of MCI to all-cause dementia [5]. Neuroimaging studies have demonstrated that structural abnormalities in several brain regions are involved in the pathological process of depressive symptoms in MCI. Xie et al. [6] reported that depressive symptoms in MCI are related to grey matter volume loss in several brain regions, including the dorsal cingulate cortex, orbitofrontal cortex (OFC), ventromedial prefrontal cortex (vmPFC), posterior middle temporal gyrus (pMTG), and insula. Sacuiu et al. and Gonzales et al. [7, 8] also reported that MCI with depressive symptoms showed increased cortical atrophy in the anterior cingulate and the frontal lobe. Studies have also shown that, compared with those with

nondepressed MCI (nD-MCI), patients with MCI and depression (D-MCI) have more white matter atrophy and white matter microstructural disruptions in the frontal, parietal, and temporal brain regions, especially in the hippocampal cingulum and fornix tracts [9–11]. Recently, researchers have used resting-state functional magnetic resonance imaging (R-fMRI) technology to study the functional changes in the brains of people with D-MCI. By analysing functional connectivity (FC), Zheng et al. [12] reported that, compared with nD-MCI, D-MCI was associated with higher effective connectivity between the right amygdala and the right lingual gyrus, right calcarine gyrus, and bilateral supplementary motor areas. Xie et al. [13] reported that, for people with MCI, scores on the Geriatric Depression Scale were positively correlated with functional connectivity in the network connecting the bilateral posterior cingulate cortex (PCC), middle temporal gyrus, and left dorsolateral prefrontal cortex (DLPFC). By analysing the amplitude of low-frequency fluctuations (ALFF), Li et al. [14] found that abnormal ALFF values in the left inferior frontal gyrus and left precuneus could effectively differentiate nD-MCI from D-MCI. Currently, the preliminary results showed that the affective network and the default mode network might be simultaneously damaged in patients with D-MCI.

FC and ALFF are two fundamental fMRI parameters. FC characterises the degree of synchronisation between low-frequency fluctuations in the resting brain and requires the definition of a relation (e.g., Pearson correlation) between the features of different voxels. Therefore, FC describes network properties, while the ALFF represents the amplitude of resting-state spontaneous brain activity by calculating the voxel-wise total power of a given fMRI time course within the low-frequency band [14]. These two measures have been shown to have a close relationship [15–17] and to be altered within the affective network and the default mode network in both MCI and major depressive disorder [12, 13, 18]. Compared with healthy elderly subjects, AD and MCI patients show absent FC density-ALFF coupling in the anterior and posterior cingulate cortex and the temporal cortex [15]. Similar methods have been used to observe changes in functional brain features in erythaematosus and epilepsy patients [16, 17]. Thus, we believe that the coupling patterns between these two parameters may provide a new measure that can help us understand the underlying neuropathophysiology of D-MCI and enhance its identifiability by resting-state fMRI.

We, therefore, utilised the measures of ALFF and FC density (FCD), a global and voxel-wise measure of FC, to investigate alterations in amplitude-connectivity coupling in D-MCI. Given the common differences that have been reported in the brain networks of patients with D-MCI [13–17], we hypothesised that those with D-MCI would have altered brain fluctuations in brain regions associated with cognitive and emotional regulation.

2. Materials and Methods

2.1. Patients. Eighteen patients with nD-MCI and 16 with D-MCI were recruited from the outpatient department of Tongde Hospital in Zhejiang Province, China, from July 2013 to August 2016. The study was approved by the local ethics committee, and all participants gave their written informed consent before the MR scanning. All participants were right-handed, and the groups did not significantly differ in age, sex, or years of education.

A diagnosis of MCI includes memory impairment that does not meet the criteria for dementia. The criteria for MCI [19] were as follows: (a) impaired memory performance on a normalised, objective verbal memory test; (b) recent history of symptomatic worsening in memory; (c) normal or near-normal performance (score > 24) on the Mini-Mental State Examination (MMSE), as well as on the activities of daily living scale (score > 24); (d) a global rating of 0.5 on the clinical dementia rating scale; and (e) the absence of dementia.

Depressive symptoms were identified by professional psychiatrists according to the *Diagnostic and Statistical Manual of Mental Disorders*, fourth edition [20]. The severity of depressive symptoms was evaluated using two clinical scales: the Hamilton Depression Rating Scale (HAMD) [21] and the Neuropsychiatric Inventory (NPI) [22]. We considered HAMD scores ≥ 7 and NPI scores ≥ 4 in the depression domain to be clinically significant [23].

Patients were excluded if they had a history of psychiatric disorders, alcohol or substance abuse/dependence during the prior five years, MMSE scores < 24, a history of neurological disease, MRI contraindications, or unstable chronic medical conditions.

2.2. MRI Scan. All scanning was collected using an 8-channel head coil in a 3T Siemens scanner (Siemens Magnetom Verio; Siemens Medical Systems, Erlangen, Germany) at Tongde Hospital in Zhejiang Province. All patients were asked to keep their heads still and their eyes closed during image acquisition. T1-weighted high-resolution anatomical images were acquired using a 3D magnetisation-prepared rapid gradient echo sequence with the following parameters: repetition time = 1900 ms, echo time = 3.44 ms, inversion time = 900 ms, flip angle = 9°, 128 sagittal slices, field of view = 256 mm, and slice thickness = 1 mm. Functional resting-state fMRI images were acquired using a T_2^*-weighted echo-planar imaging sequence with the following parameters: 33 axial slices, thickness/gap = 4.8/0 mm, in-plane resolution = $3.4 \times 3.4\,mm^2$, repetition time = 2000 ms, echo time = 30 ms, flip angle = 90°, and field of view = 200 mm. Each condition lasted for 6 min 40 s, and 200 functional volumes were obtained.

2.3. Data Preprocessing. All fMRI data were preprocessed using SPM8 (http://www.fil.ion.ucl.ac.uk/spm) and Data Processing Assistant for Resting-State fMRI (http://www.restfmri.net). The first ten time frames were discarded to ensure an MR steady state. The preprocessing steps comprised slice-timing correction for interleaved acquisitions, 3D motion correction, linear drift removal, spatial smoothing with a Gaussian smoothing kernel (full width at half maximum = 6 mm), and spatial normalisation to the standard Montreal Neurological Institute (MNI) brain space with a resampling resolution of $3 \times 3 \times 3\,mm^3$. Subjects were

discarded if head motion exceeded 1.5 mm translation in x, y, or z directions or 1.5° of maximum rotation about the three axes. All remaining smoothed images were filtered using a typical temporal bandpass (0.01–0.08 Hz) to reduce low-frequency drift and physiological high-frequency respiratory and cardiac noise. Linear trends were also removed within each time series.

2.4. ALFF Calculation. ALFF was calculated using the REST software (http://www.restfmri.net). Briefly, for a given voxel, the time series was first converted to the frequency domain using a fast Fourier transform. The square root of the power spectrum was computed and then averaged across 0.01–0.08 Hz. This averaged square root was taken as the ALFF at the given voxel [24]. Then, the ALFFs were standardised by dividing by the whole-brain average of the ALFF at each voxel, which measures the absolute strength or intensity of spontaneous low-frequency oscillations.

2.5. FCD Calculation. We performed voxel-based whole-brain correlation analysis on the preprocessed R-fMRI data, as has been well described in previous studies [25]. Pearson's correlation coefficients (r) were computed between the time series for all pairs of grey matter voxels within a grey matter mask. The FCD for a given voxel was calculated as the sum of the significant connections between a given voxel and all other voxels by thresholding each correlation at $r > 0.25$. Finally, to improve the normality of the data, the voxel-wise FCD values were transformed into a Z-score map using a Fisher Z transformation. Because of the uncertain interpretation and the detrimental effects on test-retest reliability, only positive correlations were considered in the FCD calculations.

2.6. Statistical Analysis. To examine ALFF and FCD differences between the groups, a two-sample t-test was performed between the two groups using REST. The 3dClustSim program, which is based on Monte Carlo simulation and implemented in AFNI (http://afni.nimh.nih.gov), was used for multiple comparison correction [26]. The statistical threshold was set at $P < 0.005$ and cluster size > 28 voxels, which corresponded to a corrected $P < 0.05$.

2.7. Coupling of ALFF and FCD. To test the proposal that alterations in amplitude-connectivity coupling in D-MCI and, thus, to differentiate D-MCI from nD-MCI, we computed the coupling between the FCD and ALFF across subjects in each group. Based on the two-sample t-test results of ALFF and FCD, subject-specific ALFF and FCD values were first extracted from the abnormal brain regions, respectively. Then, we performed a voxel-by-voxel Pearson correlation analysis between ALFF and FCD values in regions with alterations (between amplitude and FC) in each group, respectively.

3. Results

3.1. Neuropsychological Results. Age ($t = 0.898$, $P = 0.376$), sex distribution ($\chi^2 = 0.161$, $P = 0.735$), and years of education ($t = 0.464$, $P = 0.645$) did not differ between the two groups. Detailed demographics and the corresponding statistical tests are presented in Table 1.

Table 1: Demographics and neuropsychological data.

	D-MCI group	nD-MCI group	t/χ^2	P value
Gender, n (M/F)	16 (6/10)	18 (7/11)	0.007	1.000
Age, years	69.6 ± 6.2	72.1 ± 9.7	0.898	0.376
Education, years	8.3 ± 2.1	8.5 ± 1.8	0.464	0.645
MMSE	26.6 ± 1.1	26.6 ± 1.0	−0.037	0.971
HAMD	11.7 ± 3.1	0	16.0652	0.000
D-NPI	7.19 ± 2.3	0	13.3614	0.000

Data represent mean ± SD. Data were analysed using independent-samples t-tests. D-MCI: mild cognitive impairment with depression; nD-MCI: nondepressed mild cognitive impairment; M: male; F: female; MMSE: Mini-Mental State Examination; D-NPI: depression domain on the Neuropsychiatric Inventory; HAMD: Hamilton Depression Rating Scale.

3.2. ALFF Results. The two-sample t-tests revealed several related brain regions in which the ALFF values differed significantly between the D-MCI and nD-MCI groups ($P < 0.005$, 3dClustSim-corrected; Table 2). In particular, we found that the D-MCI group exhibited significantly higher ALFF values than the nD-MCI group in the right precentral cortex and significantly lower ALFF values in the left medial prefrontal cortex (Figure 1).

3.3. FCD Results. Similar to the ALFF values, the two-sample t-tests revealed significant differences in FCD between the D-MCI and nD-MCI groups ($P < 0.005$, 3dClustSim-corrected; Table 2). Specifically, we found that FCD values in the right middle temporal gyrus were greater in those with D-MCI than in those with nD-MCI (Figure 1).

3.4. Altered Coupling between ALFF and FCD. Correlation analyses between the abnormal ALFF and FCD brain regions revealed a negative correlation between mPFC and MTG coupling in the nD-MCI (Figure 2) but not in the D-MCI group. Thus, for patients with nD-MCI, coupling was high in the mPFC when it was low in the MTG and vice versa.

4. Discussion

Here, we investigated alterations in ALFF-FCD and coupling of ALFF with FCD in patients with D-MCI and nD-MCI. The D-MCI group exhibited significantly higher FCD in the right MTG, significantly higher ALFF in the left mPFC, and significantly lower ALFF in the right precentral gyrus (preCG) than the nD-MCI group. We also found a negative correlation between ALFF-FCD coupling in the mPFC and the MTG but only in patients with D-MCI.

The mPFC is an important node in the cortico-striato-pallido-thalamic loops and in the medial network, contributing to emotional processes and regulation [27]. Several neuroimaging studies have demonstrated that the mPFC is a key brain region in depressive symptomatology. Xie et al. [6] reported that depressive symptoms in MCI are related to grey matter volume loss in several brain regions, including the mPFC, posterior MTG, and insula. Furthermore, Sacuiu

Table 2: Brain regions with significantly lower ALFF-FCD values in the D-MCI group than in the nD-MCI group.

Brain regions	Voxels	BA	MNI coordinates			t value
			X	Y	Z	
ALFF						
Prefrontal_medial_L	32	10	−9	63	27	4.6674
Precentral_R	28	6	27	−3	51	−5.7117
FCD						
Temporal_mid_R	117	37	51	−66	6	4.9394

D-MCI: mild cognitive impairment with depression; nD-MCI: nondepressed mild cognitive impairment; MNI: Montreal Neurological Institute; BA: Brodmann area.

et al. and Gonzales et al. reported that D-MCI patients have increased cortical atrophy in the anterior cingulate and the frontal lobe, and decreased left mPFC thickness was associated with increased negative affect [7, 8]. Other studies have also demonstrated that depressed individuals with MCI had more white matter atrophy in the frontal, parietal, and temporal cortices than those with no-symptom MCI did [9–11]. Based on R-fMRI and ALFF analyses, Wang et al. [28] found that MDD patients had abnormal ALFF values in the mPFC, precentral gyrus, and other regions. Using magnetic resonance spectroscopy, McEwen et al. [29] reported that glutamate levels in the mPFC were higher in women with postpartum depression than in controls. Savitz et al. [30] found that dysfunction of the serotonin-1A receptor in the mPFC might play a role in the genesis of MDD. Additionally, a recent animal study [31] suggested that synaptogenic activity in the mPFC is associated with a rapid antidepressant response to ketamine. Thus, our results are in line with previous findings, suggesting that the altered spontaneous ALFF values in the mPFC might be a characteristic of the neurological impairments of MCI with depressive symptoms.

A neuroimaging study reported that the preCG was involved in MDD [32]. Peng et al. [33] observed decreased cortical thickness in the preCG in patients with untreated first-episode MDD. Using voxel-based morphometry, Taki et al. [34] found that male patients with subthreshold depression had significantly smaller right preCG volumes than healthy controls. Several studies have also demonstrated that grey matter structural changes in the right preCG can predict the subsequent onset of MDD and pose an increased risk for mood disorders [35–37]. A study by Ho et al. [38] revealed that the symptom of alexithymia that occurs in MDD was associated with reduced functional connectivity in the right preCG and several other right hemisphere regions that are associated with cognitive regulation in the default mode network (DMN). They found that subjective pleasantness was related to the preCG, right cerebellum, and right inferior frontal gyrus [39]. The preCG is located at the primary motor cortex, which is required for the initiation of purposeful movements via integration of information sent from the sensorimotor cortex [40]. Several studies have confirmed the association between psychomotor retardation, poor action planning, and alterations in the preCG [41, 42]. Therefore, the abnormal ALFF in the preCG of our study might be related to the depressive symptoms in our D-MCI patients.

MTG is an important node within the DMN and the affective network (AN), which are involved in self-referential processing, emotion, and regulation [43–45]. Neuroimaging evidence has demonstrated that altered FC occurs in MDD patients between the MTG and other nodes within the DMN and AN. For the FC of the right MTG, Ma et al. [46] found that patients with treatment-resistant depression as well as those with treatment-responsive depression showed abnormal connectivity mainly in the DMN. Based on FC analyses of the subgenual anterior cingulate cortex (sgACC), MDD patients showed disruptions in FC between the sgACC and MTG [47]. Du et al. [48] investigated the brain-circuit mechanisms of suicidal ideation (SI) in MDD, finding that the SI group exhibited decreased intrinsic FC among the rostral anterior cingulate cortex (rACC), the orbitomedial prefrontal cortex, and the right MTG compared with healthy controls and those with MDD without SI. In the SI group, the FC strength between the right rACC and the MTG positively correlated with SI severity. The altered FCD in the MTG in the present study expands the knowledge gained from previous studies of abnormal FC in MDD patients by investigating the FC in the right MTG. MDD is characterised by the presence of negative thoughts about oneself, the world, or the future. We hypothesised that the altered FC in the right MTG might contribute to the negative thoughts and negative emotions observed in patients with MCI and depressive symptoms.

Interestingly, we found a negative correlation between ALFF-FCD coupling in the mPFC and the MTG but only in the nD-MCI group. De Bellis and Hooper [49] reported that maltreated youth with depressive disorders had significantly weaker activation of the mPFC in response to attentional targets and stronger activation in the MTG in response to sad distracters during an emotional oddball task than controls. They concluded that maltreated youth with depressive disorders had dysfunctional cognitive and emotional processing because of the mPFC involvement in cognitive control circuits and the MTG involvement in ventral emotional circuits. Du et al. [48] also reported that depressed patients with suicidal ideation had decreased intrinsic FC between the mPFC and the right MTG, and they suggested that the disrupted frontolimbic circuits might impact decision-making and emotional processing in depressed patients with suicidal ideation. The mPFC and right MTG are two nodes within the DMN. According to previous neuroimaging studies, the DMN can be generally divided into anterior (aDMN) and posterior (pDMN) subnetworks. The former is related to self-referential thought, and the latter is related to episodic memory retrieval and scene construction [50–52]. The aDMN mostly consists of the mPFC, anterior cingulate cortex, anterior temporal lobe, and inferior frontal gyrus, whereas the pDMN mostly contains the posterior cingulate cortex (PCC), precuneus, angular gyrus, hippocampus, and temporal lobe. A recent fMRI study revealed that the activation within these subsystems and the connectivity between the aDMN and pDMN contribute differently to

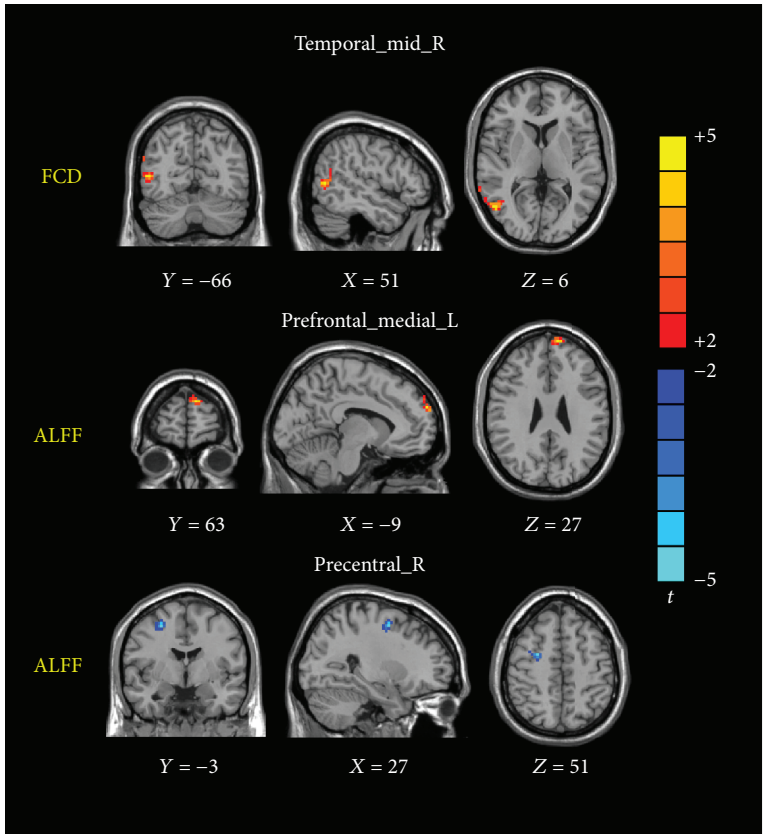

Figure 1: Brain regions showing differences in FCD or ALFF values between the D-MCI and nD-MCI groups (contrast = D-MCI − nD-MCI).

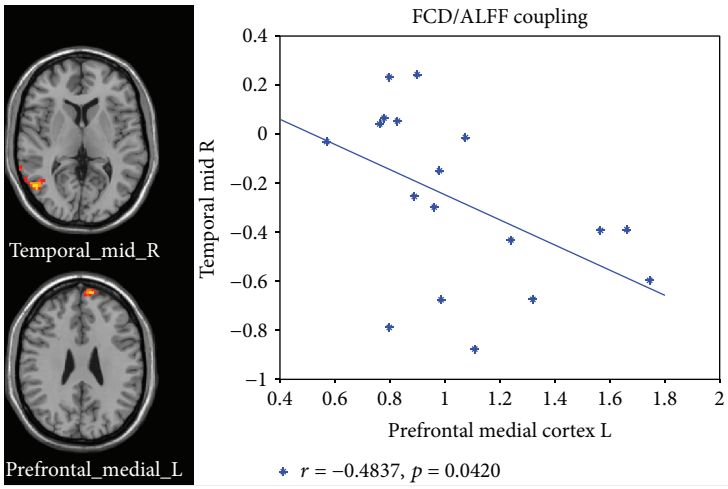

Figure 2: Significant correlations between FCD and ALFF in the nD-MCI brain. FCD values of the right temporal middle gyrus and ALFF values of the medial prefrontal cortex were subtracted from the abnormal brain regions resulting from *t*-contrast nD-MCI versus D-MCI.

future-oriented thoughts [53]. How the brain creates emotions is complex and esoteric. Using a psychological constructionist approach, Lindquist et al. hypothesised that several brain regions, including the mPFC, medial temporal lobe (MTL), and PCC, are important for realising instances of emotional experiences and perceptions [54]. The negative correlation in ALFF-FCD coupling between the mPFC and the MTG in our study might contribute to decision-making, future-oriented thoughts, and experiences and perceptions of emotion in MCI with depressive symptoms.

This study had several potential limitations. First, the sample size was relatively small, which might have resulted in low statistical power and the absence of correlations between FCD/ALFF and physiological measurements. Second, previous studies have suggested that neuronal oscillations in various frequency intervals have different specific

properties and physiological functions [14]. While short- and long-range FCD have been used in fMRI studies [55], further investigations into coupling between long- or short-range FCD with ALFF at various frequency intervals should be performed. Finally, the choice of a clinical assessment scale is very important. In our study, we selected the HAMD and the NPI to evaluate depressive symptoms in MCI, as a previous study did [9]. However, other studies have used different scales, such as the Geriatric Depression Scale [56], the Cornell Scale for Depression in Dementia [57], and the Center for Epidemiologic Studies Depression Scale [58]. Evaluating depressive symptoms comprehensively and accurately in MCI is difficult because of the cognitive impairment. Therefore, in future studies, we should evaluate clinical depressive symptoms with multiple scales, based on the characteristics of each scale.

5. Conclusions

In the current study, we observed differences between D-MCI and nD-MCI in terms of FCD and ALFF values that were derived from R-fMRI. We also examined differences in ALFF-FCD coupling in D-MCI and nD-MCI. The findings indicated that pathological factors lead to dysfunctional ALFF-FCD coupling between the mPFC and the MTG in D-MCI. Investigation of imaging coupling provides a synergistic approach to unravelling the features of the functional changes in MCI and provides a new insight into the underlying neural mechanism of MCI with depressive symptoms.

Conflicts of Interest

The authors declare no conflict of interest.

Acknowledgments

This research was supported by the Doctoral Scientific Research Foundation of the Second Affiliated Hospital, Wenzhou Medical University, the General Project of the Department of Science and Technology of Zhejiang Province (2017KY109) (to Xiaozheng Liu), the Public Project of the Department of Science and Technology of Wen Zhou (H20160002) (to Bangli Shen), and the General Project of the Department of Science and Technology of Zhejiang Province (2013KYB065, 2018KY031) (to Zhongwei Guo).

References

[1] J. D. Grill, L. G. Apostolova, S. Bullain et al., "Communicating mild cognitive impairment diagnoses with and without amyloid imaging," *Alzheimer's Research & Therapy*, vol. 9, no. 1, p. 35, 2017.

[2] R. C. Petersen, R. O. Roberts, D. S. Knopman et al., "Mild cognitive impairment: ten years later," *Archives of Neurology*, vol. 66, no. 12, pp. 1447–1455, 2009.

[3] Z. Ismail, H. Elbayoumi, C. E. Fischer et al., "Prevalence of depression in patients with mild cognitive impairment: a systematic review and meta-analysis," *JAMA Psychiatry*, vol. 74, no. 1, pp. 58–67, 2017.

[4] Y. Gao, C. Huang, K. Zhao et al., "*Retracted*: depression as a risk factor for dementia and mild cognitive impairment: a meta-analysis of longitudinal studies," *International Journal of Geriatric Psychiatry*, vol. 28, no. 5, pp. 441–449, 2013.

[5] R. J. Mourao, G. Mansur, L. F. Malloy-Diniz, E. C. Costa, and B. S. Diniz, "Depressive symptoms increase the risk of progression to dementia in subjects with mild cognitive impairment: systematic review and meta-analysis," *International Journal of Geriatric Psychiatry*, vol. 31, no. 8, pp. 905–911, 2016.

[6] C. Xie, W. Li, G. Chen et al., "The co-existence of geriatric depression and amnestic mild cognitive impairment detrimentally affect gray matter volumes: voxel-based morphometry study," *Behavioural Brain Research*, vol. 235, no. 2, pp. 244–250, 2012.

[7] S. Sacuiu, P. S. Insel, S. Mueller et al., "Chronic depressive symptomatology in mild cognitive impairment is associated with frontal atrophy rate which hastens conversion to Alzheimer dementia," *The American Journal of Geriatric Psychiatry*, vol. 24, no. 2, pp. 126–135, 2016.

[8] M. M. Gonzales, P. S. Insel, C. Nelson et al., "Cortical atrophy is associated with accelerated cognitive decline in mild cognitive impairment with subsyndromal depression," *The American Journal of Geriatric Psychiatry*, vol. 25, no. 9, pp. 980–991, 2017.

[9] G. J. Lee, P. H. Lu, X. Hua et al., "Depressive symptoms in mild cognitive impairment predict greater atrophy in Alzheimer's disease-related regions," *Biological Psychiatry*, vol. 71, no. 9, pp. 814–821, 2011.

[10] R. S. Mackin, P. Insel, D. Tosun et al., "The effect of subsyndromal symptoms of depression and white matter lesions on disability for individuals with mild cognitive impairment," *The American Journal of Geriatric Psychiatry*, vol. 21, no. 9, pp. 906–914, 2013.

[11] W. Li, L. T. Muftuler, G. Chen et al., "Effects of the coexistence of late-life depression and mild cognitive impairment on white matter microstructure," *Journal of the Neurological Sciences*, vol. 338, no. 1-2, pp. 46–56, 2014.

[12] L. J. Zheng, G. F. Yang, X. Y. Zhang et al., "Altered amygdala and hippocampus effective connectivity in mild cognitive impairment patients with depression: a resting-state functional MR imaging study with granger causality analysis," *Oncotarget*, vol. 8, no. 15, pp. 25021–25031, 2017.

[13] C. Xie, J. Goveas, Z. Wu et al., "Neural basis of the association between depressive symptoms and memory deficits in nondemented subjects: resting-state fMRI study," *Human Brain Mapping*, vol. 33, no. 6, pp. 1352–1363, 2012.

[14] Y. Li, B. Jing, H. Liu et al., "Frequency-dependent changes in the amplitude of low-frequency fluctuations in mild cognitive impairment with mild depression," *Journal of Alzheimer's Disease*, vol. 58, no. 4, pp. 1175–1187, 2017.

[15] D. Mascali, M. DiNuzzo, T. Gili et al., "Intrinsic patterns of coupling between correlation and amplitude of low-frequency fMRI fluctuations are disrupted in degenerative dementia mainly due to functional disconnection," *PLoS One*, vol. 10, no. 4, article e0120988, 2015.

[16] Z. Zhang, Q. Xu, W. Liao et al., "Pathological uncoupling between amplitude and connectivity of brain fluctuations in epilepsy," *Human Brain Mapping*, vol. 36, no. 7, pp. 2756–2766, 2015.

[17] X. D. Zhang, X. L. Jiang, Z. Cheng et al., "Decreased coupling between functional connectivity density and amplitude of low frequency fluctuation in non-neuropsychiatric systemic

lupus erythematosus: a resting-stage functional MRI study," *Molecular Neurobiology*, vol. 54, no. 7, pp. 5225–5235, 2017.

[18] B. Zhang, M. Li, W. Qin et al., "Altered functional connectivity density in major depressive disorder at rest," *European Archives of Psychiatry and Clinical Neuroscience*, vol. 266, no. 3, pp. 239–248, 2016.

[19] R. C. Petersen, G. E. Smith, S. C. Waring, R. J. Ivnik, E. G. Tangalos, and E. Kokmen, "Mild cognitive impairment: clinical characterization and outcome," *Archives of Neurology*, vol. 56, no. 3, pp. 303–308, 1999.

[20] A. Gmitrowicz and A. Kucharska, "Developmental disorders in the fourth edition of the American classification: diagnostic and statistical manual of mental disorders (DSM IV – optional book)," *Psychiatria Polska*, vol. 28, no. 5, pp. 509–521, 1994.

[21] M. Hamilton, "Development of a rating scale for primary depressive illness," *British Journal of Social and Clinical Psychology*, vol. 6, no. 4, pp. 278–296, 1967.

[22] J. L. Cummings, M. Mega, K. Gray, S. Rosenberg-Thompson, D. A. Carusi, and J. Gornbein, "The Neuropsychiatric Inventory: comprehensive assessment of psychopathology in dementia," *Neurology*, vol. 44, no. 12, pp. 2308–2314, 1994.

[23] L. S. Schneider, P. N. Tariot, C. G. Lyketsos et al., "National Institute of Mental Health Clinical Antipsychotic Trials of Intervention Effectiveness (CATIE): Alzheimer disease trial methodology," *The American Journal of Geriatric Psychiatry*, vol. 9, no. 4, pp. 346–360, 2001.

[24] Y. F. Zang, Y. He, C. Z. Zhu et al., "Altered baseline brain activity in children with ADHD revealed by resting-state functional MRI," *Brain & Development*, vol. 29, no. 2, pp. 83–91, 2007.

[25] R. L. Buckner, J. Sepulcre, T. Talukdar et al., "Cortical hubs revealed by intrinsic functional connectivity: mapping, assessment of stability, and relation to Alzheimer's disease," *The Journal of Neuroscience*, vol. 29, no. 6, pp. 1860–1873, 2009.

[26] A. Ledberg, S. Akerman, and P. E. Roland, "Estimation of the probabilities of 3D clusters in functional brain images," *NeuroImage*, vol. 8, no. 2, pp. 113–128, 1998.

[27] J. L. Price and W. C. Drevets, "Neurocircuitry of mood disorders," *Neuropsychopharmacology*, vol. 35, no. 1, pp. 192–216, 2010.

[28] L. Wang, Q. Kong, K. Li et al., "Frequency-dependent changes in amplitude of low-frequency oscillations in depression: a resting-state fMRI study," *Neuroscience Letters*, vol. 614, pp. 105–111, 2016.

[29] A. M. McEwen, D. T. A. Burgess, C. C. Hanstock et al., "Increased glutamate levels in the medial prefrontal cortex in patients with postpartum depression," *Neuropsychopharmacology*, vol. 37, no. 11, pp. 2428–2435, 2012.

[30] J. Savitz, I. Lucki, and W. C. Drevets, "5-HT_{1A} receptor function in major depressive disorder," *Progress in Neurobiology*, vol. 88, no. 1, pp. 17–31, 2009.

[31] N. Li, B. Lee, R. J. Liu et al., "mTOR-dependent synapse formation underlies the rapid antidepressant effects of NMDA antagonists," *Science*, vol. 329, no. 5994, pp. 959–964, 2010.

[32] X. L. Wang, M. Y. du, T. L. Chen et al., "Neural correlates during working memory processing in major depressive disorder," *Progress in Neuro-Psychopharmacology & Biological Psychiatry*, vol. 56, pp. 101–108, 2015.

[33] D. Peng, F. Shi, G. Li et al., "Correction: surface vulnerability of cerebral cortex to major depressive disorder," *PLoS One*, vol. 10, no. 6, article e0128947, 2015.

[34] Y. Taki, S. Kinomura, S. Awata et al., "Male elderly subthreshold depression patients have smaller volume of medial part of prefrontal cortex and precentral gyrus compared with age-matched normal subjects: a voxel-based morphometry," *Journal of Affective Disorders*, vol. 88, no. 3, pp. 313–320, 2005.

[35] L. C. Foland-Ross, M. D. Sacchet, G. Prasad, B. Gilbert, P. M. Thompson, and I. H. Gotlib, "Cortical thickness predicts the first onset of major depression in adolescence," *International Journal of Developmental Neuroscience*, vol. 46, pp. 125–131, 2015.

[36] M. Papmeyer, S. Giles, J. E. Sussmann et al., "Cortical thickness in individuals at high familial risk of mood disorders as they develop major depressive disorder," *Biological Psychiatry*, vol. 78, no. 1, pp. 58–66, 2015.

[37] X. Zhang, S. Yao, X. Zhu, X. Wang, X. Zhu, and M. Zhong, "Gray matter volume abnormalities in individuals with cognitive vulnerability to depression: a voxel-based morphometry study," *Journal of Affective Disorders*, vol. 136, no. 3, pp. 443–452, 2012.

[38] N. S. P. Ho, M. M. C. Wong, and T. M. C. Lee, "Neural connectivity of alexithymia: specific association with major depressive disorder," *Journal of Affective Disorders*, vol. 193, pp. 362–372, 2016.

[39] S. Kühn and J. Gallinat, "The neural correlates of subjective pleasantness," *NeuroImage*, vol. 61, no. 1, pp. 289–294, 2012.

[40] V. Taschereau-Dumouchel and S. Hetu, "Visuomotor representations within the human primary motor cortex: the elusive markers of visuomotor associative learning," *The Journal of Neuroscience*, vol. 32, no. 3, pp. 759-760, 2012.

[41] S. Walther, S. Hügli, O. Höfle et al., "Frontal white matter integrity is related to psychomotor retardation in major depression," *Neurobiology of Disease*, vol. 47, no. 1, pp. 13–19, 2012.

[42] J. S. Buyukdura, S. M. McClintock, and P. E. Croarkin, "Psychomotor retardation in depression: biological underpinnings, measurement, and treatment," *Progress in Neuro-Psychopharmacology & Biological Psychiatry*, vol. 35, no. 2, pp. 395–409, 2011.

[43] G. Northoff and F. Bermpohl, "Cortical midline structures and the self," *Trends in Cognitive Sciences*, vol. 8, no. 3, pp. 102–107, 2004.

[44] R. N. Spreng, R. A. Mar, and A. S. N. Kim, "The common neural basis of autobiographical memory, prospection, navigation, theory of mind, and the default mode: a quantitative meta-analysis," *Journal of Cognitive Neuroscience*, vol. 21, no. 3, pp. 489–510, 2009.

[45] L.-L. Zeng, H. Shen, L. Liu et al., "Identifying major depression using whole brain functional connectivity: a multivariate pattern analysis," *Brain*, vol. 135, no. 5, pp. 1498–1507, 2012.

[46] C. Ma, J. Ding, J. Li et al., "Resting-state functional connectivity bias of middle temporal gyrus and caudate with altered gray matter volume in major depression," *PLoS One*, vol. 7, no. 9, article e45263, 2012.

[47] H. Wu, H. Sun, J. Xu et al., "Changed hub and corresponding functional connectivity of subgenual anterior cingulate cortex in major depressive disorder," *Frontiers in Neuroanatomy*, vol. 10, p. 120, 2016.

[48] L. Du, J. Zeng, H. Liu et al., "Fronto-limbic disconnection in depressed patients with suicidal ideation: a resting-state functional connectivity study," *Journal of Affective Disorders*, vol. 215, pp. 213–217, 2017.

[49] M. D. De Bellis and S. R. Hooper, "Neural substrates for processing task-irrelevant emotional distracters in maltreated adolescents with depressive disorders: a pilot study," *Journal of Traumatic Stress*, vol. 25, no. 2, pp. 198–202, 2012.

[50] J. S. Damoiseaux, C. F. Beckmann, E. J. S. Arigita et al., "Reduced resting-state brain activity in the "default network" in normal aging," *Cerebral Cortex*, vol. 18, no. 8, pp. 1856–1864, 2008.

[51] X. Lei, Z. Zhao, and H. Chen, "Extraversion is encoded by scale-free dynamics of default mode network," *NeuroImage*, vol. 74, pp. 52–57, 2013.

[52] X. Lei, Y. Wang, H. Yuan, and D. Mantini, "Neuronal oscillations and functional interactions between resting state networks," *Human Brain Mapping*, vol. 35, no. 7, pp. 3517–3528, 2014.

[53] X. Xu, H. Yuan, and X. Lei, "Activation and connectivity within the default mode network contribute independently to future-oriented thought," *Scientific Reports*, vol. 6, no. 1, article 21001, 2016.

[54] K. A. Lindquist, T. D. Wager, H. Kober, E. Bliss-Moreau, and L. F. Barrett, "The brain basis of emotion: a meta-analytic review," *Behavioral and Brain Sciences*, vol. 35, no. 3, pp. 121–143, 2012.

[55] W. Qin, Y. Xuan, Y. Liu, T. Jiang, and C. Yu, "Functional connectivity density in congenitally and late blind subjects," *Cerebral Cortex*, vol. 25, no. 9, pp. 2507–2516, 2015.

[56] C. M. Sarabia-Cobo, B. García-Rodríguez, M. J. Navas, and H. Ellgring, "Emotional processing in patients with mild cognitive impairment: the influence of the valence and intensity of emotional stimuli: the valence and intensity of emotional stimuli influence emotional processing in patients with mild cognitive impairment," *Journal of the Neurological Sciences*, vol. 357, no. 1-2, pp. 222–228, 2015.

[57] M. L. Barca, K. Persson, R. Eldholm et al., "Trajectories of depressive symptoms and their relationship to the progression of dementia," *Journal of Affective Disorders*, vol. 222, pp. 146–152, 2017.

[58] C. L. Li, Y. C. Chiu, Y. B. Bai, J. D. Lin, F. Stanaway, and H. Y. Chang, "The co-occurrence of depressive symptoms and cognitive impairment and its relationship with self-care behaviors among community dwelling older adults with diabetes," *Diabetes Research and Clinical Practice*, vol. 129, pp. 73–78, 2017.

Hindawi
Neural Plasticity
Volume 2018, Article ID 3432649, 13 pages
https://doi.org/10.1155/2018/3432649

Research Article

Oscillatory Corticospinal Activity during Static Contraction of Ankle Muscles Is Reduced in Healthy Old versus Young Adults

Meaghan Elizabeth Spedden,[1] Jens Bo Nielsen,[2,3] and Svend Sparre Geertsen [1,2]

[1]*Department of Nutrition, Exercise and Sports, University of Copenhagen, Copenhagen, Denmark*
[2]*Department of Neuroscience, University of Copenhagen, Copenhagen, Denmark*
[3]*Elsass Institute, Charlottenlund, Denmark*

Correspondence should be addressed to Svend Sparre Geertsen; ssgeertsen@nexs.ku.dk

Received 1 March 2018; Accepted 26 March 2018; Published 26 April 2018

Academic Editor: Claudio A. Mastronardi

Aging is accompanied by impaired motor function, but age-related changes in neural networks responsible for generating movement are not well understood. We aimed to investigate the functional oscillatory coupling between activity in the sensorimotor cortex and ankle muscles during static contraction. Fifteen young (20–26 yr) and fifteen older (65–73 yr) subjects were instructed to match a target force by performing static ankle dorsi- or plantar flexion, while electroencephalographic (EEG) activity was recorded from the cortex and electromyographic (EMG) activity was recorded from dorsi- (proximal and distal anterior tibia) and plantar (soleus and medial gastrocnemius) flexor muscles. EEG-EMG and EMG-EMG beta band (15–35 Hz) coherence was analyzed as an index of corticospinal activity. Our results demonstrated that beta cortico-, intra-, and intermuscular coherence was reduced in old versus young subjects during static contractions. Old subjects demonstrated significantly greater error than young subjects while matching target forces, but force precision was not related to beta coherence. We interpret this as an age-related decrease in effective oscillatory corticospinal activity during steady-state motor output. Additionally, our data indicate a potential effect of alpha coherence and tremor on performance. These results may be instrumental in developing new interventions to strengthen sensorimotor control in elderly subjects.

1. Introduction

Aging is accompanied by increased incidence of gait and balance problems, greater movement variability, reduced force steadiness, and worsened coordination [1–3], but age-related changes in neural control of motor function have yet to be fully elucidated. Previous studies have primarily focused on characterizing structural mechanisms, whereas knowledge regarding functional changes in the neural networks involved in generating movements is limited. A better understanding of how activity patterns in descending tracts controlling motor function are modified with age is of particular importance, as these tracts directly mediate motor signals from the brain to the spinal cord.

The corticospinal tract is a major descending pathway governing voluntary movement in humans and appears to be vulnerable to age-related deterioration. Diffusion tensor imaging has revealed declining fractional anisotropy (FA) in the posterior limb of the internal capsule, indicating degeneration in white matter microstructure [4, 5]. The functional significance of these declines is supported by associations between internal capsule FA and motor performance [6]. Input-output characteristics of the corticospinal system also appear to be modulated with age. Studies using transcranial magnetic stimulation indicate that the amplitude of motor-evoked responses is lower in old than in young adults [7–9], which suggests that aging may entail reduced excitability in the corticospinal pathway.

Another functional marker of corticospinal integrity is corticomuscular coherence, which quantifies the degree of task-related oscillatory coupling between the sensorimotor cortex and contralateral muscle. In healthy young adults, coherent oscillations are present between the cortex and muscle at beta frequencies (15–35 Hz) during isometric

contractions and are mediated by the corticospinal tract [10–16]. Coherent beta oscillations may also be seen between different pools of motor neurons in synergists and within the same muscle [15, 17–19]. This intra- and intermuscular coherence shares several similarities with corticomuscular coherence and is generally assumed to be generated by similar mechanisms, and both inter- and intramuscular coherence are therefore often used as an indirect measure of the corticospinal activity [18, 19]. Coherent oscillations are also present in the alpha band (5–15 Hz) between pairs of motor units [17] but are only rarely seen between the cortex and the muscles [20, 21]. The origin of alpha coherence is debated, but some evidence suggests a central origin [21] and a relation to physiological tremor [22].

Previous investigations of age-related changes in beta band coherence have produced equivocal results. Studies have demonstrated reduced [23], increased [24], and unchanged [25] amplitudes of corticomuscular coherence in old versus young adults, whereas studies examining inter- or intramuscular coherence have shown both unchanged [26, 27] and increased [27, 28] magnitudes. However, the use of different motor tasks and muscle groups may render direct comparisons across studies inappropriate or, in the least, less straightforward. Studies exploring age-related changes in coherence have primarily focused on hand and arm muscles [23–25, 28]. Less is known about the cortical control of ankle muscles, which is of interest due to their important role in postural control and gait. For example, during gait, ankle dorsiflexors lift the toes in order to clear the ground in the swing phase, and plantar flexors play a crucial role in forward propulsion during the late stance phase [29]. To date, age-related changes in intermuscular coherence in ankle muscles during a simple phasic task [26] and during uni- and bipedal stance [27] have been explored, but investigation of the direct corticomuscular coupling is lacking.

We aimed to investigate cortico-, intra-, and intermuscular coherence in ankle muscles during static dorsi- and plantar flexion in old versus young adults. It was hypothesized that older adults would display less beta coherence than young adults, indicative of reduced oscillatory corticospinal activity. Additionally, we wanted to explore if beta coherence estimates were positively associated with task performance.

2. Methods

2.1. Subjects. Fifteen young (mean: 22.1 ± 1.7, range 20–26 yr; 7 men) and fifteen older (mean: 68.3 ± 2.7, range 65–73 yr; 7 men) participants were recruited (see Table 1). The sample size was chosen based on previous studies comparing coherence between groups [24, 25]. Subjects were free from neurological disorders and afflictions impairing leg motor function. No subjects were taking medication expected to affect neuromuscular function. There was no indication of cognitive impairment in any subjects as determined by the Mini-Mental State Examination (MMSE; all scores ≥ 26 out of 30) [30]. According to the Waterloo Footedness Questionnaire [31], 21 subjects were right-footed, 2 were left-footed, and 7 were equally right- and left-footed.

Table 1: Subject characteristics.

Group	Young ($n = 15$)	Old ($n = 15$)
Age (years)	22.1 ± 1.7	68.3 ± 2.7
Gender (M/F)	7/8	7/8
Body mass (kg)	72.95 ± 15.89	81.45 ± 14.12
Height (m)	1.76 ± 0.08	1.73 ± 0.11
BMI	23.43 ± 4.29	27.31 ± 4.14*
MMSE (score out of 30)	29.0 ± 1.1	28.9 ± 1.0
Footedness (R/L/B)	11/1/3	10/1/4

Values are presented at mean ± standard deviation where applicable. Significant differences between young and old groups are indicated by $^*p < 0.05$. MMSE: Mini-Mental State Examination. Footedness indicates foot preference. R: right; L: left; B: both.

Prior to participation in the study, subjects provided written, informed consent. All procedures were approved by the ethics committee for the Capital Region of Denmark (approval number H-16021214), and experiments were conducted in accordance with the Helsinki declaration.

2.2. Protocol. Subjects were seated in a rigid chair with the left foot firmly fastened to a force pedal containing a strain gauge that measured force exerted on the pedal. The leg was positioned with ~90° flexion at the hip joint, ~115° flexion at the knee joint, and ~120° dorsiflexion at the ankle joint.

First, subjects performed three maximal isometric dorsiflexion contractions (MVC), separated by 30 s rest, as a measure of maximal voluntary dorsiflexion strength. Online visual feedback of force production was projected onto the wall in front of subjects as a moving yellow trace on a black background. The projector (TDP-T 255; Toshiba) was attached to the ceiling 148 cm from the wall, resulting in a screen size of 125 cm by 167 cm. During MVC, verbal encouragement was provided to ensure maximal efforts. MVC was determined as peak force production across the three trials.

Subsequently, subjects performed a static contraction, where they were asked to maintain a force level of 10% MVC during isometric dorsiflexion for two minutes. The target force level was displayed on the wall as a horizontal line, and subjects were instructed to follow this line as precisely as possible with the moving yellow trace depicting real-time force production (Figure 1).

Following a short rest, subjects repeated the MVC procedure and static contraction for plantar flexion. During periods where data was recorded, subjects were asked to relax face and neck muscles to minimize artifacts in electroencephalographic (EEG) signals.

2.3. Electrophysiological Recordings. EEG and electromyographic (EMG) activity were recorded using active surface electrodes (BioSemi, The Netherlands) and ActiView acquisition software (version 6.05). EEG was measured using 64 pin electrodes plugged into a headcap (BioSemi) that ensured positioning in accordance with the 10/20 layout system. EMG was recorded from four pairs of electrodes placed on left lower leg muscles (interelectrode distance ~ 1.5 cm) after

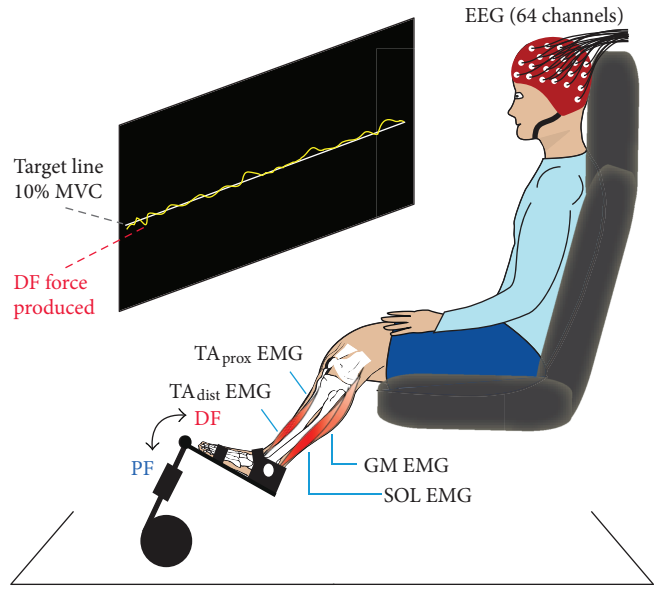

Figure 1: Experimental setup and static contractions. Subjects sat in a chair with their left foot fastened to a force pedal and maintained a force level of 10% of their maximal voluntary contraction (MVC) for 2 min, first for dorsiflexion (DF) and subsequently for plantar flexion (PF). The target force level was projected onto the wall as a horizontal line that subjects were asked to follow as precisely as possible with a yellow force trace showing online force production. During contractions, electroencephalographic (EEG) and electromyographic (EMG) signals from the proximal and distal ends of the anterior tibial muscle (TA_{prox} and TA_{dist}), soleus (SOL), and medial gastrocnemius (GM) were recorded.

preparation of the skin with shaving, abrasion, and cleaning with alcohol. Pairs of EMG electrodes were positioned over the proximal (TA_{prox}) and distal (TA_{dist}) ends of the anterior tibial muscle (mean distance between electrode pairs ~ 12 cm) and over the center of the medial gastrocnemius (MG) and soleus (SOL) muscles. As per the BioSemi system design, signals were recorded in reference to a common mode sense active electrode, while a driven right leg electrode was used to cancel signals measured at the common mode sense electrode. Analog signals were sampled at 2048 Hz, and offset was contained to $\pm 25\,\mu$V.

2.4. Data Analysis and Statistics. All data analysis was performed in MATLAB (Version R2016b, MathWorks, MA, USA). Electrophysiological data was preprocessed using the EEGLAB toolbox (v14.0.0). Initially, EEG and EMG signals were downsampled to 256 Hz. EEG signals were then rereferenced to an average reference excluding noisy and high impedance channels and band pass filtered between 0.5 to 120 Hz. Independent component analysis was performed in EEGLAB [32] and was used to remove EEG signal components displaying unequivocal spatial and temporal characteristics of eye blinks and/or face and neck muscle activity [33]. EMG signals were band pass filtered between 5 and 120 Hz then full-wave rectified to emphasize information about timing of motor unit action potentials in the signals [34] and to improve coherence detection [35].

In order to examine the coupling between EEG-EMG and EMG-EMG signals in the frequency domain, coherence estimates were constructed [36]. Coherence describes the linear association between two signals at each frequency of interest and is a measure of phase consistency between signals. Coherence estimates are defined over the range [0, 1] where 0 indicates no association between signals and 1 indicates a strong association. To calculate coherence, auto- and cross-spectra were constructed by dividing signals into nonoverlapping segments, after which discrete Fourier transforms were performed on each segment and averaged. Coherence was then determined as the squared modulus of the cross-spectrum for the two signals $f_{xy}(\lambda)$ normalized by the product of the two autospectra, $f_{xx}(\lambda)$ and $f_{yy}(\lambda)$:

$$|Rxy(\lambda)|^2 = \frac{\left|f_{xy}(\lambda)\right|^2}{f_{xx}(\lambda) f_{yy}(\lambda)}. \quad (1)$$

EEG-EMG coherence thus quantifies the strength and frequency range of the coupling between cortical and muscular activity, whereas EMG-EMG coherence quantifies common rhythmic drive to two muscles or motor neuron pools. The statistical significance of individual coherence estimates was assessed according to an upper 95% confidence limit determined as

$$1 - 0.05^{\frac{1}{(L-1)}}, \quad (2)$$

where L indicates the number of data segments used for the analysis [36].

For data obtained during static dorsiflexion, coherence was calculated between EEG and TA_{prox}; EEG and TA_{dist}; and between TA_{prox} and TA_{dist}. For static plantar flexion, coherence analysis was likewise performed for EEG and SOL; EEG and MG; and between SOL and MG. For all

analyses, 120 seconds of data and a frequency resolution of 1 Hz were utilized.

Initially, EEG-EMG coherence was calculated for all EEG electrodes. Scalp plots indicated that beta band (15–35 Hz) coherence was localized at the vertex (Cz), assumedly corresponding to the sensorimotor cortex (Figure 2). Accordingly, further analysis was performed using coherence at the Cz electrode (see example in Figure 3).

All EMG-EMG coherence data was visually inspected for signs of crosstalk, that is, high coherence across a wide range of frequencies and close to zero lag synchronization in the time domain as evidenced in cumulant density plots [37]. No data was observed displaying these characteristics, so all data was included in pooled analyses.

To undertake a population analysis, coherence for each age group was pooled, resulting in single group estimates at each frequency of interest. Group differences were investigated using the χ^2 extended difference of coherence test [38], a nonparametric test that provides the amount of pooled coherence difference between groups at each frequency in relation to an upper 95% confidence interval limit.

Coherence was also quantified as the sum (i.e., area) of alpha (5–15 Hz), total beta (15–35), low (15–25 Hz), and high (25–35 Hz) beta coherence. These values were transformed logarithmically to symmetrize distributions for statistical analyses. Additionally, we registered the frequency at which peak beta coherence occurred as well as the sum of EMG power in alpha and beta bands.

Performance during static contractions was quantified as the root mean square (RMS) error, that is, the RMS deviation of the raw force signal from the target force level.

One-way ANOVA was used to evaluate effects of age group on dependent variables, that is, logarithmic coherence area estimates, frequency for peak beta coherence, summed EMG power, RMS error, and subject characteristics (MMSE score, height, weight, and body mass index (BMI)). Model assumptions were checked by visual inspection of residual and normal probability plots. ANOVA was also utilized to explore if gender and/or laterality (footedness) affected the area of beta coherence.

Associations between task performance and coherence estimates, as well as performance and power were assessed by means of Pearson correlations. The significance level used to reject the null hypothesis was $\alpha = 0.05$, but tendencies were also noted for $p < 0.1$. Values are presented as mean ± standard deviation where applicable.

3. Results

Subject characteristics are summarized in Table 1. Young and old subjects were comparable in height ($p = 0.349$), body mass ($p = 0.133$), and MMSE score ($p = 0.726$), whereas older subjects had significantly greater BMI ($p = 0.018$).

EEG, EMG, autospectra, and coherence results from a single young subject during static dorsiflexion are shown in Figure 3. For this subject, sizeable coherence peaks were observed in the beta band (~20 Hz) for both cortico- and intramuscular coherence.

3.1. EMG Power. Figure 4 shows summed EMG power for young and older subjects. Alpha EMG power was greater in old subjects for TA_{dist} ($p = 0.011$) and SOL ($p = 0.023$), whereas group differences were not significant for TA_{prox} ($p = 0.312$) or GM ($p = 0.218$). In the beta band, old subjects had significantly greater power for TA_{prox} ($p = 0.005$), but no other differences were detected (TA_{dist}, $p = 0.413$; SOL, $p = 0.666$; GM, $p = 0.363$).

3.2. Coherence during Static Dorsiflexion. Pooled coherence for young and old groups during the dorsiflexion task is presented in Figure 5. For both groups, pooled beta coherence estimates exceeded significance levels for cortico- and intramuscular coherence measures and indicated greater coherence in young than in old subjects (Figures 5(a), 5(c), and 5(e)). The χ^2 extended difference of coherence test confirmed that group means differed significantly at beta frequencies for both cortico- and intramuscular coherence (Figures 5(b), 5(d), and 5(f)). The χ^2 test also revealed significant group differences in intramuscular coherence in the alpha band (~10 Hz), where young subjects had greater coherence than old subjects.

Estimates for coherence area in alpha, beta, and high and low beta bands are presented in Figure 6. Differences between young and old subjects were most consistent in the high beta band, where coherence area was greater for young than old subjects for all three coherence measures, though group differences in total and low beta area were also significant for TA_{prox}-TA_{dist} coherence and tended towards significance for the total beta band in Cz-TA_{prox}. Using this approach, no differences between young and old subjects were present in the area of alpha coherence.

Visual inspection of pooled group plots suggested that coherence in old adults appeared to be slightly shifted toward earlier frequencies, but review of single-subject plots indicated that this trend was driven by three older subjects showing pronounced coherence at alpha to early beta frequencies. In addition, the frequency at which peak beta coherence occurred did not differ significantly between groups for corticomuscular coherence (Cz-TA_{prox}, $p = 0.420$, Cz-TA_{dist}, $p = 0.742$), although it tended to be lower in old subjects for intramuscular coherence (TA_{prox}-TA_{dist}, $p = 0.088$).

No significant effects of gender (all $p > 0.2$) or footedness (all $p > 0.3$) on beta band coherence area during dorsiflexion were present.

3.3. Coherence during Static Plantar Flexion. Pooled coherence data from the plantar flexion task demonstrated trends similar to those observed for the dorsiflexion task, though amplitudes were lower in both age groups (Figures 7(a), 7(c), and 7(e)). Group estimates indicated statistically significant beta coherence in both young and old subjects for all three measures. Pooled plots suggested that the magnitude of beta coherence was consistently larger for young subjects, which was corroborated by the χ^2 extended difference of coherence test (Figures 7(b), 7(d), and 7(f)). For intermuscular coherence, pooled estimates indicated the presence of alpha coherence in both age groups, but group differences at these frequencies did not reach the significance level. Thus,

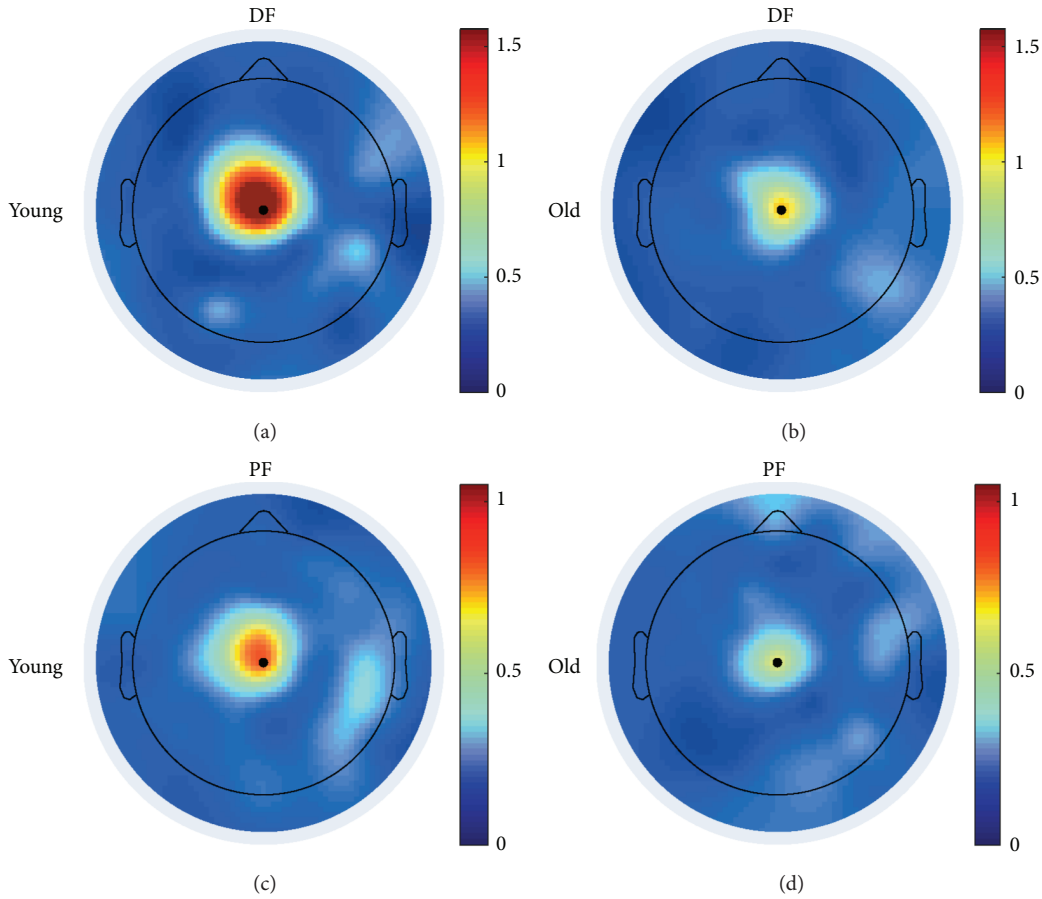

FIGURE 2: Coherence head plots. Spatial localization of summed beta band (15–35 Hz) corticomuscular coherence for single young (a, c) and old (b, d) subjects during static dorsiflexion (a, b; EEG-TA_{prox} coherence) and plantar flexion (c, d; EEG-SOL coherence).

the χ^2 test indicated that group differences were confined to the beta band.

The area of beta coherence differed between groups in a more widespread manner than for dorsiflexion (Figure 6); Cz-SOL coherence only tended to be greater in young subjects for the high beta band, whereas for Cz-GM and SOL-GM, significant differences in total, low, and high beta bands were observed. In the alpha band, a significant group difference was observed for Cz-GM, where coherence area was greater in old subjects.

Similar to what was observed in dorsiflexion, pooled coherence data suggested that coherence in old subjects was present at slightly lower frequencies than in young subjects. Upon inspection of individual coherence estimates, it was again apparent that the same three old subjects were responsible for this trend. Correspondingly, the frequency at which peak beta coherence occurred did not differ in young and old adults for Cz-GM ($p = 0.754$) or SOL-GM ($p = 0.673$), but a tendency towards lower frequency beta coherence in older adults was present for Cz-SOL ($p = 0.081$).

As for dorsiflexion, beta band coherence during plantar flexion was neither affected by gender (all $p > 0.4$) nor footedness (all $p > 0.3$).

3.4. Task Performance and Associations with Power and Coherence. Figure 8 shows group differences in force precision during static dorsi- and plantar flexion contractions. RMS error during dorsiflexion was greater for old (14.5 ± 8.2 mV) than for young (9.5 ± 3.1 mV) adults ($p = 0.035$). During plantar flexion, RMS error for old adults (16.8 ± 6.3 mV) was likewise greater than for young adults (11.1 ± 3.1 mV; $p = 0.004$).

To examine if low-frequency rhythmicity in EMG bursts was related to task performance, associations between EMG alpha power and RMS error were explored. EMG alpha power in TA_{prox} was positively associated with RMS error ($r = 0.47$, $p = 0.008$), and a tendency towards a positive correlation between TA_{dist} and RMS error was also present ($r = 0.36$, $p = 0.054$), while alpha power in SOL and GM was not related to RMS error during plantar flexion (SOL, $p = 0.323$, GM, $p = 0.776$).

Furthermore, we investigated possible associations between coherence estimates and performance. Surprisingly, neither cortico- nor intramuscular beta coherence area was correlated with RMS error during the dorsiflexion task (Cz-TA_{prox}, $p = 0.783$; Cz-TA_{dist}, $p = 0.745$; TA_{prox}-TA_{dist}, $p = 0.306$), suggesting that the amount of beta coherence was not related to task performance. For the plantar flexion task, RMS error was also unrelated to beta coherence area (Cz-SOL, $p = 0.327$; Cz-GM, $p = 0.870$; SOL-GM, $p = 0.946$). Correlations between RMS error and low and high beta coherence were similarly nonsignificant for

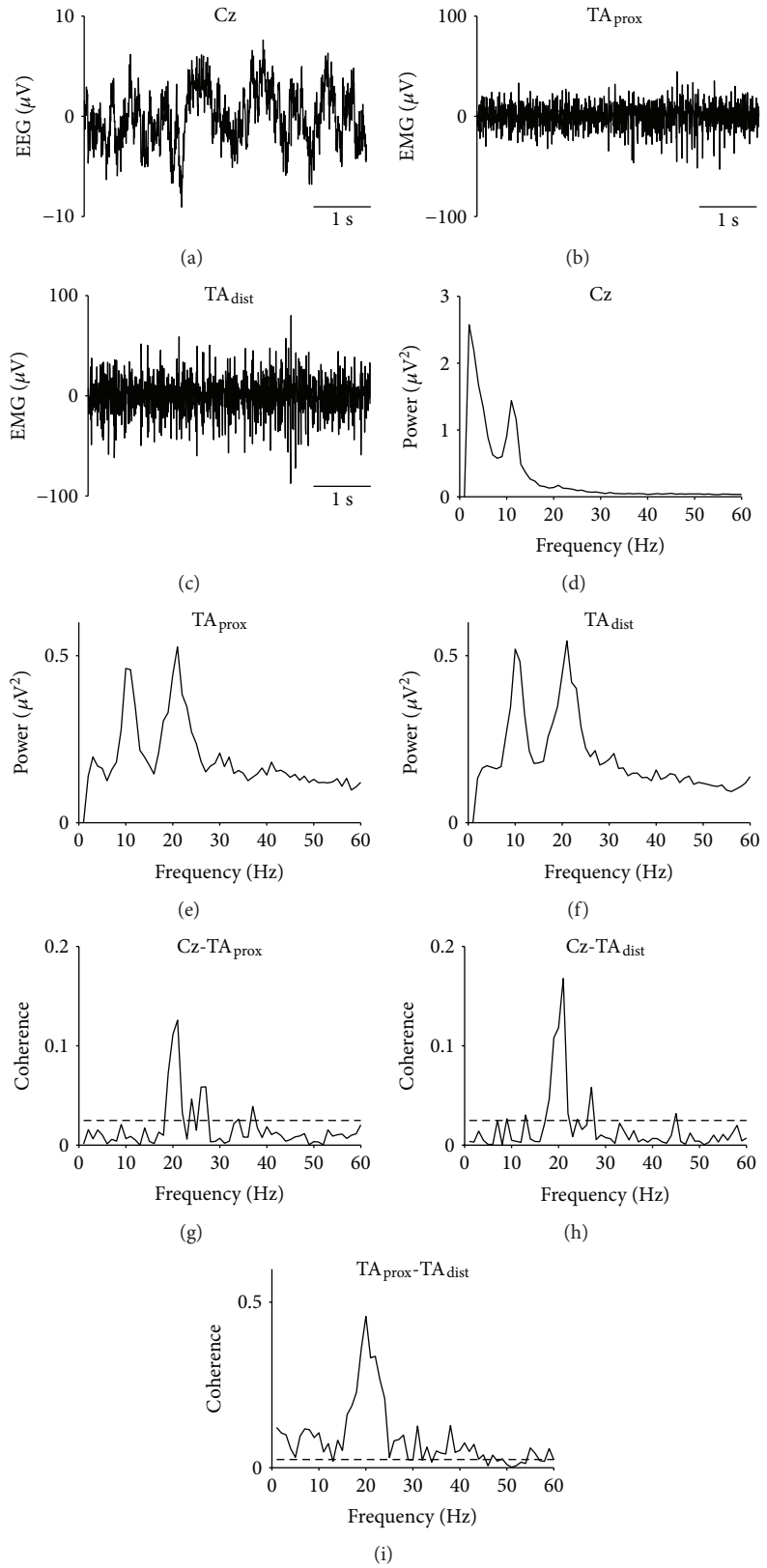

Figure 3: Raw EEG and EMG traces, autospectra, and coherence results from a single young subject. EEG from Cz (a), EMG from proximal (b), and distal (c) ends of the anterior tibial muscle (TA_{prox} and TA_{dist}, resp.); autospectra for Cz (d), TA_{prox} (e), TA_{dist} (f); and coherence for Cz-TA_{prox} (g), Cz-TA_{dist} (h), and TA_{prox}-TA_{dist} (i) during static dorsiflexion. Dashed lines on coherence plots indicate upper 95% confidence interval limits.

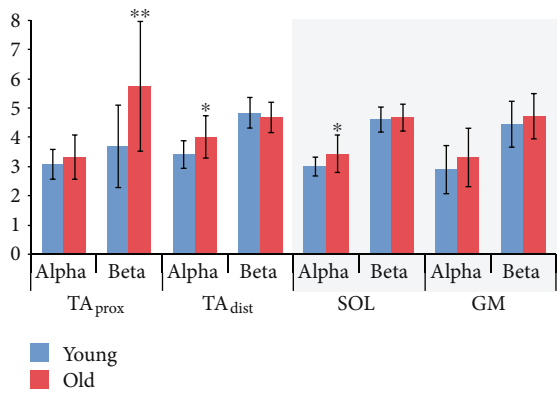

Figure 4: EMG power. Summed EMG power in alpha (5–15 Hz) and beta (15–35 Hz) bands for young and old subjects during dorsiflexion (white background) and plantar flexion (grey background). Significant differences between young and old groups are indicated by $^{*}p < 0.05$; $^{**}p < 0.01$. TA_{prox}: proximal end of anterior tibial; TA_{dist}: distal end of anterior tibial; SOL: soleus; GM: medial gastrocnemius.

both dorsi- and plantar flexion tasks (range for p values: 0.175–0.971). Interestingly, alpha coherence area was positively correlated with RMS error for both tasks in five out of six coherence measures (range for p values: 0.010–0.062, range for r: 0.34–0.46), demonstrating that greater coherence in the alpha band was accompanied by less precision in force production across groups.

4. Discussion

The aim of this study was to examine age-related changes in cortico-, intra-, and intermuscular beta band coherence in lower leg muscles during static dorsi- and plantar flexion. We found that beta band coherence estimates were significantly lower in old versus young adults for all coherence measures during both tasks. Error during force tasks was greater for old than young subjects, but no associations were observed between task performance and coherence area in the beta band. Collectively, our results suggest an age-related reduction in oscillatory corticospinal activity in the beta band during a simple task requiring steady state motor output, but the amount of beta coherence was not related to precision in force production. Interestingly, our data indicate a potential effect of alpha coherence and EMG alpha power on task performance.

4.1. Beta Band Coherence. For subjects with significant coherence, cortico-, intra-, and intermuscular coherence was most prominent in the beta band, which agrees with previous results demonstrating beta coherence during isometric contractions [10, 11, 13–17, 20]. That this oscillatory coupling in the beta band specifically reflects task-related corticospinal activity is confirmed by multiple lines of evidence. In the monkey, it has been demonstrated that local field potentials in the primary motor cortex are coherent with EMG in the beta band during static contractions, and that these local field potentials were phase-locked with pyramidal cell firing, indicating that corticomuscular coherence is, in the least, partially mediated by the corticospinal tract [39]. Moreover, beta coherence is weakened or absent in patients with central stroke [40]. The use of EEG, MRI, and TMS in combination has also shown, in healthy humans, that corticomuscular coherence is localized at the same site as the muscle's hotspot for TMS [41]. Finally, it has been shown that subthreshold TMS increases corticomuscular coherence, suggesting a role for cortical cells in the generation of beta band coherence [42]. Cortico-, intra-, and intermuscular coherence are thought to generally reflect the same oscillatory corticospinal activity [19], but when considering the indirect measures of intra and intermuscular coherence, contributions from other common neural drives cannot be excluded.

4.2. Age-Related Changes in Beta Band Coherence. Our findings of reduced beta band coherence in older subjects are in line with results from a previous study suggesting weakened corticomuscular coherence in older adults during static contractions of arm muscles [23], although other studies have demonstrated unchanged or greater beta coherence in older adults [24–28]. These inconsistencies are not easily reconciled, but considering that beta coherence is task-dependent, differences in task details across studies are likely of utmost importance. One study examined intermuscular coherence in ankle muscles during a simple motor task across the adult lifespan and found no evidence of age-related changes in beta coherence amplitude [26]. However, this study utilized a task consisting of brief phasic dorsiflexions, where visual feedback of EMG traces was provided, but where contraction strength was not controlled, which may contribute to explaining the seemingly divergent results. What is more, this study only examined the corticomuscular coupling indirectly, that is, via intermuscular coherence.

Another recent study investigated intermuscular coherence in triceps surae muscles during stance and found greater beta band coherence in older versus young adults during the uni- but not bipedal posture [27]. These findings indicate that older adults deployed greater oscillatory corticospinal activity during a demanding task, possibly as a strategy to manage their increased postural sway. Interestingly, beta coherence was not greater in older adults during the simpler task, that is, bipedal stance, suggesting that task difficulty may modulate the age-related mobilization of oscillatory corticospinal activity. Our task differed considerably from uni- and bipedal stance, making direct comparisons difficult, but one interesting factor may be differences in the costs of failure in task performance; for static dorsiflexion, there is no consequence to poor performance, whereas during unipedal stance, there is likely a perceived risk of falling that could affect the neural strategy employed.

The age-related reduction we observed in beta coherence, indicative of decreased oscillatory corticospinal activity, is plausibly related to both structural and functional declines in the nervous system. There does not appear to be an age-related loss of neurons in the primary motor cortex [43], but the deterioration in white matter microstructure that occurs with aging likely affects corticospinal connectivity [4, 5]. Decreases in synaptic density [44] and dendritic

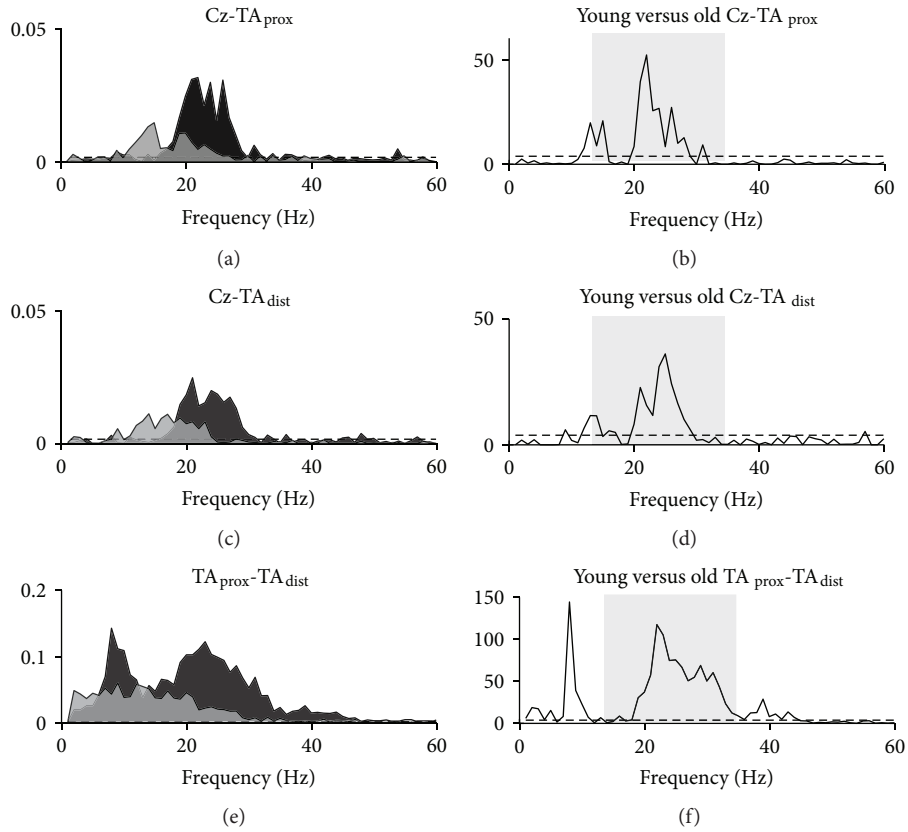

Figure 5: Pooled coherence during dorsiflexion. Pooled coherence estimates for young (black areas) and old (light grey areas) groups during static dorsiflexion (a, c, e) and χ^2 test statistics as a function of frequency (b, d, f) illustrating frequencies at which group means differed. Shaded boxes in b, d, and f mark the beta band (15–35 Hz). Dashed lines indicate upper 95% confidence interval limits. TA_{prox}: proximal end of anterior tibial muscle; TA_{dist}: distal end of anterior tibial muscle.

arborization [45] may likewise contribute to reduced corticomuscular coherence in older adults.

Age-related changes in the functional organization of sensorimotor networks have also been demonstrated. Functional MRI studies suggest that aging entails greater and more widespread cortical activation including regions involved in sensory processing and cognitive control, even during simple motor tasks [46–48]. The reduction we observed in functional corticospinal involvement is not necessarily inconsistent with these findings but may rather be a consequence of age-related de-differentiation of networks, that is, more defocalized and nonspecific activation patterns may entail a less focused and effective corticospinal coupling. Alternatively, decreased corticospinal involvement may represent a fundamental decline in the sensorimotor system compelling compensatory activation in, for example, cognitive or sensory processing regions. Synchronous activity has been theorized as a particularly efficient mode of corticospinal interaction in tasks with relatively low computational demands [39, 49]; accordingly, decreased coherence in older adults may indicate decreased efficiency in the corticospinal system necessitating compensatory strategies in order to perform a given task. The relationship between age-related reductions in beta coherence and modifications of sensorimotor networks should be explored in future studies.

When we examined group estimates for pooled coherence, we noticed that the area of significant coherence was shifted towards lower frequencies (late alpha-early beta) in older subjects. However, this shift appeared to be primarily driven by three older subjects and was not statistically evident when comparing the frequency for peak beta coherence in old versus young groups. We only investigated this apparent shift within the confines of the beta band, as the origin of this activity is well-established, but it is possible that the frequency band reflecting oscillatory corticospinal activity shifts slightly with aging and is thus present at somewhat lower frequencies (~10–25 Hz). This would be in line with previous results indicating that cortical activity and corticomuscular coherence slow with aging [24]; thus, this potential shift towards lower frequencies should be explored in further projects.

It should be noted that we found higher BMI in the older subjects, but we do not believe that this could explain the observed differences in coherence. Although more subcutaneous fat could affect the EMG amplitude, it would not be expected to affect the frequency of the signals, which is what is used for coherence analyses.

4.3. Mechanisms Contributing to Decreased Performance in Older Subjects. The functional significance of the observed decline in beta band coherence is unclear. We expected that

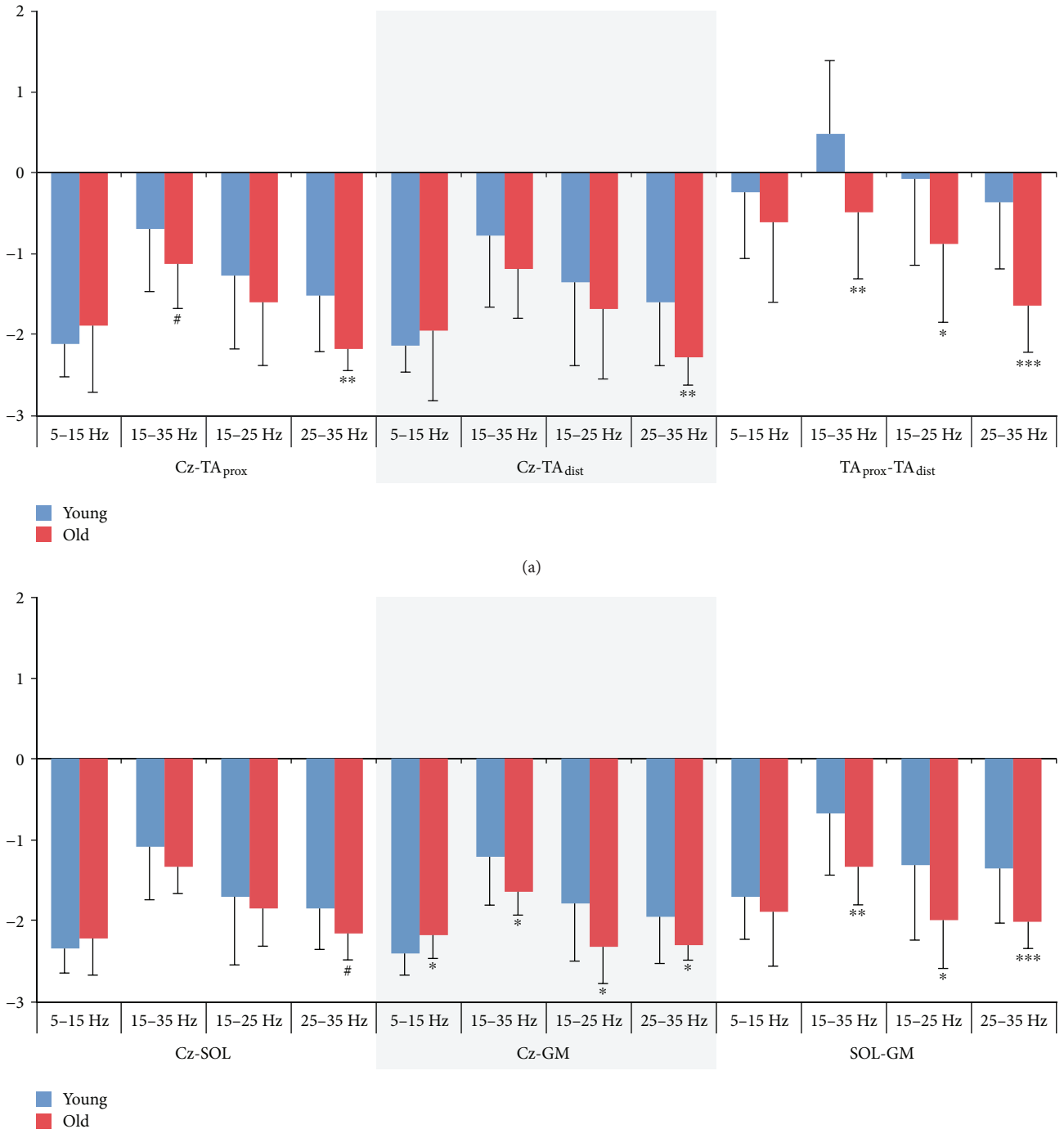

Figure 6: Coherence area estimates. Logarithmic coherence area in alpha (5–15 Hz), beta (15–35 Hz), low (15–25 Hz), and high (25–35 Hz) beta during static dorsiflexion (a) and plantar flexion (b) for young and old subjects. Significant differences between young and old groups are indicated by $^{*}p < 0.05$; $^{**}p < 0.01$; $^{***}p < 0.001$; $^{\#}p < 0.1$. TA_{prox}: proximal end of anterior tibial; TA_{dist}: distal end of anterior tibial; SOL: soleus; GM: medial gastrocnemius.

greater oscillatory corticospinal activity would be positively related to precision in force production, as suggested by a previous study [49], but our results indicated no association between beta coherence and force precision; older adults demonstrated greater error and less beta coherence, but the two parameters were not related. As a more challenging visuomotor task was used by Kristeva and colleagues [49], requiring subjects to respond precisely to an applied force of 4% MVC, this divergence may reflect that our task was not sufficiently demanding to detect a positive effect of beta coherence on performance. On the other hand, other studies have found that greater beta coherence was associated with

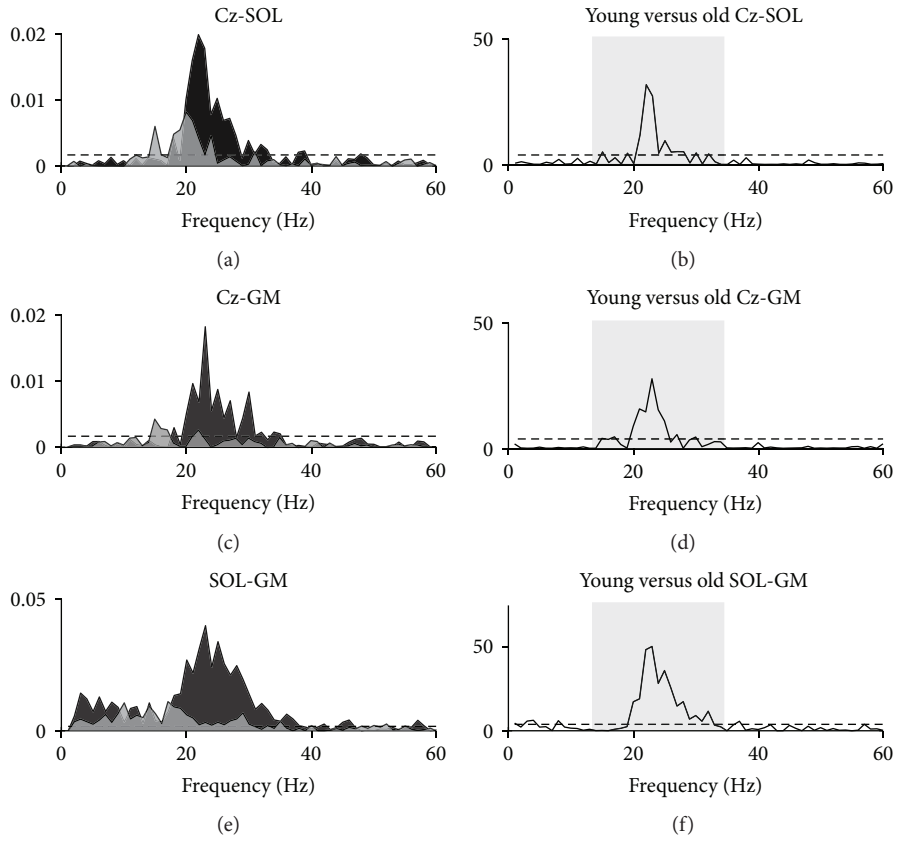

Figure 7: Pooled coherence during plantar flexion. Pooled coherence estimates for young (black areas) and old (light grey areas) groups during static plantar flexion (a, c, e) and χ^2 test statistics as a function of frequency (b, d, f) illustrating frequencies at which group means differed. Shaded boxes in b, d, and f mark the beta band (15–35 Hz). Dashed lines indicate upper 95% confidence interval limits. SOL: soleus; GM: medial gastrocnemius.

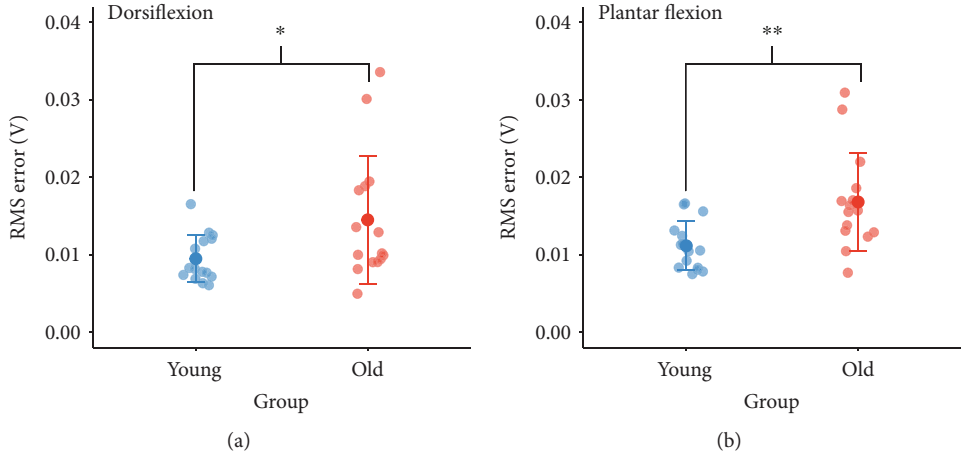

Figure 8: Performance during static contractions. Group differences in force precision during submaximal dorsiflexion (a) and plantar flexion (b). Significant differences between young and old groups are indicated by $^{*}p < 0.05$, $^{**}p < 0.01$. RMS: root mean square.

worsened precision [14, 25], which emphasizes that the functional significance of beta coherence probably also differs according to task demands.

We also investigated the presence of age-related physiological (or essential) tremor as a possible explanation for decreased force precision in older adults [50]. EMG power in the alpha band was greater in TA_{dist} and SOL for old versus young subjects, indicating greater tremor in older subjects in these muscles, as would be expected. Alpha power was also positively associated with RMS error across groups for TA_{prox} and tended strongly to be associated with error for TA_{dist}, which suggests that the degree of rhythmic

bursting in EMG had a negative effect on the ability to precisely maintain the target force. Interestingly, we also found positive correlations between the area of alpha coherence and RMS error for five out of six coherence measures. It has been suggested that alpha coherence is related to the central component of physiological tremor [22, 51]; however, group differences in the area of alpha coherence were only significant for Cz-GM, indicating that the area of alpha coherence is not a likely explanation for worsened force precision in older subjects but rather a factor contributing to individual differences in the ability to maintain a target force precisely. This is also supported by the observation that young subjects had greater magnitude of intramuscular alpha coherence at ~10 Hz when coherence was compared between groups at each frequency of interest. Altogether, the significance of these correlations is ambiguous, particularly when taking into account the low magnitudes of alpha coherence area estimates, but the consistency of correlations across different muscles and coherence measures warrants further investigation in future studies.

Nonetheless, greater physiological tremor in older adults may by some means be related to the lack of association observed between beta band coherence and force precision. Though speculative, it is plausible that mechanisms leading to increased tremor in older subjects may have a detrimental effect on the ability to effectively regulate force precision via beta oscillations and thus obscure any positive influence of beta coherence on performance.

5. Conclusion

We have shown that the amount of beta band cortico-, intra-, and intermuscular coherence in ankle muscles is reduced in old versus young adults during static contraction, suggesting an age-related decrease in the strength of oscillatory corticospinal activity during steady-state motor output. Our data also indicate a potential effect of alpha band coherence and tremor on precision control of muscle force. These results may be instrumental in developing new preventive and therapeutic interventions that may strengthen sensorimotor control in elderly subjects. Future projects should focus on delineating the relationship between beta band coherence and specific motor deficits in older adults and exploring mechanisms underlying the observed reduction in effective corticospinal coupling.

Conflicts of Interest

The authors declare that there is no conflict of interest regarding the publication of this article.

Funding

This work was supported by grants from the Danish Medical Research Council (FSS) and the Elsass Fonden.

References

[1] R. D. Seidler, J. A. Bernard, T. B. Burutolu et al., "Motor control and aging: links to age-related brain structural, functional, and biochemical effects," *Neuroscience & Biobehavioral Reviews*, vol. 34, no. 5, pp. 721–733, 2010.

[2] M. Cruz-Jimenez, "Normal changes in gait and mobility problems in the elderly," *Physical Medicine and Rehabilitation Clinics of North America*, vol. 28, no. 4, pp. 713–725, 2017.

[3] N. M. C. W. Oomen and J. H. van Dieën, "Effects of age on force steadiness: s literature review and *meta*-analysis," *Ageing Research Reviews*, vol. 35, pp. 312–321, 2017.

[4] D. H. Salat, D. S. Tuch, D. N. Greve et al., "Age-related alterations in white matter microstructure measured by diffusion tensor imaging," *Neurobiology of Aging*, vol. 26, no. 8, pp. 1215–1227, 2005.

[5] S. Sala, F. Agosta, E. Pagani, M. Copetti, G. Comi, and M. Filippi, "Microstructural changes and atrophy in brain white matter tracts with aging," *Neurobiology of Aging*, vol. 33, no. 3, pp. 488–498.e2, 2012.

[6] E. V. Sullivan, T. Rohlfing, and A. Pfefferbaum, "Quantitative fiber tracking of lateral and interhemispheric white matter systems in normal aging: relations to timed performance," *Neurobiology of Aging*, vol. 31, no. 3, pp. 464–481, 2010.

[7] H. Fujiyama, M. I. Garry, O. Levin, S. P. Swinnen, and J. J. Summers, "Age-related differences in inhibitory processes during interlimb coordination," *Brain Research*, vol. 1262, pp. 38–47, 2009.

[8] A. Oliviero, P. Profice, P. A. Tonali et al., "Effects of aging on motor cortex excitability," *Neuroscience Research*, vol. 55, no. 1, pp. 74–77, 2006.

[9] J. B. Pitcher, K. M. Ogston, and T. S. Miles, "Age and sex differences in human motor cortex input–output characteristics," *The Journal of Physiology*, vol. 546, no. 2, pp. 605–613, 2003.

[10] B. A. Conway, D. M. Halliday, S. F. Farmer et al., "Synchronization between motor cortex and spinal motoneuronal pool during the performance of a maintained motor task in man," *The Journal of Physiology*, vol. 489, no. 3, pp. 917–924, 1995.

[11] D. M. Halliday, B. A. Conway, S. F. Farmer, and J. R. Rosenberg, "Using electroencephalography to study functional coupling between cortical activity and electromyograms during voluntary contractions in humans," *Neuroscience Letters*, vol. 241, no. 1, pp. 5–8, 1998.

[12] S. N. Baker, "Synchronization in monkey motor cortex during a precision grip task. II. Effect of oscillatory activity on corticospinal output," *Journal of Neurophysiology*, vol. 89, no. 4, pp. 1941–1953, 2002.

[13] S. Chen, J. Entakli, M. Bonnard, E. Berton, and J. B. De Graaf, "Functional corticospinal projections from human supplementary motor area revealed by corticomuscular coherence during precise grip force control," *PLoS One*, vol. 8, no. 3, article e60291, 2013.

[14] J. Ushiyama, J. Yamada, M. Liu, and J. Ushiba, "Individual difference in β-band corticomuscular coherence and its relation to force steadiness during isometric voluntary ankle dorsiflexion in healthy humans," *Clinical Neurophysiology*, vol. 128, no. 2, pp. 303–311, 2017.

[15] A. Reyes, C. M. Laine, J. J. Kutch, and F. J. Valero-Cuevas, "Beta band corticomuscular drive reflects muscle coordination strategies," *Frontiers in Computational Neuroscience*, vol. 11, p. 17, 2017.

[16] R. Matsuya, J. Ushiyama, and J. Ushiba, "Inhibitory interneuron circuits at cortical and spinal levels are associated with individual differences in corticomuscular coherence during isometric voluntary contraction," *Scientific Reports*, vol. 7, article 44417, 2017.

[17] S. F. Farmer, F. D. Bremner, D. M. Halliday, J. R. Rosenberg, and J. A. Stephens, "The frequency content of common synaptic inputs to motoneurones studied during voluntary isometric contraction in man," *Physiology*, vol. 470, no. 1, pp. 127–155, 1993.

[18] P. Grosse, M. J. Cassidy, and P. Brown, "EEG–EMG, MEG–EMG and EMG–EMG frequency analysis: physiological principles and clinical applications," *Clinical Neurophysiology*, vol. 113, no. 10, pp. 1523–1531, 2002.

[19] J. M. Kilner, S. N. Baker, S. Salenius, V. Jousmäki, R. Hari, and R. N. Lemon, "Task-dependent modulation of 15-30 Hz coherence between rectified EMGs from human hand and forearm muscles," *The Journal of Physiology*, vol. 516, no. 2, pp. 559–570, 1999.

[20] S. Salenius, K. Portin, M. Kajola, R. Salmelin, and R. Hari, "Cortical control of human motoneuron firing during isometric contraction," *Journal of Neurophysiology*, vol. 77, no. 6, pp. 3401–3405, 1997.

[21] S. Hansen, N. L. Hansen, L. O. D. Christensen, N. T. Petersen, and J. B. Nielsen, "Coupling of antagonistic ankle muscles during co-contraction in humans," *Experimental Brain Research*, vol. 146, no. 3, pp. 282–292, 2002.

[22] J. Raethjen, M. Lindemann, M. Dümpelmann et al., "Corticomuscular coherence in the 6–15 Hz band: is the cortex involved in the generation of physiologic tremor?," *Experimental Brain Research*, vol. 142, no. 1, pp. 32–40, 2002.

[23] M. B. Bayram, V. Siemionow, and G. H. Yue, "Weakening of corticomuscular signal coupling during voluntary motor action in aging," *The Journals of Gerontology: Series A*, vol. 70, no. 8, pp. 1037–1043, 2015.

[24] D. Kamp, V. Krause, M. Butz, A. Schnitzler, and B. Pollok, "Changes of cortico-muscular coherence: an early marker of healthy aging?," *Age*, vol. 35, no. 1, pp. 49–58, 2013.

[25] S. Graziadio, A. Basu, L. Tomasevic, F. Zappasodi, F. Tecchio, and J. A. Eyre, "Developmental tuning and decay in senescence of oscillations linking the corticospinal system," *The Journal of Neuroscience*, vol. 30, no. 10, pp. 3663–3674, 2010.

[26] S. R. Jaiser, M. R. Baker, and S. N. Baker, "Intermuscular coherence in normal adults: variability and changes with age," *PLoS One*, vol. 11, no. 2, article e0149029, 2016.

[27] T. Watanabe, K. Saito, K. Ishida, S. Tanabe, and I. Nojima, "Coordination of plantar flexor muscles during bipedal and unipedal stances in young and elderly adults," *Experimental Brain Research*, pp. 1–11, 2018.

[28] J. G. Semmler, "Motor-unit coherence during isometric contractions is greater in a hand muscle of older adults," *Journal of Neurophysiology*, vol. 90, no. 2, pp. 1346–1349, 2003.

[29] J. B. Nielsen, "How we walk: central control of muscle activity during human walking," *The Neuroscientist*, vol. 9, no. 3, pp. 195–204, 2003.

[30] M. F. Folstein, S. E. Folstein, and P. R. McHugh, "'Mini-mental state'. A practical method for grading the cognitive state of patients for the clinician," *Journal of Psychiatric Research*, vol. 12, no. 3, pp. 189–198, 1975.

[31] L. J. Elias and M. P. Bryden, "Footedness is a better predictor of language lateralisation than handedness," *Laterality: Asymmetries of Body, Brain and Cognition*, vol. 3, no. 1, pp. 41–52, 1998.

[32] A. Delorme and S. Makeig, "EEGLAB: an open source toolbox for analysis of single-trial EEG dynamics including independent component analysis," *Journal of Neuroscience Methods*, vol. 134, no. 1, pp. 9–21, 2004.

[33] M. Chaumon, D. V. M. Bishop, and N. A. Busch, "A practical guide to the selection of independent components of the electroencephalogram for artifact correction," *Journal of Neuroscience Methods*, vol. 250, pp. 47–63, 2015.

[34] D. M. Halliday and S. F. Farmer, "On the need for rectification of surface EMG," *Journal of Neurophysiology*, vol. 103, no. 6, article 3547, 2010.

[35] N. J. Ward, S. F. Farmer, L. Berthouze, and D. M. Halliday, "Rectification of EMG in low force contractions improves detection of motor unit coherence in the beta-frequency band," *Journal of Neurophysiology*, vol. 110, no. 8, pp. 1744–1750, 2013.

[36] D. M. Halliday, J. R. Rosenberg, A. M. Amjad, P. Breeze, B. A. Conway, and S. F. Farmer, "A framework for the analysis of mixed time series/point process data—theory and application to the study of physiological tremor, single motor unit discharges and electromyograms," *Progress in Biophysics and Molecular Biology*, vol. 64, no. 2-3, pp. 237–278, 1995.

[37] S. F. Farmer, J. Gibbs, D. M. Halliday et al., "Changes in EMG coherence between long and short thumb abductor muscles during human development," *The Journal of Physiology*, vol. 579, no. 2, pp. 389–402, 2007.

[38] A. M. Amjad, D. M. Halliday, J. R. Rosenberg, and B. A. Conway, "An extended difference of coherence test for comparing and combining several independent coherence estimates: theory and application to the study of motor units and physiological tremor," *Journal of Neuroscience Methods*, vol. 73, no. 1, pp. 69–79, 1997.

[39] S. N. Baker, J. M. Kilner, E. M. Pinches, and R. N. Lemon, "The role of synchrony and oscillations in the motor output," *Experimental Brain Research*, vol. 128, no. 1-2, pp. 109–117, 1999.

[40] S. F. Farmer, M. Swash, D. A. Ingram, and J. A. Stephens, "Changes in motor unit synchronization following central nervous lesions in man," *The Journal of Physiology*, vol. 463, no. 1, pp. 83–105, 1993.

[41] T. Mima, C. Gerloff, J. Steger, and M. Hallett, "Frequency-coding of motor control system—coherence and phase estimation between cortical rhythm and motoneuronal firing in humans," *Society for Neuroscience – Abstracts*, vol. 24, article 1768, 1998.

[42] N. L. Hansen and J. B. Nielsen, "The effect of transcranial magnetic stimulation and peripheral nerve stimulation on corticomuscular coherence in humans," *The Journal of Physiology*, vol. 561, no. 1, pp. 295–306, 2004.

[43] H. Haug and R. Eggers, "Morphometry of the human cortex cerebri and corpus striatum during aging," *Neurobiology of Aging*, vol. 12, no. 4, pp. 336–338, 1991.

[44] P. R. Huttenlocher, "Synaptic density in human frontal cortex — developmental changes and effects of aging," *Brain Research*, vol. 163, no. 2, pp. 195–205, 1979.

[45] B. Anderson and V. Rutledge, "Age and hemisphere effects on dendritic structure," *Brain*, vol. 119, no. 6, pp. 1983–1990, 1996.

[46] V. S. Mattay, F. Fera, A. Tessitore et al., "Neurophysiological correlates of age-related changes in human motor function," *Neurology*, vol. 58, no. 4, pp. 630–635, 2002.

[47] S. Heuninckx, N. Wenderoth, F. Debaere, R. Peeters, and S. P. Swinnen, "Neural basis of aging: the penetration of cognition into action control," *The Journal of Neuroscience*, vol. 25, no. 29, pp. 6787–6796, 2005.

[48] S. Heuninckx, N. Wenderoth, and S. P. Swinnen, "Systems neuroplasticity in the aging brain: recruiting additional neural resources for successful motor performance in elderly persons," *The Journal of Neuroscience*, vol. 28, no. 1, pp. 91–99, 2008.

[49] R. Kristeva, L. Patino, and W. Omlor, "Beta-range cortical motor spectral power and corticomuscular coherence as a mechanism for effective corticospinal interaction during steady-state motor output," *NeuroImage*, vol. 36, no. 3, pp. 785–792, 2007.

[50] F. Gövert, J. S. Becktepe, and G. Deuschl, "Current concepts of essential tremor," *Revue Neurologique*, vol. 172, no. 8-9, pp. 416–422, 2016.

[51] J. F. Marsden, P. Brown, and S. Salenius, "Involvement of the sensorimotor cortex in physiological force and action tremor," *Neuroreport*, vol. 12, no. 9, pp. 1937–1941, 2001.

Hindawi
Neural Plasticity
Volume 2018, Article ID 5257285, 9 pages
https://doi.org/10.1155/2018/5257285

Review Article

Proton Pump Inhibitors and Dementia: Physiopathological Mechanisms and Clinical Consequences

Gloria Ortiz-Guerrero,[1] Diana Amador-Muñoz,[2] Carlos Alberto Calderón-Ospina,[3] Daniel López-Fuentes,[4] and Mauricio Orlando Nava Mesa[2]

[1]*Individualized Research Learner Program, Neuromuscular Research Division, University of Kansas Medical Center, 3901 Rainbow Blvd., Kansas City, KS 66160, USA*
[2]*Neuroscience (NEUROS) Research Group, School of Medicine and Health Sciences, Universidad del Rosario, Carrera 24 No. 63C–69, Bogotá 111221, Colombia*
[3]*Unidad de Farmacología, School of Medicine and Health Sciences, Universidad del Rosario, Carrera 24 No. 63C–69, Bogotá 111221, Colombia*
[4]*Medical Social Service, Hospital de San Francisco, Kra 8 No. 6A–121, Gacheta 251230, Colombia*

Correspondence should be addressed to Mauricio Orlando Nava Mesa; monavam@usal.es

Received 14 November 2017; Accepted 14 February 2018; Published 21 March 2018

Academic Editor: Francisco Lopera

Alzheimer's disease (AD) is the most common type of dementia, mainly encompassing cognitive decline in subjects aged ≥65 years. Further, AD is characterized by selective synaptic and neuronal degeneration, vascular dysfunction, and two histopathological features: extracellular amyloid plaques composed of amyloid beta peptide (Aβ) and neurofibrillary tangles formed by hyperphosphorylated tau protein. Dementia and AD are chronic neurodegenerative conditions with a complex physiopathology involving both genetic and environmental factors. Recent clinical studies have shown that proton pump inhibitors (PPIs) are associated with risk of dementia, including AD. However, a recent case-control study reported decreased risk of dementia. PPIs are a widely indicated class of drugs for gastric acid-related disorders, although most older adult users are not treated for the correct indication. Although neurological side effects secondary to PPIs are rare, several preclinical reports indicate that PPIs might increase Aβ levels, interact with tau protein, and affect the neuronal microenvironment through several mechanisms. Considering the controversy between PPI use and dementia risk, as well as both cognitive and neuroprotective effects, the aim of this review is to examine the relationship between PPI use and brain effects from a neurobiological and clinical perspective.

1. Introduction

Dementia is a clinical syndrome that represents a wide spectrum of cognitive dysfunction and leads to progressive and chronic deterioration of social and occupational activities. According to the World Alzheimer Report, over 46.8 million people worldwide lived with dementia in 2015, with a predicted increase of cases to 74.7 million by 2030 and 131.5 million by 2050. In addition, 63% and 68% of all people with dementia will live in low- and middle-income countries by 2030 and 2050, respectively [1]. Because of this increased number of cases, the high cost of dementia is another issue that health systems will be dealing with in the future. Currently, the cost is estimated at $18 billion per year in the US, with an increase expected over upcoming years. Owing to the economic and social impact caused by dementia, the World Health Organization designated dementia a public health priority [2]. There are different types of dementia, with Alzheimer's disease (AD) being the most prevalent in humans, accounting for 50–70% of all cases [3]. The prevalence rate for AD increases predominantly with age, surging from 3.5% in people aged 75 years old to 46.3% in people aged 95 years old or older [4]. The histopathological hallmarks of AD include extracellular deposition of amyloid-β (Aβ) plaques, formation of neurofibrillary tangles (NFTs) from hyperphosphorylated tau protein, and

neurodegeneration caused by progressive loss of neurons and their processes [5]. Moreover, the most accepted theory to explain the pathogenesis of AD is the amyloid hypothesis, which states that the cognitive disease phenotype is due to Aβ dyshomeostasis [6].

Proton pump inhibitors (PPIs) are a class of drugs used to treat gastric acid-related disorders, such as gastroesophageal reflux and peptic ulcer disease, and which act mainly as irreversible inhibitors of the H^+/K^+-ATPase pump to decrease gastric acid production [7]. PPIs have an excellent safety profile and have become one of the most prescribed drugs in recent years. According to the National Health and Nutrition Examination Survey, from 1999 to 2012, the percentage of adults aged 40–60 who received a prescription for PPIs almost doubled from 4.9% to 8.3% in the United States, surging concerns about their widespread use among this age group [8, 9]. Furthermore, various studies have shown that 50–70% of patients prescribed PPIs do not have the correct indication, especially in hospitalized elderly patients [10–12]. Overall, long-term use of PPIs has increased, leading to potential adverse effects such as nutritional deficiencies (vitamin B_{12}, magnesium, and iron), renal damage, osteoporotic fracture, infection by *Clostridium difficile*, rhabdomyolysis, anemia, and thrombocytopenia [13]. Because of these adverse effects, their safety and role in cognitive function (including risk of developing dementia and AD) have been questioned lately. Several studies described association between PPIs and greater risk of developing dementia and AD in older people [9, 14, 15]. However, other study has not shown that PPIs were associated with greater risk of dementia neither AD [7]. In addition, a recent case-control study conducted in German primary care patients reported decreased risk of dementia with PPI use [16]. In fact, neuroprotective effects of PPIs have been recently described [17, 18]. Due to these controversial findings, and also the role of PPIs in progression from mild to severe cognitive dysfunction, the aim of this article is to review the relationship between PPI use and basic mechanisms of neuronal dysfunction. In this regard, we discuss if PPI use is associated with greater susceptibility to developing dementia, focusing on a neurobiological basis of AD. Consequently, we propose new hypothesis regarding the physiopathological mechanisms of cognitive impairment induced by acute and chronic PPI use and examine some associated factors that increase dementia susceptibility after PPI exposure.

2. The Effect of PPIs on the Central Nervous System

One of the human genes encoding H^+/K^+-ATPase (ATP12A/ATP1AL1) is expressed in the brain, colon, and placenta, while the other gene (ATP4A) is only expressed in gastric epithelial cells [19]. Accordingly, there is evidence of H^+/K^+-ATPase activity in the central nervous system (CNS), with certain isoforms expressed [20]. Proton pumps have several physiological functions in neurons and contribute to acid–base and potassium homeostasis [19]. Vesicular proton pumps (H^+-ATPases or V-ATPases) create the proton gradient that is required for packaging of neurotransmitters into synaptic vesicles. Furthermore, new evidence indicates that vesicular H^+/K^+-ATPase plays an interesting role in both exocytosis and endocytosis in nerve terminals [21, 22]. Ca^{2+}-ATPase, Na^+/K^+-ATPase, and H^+/K^+-ATPase are included in the PII subfamily of P-type ATPases [23]. P-type ATPases share common structural motifs and likely arise from a common ancestral gene [19]. Interestingly, the primary structure of the α subunit of gastric H^+/K^+-ATPase is 98% homologous within species and highly homologous to the catalytic subunit of Na^+/K^+-ATPase (~63%) and sarcoplasmic/endoplasmic reticulum Ca^{2+}-ATPase (SERCA) (~25%) [24, 25].

Proton pump inhibitors (e.g., omeprazole, lansoprazole, dexlansoprazole, rabeprazole, pantoprazole, and esomeprazole) effectively block acid secretion by covalent and irreversible binding to H^+/K^+-ATPases on the luminal surface of the parietal cell membrane [26, 27]. The site of reaction on the enzyme differs according to the particular PPI. However, all PPIs react with cysteine 813 in the active E2 configuration (ion-site-out) [27]. Considering the high homology between P-type ATPases, it is possible that PPIs can inhibit other ionic pumps in different organs or even induce systemic physiological changes. Indeed, the CNS may be one system affected, with its interaction facilitated by pathological conditions exhibiting reduced pH in the brain, cerebrospinal fluid, and blood (i.e., metabolic stress).

Passage of PPIs through the blood-brain barrier (BBB) has been calculated. After administering 10 mg/kg intravenous (IV) omeprazole to male Sprague Dawley rats, the area under the curve (AUC) of concentration versus time in the brain divided by AUC in blood was calculated [28]. The resulting blood-to-brain distribution coefficient was 0.15, indicating that up to 15% of a single IV dose of omeprazole can reach the CNS and potentially affect cognitive function with either acute or repetitive long-term use. Corroboratively, *in vitro* and *in vivo* pharmacokinetic studies have shown that lansoprazole may also penetrate the BBB [29].

Some PPIs, such as lansoprazole, esomeprazole, and pantoprazole, are reported to cause adverse neurological effects, mainly headaches [30, 31] and dizziness/vertigo [32]. Other adverse effects that involve the CNS (at a frequency of <1%) include depression, diplopia, disturbed sleep, drowsiness, insomnia, nervousness, and tremor. There have also been reports of sensoperceptual abnormalities (i.e., hallucinations) [33, 34] and delirium [35]. Neurological side effects induced by chronic PPI use may be related to indirect systemic abnormalities (i.e., magnesium and vitamin B_{12} deficiency) [36] or direct effects on neurons after passage through the BBB. Although the exact mechanisms on brain circuits have not been fully described, most neurological side effects are reported with chronic administration of PPIs.

3. PPIs and Physiopathological Effects in Dementia

PPI drugs can facilitate tau and Aβ-induced neurotoxicity, which may increase AD progression and cognitive decline. Below, we discuss relevant physiopathological mechanisms.

3.1. PPIs and Aβ Plaques. One of the most described effects in dementia relates to increased production of Aβ plaques by PPIs [37]. As already stated, one of the major hallmarks of AD is extracellular accumulation of Aβ plaques, which lead to oxidative and inflammatory damage in the brain [3]. These Aβ species are produced by cleavage of amyloid precursor protein (APP) by β-secretase (also known as β-site APP-cleaving enzyme 1 [BACE1]) and γ-secretase [38]. Although the total number of Aβ plaques does not correlate well with AD severity, there is a direct effect on cognition and cell death in APP/tau transgenic mice because of neuronal loss and the astrocyte inflammatory response [39]. In 2013, Badiola et al. [37] investigated the effect of PPIs on Aβ production using cell and animal models and suggested a novel hypothesis: they suggested that PPIs act as inverse γ-secretase modulators (iGSM), which change the γ-secretase cleavage site and thereby increase Aβ42 levels and decrease Aβ38 levels. In addition, PPIs can increase BACE1 activity, raising production of Aβ37 and Aβ40 levels. In AD, the major pathological species is thought to be Aβ42, but the most produced is Aβ40 [38]. Ultimately, PPIs (specifically lansoprazole) may alter media pH, amplifying the activity of other proteases, such as memprin-β, and generating Aβ2-x peptides (e.g., Aβ2-37, Aβ2-40, and Aβ2-42 species). Moreover, Badiola et al. were able to demonstrate that lansoprazole enhances Aβ production using *in vivo* and *in vitro* models, supporting the theory that PPIs effect AD by boosting Aβ production [37]. It has also been shown that PPIs can inhibit vacuolar proton pumps, which acidify lysosomes by pumping protons from the cytoplasm to the lumen of vacuoles in microglia and macrophages [40, 41]. Normally, this acid environment in lysosomes permits degradation of fibrillary Aβ. As PPIs can cross the BBB, they act on V-ATPases in an inhibitory manner, causing less degradation of fibrillary Aβ and hence a reduction in its clearance [28, 41]. To date, there are few studies that explain the relationship between the effects of PPIs and presence of Aβ plaques. It would be interesting if future studies determine why Aβ plaque production increases or their clearance decreases with PPI use.

3.2. PPIs and Tau Protein. Currently, AD diagnosis is based on neuropsychological tests (cognitive criteria), neuroimaging (i.e., MRI and amyloid deposits by PET), and tau/amyloid in CSF (biomarker criteria) that rule out other causes of dementia [42–44]. However, a definitive diagnosis can only be confirmed histopathologically by the extensive presence of Aβ and NFTs in the neocortex of postmortem brain tissue [45]. The main component of NFTs is paired helical filaments (PHFs) formed from hyperphosphorylated tau protein [46, 47]. Tau protein plays an important role as a microtubule-associated protein in neuronal axons, stabilizing microtubules and inducing their assembly [48]. When tau protein is hyperphosphorylated, it is unable to bind and stabilize microtubules, which leads to degeneration of affected neurons [49]. According to the neuroimmunomodulation theory of AD, the earliest CNS changes before the clinical onset of AD result from a chronic inflammatory response, which leads to abnormal tau phosphorylation and induces formation of PHFs and tau protein aggregates, ultimately resulting in cytoskeletal alterations [50]. Consequently, these lesions are present before the presentation of clinical symptoms of AD [51]. The first NFT lesion appears in the transentorhinal cortex and is proceeded by the entorhinal cortex and hippocampus and finally the neocortex [52]. Several studies have shown that NFTs correlate with cognitive decline and severity in AD, positioning tau NFTs as suitable targets for therapy and diagnosis in AD patients. Several researchers have focused on developing different radiotracer components based on their high affinity for tau protein. This will allow future quantification of tau burden using noninvasive diagnostic imaging such as positron emission tomography (PET) [53]. Okamura and coworkers have found that PPIs show high affinity to tau protein. They screened more than 2000 compounds to develop agents for use in PET and identified quinoline and benzimidazole as high affinity components of NFTs rather than senile plaques [51]. Subsequently, Rojo and colleagues found that lansoprazole, a Food and Drug Administration- (FDA-) approved PPI with a benzimidazole ring structure, had nanomolar binding affinity for tau aggregates, in agreement with Okamura's findings. They also showed that lansoprazole has high lipophilicity and can cross the BBB, reaching the brain within 37 min after administration and therefore showing suitability as a radiotracer for PET imaging. However, during kinetic analysis, lansoprazole interactions with tau NFTs did not fit the classical one-site or two-site binding models [29]. We hypothesize that this can be explained by the six tau protein isoforms expressed in the human CNS. These tau isoforms are divided into two sets with three (3R) and four (4R) microtubule-binding domains. In usual conditions, both sets of isoforms are expressed in an equal ratio, while under pathological conditions, different tauopathies show different isoform ratios with diverse morphologies [54]. Additionally, tau undergoes multiple posttranslational changes resulting in conformational modifications in aggregates, as well as alterations in binding affinities and binding sites of tau protein [55]. Further, Rojo et al. performed docking studies and identified strong hydrogen bond interactions between the NH group of the benzimidazole ring of lansoprazole and the C-terminal hexapeptide (386TDHGAE391) of the tau core [29]. Corroboratively, studies by Fawaz and coworkers determined that replacing the NH group of the benzimidazole ring affected tau protein affinity, which has enabled development of new radiotracers with higher affinities, such as [18F]N-methyl lansoprazole [53]. This research field is based on the study of lansoprazole, and indeed its high affinity to tau protein is a striking and open avenue for researchers to create and improve noninvasive techniques for diagnosing AD in the early stages. Many of these studies are still in preclinical or early clinical trial stages. Further investigations are needed to specifically understand PPI interactions with tau protein.

3.3. PPIs and Vitamin B_{12} Deficiency. Gastric acidity is necessary for absorption of vitamin B_{12}, which is an essential water-soluble vitamin obtained from different dietary sources such as fish, meat, dairy products, and fortified cereal [56]. Statistically, approximately 6–20% of American adults have vitamin B_{12} deficiency, likely as a natural phenomenon.

Nonetheless, the risk of B_{12} deficiency increases with age [57]. During digestion, vitamin B_{12} binds to salivary R proteins and then to intrinsic factors, reaching the whole intestine and ileum terminal intact, where B_{12} absorption occurs. B_{12} is firmly bound to proteins and consequently requires acid-activated proteolytic digestion. Use of PPIs causes hypochlorhydria, which results in vitamin B_{12} malabsorption as B_{12} remains tightly bound to proteins in the stomach [58]. Several studies have shown controversial results between long-term PPI use and vitamin B_{12} deficiency. For instance, in a case-control study, patients treated with PPIs for 2 years or longer showed a statistically significant association with increased risk of B_{12} deficiency [59]. In contrast, in a cross-sectional study, patients prescribed PPIs for 3 years or longer had similar B_{12} levels as non-PPI users [60]. It is important to note that most of these trials show association and not causation. Likely, other factors will contribute to these findings in addition to acid-suppressive therapy [61].

Vitamin B_{12} deficiency caused by PPI use has been associated with dementia and cognitive impairment [62]. Vitamin B_{12} is required for one-carbon transfer reactions such as methylation, which are needed for processing and production of nucleotides, phospholipids, and monoamine neurotransmitters [63]. Usually, vitamin B_{12} removes a methyl group from tetrahydrofolate, turning it into methylcobalamin. Methylcobalamin then presents its methyl group to homocysteine, which is finally converted to methionine by methionine synthase [62]. Thus, vitamin B_{12} deficiency is one of the main causes of hyperhomocysteinemia. Both hyperhomocysteinemia and B_{12} deficiency are considered risk factors for brain atrophy, cognitive impairment, and dementia [64]. Studies have shown that hyperhomocysteinemia may activate several protein kinases, such as glycogen synthase kinase 3β (GSK-3β), cyclin-dependent kinase-5 (Cdk-5), c-Jun N-terminal kinase (JNK), extracellular signal-regulated kinase (ERK), and p38 mitogen-activated protein kinase (MAPK), and inhibit protein phosphatase 2A (PP2A) (41), which are all pivotal enzymes in regulating the phosphorylation state of tau protein [65]. Among these enzymes, PP2A plays a crucial role as it is the main brain serine/threonine phosphatase and prevents tau hyperphosphorylation [66]. Decreased methylation may affect PP2A function by leading to hyperphosphorylation and aggregation of tau protein [62]. In animal models, aside from inducing tau protein hyperphosphorylation, hyperhomocysteinemia can increase Aβ production, while folate/vitamin B_{12} supplementation may attenuate these effects [67–69]. Based on these findings, high homocysteine levels are a strong and independent risk factor for developing AD [70]. Alternative mechanisms for linking AD with vitamin B_{12} deficiency have also been described, which are distinct from PP2A inactivation and tau hyperphosphorylation. Using the structure and function of vitamin B_{12} inside cells, Rafiee and colleagues (38) [62] studied direct binding between B_{12} and tau protein *in vitro* by fluorometry and circular dichroism. Because vitamin B_{12} can interact with thiol groups, they determined that cobalamin can directly bind to tau via cysteine residues on tau protein. Hence, the resulting B_{12}/tau protein complex prevents tau protein fibrillation. Besides, tau aggregation is inhibited by vitamin B_{12} capping on cysteine residues of tau. In summary, the effect exerted on neurodegeneration by vitamin B_{12} deficiency and hyperhomocysteinemia is not only due to PP2A inactivation and tau hyperphosphorylation but also direct binding of vitamin B_{12} to tau protein, inhibiting its fibrillation and aggregation [62].

Although different mechanisms have been described to explain the effects of vitamin B_{12} deficiency in dementia, more clinical trials are needed to understand this relationship. In addition, more studies are required to establish if vitamin B_{12} deficiency is a causal event in dementia or an associated factor, as shown in other studies.

4. PPIs and Antineurotoxicity

In contrast to the effect of PPIs on Aβ plaque production, tau protein, and vitamin B_{12} deficiency in AD development, different studies have shown antineurotoxic effects of PPIs on astrocytes and microglia [17]. In AD patients, activated astrocytes exist in close relationship with senile plaques and neuronal degeneration [71]. These activated cells release powerful neurotoxic products, including proinflammatory cytokines, reactive oxygen species, and nitric oxide [72, 73]. Although astrocytes show neuroprotective activity, activated astrocytes may aggravate neurodegenerative diseases [74]. Hashioka et al. [17] demonstrated that lansoprazole and omeprazole decrease interferon- (IFN-) γ-induced astrocytic neurotoxicity as a result of inhibition of signal transducer and activator of transcription 3 (STAT3) activation. They also confirmed that PPIs slightly reduce production of T-cell alpha chemoattractant (I-TAC) by IFN-γ-activated astrocytes, although only lansoprazole shows a significant effect. These findings are in agreement with another study by Hashioka et al. [18] showing that lansoprazole and omeprazole may suppress tumor necrosis factor- (TNF-) α production from THP-1 cells and decrease human microglial and monocyte neurotoxicity. In addition, they showed that nonsteroidal anti-inflammatory drugs (NSAID) can increase antineurotoxic effect of PPIs due to their synergic effect. Furthermore, a recent study identified lansoprazole as a liver X receptor (LXR) agonist [75]. LXRs are transcription factors that modify expression of genes related to cholesterol metabolism. Hence, lansoprazole increases ATP-binding cassette transporter (Abca1) and apolipoprotein- (Apo-) E levels in primary astrocytes, both genes regulated by LXR [75]. Moreover, ApoE lipid complexes mediated by ABCA1 inhibit Aβ plaque aggregation, thereby supporting the theory that lansoprazole can act as a therapeutic agent in AD [17].

5. Clinical Association between PPIs and Risk of Dementia, AD, and Cognitive Impairment

Based on a systematic review from 2017, four European observational studies have investigated association between PPI use and dementia. Three studies have found a positive association between dementia and omeprazole, esomeprazole, lansoprazole, and pantropazole, with an approximately 1.4-fold increased risk of any dementia in cohorts using PPIs

(95% CI, 1.36–1.52; $P < 0.001$) [76]. Similarly, in a recent prospective cohort study in Asian population ($n = 15726$, 7863 PPI users), an association with dementia has been found (aHR, 1.22; 95% confidence interval, 1.05–1.42) [15]. In contrast, the fourth European report included in the systematic review found a negative association (OR dementia with PPI use = 0.94 (95% CI, 0.90–0.97) $P = 0.0008$) [76]. Herghelegiu and colleagues [77] conducted a single-center case-control study that compared 148 PPI users (aged at least 65 years old) with a control group of nonusers during an 8-month period. They confirmed statistically significant association between PPI use and dementia. However, bias was influenced by the small study sample. Further, they did not take into account fundamental cofounders such as age, sex, history of stroke, and smoking status, which are considered risk factors for dementia. Conversely, Booker and coworkers [16] found statistically significant reduction between dementia and PPI use with a case-control study using a database of general practice medical records in Germany and including 11,956 patients with initial dementia diagnoses over a 4-year period. This study was considered to have a moderate risk of bias due to codes being entered by general practitioners. The other two cohort studies performed by Haenisch et al. and Gomm et al. [9, 14] used data from two different German databases (KNDD and AgeCoDe, resp.) which reported positive association between PPI use and dementia. Although both studies included a wide range of cofounders, neither took into account either hypertension or family history of dementia (again well-known risk factors for dementia) nor sugar intake, physical exercise, or air pollution, recently considered risk factors for dementia [76]. In contrast, Haenisch et al. [14] performed the only study to include a subgroup for evaluating AD risk. Their results were in favor of elevated risk for AD associated with PPI use. Besides, exclusion of cofounders (such as age, sex, education, ApoE4 allele status, polypharmacy, depression, ischemic heart disease, and stroke) did not influence the effect of PPI use on AD.

In the same systematic review, weak association between PPI use and acute cognitive impairment was demonstrated in a series of case reports and small observational studies [76]. Regarding these, four were hypomagnesemia-associated delirium or confusion cases [78, 79], one was associated with hyponatremic delirium [80], and one was delirium of unknown cause [35]. PPIs were implied as a main cause in these effects because they can lower magnesium and sodium levels, and the majority of studies were associated with omeprazole use [35, 78, 80]. In one case, withdrawing esomeprazole therapy provided symptomatic relief and reestablishment of magnesium levels [78]. With these observational studies, data on PPI use and risk of delirium was incorporated [81, 82]. For instance, Otremba and coworkers performed a cross-sectional study, including 675 patients of 60–100 years old, who were admitted to a subacute geriatric ward over a 12-month period. They found that PPI use was a predictive factor for developing delirium in these patients. The Confusion Assessment Method and Delirium-O-Meter were the scales used for diagnosing delirium and its severity, respectively [82]. However, Fujii and coworkers, who compared incidence and severity of delirium in H(2) blocker users and PPI users, found that delirium can be reduced by switching H(2) blockers to PPIs [81]. However, there are major difficulties in evaluating these studies as the data does not contain reliable information. Also, the majority of studies used different group characteristics, which makes comparisons among them challenging [76].

Other studies have focused on short-term PPI use and its influence on different cognitive functions. For instance, Akter et al. used the Cambridge Neuropsychological Test Automated Battery (the well-known CANTAB software) to evaluate each PPI and its effect in different cognitive domain functions of young patients (20–26 years old) over 7 days [12]. CANTAB software can accurately determine amyloid-related cognitive decline and quantify the severity of impairment in prodromal AD patients [83]. This study found that taking different PPIs may influence several degrees of cognitive capacity. For instance, omeprazole led to deterioration of visual and episodic memory, motor and mental response speed, new learning, short-term and sustained attention, retention and manipulation of visuospatial information, and strategy development [12]. Lansoprazole, in addition to the mentioned effects of omeprazole, can restrict manipulation of remembered memory to generate a complex task or strategy and also limit retention of spatial information. Contrary to lansoprazole and omeprazole, esomeprazole induced difficulties in maintaining sustained attention, retaining and manipulating spatial memory, and planning strategy [12]. In contrast, a very recent study including data from the Nurses' Health Study II has not shown association between PPI use and cognitive dysfunction or dementia risk. However, this study indicates a modest association for psychomotor speed and attention among PPI users [84]. To explain some acute and chronic cognitive effects, it is possible that PPIs may preferentially affect the hippocampus and associative neocortex via a neuroplasticity mechanism. Still to our knowledge, there is no evidence of *in vivo* or *in vitro* experiments using long-term potentiation protocols to confirm this theory.

6. Final Considerations and Conclusion

There is currently no consensus on the role of PPIs and the associated risk of developing dementia. Because of the multifactorial origin of dementia (Alzheimer–vascular spectrum dementia), future studies are required to consider associated environmental and genetic factors, as well as biomarkers (i.e., APOE-ε4) and other covariates (i.e., chronic stress) that may increase the risk of dementia in patients who consume PPIs. It is possible that the cognitive effects of PPIs are due to drug interactions, especially in polymedicated elderly patients. For instance, omeprazole may increase blood levels of diazepam (a γ-aminobutyric acid [GABA]-A agonist) by decreasing plasma clearance (via cytochrome P450) and then increasing neurological side effects [85]. In a retrospective study in six residential care homes in England ($n = 133$), it was found that 9.2% of older people with dementia were prescribed with two or more

potentially inappropriate medications, including PPIs and long-acting benzodiazepines [86]. In addition, an FDA study has shown that some adverse events with PPIs (including omeprazole, lansoprazole, and pantoprazole) could be associated with benzodiazepine drug interactions [87]. As long-term benzodiazepine use might increase dementia risk [88, 89], it is possible that combined treatment of GABA-A agonists and PPIs may increase this susceptibility, considering the close association between GABAergic system dysfunction and the physiopathology of AD and mild cognitive impairment [90]. In fact, cognitive impairment has been reported after lorazepam treatment in patients with higher risk for AD (APOE-ε4 allele carriers) [91]. At recommended doses, a pharmacokinetic interaction between benzodiazepines and PPIs is less probable with pantoprazole, lansoprazole, and rabeprazole than with omeprazole [92–94]. Accordingly, those PPI drugs might be considered in polymedicated subjects.

Cumulative evidence indicates that chronic treatment with NSAIDs (e.g., ibuprofen) may delay AD onset and reduce AD rate of progression [95, 96]. As mentioned earlier, *in vitro* evidence indicates that PPIs might have neuroprotective and anti-inflammatory effects that act synergistically with NSAIDs. Some limitations of *in vitro* studies include the experimental duration, as well as complex specific microenvironment factors observed only *in vivo* [97]. In fact, dementia and AD are chronic neurodegenerative diseases with a complex physiopathology and several compensatory neuronal-glial mechanisms after long-term Aβ peptide exposure. To simulate environmental cellular conditions of AD, it is necessary to design durable *in vitro* studies that involve persistent oxidative stress and metabolic dysfunction.

Vascular and BBB dysfunctions have been observed in AD patients [98]. Taking into account age-related changes of BBB function, as well as vulnerability to disruption by external factors such as hypertension and drugs [99, 100], we suggest that neurological susceptibility to PPIs may be related to changes in BBB permeability, as well as changes in the brain microenvironment related to aging. However, more studies are necessary to identify other factors that contribute to this susceptibility.

Although the mechanisms of brain dysfunction induced by PPIs are not known with certainty, it is possible they influence ionic pumps controlling the membrane potential and electrochemical gradient in neurons. Considering the preferential effects of PPIs on Aβ and tau protein, as well as on endothelial function, further studies are needed to contemplate differential susceptibility between AD and vascular dementia. Taking into account the effects of PPIs on vitamin B_{12} levels, and possibly indirect effects on membrane ionic transporters, nutritional and electrolyte monitoring is required in patients who chronically use PPIs, mainly older adults and patients with chronic malnutrition or debilitating chronic conditions. Also, it is necessary to determine the previous cognitive status of patients and whether they have risk factors for dementia, as well as pharmacokinetic drug interactions. Altogether, it is necessary to consider the risk–benefit of chronic PPI use and, above all, strictly establish an adequate therapeutic indication.

Conflicts of Interest

The authors declare that they have no conflicts of interest.

Acknowledgments

The authors thank Rachel James, Ph.D., from Edanz Group (http://www.edanzediting.com/ac) for editing a draft of this manuscript. This work was supported by the Universidad del Rosario (Bogotá, Colombia).

References

[1] M. Prince, A. Wimo, M. Guerchet, G. Claire Ali, Y.-T. Wu, and M. Prina, *World Alzheimer Report 2015: the Global Impact of Dementia: an Analysis of Prevalence, Incidence, Cost and Trends*, Alzheimer's Disease International (ADI), London, 2015.

[2] World Health Organization, *Dementia: a Public Health Priority. World Health Organization*, World Health Organization, Geneva, 2012.

[3] H. W. Querfurth and F. M. LaFerla, "Alzheimer's disease," *The New England Journal of Medicine*, vol. 362, no. 4, pp. 329–344, 2010.

[4] N. Matyas, S. Auer, C. Gisinger et al., "Continuing education for the prevention of mild cognitive impairment and Alzheimer's-type dementia: a systematic review protocol," *Systematic Reviews*, vol. 6, no. 1, p. 157, 2017.

[5] P. S. Aisen, J. Cummings, C. R. Jack et al., "On the path to 2025: understanding the Alzheimer's disease continuum," *Alzheimer's Research & Therapy*, vol. 9, no. 1, p. 60, 2017.

[6] D. J. Selkoe and J. Hardy, "The amyloid hypothesis of Alzheimer's disease at 25 years," *EMBO Molecular Medicine*, vol. 8, no. 6, pp. 595–608, 2016.

[7] F. C. Goldstein, K. Steenland, L. Zhao, W. Wharton, A. I. Levey, and I. Hajjar, "Proton pump inhibitors and risk of mild cognitive impairment and dementia," *Journal of the American Geriatrics Society*, vol. 65, no. 9, pp. 1969–1974, 2017.

[8] E. D. Kantor, C. D. Rehm, J. S. Haas, A. T. Chan, and E. L. Giovannucci, "Trends in prescription drug use among adults in the United States from 1999-2012," *JAMA*, vol. 314, no. 17, pp. 1818–1831, 2015.

[9] W. Gomm, K. von Holt, F. Thomé et al., "Association of proton pump inhibitors with risk of dementia: a pharmacoepidemiological claims data analysis," *JAMA Neurology*, vol. 73, no. 4, pp. 410–416, 2016.

[10] J. J. Heidelbaugh and J. M. Inadomi, "Magnitude and economic impact of inappropriate use of stress ulcer prophylaxis in non-ICU hospitalized patients," *The American Journal of Gastroenterology*, vol. 101, no. 10, pp. 2200–2205, 2006.

[11] S. M. Eid, A. Boueiz, S. Paranji, C. Mativo, R. Landis, and M. S. Abougergi, "Patterns and predictors of proton pump inhibitor overuse among academic and non-academic hospitalists," *Internal Medicine*, vol. 49, no. 23, pp. 2561–2568, 2010.

[12] S. Akter, M. R. Hassan, M. Shahriar, N. Akter, M. G. Abbas, and M. A. Bhuiyan, "Cognitive impact after short-term exposure to different proton pump inhibitors: assessment using CANTAB software," *Alzheimer's Research & Therapy*, vol. 7, no. 1, p. 79, 2015.

[13] L. Y. Yu, L. N. Sun, X. H. Zhang et al., "A review of the novel application and potential adverse effects of proton pump inhibitors," *Advances in Therapy*, vol. 34, no. 5, pp. 1070–1086, 2017.

[14] B. Haenisch, K. von Holt, B. Wiese et al., "Risk of dementia in elderly patients with the use of proton pump inhibitors," *European Archives of Psychiatry and Clinical Neuroscience*, vol. 265, no. 5, pp. 419–428, 2015.

[15] S.-Y. Tai, C.-Y. Chien, D.-C. Wu et al., "Risk of dementia from proton pump inhibitor use in Asian population: a nationwide cohort study in Taiwan," *PLoS One*, vol. 12, no. 2, article e0171006, 2017.

[16] A. Booker, L. E. Jacob, M. Rapp, J. Bohlken, and K. Kostev, "Risk factors for dementia diagnosis in German primary care practices," *International Psychogeriatrics*, vol. 28, no. 7, pp. 1059–1065, 2016.

[17] S. Hashioka, A. Klegeris, and P. L. McGeer, "Proton pump inhibitors reduce interferon-γ-induced neurotoxicity and STAT3 phosphorylation of human astrocytes," *Glia*, vol. 59, no. 5, pp. 833–840, 2011.

[18] S. Hashioka, A. Klegeris, and P. L. McGeer, "Proton pump inhibitors exert anti-inflammatory effects and decrease human microglial and monocytic THP-1 cell neurotoxicity," *Experimental Neurology*, vol. 217, no. 1, pp. 177–183, 2009.

[19] I. R. Driel and J. M. Callaghan, "Proton and potassium transport by H^+/K^+-ATPases," *Clinical and Experimental Pharmacology and Physiology*, vol. 22, no. 12, pp. 952–960, 1995.

[20] N. N. Modyanov, K. E. Petrukhin, V. E. Sverdlov et al., "The family of human Na, K-ATPase genes. *ATP1AL1* gene is transcriptionally competent and probably encodes the related ion transport ATPase," *FEBS Letters*, vol. 278, no. 1, pp. 91–94, 1991.

[21] D. Wang and P. R. Hiesinger, "The vesicular ATPase: a missing link between acidification and exocytosis," *The Journal of Cell Biology*, vol. 203, no. 2, pp. 171–173, 2013.

[22] L. Tabares and B. Betz, "Multiple functions of the vesicular proton pump in nerve terminals," *Neuron*, vol. 68, no. 6, pp. 1020–1022, 2010.

[23] M. Bublitz, H. Poulsen, J. P. Morth, and P. Nissen, "In and out of the cation pumps: P-type ATPase structure revisited," *Current Opinion in Structural Biology*, vol. 20, no. 4, pp. 431–439, 2010.

[24] K. J. Sweadner and C. Donnet, "Structural similarities of Na, K-ATPase and SERCA, the Ca2+-ATPase of the sarcoplasmic reticulum," *The Biochemical Journal*, vol. 356, no. 3, pp. 685–704, 2001.

[25] F. Jaisser, J. D. Horisberger, K. Geering, and B. C. Rossier, "Mechanisms of urinary K+ and H+ excretion: primary structure and functional expression of a novel H, K-ATPase," *The Journal of Cell Biology*, vol. 123, no. 6, pp. 1421–1429, 1993.

[26] J. M. Shin and N. Kim, "Pharmacokinetics and pharmacodynamics of the proton pump inhibitors," *Journal of Neurogastroenterology and Motility*, vol. 19, no. 1, pp. 25–35, 2013.

[27] J. M. Shin, K. Munson, O. Vagin, and G. Sachs, "The gastric HK-ATPase: structure, function, and inhibition," *Pflugers Archiv: European Journal of Physiology*, vol. 457, no. 3, pp. 609–622, 2009.

[28] F. C. Cheng, Y. F. Ho, L. C. Hung, C. F. Chen, and T. H. Tsai, "Determination and pharmacokinetic profile of omeprazole in rat blood, brain and bile by microdialysis and high-performance liquid chromatography," *Journal of Chromatography A*, vol. 949, no. 1-2, pp. 35–42, 2002.

[29] L. E. Rojo, J. Alzate-Morales, I. N. Saavedra, P. Davies, and R. B. Maccioni, "Selective interaction of lansoprazole and astemizole with tau polymers: potential new clinical use in diagnosis of Alzheimer's disease," *Journal of Alzheimer's Disease*, vol. 19, no. 2, pp. 573–589, 2010.

[30] J.-F. Liang, Y.-T. Chen, J.-L. Fuh et al., "Proton pump inhibitor-related headaches: a nationwide population-based case-crossover study in Taiwan," *Cephalalgia*, vol. 35, no. 3, pp. 203–210, 2014.

[31] R. M. Martin, N. R. Dunn, S. Freemantle, and S. Shakir, "The rates of common adverse events reported during treatment with proton pump inhibitors used in general practice in England: cohort studies," *British Journal of Clinical Pharmacology*, vol. 50, no. 4, pp. 366–372, 2000.

[32] S. Chimirri, R. Aiello, C. Mazzitello et al., "Vertigo/dizziness as a drugs' adverse reaction," *Journal of Pharmacology & Pharmacotherapeutics*, vol. 4, no. 5, pp. 104–109, 2013.

[33] J. J. Sebastian Domingo, "Omeprazole-induced hallucinations. Not as rare as you might think," *Gastroenterología y Hepatología*, vol. 41, no. 3, 2017.

[34] A. M. Hanneken, N. Babai, and W. B. Thoreson, "Oral proton pump inhibitors disrupt horizontal cell-cone feedback and enhance visual hallucinations in macular degeneration patients," *Investigative Ophthalmology & Visual Science*, vol. 54, no. 2, pp. 1485–1489, 2013.

[35] J. G. Heckmann, F. Birklein, and B. Neundörfer, "Omeprazole-induced delirium," *Journal of Neurology*, vol. 247, no. 1, pp. 56-57, 2000.

[36] C. de la Coba Ortiz, F. Argüelles Arias, C. Martín de Argila de Prados et al., "Proton-pump inhibitors adverse effects: a review of the evidence and position statement by the Sociedad Española de Patología Digestiva," *Revista Española de Enfermedades Digestivas*, vol. 108, no. 4, pp. 207–224, 2016.

[37] N. Badiola, V. Alcalde, A. Pujol et al., "The proton-pump inhibitor lansoprazole enhances amyloid beta production," *PLoS One*, vol. 8, no. 3, article e58837, 2013.

[38] S. G. Younkin, "The role of Aβ42 in Alzheimer's disease," *Journal of Physiology-Paris*, vol. 92, no. 3-4, pp. 289–292, 1998.

[39] B. DaRocha-Souto, T. C. Scotton, M. Coma et al., "Brain oligomeric β-amyloid but not total amyloid plaque burden correlates with neuronal loss and astrocyte inflammatory response in amyloid precursor protein/tau transgenic mice," *Journal of Neuropathology & Experimental Neurology*, vol. 70, no. 5, pp. 360–376, 2011.

[40] M. K. Fallahzadeh, A. Borhani Haghighi, and M. R. Namazi, "Proton pump inhibitors: predisposers to Alzheimer disease?," *Journal of Clinical Pharmacy and Therapeutics*, vol. 35, no. 2, pp. 125-126, 2010.

[41] M. R. Namazi and F. Jowkar, "A succinct review of the general and immunological pharmacologic effects of proton pump inhibitors," *Journal of Clinical Pharmacy and Therapeutics*, vol. 33, no. 3, pp. 215–217, 2008.

[42] P. J. Visser, S. Vos, I. van Rossum, and P. Scheltens, "Comparison of International Working Group criteria and National Institute on Aging–Alzheimer's Association criteria for Alzheimer's disease," *Alzheimer's & Dementia*, vol. 8, no. 6, pp. 560–563, 2012.

[43] G. M. McKhann, D. S. Knopman, H. Chertkow et al., "The diagnosis of dementia due to Alzheimer's disease: recommendations from the National Institute on Aging-Alzheimer's Association workgroups on diagnostic guidelines for Alzheimer's disease," *Alzheimer's & Dementia*, vol. 7, no. 3, pp. 263–269, 2011.

[44] M. C. Carrillo, R. A. Dean, F. Nicolas et al., "Revisiting the framework of the National Institute on Aging-Alzheimer's Association diagnostic criteria," *Alzheimer's & Dementia*, vol. 9, no. 5, pp. 594–601, 2013.

[45] D. Dawbarn and S. J. Allen, *Neurobiology of Alzheimer's Disease*, Bios Scientific, Oxford, 1995.

[46] G. A. Farías, C. Vial, and R. B. Maccioni, "Specific macromolecular interactions between tau and the microtubule system," *Molecular and Cellular Biochemistry*, vol. 112, no. 1, pp. 81–88, 1992.

[47] K. S. Kosik, C. L. Joachim, and D. J. Selkoe, "Microtubule-associated protein tau (tau) is a major antigenic component of paired helical filaments in Alzheimer disease," *Proceedings of the National Academy of Sciences of the United States of America*, vol. 83, no. 11, pp. 4044–4048, 1986.

[48] R. B. Maccioni and V. Cambiazo, "Role of microtubule-associated proteins in the control of microtubule assembly," *Physiological Reviews*, vol. 75, no. 4, pp. 835–864, 1995.

[49] M. L. Billingsley and R. L. Kincaid, "Regulated phosphorylation and dephosphorylation of tau protein: effects on microtubule interaction, intracellular trafficking and neurodegeneration," *The Biochemical Journal*, vol. 323, no. 3, Part 3, pp. 577–591, 1997.

[50] L. E. Rojo, J. A. Fernández, A. A. Maccioni, J. M. Jimenez, and R. B. Maccioni, "Neuroinflammation: implications for the pathogenesis and molecular diagnosis of Alzheimer's disease," *Archives of Medical Research*, vol. 39, no. 1, pp. 1–16, 2008.

[51] N. Okamura, T. Suemoto, S. Furumoto et al., "Quinoline and benzimidazole derivatives: candidate probes for *in vivo* imaging of tau pathology in Alzheimer's disease," *The Journal of Neuroscience*, vol. 25, no. 47, pp. 10857–10862, 2005.

[52] H. Braak and E. Braak, "Neuropathological stageing of Alzheimer-related changes," *Acta Neuropathologica*, vol. 82, no. 4, pp. 239–259, 1991.

[53] M. V. Fawaz, A. F. Brooks, M. E. Rodnick et al., "High affinity radiopharmaceuticals based upon lansoprazole for PET imaging of aggregated tau in Alzheimer's disease and progressive supranuclear palsy: synthesis, preclinical evaluation, and lead selection," *ACS Chemical Neuroscience*, vol. 5, no. 8, pp. 718–730, 2014.

[54] V. L. Villemagne and N. Okamura, "Tau imaging in the study of ageing, Alzheimer's disease, and other neurodegenerative conditions," *Current Opinion in Neurobiology*, vol. 36, pp. 43–51, 2016.

[55] M. G. Spillantini and M. Goedert, "Tau pathology and neurodegeneration," *The Lancet Neurology*, vol. 12, no. 6, pp. 609–622, 2013.

[56] R. Oh and D. L. Brown, "Vitamin B_{12} deficiency," *American Family Physician*, vol. 67, no. 5, pp. 979–986, 2003.

[57] A. Hunt, D. Harrington, and S. Robinson, "Vitamin B_{12} deficiency," *BMJ*, vol. 349, article g5226, 2014.

[58] V. Savarino, P. Dulbecco, and E. Savarino, "Are proton pump inhibitors really so dangerous?," *Digestive and Liver Disease*, vol. 48, no. 8, pp. 851–859, 2016.

[59] J. R. Lam, J. L. Schneider, W. Zhao, and D. A. Corley, "Proton pump inhibitor and histamine 2 receptor antagonist use and vitamin B_{12} deficiency," *JAMA*, vol. 310, no. 22, pp. 2435–2442, 2013.

[60] L. Lombardo, M. Foti, O. Ruggia, and A. Chiecchio, "Increased incidence of small intestinal bacterial overgrowth during proton pump inhibitor therapy," *Clinical Gastroenterology and Hepatology*, vol. 8, no. 6, pp. 504–508, 2010.

[61] L. Linder, C. Tamboue, and J. N. Clements, "Drug-induced vitamin B_{12} deficiency: a focus on proton pump inhibitors and histamine-2 antagonists," *Journal of Pharmacy Practice*, vol. 30, no. 6, pp. 639–642, 2017.

[62] S. Rafiee, K. Asadollahi, G. Riazi, S. Ahmadian, and A. A. Saboury, "Vitamin B12 inhibits tau fibrillization via binding to cysteine residues of tau," *ACS Chemical Neuroscience*, vol. 8, no. 12, pp. 2676–2682, 2017.

[63] B. W. Penninx, J. M. Guralnik, L. Ferrucci, L. P. Fried, R. H. Allen, and S. P. Stabler, "Vitamin B_{12} deficiency and depression in physically disabled older women: epidemiologic evidence from the Women's Health and Aging Study," *The American Journal of Psychiatry*, vol. 157, no. 5, pp. 715–721, 2000.

[64] F. Ma, T. Wu, J. Zhao et al., "Plasma homocysteine and serum folate and vitamin B_{12} levels in mild cognitive impairment and Alzheimer's disease: a case-control study," *Nutrients*, vol. 9, no. 12, 2017.

[65] E. M. Mandelkow and E. Mandelkow, "Biochemistry and cell biology of tau protein in neurofibrillary degeneration," *Cold Spring Harbor Perspectives in Medicine*, vol. 2, no. 7, article a006247, 2012.

[66] T. Bottiglieri, E. Arning, B. Wasek, V. Nunbhakdi-Craig, J. M. Sontag, and E. Sontag, "Acute administration of L-DOPA induces changes in methylation metabolites, reduced protein phosphatase 2A methylation, and hyperphosphorylation of tau protein in mouse brain," *The Journal of Neuroscience*, vol. 32, no. 27, pp. 9173–9181, 2012.

[67] W. Wei, Y. H. Liu, C. E. Zhang et al., "Folate/vitamin-B12 prevents chronic hyperhomocysteinemia-induced tau hyperphosphorylation and memory deficits in aged rats," *Journal of Alzheimer's Disease*, vol. 27, no. 3, pp. 639–650, 2011.

[68] C. E. Zhang, Q. Tian, W. Wei et al., "Homocysteine induces tau phosphorylation by inactivating protein phosphatase 2A in rat hippocampus," *Neurobiology of Aging*, vol. 29, no. 11, pp. 1654–1665, 2008.

[69] C. E. Zhang, W. Wei, Y. H. Liu et al., "Hyperhomocysteinemia increases β-amyloid by enhancing expression of γ-secretase and phosphorylation of amyloid precursor protein in rat brain," *The American Journal of Pathology*, vol. 174, no. 4, pp. 1481–1491, 2009.

[70] G. Ravaglia, P. Forti, F. Maioli et al., "Homocysteine and folate as risk factors for dementia and Alzheimer disease," *The American Journal of Clinical Nutrition*, vol. 82, no. 3, pp. 636–643, 2005.

[71] M. T. Heneka, J. J. Rodríguez, and A. Verkhratsky, "Neuroglia in neurodegeneration," *Brain Research Reviews*, vol. 63, no. 1-2, pp. 189–211, 2010.

[72] T. Mizuno, R. Kuno, A. Nitta et al., "Protective effects of nicergoline against neuronal cell death induced by activated microglia and astrocytes," *Brain Research*, vol. 1066, no. 1-2, pp. 78–85, 2005.

[73] R. E. Gonzalez-Reyes, M. O. Nava-Mesa, K. Vargas-Sanchez, D. Ariza-Salamanca, and L. Mora-Muñoz, "Involvement of astrocytes in Alzheimer's disease from a neuroinflammatory and oxidative stress perspective," *Frontiers in Molecular Neuroscience*, vol. 10, p. 427, 2017.

[74] M. V. Sofroniew and H. V. Vinters, "Astrocytes: biology and pathology," *Acta Neuropathologica*, vol. 119, no. 1, pp. 7–35, 2010.

[75] A. A. Cronican, N. F. Fitz, T. Pham et al., "Proton pump inhibitor lansoprazole is a nuclear liver X receptor agonist," *Biochemical Pharmacology*, vol. 79, no. 9, pp. 1310–1316, 2010.

[76] R. Batchelor, J. F. Gilmartin, W. Kemp, I. Hopper, and D. Liew, "Dementia, cognitive impairment and proton pump inhibitor therapy: a systematic review," *Journal of Gastroenterology and Hepatology*, vol. 32, no. 8, pp. 1426–1435, 2017.

[77] A. M. Herghelegiu, G. I. Prada, and R. Nacu, "Prolonged use of proton pomp inhibitors and cognitive function in older adults," *Farmácia*, vol. 64, no. 2, pp. 262–267, 2016.

[78] M. G. Delgado, S. Calleja, L. Suarez, and J. Pascual, "Recurrent confusional episodes associated with hypomagnesaemia due to esomeprazol," *BMJ Case Reports*, vol. 2013, article bcr2013200501, 2013.

[79] L. Pasina, D. Zanotta, S. Puricelli, and G. Bonoldi, "Acute neurological symptoms secondary to hypomagnesemia induced by proton pump inhibitors: a case series," *European Journal of Clinical Pharmacology*, vol. 72, no. 5, pp. 641–643, 2016.

[80] V. S. Bebarta, J. A. King, and M. McDonough, "Proton pump inhibitor-induced rhabdomyolysis and hyponatremic delirium," *The American Journal of Emergency Medicine*, vol. 26, no. 4, pp. 519.e1–519.e2, 2008.

[81] S. Fujii, H. Tanimukai, and Y. Kashiwagi, "Comparison and analysis of delirium induced by histamine H2 receptor antagonists and proton pump inhibitors in cancer patients," *Case Reports in Oncology*, vol. 5, no. 2, pp. 409–412, 2012.

[82] I. Otremba, K. Wilczyński, and J. Szewieczek, "Delirium in the geriatric unit: proton-pump inhibitors and other risk factors," *Clinical Interventions in Aging*, vol. 11, pp. 397–405, 2016.

[83] F. C. Soares, T. C. de Oliveira, L. D. de Macedo et al., "CANTAB object recognition and language tests to detect aging cognitive decline: an exploratory comparative study," *Clinical Interventions in Aging*, vol. 10, pp. 37–48, 2015.

[84] P. Lochhead, K. Hagan, A. D. Joshi et al., "Association between proton pump inhibitor use and cognitive function in women," *Gastroenterology*, vol. 153, no. 4, pp. 971–979.e4, 2017.

[85] W. Li, S. Zeng, L.-S. Yu, and Q. Zhou, "Pharmacokinetic drug interaction profile of omeprazole with adverse consequences and clinical risk management," *Therapeutics and Clinical Risk Management*, vol. 9, pp. 259–271, 2013.

[86] C. Parsons, S. Johnston, E. Mathie et al., "Potentially inappropriate prescribing in older people with dementia in care homes," *Drugs & Aging*, vol. 29, no. 2, pp. 143–155, 2012.

[87] J. Labenz, K. U. Petersen, W. Rösch, and H. R. Koelz, "A summary of Food and Drug Administration-reported adverse events and drug interactions occurring during therapy with omeprazole, lansoprazole and pantoprazole," *Alimentary Pharmacology and Therapeutics*, vol. 17, no. 8, pp. 1015–1019, 2003.

[88] J. Gallacher, P. Elwood, J. Pickering, A. Bayer, M. Fish, and Y. Ben-Shlomo, "Benzodiazepine use and risk of dementia: evidence from the Caerphilly Prospective Study (CaPS)," *Journal of Epidemiology & Community Health*, vol. 66, no. 10, pp. 869–873, 2012.

[89] S. Billioti de Gage, A. Pariente, and B. Begaud, "Is there really a link between benzodiazepine use and the risk of dementia?," *Expert Opinion on Drug Safety*, vol. 14, no. 5, pp. 733–747, 2015.

[90] M. O. Nava-Mesa, L. Jimenez-Diaz, J. Yajeya, and J. D. Navarro-Lopez, "GABAergic neurotransmission and new strategies of neuromodulation to compensate synaptic dysfunction in early stages of Alzheimer's disease," *Frontiers in Cellular Neuroscience*, vol. 8, p. 167, 2014.

[91] C. M. Stonnington, P. J. Snyder, J. G. Hentz, E. M. Reiman, and R. J. Caselli, "Double-blind crossover study of the cognitive effects of lorazepam in healthy apolipoprotein E (*APOE*)-ε4 carriers," *The Journal of Clinical Psychiatry*, vol. 70, no. 10, pp. 1379–1384, 2009.

[92] R. Gugler, M. Hartmann, J. Rudi et al., "Lack of pharmacokinetic interaction of pantoprazole with diazepam in man," *British Journal of Clinical Pharmacology*, vol. 42, no. 2, pp. 249–252, 1996.

[93] R. A. Lefebvre, B. Flouvat, S. Karolac-Tamisier, E. Moerman, and E. V. Ganse, "Influence of lansoprazole treatment on diazepam plasma concentrations," *Clinical Pharmacology & Therapeutics*, vol. 52, no. 5, pp. 458–463, 1992.

[94] T. Ishizaki, K. Chiba, K. Manabe et al., "Comparison of the interaction potential of a new proton pump inhibitor, E3810, versus omeprazole with diazepam in extensive and poor metabolizers of *S*-mephenytoin 4′-hydroxylation," *Clinical Pharmacology & Therapeutics*, vol. 58, no. 2, pp. 155–164, 1995.

[95] G. M. Pasinetti, "From epidemiology to therapeutic trials with anti-inflammatory drugs in Alzheimer's disease: the role of NSAIDs and cyclooxygenase in β-amyloidosis and clinical dementia," *Journal of Alzheimer's Disease*, vol. 4, no. 5, pp. 435–445, 2002.

[96] P. L. McGeer, E. McGeer, J. Rogers, and J. Sibley, "Anti-inflammatory drugs and Alzheimer disease," *The Lancet*, vol. 335, no. 8696, p. 1037, 1990.

[97] A. Ghallab, "In vitro test systems and their limitations," *EXCLI Journal*, vol. 12, pp. 1024–1026, 2013.

[98] R. D. Bell and B. V. Zlokovic, "Neurovascular mechanisms and blood-brain barrier disorder in Alzheimer's disease," *Acta Neuropathologica*, vol. 118, no. 1, pp. 103–113, 2009.

[99] G. N. Shah and A. D. Mooradian, "Age-related changes in the blood-brain barrier," *Experimental Gerontology*, vol. 32, no. 4-5, pp. 501–519, 1997.

[100] T. O. Kleine, R. Hackler, and P. Zofel, "Age-related alterations of the blood-brain-barrier (bbb) permeability to protein molecules of different size," *Zeitschrift für Gerontologie*, vol. 26, no. 4, pp. 256–259, 1993.